

Physiochemical responses of an asterinid starfish (Echinodermata: Asteroidea) to global ocean change

Dissertation

for obtaining a Doctoral Degree in Science (Dr. rer. nat)
at the Faculty of Geosciences (FB5), the University of Bremen



Munawar Khalil

November 2024

Physiochemische Reaktionen eines Asteriniden- Seesterns (Echinodermata: Asteroidea) auf globale Ozeanveränderungen

Dissertation

zur Erlangung des Doktorgrades der Naturwissenschaften (Dr. rer. nat)
am Fachbereich Geowissenschaften (FB5), der Universität Bremen



Munawar Khalil

November 2024

The work contained within this dissertation took place between January 2020 and July 2024 at the Leibniz Centre for Tropical Marine Research (ZMT) in Bremen, Germany.

Supported financially by the Leibniz Centre for Tropical Marine Research (ZMT) Academy – Doctoral Research Grant and the Ministry of Education, Culture, Research, and Technology (MoECRT), Republic of Indonesia – Asian Development Bank (ADB) AKSI Project [grant number L3749-INO].

First Reviewer:

Prof. Dr. Hildegard Westphal

University of Bremen, Germany

Leibniz Centre for Tropical Marine Research (ZMT), Bremen, Germany

Second Reviewer:

Prof. Dr. Ingrid Kröncke

Carl von Ossietzky University of Oldenburg, Germany

Senckenberg – Marine Research Department, Wilhelmshaven, Germany

Colloquium: 12 November 2024

Die in dieser Dissertation enthaltenen Arbeiten fanden zwischen Januar 2020 und Juli 2024 am Leibniz-Zentrum für Marine Tropenforschung (ZMT) in Bremen, Deutschland.

Finanziell unterstützt durch das Leibniz - Zentrum für Marine Tropenforschung (ZMT) Akademie – Doktorandenstipendium und das Ministerium für Bildung, Kultur, Forschung und Technologie (MfBKFuT), Republik Indonesien – Asian Development Bank (ADB) AKSI Projekt [Zuschussnummer L3749-INO].

Erstprüferin:

Prof. Dr. Hildegard Westphal

Universität Bremen, Deutschland

Leibniz-Zentrum für Marine Tropenforschung (ZMT), Bremen, Deutschland

Zweiter Prüfer:

Prof. Dr. Ingrid Kröncke

Carl von Ossietzky Universität Oldenburg, Deutschland

Senckenberg am Meer, Wilhelmshaven, Germany

Kolloquium: 12 November 2024

Table of contents

	Page
Table of contents	i
Affirmation/Erklärung	v
Summary	vi
Zusammenfassung	viii
Overview of publications and conference’s contribution	xi
List of figures	xiv
List of tables.....	xxi
Acknowledgments	xxv
Abbreviations.....	xxvii
Chapter 1. General introduction.....	1
1.1. Global ocean change	1
1.2. Effect of ocean acidification and ocean warming on marine organisms	7
1.3. The adaptive potential of marine organisms to global ocean change	20
1.4. Bioindicator species for assessing the effects of ocean warming and ocean acidification	22
1.5. Research aim and approach.....	24
1.5.1. Study objective and hypothesis	24
1.5.2. Model species: asterinid starfish	25
1.5.3. Experimental design and procedures.....	28
1.5.4. Outline of the thesis	31
Chapter 2. Ocean warming amplifies the effects of ocean acidification on skeletal mineralogy and microstructure in the asterinid starfish <i>Aquilonastra yairi</i>	35

2.1.	Introduction	39
2.2.	Materials and methods.....	42
2.2.1.	Experimental design and control of seawater chemistry	42
2.2.2.	Skeletal mineral composition analysis	44
2.2.3.	Analysis of the skeleton microstructure.....	44
2.2.4.	Statistical analysis.....	45
2.3.	Result	45
2.3.1.	Elemental composition of skeletal carbonate	45
2.3.2.	Skeletal microstructure	50
2.4.	Discussion.....	54
2.5.	Acknowledgements	57
2.6.	Supplementary materials.....	58
Chapter 3.	Long-term physiological responses to combined ocean acidification and warming show energetic trade-offs in an asterinid starfish.....	65
3.1.	Introduction	69
3.2.	Material and methods	71
3.2.1.	Experimental design and seawater chemistry control and measurement.....	71
3.2.2.	Metabolic rate.....	72
3.2.3.	Mortality	72
3.2.3.	Righting behaviour	72
3.2.5.	Calcification rate	73
3.2.6.	Statistical analysis.....	73
3.3.	Results.....	74
3.3.1.	Metabolic rate.....	74
3.3.2.	Mortality	74
3.3.3.	Righting activity.....	76
3.3.4.	Calcification rate	76

3.4.	Discussion.....	80
3.4.1.	Metabolic response under multiple stressors	80
3.4.2.	Ocean warming and $p\text{CO}_2$ impact on mortalit.....	82
3.4.3.	Ocean warming influence on righting response	83
3.4.4.	Potential antagonistic effect of elevated temperature and $p\text{CO}_2$ on calcification	84
3.5.	Conclusion.....	86
3.6.	Acknowledgements	86
3.7.	Supplementary materials.....	87
Chapter 4. Simultaneous ocean acidification and warming do not alter the lipid-associated biochemistry but induce enzyme activities in an asterinid starfish		
		100
4.1.	Introduction	104
4.2.	Methods.....	107
4.2.1.	Experimental design and exposure conditions.....	107
4.2.2.	Total lipid and fatty acids analysis.....	108
4.2.3.	Ca-ATPase and Mg-ATPase activity assays	109
4.2.4.	Statistical analysis.....	110
4.3.	Results.....	111
4.3.1.	Total lipid	111
4.3.2.	Fatty acids composition.....	112
4.3.3.	Ca-ATPase and Mg-ATPase activities	118
4.4.	Discussion.....	120
4.4.1.	Lipid-associated resilience and homeoviscous adaptations	120
4.4.2.	Enzyme activities under multiple stressors and their potential role in calcification	124
4.5.	Conclusions	127
4.6.	Acknowledgments	127
4.7.	Data availability	128

4.8. Supplementary materials.....	128
Chapter 5. General discussion	145
5.1. Temperature is a key driver affecting physiochemical functions of starfish.....	146
5.2. Effect of ocean warming and acidification on physiology- related functions of the starfish and their ecological implication	148
Chapter 6. Conclusion and future research.....	151
6.1. Conclusion.....	151
6.2. Potential further research.....	155
References.....	158
Appendix	212
Index.....	221

Affirmation/Erklärung

Versicherung an Eides Statt / *Affirmation in lieu of an oath*

gem. § 5 Abs. 5 der Promotionsordnung vom 18.06.2018 /
according to § 5 (5) of the Doctoral Degree Rules and Regulations of 18 June, 2018

Ich / I, _____
(Vorname / First Name, Name / Name, Anschrift / Address, ggf. Matr.-Nr. / student ID no., if applicable)

versichere an Eides Statt durch meine Unterschrift, dass ich die vorliegende Dissertation selbständig und ohne fremde Hilfe angefertigt und alle Stellen, die ich wörtlich dem Sinne nach aus Veröffentlichungen entnommen habe, als solche kenntlich gemacht habe, mich auch keiner anderen als der angegebenen Literatur oder sonstiger Hilfsmittel bedient habe und die zu Prüfungszwecken beigelegte elektronische Version (PDF) der Dissertation mit der abgegebenen gedruckten Version identisch ist. / *With my signature I affirm in lieu of an oath that I prepared the submitted dissertation independently and without illicit assistance from third parties, that I appropriately referenced any text or content from other sources, that I used only literature and resources listed in the dissertation, and that the electronic (PDF) and printed versions of the dissertation are identical.*

Ich versichere an Eides Statt, dass ich die vorgenannten Angaben nach bestem Wissen und Gewissen gemacht habe und dass die Angaben der Wahrheit entsprechen und ich nichts verschwiegen habe. / *I affirm in lieu of an oath that the information provided herein to the best of my knowledge is true and complete.*

Die Strafbarkeit einer falschen eidesstattlichen Versicherung ist mir bekannt, namentlich die Strafandrohung gemäß § 156 StGB bis zu drei Jahren Freiheitsstrafe oder Geldstrafe bei vorsätzlicher Begehung der Tat bzw. gemäß § 161 Abs. 1 StGB bis zu einem Jahr Freiheitsstrafe oder Geldstrafe bei fahrlässiger Begehung. / *I am aware that a false affidavit is a criminal offence which is punishable by law in accordance with § 156 of the German Criminal Code (StGB) with up to three years imprisonment or a fine in case of intention, or in accordance with § 161 (1) of the German Criminal Code with up to one year imprisonment or a fine in case of negligence.*

Ort / Place, Datum / Date

Unterschrift / Signature

Summary

The continuous increase in greenhouse gas (GHG) emissions, especially carbon dioxide (CO₂), since the beginning of global industrialization has resulted in significant alterations in seawater physicochemical properties, particularly elevated seawater temperatures (ocean warming, OW) and ocean acidification (OA). These changes have wide-ranging consequences for marine organisms, affecting their biological functions and ecological roles. The combined effects of OW and OA may amplify adverse outcomes compared to individual stressors due to the complex reorganization of cellular mechanisms and molecular pathways, which subsequently appear in behavioral modifications. However, organismal reactions and thresholds to these stressors are variable, which might differ within organism ontogeny or among taxa, making predictions challenging. Therefore, increasing research has been performed to better understand the potential mechanisms underlying the ability of marine organisms to alleviate the effects of environmental change, mainly due to OW and OA. Thus, employing multiple bioindicators, specifically keystone species such as starfish, to evaluate the impacts of OW and OA offers a comprehensive approach to examining their effects not simply on the organism concerned but also on the broader ecosystem.

The presented studies in this thesis aim to contribute to the understanding the role of physiochemistry and trade-offs on marine ectotherms, particularly asterinid starfish, in coping with environmental stress. For this purpose, mineralogic, metabolic, behavioral, lipidomics, and enzymatic activity approaches are used. The research summarized in this thesis provides the first investigation of the effects of global ocean change on biomineralization and physiological traits through long-term experiments using asterinid starfish species, *Aquilonastra yairi*, distributed in tropical to subtropical regions (across the Mediterranean Sea, Red Sea, and Gulf of Suez). The starfish were exposed to two temperature levels (27 °C and 32 °C) crossed with three pCO₂ regimes (455 µatm, 1052 µatm, and 2066 µatm), representing factorial combinations of ambient conditions and future levels of CO₂ and temperature change according to the IPCC-Representative Concentration Pathways (RCPs) 8.5 greenhouse gas emission scenario for the year 2100.

The present work revealed that asterinid starfish demonstrate high stressor tolerance and resilience to increased temperature and $p\text{CO}_2$ through adaptive adjustments in physiological functions or behavioral activities, suggesting high homeostatic capacities and the ability to regulate physiochemical response to maintain survival, fitness, and metabolic biosynthesis under chronic conditions. The temperature was the predominant factor, exerting a significant effect on the magnitude and frequency of the affected physiological-related processes; however, concurrent exposure to OA and OW stress produced synergistic effects on some of the starfish physiology-related responses tested. While decreased pH negatively affects starfish calcification performance, the increased temperature potentially mitigates these effects. However, increased temperature might also lead to more magnesium (Mg^{2+}) incorporation into the calcite lattice, potentially compromising the starfish skeleton. Furthermore, it was revealed that starfish can preserve lipid-associated biochemistry (FAs) under elevated temperature and $p\text{CO}_2$, which potentially provides molecular instruments to cope with future OA and OW scenarios. However, combined OA and OW significantly affected Ca-ATPase and Mg-ATPase enzyme activities, which are recognized to play an important role in the biomineralization pathway, raising concerns about potential susceptibilities in skeletal development and preservation.

Investigating the complex impacts of global ocean change on marine organisms requires a comprehensive research approach that encompasses diverse biological, chemical, and physical traits. Understanding the physiological and chemical responses of bioindicator species, e.g., asterinid starfish, to combined stressors OW and OA is important to comprehend the relationships and interactions between biological processes and abiotic environmental conditions, which in turn essential for accurately predicting their resilience, ecological implication, and broader ecosystem dynamics. At the ecosystem scale, this study significantly contributes to the ongoing knowledge for future studies of the impact of climate change on coral reef-associated invertebrates. Specifically, this finding is beneficial for the conservation of coral reef ecosystems under future ocean conditions.

Zusammenfassung

Der kontinuierliche Anstieg der Treibhausgasemissionen (THG), insbesondere von Kohlendioxid (CO₂), seit Beginn der globalen Industrialisierung hat zu erheblichen Veränderungen der physikalisch-chemischen Eigenschaften des Meerwassers geführt, insbesondere zu erhöhten Meerwassertemperaturen (Ozeanerwärmung, OW) und zur Versauerung der Ozeane (OA). Diese Veränderungen haben weitreichende Folgen für die Meeresorganismen und beeinträchtigen ihre biologischen Funktionen und ökologischen Aufgaben. Die kombinierten Auswirkungen von OW und OA können die negativen Folgen im Vergleich zu den einzelnen Stressoren verstärken, da sich zelluläre Mechanismen und molekulare Pfade komplex umgestalten, was sich wiederum in Verhaltensänderungen niederschlägt. Die Reaktionen und Schwellenwerte der Organismen auf diese Stressfaktoren sind jedoch komplex und variabel und können sich innerhalb der Ontogenese des Organismus oder zwischen den Taxa unterscheiden, was Vorhersagen schwierig macht. Aus diesem Grund werden immer mehr Forschungsarbeiten durchgeführt, um die potenziellen Mechanismen besser zu verstehen, die der Fähigkeit von Meeresorganismen zugrunde liegen, die Auswirkungen von Umweltveränderungen, vor allem aufgrund von OW und OA, abzumildern. Der Einsatz mehrerer Bioindikatoren, insbesondere von Schlüsselarten wie Seesternen, zur Bewertung der Auswirkungen von OW und OA bietet daher einen umfassenden Ansatz zur Untersuchung ihrer Auswirkungen nicht nur auf den betreffenden Organismus, sondern auch auf das Ökosystem im weiteren Sinne.

Die in dieser Arbeit vorgestellte Studie zielt darauf ab, die Rolle der Physiochemie und der Kompromisse bei marinen ektothermen Organismen, insbesondere bei Seesternen, bei der Bewältigung von Umweltstress zu verstehen, indem mineralogische, metabolische, verhaltensbezogene, lipidomische und enzymatische Aktivitätsansätze verwendet werden. Es handelt sich um die erste Forschungsarbeit, die die Auswirkungen des globalen Ozeanwandels auf die Biomineralisierung und physiologische Eigenschaften anhand von Langzeitexperimenten mit der Seesternart *Aquilonastra yairi* untersucht, die in tropischen bis subtropischen Regionen (Mittelmeer, Rotes Meer und Golf von Suez) verbreitet ist. Die Seesterne wurden zwei Temperaturniveaus (27 °C and 32 °C) in Kombination mit drei pCO₂-Regimen (455 µatm, 1052 µatm, und 2066 µatm) ausgesetzt, die faktorielle Kombinationen von

Umgebungsbedingungen und zukünftigen CO₂- und Temperaturänderungen gemäß dem IPCC-Szenario der repräsentativen Konzentrationspfade (RCPs) 8.5 für das Jahr 2100 darstellen.

Die vorliegende Arbeit zeigte, dass Asteriniden-Seesterne eine hohe Stresstoleranz und Widerstandsfähigkeit gegenüber erhöhten Temperaturen und pCO₂ aufweisen, und zwar durch adaptive Anpassungen der physiologischen Funktionen oder Verhaltensaktivitäten, was auf hohe homöostatische Kapazitäten und die Fähigkeit zur Regulierung physiochemischer Reaktionen zur Aufrechterhaltung des Überlebens, der Fitness und der metabolischen Biosynthese unter chronischen Bedingungen schließen lässt. Die Temperatur war der vorherrschende Faktor, der eine signifikante Auswirkung auf das Ausmaß und die Häufigkeit der betroffenen physiologischen Prozesse hatte; die gleichzeitige Exposition gegenüber OA- und OW-Stress führte jedoch zu synergistischen Effekten auf einige der getesteten physiologischen Reaktionen der Seesterne. Während sich ein niedriger pH-Wert negativ auf die Kalzifizierungsleistung der Seesterne auswirkt, mildert die erhöhte Temperatur diese Auswirkungen möglicherweise ab. Eine erhöhte Temperatur könnte jedoch auch zu einem verstärkten Einbau von Magnesium (Mg²⁺) in das Kalzitgitter führen, wodurch das Seesternskelett möglicherweise beeinträchtigt wird. Darüber hinaus zeigte sich, dass Seesterne die lipidassoziierte Biochemie (Fettsäuren) unter erhöhten Temperaturen und pCO₂ bewahren können, was möglicherweise molekulare Instrumente zur Bewältigung künftiger OA- und OW-Szenarien bietet. Allerdings beeinträchtigte die Kombination von OA und OW die Aktivitäten der Enzyme Ca-ATPase und Mg-ATPase, die bekanntermaßen eine wichtige Rolle bei der Biomineralisierung spielen, erheblich, was Anlass zur Sorge über mögliche Anfälligkeiten bei der Entwicklung und Erhaltung des Skeletts gibt.

Die Untersuchung der komplexen Auswirkungen des globalen Ozeanwandels auf Meeresorganismen erfordert einen umfassenden Forschungsansatz, der verschiedene biologische, chemische und physikalische Merkmale umfasst. Das Verständnis der physiologischen und chemischen Reaktionen von Bioindikatorarten, z. B. Asteriniden-Seesternen, auf die kombinierten Stressoren OW und OA ist wichtig, um die Beziehungen und Wechselwirkungen zwischen biologischen Prozessen und abiotischen Umweltbedingungen zu verstehen, was wiederum für eine genaue Vorhersage ihrer Widerstandsfähigkeit, der ökologischen Auswirkungen und der breiteren Ökosystemdynamik unerlässlich ist. Auf der Ebene der Ökosysteme trägt diese Studie auch zum aktuellen Wissensstand für künftige

Studien über die Auswirkungen des Klimawandels auf mit Korallenriffen assoziierte wirbellose Tiere bei. Insbesondere ist dieses Ergebnis für die Erhaltung von Korallenriff-Ökosystemen unter zukünftigen Meeresbedingungen von Nutzen.

Overview of publications and conference's contribution

The presented doctoral dissertation is based on a cumulative thesis consisting of three articles published in international peer-reviewed journals (Chapters 2, 3, and 4). The authors' contributions to the manuscripts are summarized on the back of the respective cover pages.

Chapter 2: **Khalil, M.**, Doo, S. S., Stuhr, M., & Westphal, H. (2022). Ocean warming amplifies the effects of ocean acidification on skeletal mineralogy and microstructure in the asterinid starfish *Aquilonastra yairi*. *Journal of Marine Science and Engineering*, 10(8), 1065. <https://doi.org/10.3390/jmse10081065>.

Chapter 3: **Khalil, M.**, Doo, S. S., Stuhr, M., & Westphal, H. (2023). Long-term physiological responses to combined ocean acidification and warming show energetic trade-offs in an asterinid starfish. *Coral Reefs*, 42(4), 845-858. <https://doi.org/10.1007/s00338-023-02388-2>.

Chapter 4: **Khalil, M.**, Stuhr, M., Kunzmann, A., & Westphal, H. (2024). Simultaneous ocean acidification and warming do not alter the lipid-associated biochemistry but induce enzyme activities in an asterinid starfish. *Science of the Total Environment*, 932, 173000. <https://doi.org/10.1016/j.scitotenv.2024.173000>.

In addition, four journal articles (served as author/co-author) *unrelated* to doctoral research work (2020-2024) were also published in international peer-reviewed journals. Article details are provided in the *appendix*.

During doctoral study, part of the work has been presented at the conferences outlined below: **Khalil, M.**, Doo, S. S., Stuhr, M., & Westphal, H. (2023, January 24). *Physiological effects of combined ocean acidification and warming on asterinid starfish*. ZMT Annual Conference 4 (ZAC-4), Bremen, Germany.

Understanding how marine ecosystems are impacted by environmental stressors relies on accurate predictions of species-specific responses (performances of marine organisms) to climate change. In this study, we assess the combined effects of elevated $p\text{CO}_2$ and temperature on organismal mortality, metabolic rate, righting activity, and calcification rates

of the tropical asterinid starfish *Aquilonastra yairi*. Adult specimens of *A. yairi* were acclimated at two temperature levels (27 °C and 32 °C) crossed with three pCO₂ concentrations (455 µatm, 1052 µatm, and 2066 µatm) for 90 days. At the end of the 90-day incubation, mortality was not altered by temperature and pCO₂ treatments. Elevated temperature alone increased metabolic rate, accelerated righting activity, and caused a decline in calcification rate. In contrast, elevated pCO₂ concentration increased metabolic rate and reduced calcification rate but did not significantly affect the righting activity. These results demonstrate that temperature is the main driver regulating starfish physiology. However, the combination of high temperature and high pCO₂ concentration shows nonlinear and potentially synergistic effects on organismal physiology (e.g., metabolic rate), whereby the high temperature benefits the starfish to cope with the adverse effect of high pCO₂ concentration (low pH) on calcification and minimize skeletal dissolution. Our study implies that while the temperature is the most significant stressor associated with global change for asterinid starfish, interactive effects with pCO₂ might raise physiological perturbations.

Khalil, M., Stuhr, M., Kunzmann, A., & Westphal, H. (2024, January 16). *Ocean acidification and warming effects on lipid-associated biochemistry and enzyme activities in an asterinid starfish*. ZMT Annual Conference 5 (ZAC-5), Bremen, Germany.

Ocean acidification and ocean warming as part of global climate change consequences are affecting marine organismal physiology on a microscale and are altering ecosystem functions on a broader level. However, there is still sparse information on how they interact to affect tropical and subtropical intertidal species. Driving the environmental window of marine species away from their optimum conditions triggers stress that may affect biochemical metabolic characteristics, with consequences on lipid-related biochemistry and enzyme biosynthesis. This study aims to investigate lipids and associated fatty acids (FAs) and the activity of enzymes involved in the calcification process of asterinid starfish *Aquilonastra yairi* in response to near-future global change scenarios. The *A. yairi* in our experiment were acclimatized to two temperature levels (27 °C, 32 °C) crossed with three pCO₂ concentrations (455 µatm, 1052 µatm, 2066 µatm) for 90 days. The composition of the total lipids (ΣL_C) and FAs were unaffected by combined elevated temperature and pCO₂, but at elevated temperature, there was an increase in ΣL_C , SFAs (saturated fatty acids) and PUFAs (polyunsaturated fatty acids), and a decrease in MUFAs (monounsaturated fatty acids). Furthermore, statistical tests confirmed that temperature was the sole factor significantly altering the SFAs composition. A

homeoviscous adaptation strategy appears to be employed by *A. yairi* to reduce the impacts of elevated temperatures and $p\text{CO}_2$. Parabolic responses and unstable Ca-ATPase and Mg-ATPase enzyme activities were detected at ambient temperature-elevated $p\text{CO}_2$, while stable enzyme activities were observed at high-temperature-elevated $p\text{CO}_2$. Hence, the increased temperature seems to allow the starfish to cope with the negative effect of increased $p\text{CO}_2$ on enzyme activities (antagonistic interactive effects). Our results indicate that lipid biochemistry in starfish is resilient to elevated $p\text{CO}_2$ but not temperature, while enzyme activities appear more sensitive to alterations in $p\text{CO}_2$.

List of figures

	Page
Figure 1.1. Annual-mean atmospheric main GHGs emission CO ₂ , CH ₄ , and N ₂ O (1850-2019), and CO ₂ contributions from human anthropogenic activities (modified from IPCC (2023)). GHG emissions have risen at an accelerating rate since 1850. As of 2019, the levels of CO ₂ , CH ₄ , and N ₂ O in the atmosphere all exceeded 410 parts per million (ppm), 1866 parts per billion (ppb), and 332 parts per billion (ppb), respectively (IPCC, 2023).	2
Figure 1.2. Historical and projection of global surface temperature. (a). The annual mean of earth's surface temperature anomalies from 1850 to 2022. The trends of land and ocean surface temperature anomalies are 0.09 °C/decade and 0.04 °C/decade, respectively. Datasets were extracted from NOAA (2023), (b). Cumulative temperature (1850-2019) and projected temperature (2020-2050) of the earth's surface based on GHG CO ₂ emissions (modified from IPCC (2021)). The projected temperatures are modeled using cumulative CO ₂ emissions under the IPCC-SSPs scenario.	5
Figure 1.3. Historical and projection of the global surface CO ₂ -pH trend and the potential for ocean acidification. (a) observed and current global atmospheric CO ₂ concentration trend. Datasets were extracted from (Lan et al., 2023), (b) the cumulative ocean pH (1950-2019), and the projected surface ocean pH (2020-2010) based on the GHG CO ₂ emissions (modified from IPCC (2021)). The projected surface ocean pH is modeled using cumulative CO ₂ emissions under the IPCC-SSPs scenario, (c) schematic diagram of the ocean acidification processes.	6

Figure 1.4.	The studied asternid starfish <i>Aquilonastra yairi</i> . (a) dorsal (upper) part, (b) ventral (bottom) part, (c) fissiparous-asexual reproduction (fission) fragment, (d) skeleton microstructure appearance (stereom pore).....	28
Figure 1.5.	Schematic outline of the chapter-specific objectives and overarching approach of the dissertation. The background context of ocean warming and acidification caused by GHGs-CO ₂ and its ramifications on marine life (Chapter 1), the interactive effects of OA/OW on the biomineralization process of starfish <i>A. yairi</i> which is reflected in their skeletal mineralization and microstructure (Chapter 2), potential alterations in important physiological factors and behaviour of starfish under OA/OW environment (Chapter 3), starfish micro-physiochemical profiles of lipid-FAs and its enzyme activities under OA/OW conditions (Chapter 4), the previous chapters are further synthesized (Chapter 5), general conclusion and questions that may remain unaddressed in this dissertation are highlighted for future studies (Chapter 6).	34
Figure 2.1.	Changes in skeletal properties (A) Mg/Ca ratios (mmol/mol) and (B) Sr/Ca ratios (mmol/mol) of skeletal carbonate in <i>A. yairi</i> exposed to different temperatures (27 °C and 32 °C) crossed with different pCO ₂ concentrations (455 µatm, 1052 µatm, and 2066 µatm) measured after 45 and 90 days of incubation (<i>n</i> = 36).	46
Figure 2.2.	Ratios between skeletal mineral element to total skeletal material (A) Ca _{norm} ratios (mg/g), (B) Mg _{norm} ratios (mg/g), and (C) Sr _{norm} ratios (mg/g) in <i>A. yairi</i> exposed to elevated temperatures levels (27 °C and 32 °C) crossed with increased pCO ₂ concentrations (455 µatm, 1052 µatm and 2066 µatm) measured after 45 and 90 days of incubation (<i>n</i> = 36).	48
Figure 2.3.	SEM micrographs of the skeletal microstructure of <i>A. yairi</i> cultured under two temperature levels (27 °C and 32 °C)	

crossed with three $p\text{CO}_2$ concentrations (455 μatm , 1052 μatm and 2066 μatm). Stereom microstructure after 45 (A,C,E,G,I,K) and 90 days (B,D,F,H,J,L) of incubation time. *sp*: stereom pore; *st*: skeleton trabeculae; *imp*: stereom inner matrix pore; ㉑ the galleries stereom pores are less-equal in shape; ㉒ dissolution in calcium carbonate skeleton; ㉓ increased size of inner matrix aperture pores. Technical image acquisition, SEM mode: SE, SEM HV: 5.0 kV, SEM magnification: 3000 \times 53

Figure S2.1. Schematic of ocean acidification and ocean warming experimental design with a fully factorial combination of low $p\text{CO}_2$ (455 μatm), moderate $p\text{CO}_2$ (1052 μatm), and high $p\text{CO}_2$ (2066 μatm) treatments with ambient temperature (27 °C) and high temperature (32 °C) treatments..... 61

Figure S2.2. Skeletal Sr values over incubation time in *A. yairi* exposed to elevated temperatures levels (27 °C and 32 °C) crossed with increased $p\text{CO}_2$ concentrations (455 μatm , 1052 μatm , and 2066 μatm). (A) Sr/Ca ratio (mmol/mol), (B) Sr_{norm} ratio (mg/g). Data were presented as mean ($n = 36$)..... 62

Figure S2.3. Correlation of Sr_{norm} ratios (mg/g) against Mg_{norm} ratios (mg/g) ($R^2 = 0.44$, $F_{1, 34} = 26.78$, $p = 1.019 \times 10^{-5}$) in *A. yairi* exposed to elevated temperatures levels (27 °C and 32 °C) crossed with increased $p\text{CO}_2$ concentrations (455 μatm , 1052 μatm , and 2066 μatm). $n = 36$ 63

Figure S2.4. Skeletal Ca_{norm} (mg/g) ratio over incubation time in *A. yairi* exposed to elevated temperatures levels (27 °C and 32 °C) crossed with increased $p\text{CO}_2$ concentrations (455 μatm , 1052 μatm , and 2066 μatm). Data were presented as mean ($n = 36$). 64

Figure 3.1. The metabolic rate (M_{O_2}) responses, measured as oxygen consumption of *A. yairi* (shown in the upper left corner) reared under different $p\text{CO}_2$ levels (455 μatm , 1052 μatm , and 2066 μatm) and temperatures (27 °C and 32 °C). $n = 42$

	individuals per treatment group. The yellow dots indicate the mean effect in each treatment, and green vertical bars indicate 95% confidence intervals. Dots represent individual M_{O_2} values, displayed with jitter to avoid overlap. Different letters designate significant differences between treatments ($p \leq 0.05$) based on Tukey's HSD post hoc comparison.	75
Figure 3.2.	Righting activity coefficient (RAC) of <i>A. yairi</i> exposed under different pCO_2 concentrations (455 μatm , 1052 μatm , 2066 μatm) and temperatures (27 °C, 32 °C). High RAC values indicate low righting times (s), and vice versa ($n = 36$ individuals per treatment group). Relatively higher RAC values are associated with higher levels of stress. The green vertical bar indicates 95% confidence intervals, yellow dots indicate the mean effect in each treatment. Dots represent individual RAC values, displayed with jitter to avoid overlap. Different letters designate significant differences between treatment groups ($p \leq 0.05$).	77
Figure 3.3.	Calcification rate (G_{TA}) of <i>A. yairi</i> reared under different pCO_2 concentrations (455 μatm , 1052 μatm , 2066 μatm) and temperatures (27 °C, 32 °C). Horizontal dotted lines indicate zero G_{TA} . (a) shows the relationship between mean calcification rate, temperature, and pCO_2 concentration. Error bars indicate standard deviation and different letters designate significant differences between treatments ($p \leq 0.05$) based on Tukey's HSD post hoc comparison. (b) shows the pH_{sw} (total scale)-dependence of <i>A. yairi</i> calcification rate at 27 °C and 32 °C. The symbols (cyan and orange cycles) indicate the calcification rate for the starfish in each replicate, and black symbols represent the mean effect for the starfish in each treatment. Shaded areas represent the 95% confidence interval; $n = 18$ (three samples per treatment).	78
Figure S3.1.	Asterinid starfish <i>A. yairi</i> , (a) dorsal view, (b) ventral view.....	96

Figure S3.2. Schematic of experimental design to determine the impact of ocean acidification and warming on the tropical asterinid starfish <i>A. yairi</i> (unmodified from Khalil et al. (2022)).....	97
Figure S3.3. Linear polynomial interpolation model for the metabolic rate (M_{O_2}) responses of <i>A. yairi</i> reared under different pCO_2 concentrations (455 μatm , 1052 μatm , and 2066 μatm) and temperatures (27 °C, 32 °C) for 90 days of incubation time. Colored dots indicate the mean effect on M_{O_2} in each treatment.....	98
Figure S3.4. Linear polynomial interpolation model for the righting activity coefficient (RAC) of <i>A. yairi</i> reared under different pCO_2 concentrations (455 μatm , 1052 μatm , and 2066 μatm) and temperatures (27 °C, 32 °C) for 90 days of incubation time. Colored dots indicate the mean effect on RAC in each treatment.....	99
Figure 4.1. Total lipid ($mg\ g^{-1}\ DW$) of <i>A. yairi</i> (shown in the upper left corner) for 90 days of exposure to different temperature levels (27 °C, 32 °C) and pCO_2 concentrations (455 μatm , 1052 μatm , and 2066 μatm). Boxplots display the mean effect in each treatment (black dots), median (horizontal solid bar inside the box), interquartile (upper and lower horizontal lines of the box), and 1.5x interquartile ranges (whiskers). Vertical dark-green bars denote 95% confidence intervals of ΣL_C values; $n = 54$	112
Figure 4.2. Fatty acids composition of asteroid <i>A. yairi</i> exposed to different temperature levels (27 °C, 32 °C) and pCO_2 concentrations (455 μatm , 1052 μatm , and 2066 μatm) for 90 days of incubation time. Boxplots display the mean effect in each treatment (color dots), median (horizontal solid bar inside the box), interquartile (upper and lower horizontal lines of the box), and 1.5x interquartile ranges (whiskers). Vertical dark-green bars denote 95% confidence intervals of	

	fatty acids. Letters designate significant differences between the temperature treatment ($p < 0.05$); $n = 54$	113
Figure 4.3.	Biplot of principal component analysis (PCA) based on fatty acid profiles ($n = 18$ classes) for asteroid <i>A. yairi</i> exposed to different temperature levels (27 °C, 32 °C) and $p\text{CO}_2$ concentrations (455 μatm , 1052 μatm , and 2066 μatm) for 90 days of incubation time; $n = 54$. Individual samples are color-coded according to the treatment level. The plot is shown with 95% confidence ellipses.....	115
Figure 4.4.	Enzyme activities of asteroid <i>A. yairi</i> exposed to different temperature levels (27 °C, 32 °C) and $p\text{CO}_2$ concentrations (455 μatm , 1052 μatm , and 2066 μatm) for 90 days of incubation time; (a) Ca-ATPase ($\mu\text{moles Pi mg protein}^{-1} \text{ min}^{-1}$), and (b) Mg-ATPase ($\mu\text{moles Pi mg protein}^{-1} \text{ min}^{-1}$). Boxplots display the mean effect in each treatment (black dots), median (horizontal solid bar inside the box), and interquartile (upper and lower horizontal lines of the box) and 1.5x interquartile ranges (whiskers). Vertical dark-green bars denote 95% confidence intervals of enzyme activity values. Letters designate significant differences between the treatment groups (Tukey's HSD, $p < 0.05$); $n = 53$	119
Figure S4.1.	Linear polynomial interpolation model for the total lipid content ($\text{mg g}^{-1} \text{ DW}$) of <i>A. yairi</i> reared under different temperature levels (27 °C, 32 °C) and $p\text{CO}_2$ concentrations (455 μatm , 1052 μatm , and 2066 μatm) for up to 90 days of incubation time. Colored dots indicate the mean total lipid content in each treatment; $n = 54$	140
Figure S4.2.	Fatty acids (FAs) composition of asteroid <i>A. yairi</i> exposed at different temperature levels (27 °C, 32 °C) and $p\text{CO}_2$ concentrations (455 μatm , 1052 μatm , and 2066 μatm) for 90 days. (a) Saturated fatty acids (SFAs) composition of <i>A. yairi</i> , (b) Monounsaturated fatty acids (MUFAs) composition of <i>A. yairi</i> , (c) Polyunsaturated fatty acids (PUFAs) composition of	

A. yairi. Plots display group mean (black dots). Vertical dark-green bars denote 95% confidence intervals of FAs type values. The letters designate significant differences between treatments; $n = 54$ 143

Figure S4.3. Linear polynomial interpolation model for the enzyme activity of starfish *A. yairi* reared under different temperature levels (27 °C, 32 °C) and $p\text{CO}_2$ concentrations (455 μatm , 1052 μatm , and 2066 μatm) for 90 days of incubation time. (a) Ca-ATPase ($\mu\text{moles Pi mg protein}^{-1} \text{ min}^{-1}$), and (b) Ca-ATPase ($\mu\text{moles Pi mg protein}^{-1} \text{ min}^{-1}$). Colored dots indicate the mean effect on enzyme activity in each treatment; $n = 54$ 144

List of tables

	Page
Table 1.1. Studies on the impacts of ocean acidification and ocean warming as combined stressors (OW*OA) on marine invertebrates. The studies involved factorial experimental design, level of OA (pH/pCO ₂), and OW (Temperature, °C). This study contains only descriptive statistics. OA*OW refers to the effects of combined stressors, which are statistically significant ($p < 0.05$). The pH levels are listed as published on the total scale (pH _T ^a), NBS scale (pH _{NBS} ^b), or no scale (pH ^c) if not indicated. pCO ₂ levels (µatm/ppm) indicated next to pH. Abbreviations, OA: ocean acidification; OW: ocean warming; OA*OW: ocean acidification + ocean warming (combined stressor effect); NS: not specified.....	12
Table 1.2. Observed parameters and methodology applied to examine the effect of OW and OA on the starfish <i>A. yairi</i>	30
Table 2.1. Seawater chemistry values measured during a 90-day experimental period for <i>Aquilonastra yairi</i> reared under two temperature levels (27 °C and 32 °C) crossed with three levels of pCO ₂ (455 µatm, 1052 µatm, and 2066 µatm). Data are presented as mean values ± SE. A _T , total alkalinity; DIC, dissolved inorganic carbon; pCO ₂ , partial pressure of CO ₂ ; [CO ₃ ⁻²], carbonate ion concentration; [HCO ₃ ⁻], bicarbonate ion concentration; [CO ₂], dissolved CO ₂ ; Ω _{Ca} , calcite saturation state; Ω _{Ar} , aragonite saturation state.....	43
Table 2.2. Summary of three-way ANOVA results for the skeletal mineral ratios of <i>A. yairi</i> exposed to temperature (27 °C, 32 °C) crossed with elevated pCO ₂ (455 µatm, 1052 µatm, 2066 µatm) treatments for 45 and 90 days incubation time. Bold terms indicate a significant difference ($p < 0.05$).	49

Table 2.3.	Skeletal microstructure characteristics of <i>A. yairi</i> under crossed temperatures and $p\text{CO}_2$ conditions at different incubation times as observed with scanning electron microscopy (SEM).....	51
Table S2.1.	Tukey HSD post hoc test for the interactive effects of incubation time (45 and 90 days), $p\text{CO}_2$ (455 μatm , 1052 μatm , 2066 μatm) and temperature (27 °C, 32 °C) on skeletal Mg/Ca ratio of <i>A. yairi</i> using the ‘agricolae R-package’ for multiple comparisons to interrogate the main effects of incubation time, temperature and $p\text{CO}_2$ (incubation time: $p\text{CO}_2$: temperature, $p = 0.014$, Table 2.2).....	59
Table 3.1.	Results of the multifactorial statistical analysis on metabolic rate, righting activity, and calcification rate of the starfish <i>A. yairi</i> reared under different $p\text{CO}_2$ concentrations (455 μatm , 1052 μatm , 2066 μatm) and temperatures (27 °C, 32 °C) for 90 days of incubation time. Significant effects ($p \leq 0.05$) are in bold.....	79
Table S3.1.	Seawater parameters (mean \pm SE) from treatment tanks of <i>A. yairi</i> . A_T , total alkalinity; C_T , dissolved inorganic carbon (DIC); $p\text{CO}_2$, partial pressure of CO_2 ; $[\text{CO}_3^{2-}]$, carbonate ion; $[\text{HCO}_3^-]$, bicarbonate ion; $[\text{CO}_2]$, dissolved CO_2 ; Ω_{ca} , calcite saturation state; Ω_{Ar} , aragonite saturation state; SW, seawater.	91
Table S3.2.	The effect of temperature (27 °C, 32 °C) and $p\text{CO}_2$ (455 μatm , 1052 μatm , and 2066 μatm) on the starfish <i>A. yairi</i> metabolic rate for 90 days of incubation time.	92
Table S3.3.	The effect of temperature (27 °C, 32 °C) and $p\text{CO}_2$ (455 μatm , 1052 μatm , and 2066 μatm) on the starfish <i>A. yairi</i> righting activity coefficient (RAC) for 90 days of incubation time.....	92
Table S3.4.	Tukey HSD post hoc test results for the sole and interactive effects of temperature (27 °C and 32 °C), and $p\text{CO}_2$ (455 μatm , 1052 μatm , and 2066 μatm) on the starfish <i>A. yairi</i> metabolic rate and calcification rate (Table 3.1) for 90 days of incubation time. Significant effects ($p < 0.05$) are in bold.	93

Table 4.1.	Total lipid and fatty acids composition of <i>A. yairi</i> reared under different temperature levels (27 °C, 32 °C) and $p\text{CO}_2$ concentrations (455 μatm , 1052 μatm , and 2066 μatm). Total lipid is expressed as mg g^{-1} (mean \pm SE) of asteroids tissue dry weight (DW). FAs are expressed as $\mu\text{g mg}^{-1}$ (mean \pm SE) of asteroids tissue DW. ΣSFAs : sum of SFAs, ΣMUFAs : sum of MUFAs, ΣPUFAs : sum of PUFAs, $\omega 3$: omega-3, $\omega 6$: omega-3, $\Sigma\omega 3$: $\Sigma\omega 6$: ratio of omega-3 ($\omega 3$) fatty acids to omega-6 ($\omega 6$) fatty acids, EPA:DHA: ratio of eicosapentaenoic acid (EPA) to docosahexaenoic acid (DHA).	116
Table S4.1.	Summary of water parameters from treatment tanks of <i>A. yairi</i> . A_T , total alkalinity; C_T , dissolved inorganic carbon (DIC); $p\text{CO}_2$, partial pressure of CO_2 ; $[\text{CO}_3^{-2}]$, carbonate ion; $[\text{HCO}_3^-]$, bicarbonate ion; $[\text{CO}_2]$, dissolved CO_2 ; Ω_{ca} , calcite saturation state; Ω_{Ar} , aragonite saturation state. Salinity, temperature, $\text{pH}_{\text{NBS scale}}$, $\text{pH}_{\text{T (total scale)}}$, A_T , and C_T were measured in water samples collected during the exposure. Other parameters are calculated using CO_2SYS software. Data are represented as means \pm SE.....	130
Table S4.2.	Summary of 2-way ANCOVA multifactorial analysis examining the effect of elevated temperature (27 °C, 32 °C) and $p\text{CO}_2$ (455 μatm , 1052 μatm , and 2066 μatm) on the total lipid, fatty acids composition, and enzyme (Ca-ATPase and Mg-ATPase) activities of the asterinid starfish <i>A. yairi</i> for 90 days of incubation time. Significant effects ($p < 0.05$) are in bold.	131
Table S4.3.	Summary of 2-way MANCOVA multifactorial analysis examining the effect of elevated temperature (27 °C, 32 °C) and $p\text{CO}_2$ (455 μatm , 1052 μatm , 2066 μatm) on SFAs, MUFAs, and PUFAs of asterinid starfish <i>A. yairi</i> for 90 days of incubation time. Significant effects ($p < 0.05$) are in bold.	137
Table S4.4.	Tukey HSD post hoc test results for the sole and interactive effects of temperature (27 °C and 32 °C) and $p\text{CO}_2$ (455 μatm , 1052 μatm , and 2066 μatm) on the asterinid starfish <i>A. yairi</i>	

total lipid content (Table S4.1) for 90 days of incubation time.

Significant effects ($p \leq 0.05$) are in bold..... 138

Table 6.1. Overview of the effect of $p\text{CO}_2$, temperature, and combined stressors on the physiochemical traits of asterinid starfish *A. yairi*. Arrows ($\uparrow\downarrow$) indicate the significance and direction of response to elevated stressor levels; (\leftrightarrow) denotes combined stressors acting in a significant and interactive fashion to affect the traits; (-) implies no significant effect was measured, and (\ddagger) indicates an effect of stressor was observed..... 153

Acknowledgments

This dissertation would not have been possible without the help, support, and assistance in various ways from a remarkable group of individuals and organizations. First, I express my deepest gratitude to my supervisor, Prof. Dr. Hildegard Westphal, who has accepted me as her student and guided, mentored, and advised me through my doctoral degree. She dedicated tremendous energy, dedication, and patience during this challenging PhD journey. I am very grateful and honored to be your student. Thank you for all the opportunities, independence, and freedom to work that have contributed significantly to my personal and scientific development.

I would like to acknowledge the Leibniz Centre for Tropical Marine Research (ZMT), which has hosted my doctoral studies and provided the necessary infrastructure, support, research grant, and facilities to conduct my research. I am very grateful to the Ministry of Education, Culture, Research and Technology (MoECRT), Republic of Indonesia - Asian Development Bank (ADB), for awarding me with a doctoral scholarship through the Advance Knowledge and Skills for Sustainable Growth (AKSI) Project. Thanks to the Bremen International Graduate School for Marine Science (GLOMAR) for its valuable courses and training that helped improve my knowledge and skills.

My appreciation also goes to the members of the doctoral panel, Dr. Andreas Kunzmann, Dr. Sebastian Ferse, and Dr. Henry C. Wu, who have provided a lot of input and advice on my research project, especially during the difficult times of the pandemic. Dr. Marleen Stuhr and Dr. Steve Doo, I thank you for offering ideas, insights, and solutions in the process of completing my research project. I gratefully acknowledge Silvia Hardenberg, José Garcia, and Nico Steinel from the ZMT Marine Experimental Ecology Facility (MAREE) for providing technical support and assistance, as well as ZMT staff Donata Monien, Matthias Birkicht, Stefanie Bröhl, Fabian Hüge, Raika Himmelsbach, Jule Mawick, Sebastian Flotow, Sonja Peters, and Constanze von Waldthausen for their excellent support in the ZMT chemistry, biology, and geology laboratories. I also extend my warmest compliments to all Carbonate Geoecology and Sedimentology Working Group members for their encouragement, feedback, and great friendship.

Heartfelt and profoundly grateful to my family for their unrivaled and continuous unconditional love, care, support, and prayers. Special gratitude goes to my dear wife, Angie Adrianie, and my sons, Keyaan Khalil and Kenaan Khalil, for their sacrifice and encouragement. I dedicate this milestone to my beloved parents (may God always bless them). Also, thanks to all my Indonesian fellows for their sincere friendship, help, and concern. Finally, I express my deep gratitude to all the examination committee members for their precious time and helpful, constructive suggestions and comments, which immensely helped improve the quality of this dissertation.

Abbreviations

A_T	total alkalinity of seawater
$[\text{CO}_2]$	dissolved carbon dioxide
$[\text{CO}_3^{-2}]$	carbonate ion concentration
$[\text{HCO}_3^-]$	bicarbonate ion concentration
$^{\circ}\text{C}$	degree Celsius
ANCOVA	analysis of covariance
ANOVA	analysis of variance
atm	atmospheres; used in microatm (μatm)
ATPase	adenosine triphosphate(ase); enzyme
Ca, Ca^{2+}	calcium, calcium ion
CaCO_3	calcium carbonate
CO_2	carbon dioxide; <i>p</i> (partial)
DIC	dissolved inorganic carbon
e.g.	<i>exempli gratia</i> in Latin; for example
g	gram(s)
<i>g</i>	force of gravity
h	hour(s)
H^+	hydrogen ion; proton
H_2O_2	hydrogen peroxide
HMC	High magnesium calcite
HNO_3	nitric acid
ICP-OES	inductively coupled plasma-optical emission spectroscopy
i.e.	<i>id est</i> in Latin; that is
IMC	intermediate magnesium calcite
IPCC	Intergovernmental Panel on Climate Change
Kg	kilogram(s)
L	liter(s)
LMC	low magnesium calcite
M	molar concentration

MANCOVA	multivariate analysis of covariance
Mg	milligram(s)
Mg, Mg ²⁺	magnesium, magnesium ion
Mg/Ca	magnesium/calcium
MgCO ₃	Magnesium calcite
mg/g	milligram/gram(s)
ml	milliliter(s)
ml/mg	milliliter(s)/milligram(s)
mmol	millimole(s)
NaOH	sodium hydroxide
O ₂	oxygen
OA	ocean acidification
OW	ocean warming
Pa	Pascal (unit of pressure)
pH _{NBS}	pH, measured on the National Bureau of Standards (NBS) scale
pH _T	pH, measured on the total scale
ppm	parts per million
PSU	practical salinity unit
rpm	revolutions per minute
s	second(s)
SEM	scanning electron microscope
SEM-HV	SEM-high voltage
SEM-SE	SEM-secondary electrons
Sr, Sr ²⁺	strontium, strontium ion
Sr/Ca	strontium/calcium
wt%	weight percent
μmol	micromole(s)
Ω	calcium carbonate saturation state of seawater
Ω _{Ar}	aragonite saturation state of the seawater
Ω _{Ca}	calcite saturation state of seawater

Chapter 1. General introduction

1.1. Global ocean change

The release of anthropogenic greenhouse gases (GHGs) emission (e.g., carbon dioxide (CO₂), methane (CH₄), nitrous oxide (N₂O), and fluorinated gases) into the atmosphere as a result of human activities has changed the physical and chemical properties of the world's oceans since the industrial revolution in the early 19th century (IPCC, 2023; Yoro & Daramola, 2020), referred to as global ocean change (Boyd et al., 2018). In particular, GHGs CO₂, CH₄, and N₂O have increased and are projected to continue growing in line with population and economic growth (Le Quéré et al., 2009). In 2019, net anthropogenic GHG emissions were reached 56 ± 6.6 gigaton CO₂ equivalent (GtCO₂-eq), which is approximately 6.5 GtCO₂-eq (12%) higher than in 2010 and 54 GtCO₂-eq (54%) higher than in 1990 (IPCC (2023); Figure 1.1). This increased emission has been primarily attributed to anthropogenic activities via fossil fuel combustion, cement production, deforestation, agricultural expansion and intensification, industrial processes, and waste management (Friedlingstein et al., 2023; IPCC, 2019, 2023; Sabine et al., 2004).

CO₂ is one of the most significant GHGs in the earth's atmosphere. During 1851-2022, the world emitted 2550 ± 260 Gt CO₂ into the atmosphere (Friedlingstein et al., 2023). CO₂ concentrations in the atmosphere have been recorded to increase linearly $\approx 47\%$ since 1850, with the accelerated rate achieving ≈ 2.2 ppm/year over the last decade (Ramonet et al., 2023). Emissions rose from mean levels of ≈ 278 ppm in 1750 (IPCC, 2021), the beginning of the industrial era, to ≈ 417.1 ppm in 2022 (Lan et al. (2023); Figure 1.3a) and is estimated to reach ≈ 419.3 ppm in 2023 (Friedlingstein et al., 2023) which is higher than in the last 800,000 years (Friedlingstein et al., 2023; IPCC, 2023; Lindsey, 2023). By the end of the year 2100, the atmospheric CO₂ concentration is estimated to range from ≈ 580 ppm (RCP4.5) to ≈ 1000 ppm (RCP8.5) (IPCC (2014); Figure 1.3b), resulting in an increase in heat trapped and re-emitted

within the earth (greenhouse effect) and generating positive radiative forcing¹ (Doney et al., 2014; Fawzy et al., 2020; Gattuso et al., 2015; IPCC, 2023).

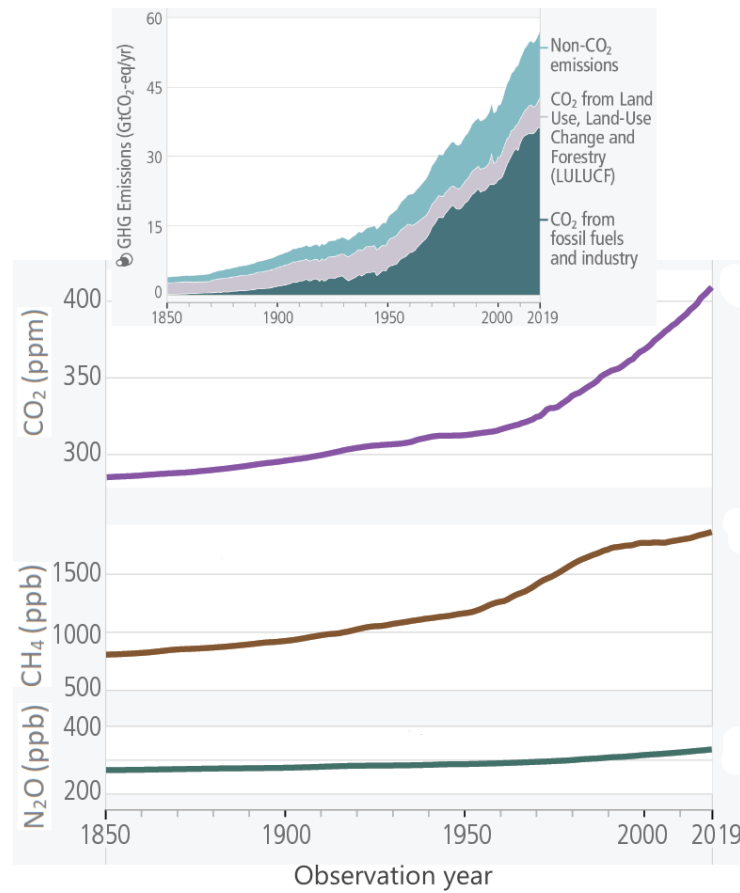


Figure 1.1. Annual-mean atmospheric main GHGs emission CO₂, CH₄, and N₂O (1850-2019), and CO₂ contributions from human anthropogenic activities (modified from IPCC (2023). GHG emissions have risen at an accelerating rate since 1850. As of 2019, the levels of CO₂, CH₄, and N₂O in the atmosphere all exceeded 410 parts per million (ppm), 1866 parts per billion (ppb), and 332 parts per billion (ppb), respectively (IPCC, 2023).

The ramifications of disturbances to the earth's heat balance may have extensive and profound impacts on the planet and its inhabitants, including increased global average temperatures,

¹ Positive radiative forcing refers to a situation where there is an increase in the amount of energy (in watts per square meter, Wm⁻²) entering the earth's atmosphere compared to the amount of energy leaving it. As simpler form, more energy from the sun is being absorbed by the earth and its atmosphere than is being radiated back to space. This imbalance leads to a net gain of energy within the earth's climate system and results in warming (Etminan et al., 2016). Positive radiative forcing is primarily driven by increasing concentration of GHGs in the atmosphere (Doney et al., 2014; Etminan et al., 2016).

changes in weather systems and climatic conditions, accelerated melting of glaciers and ice sheets, acidification (soil and ocean), intensifying extreme weather events, rising sea levels; leading to ecosystem shifts and potential extinctions, affecting agricultural-fisheries productivity and food availability, and driving migration and population displacement (Hegerl et al., 2018; Hughes, 2000; IPCC, 2019, 2022, 2023). Therefore, understanding the impacts of global change is imperative to grasp the potential effects on organisms, ecosystems, and human societies, as well as exploring potential strategies to reverse events and mitigate existing and emerging problems.

Oceans are a critical component of the earth's climate system; serve as a heat reservoir and carbon sink, by absorbing $\approx 89\%$ of atmospheric heat (Cheng et al., 2022; von Schuckmann et al., 2023) and $\approx 25\%$ of CO_2 (Gruber et al., 2023), respectively. About 61.9% of absorbed heat warms the upper 0-700 m of the ocean's water column (Cheng et al., 2021). Increasing heat in the atmosphere due to intensifying anthropogenic climate change over the past few decades leads to increasing ocean heat content (Li et al., 2023), resulting in an increase of its interior temperature and further referred to as ocean warming (OW) (Cheng et al., 2021; Cheng et al., 2022; Ruela et al., 2020). This phenomenon (i.e., OW) has permeated and dispersed into entire ocean layers, spanning from the surface to the abyssal zone (Durack et al., 2018). Since the 1970s, ocean temperatures have exhibited a linear increasing trend (NOAA (2023); Figure 1.2a), with the global sea surface temperature (SST) reaching its highest record in 2023 (SST anomaly $0.54\text{ }^\circ\text{C}$; Cheng et al. (2024)). The global average ocean temperature has risen by $\approx 1.5\text{ }^\circ\text{C}$ since 1850 and is projected to increase in the range of $3.3\text{ }^\circ\text{C}$ to $5.7\text{ }^\circ\text{C}$ by the end of 2100 relative to 1850 to 1900 under the Shared Socioeconomic Pathways (SSPs) SSP5-8.5 high CO_2 emission scenario (IPCC (2021, 2023); Figure 1.2b). Furthermore, OW has frequently been associated with an increased frequency of extreme regional warming episodes referred to as marine heatwaves (Frolicher et al., 2018), which may pose a higher risk to marine organisms and ecosystem services (Smith et al., 2023).

Meanwhile, increased atmospheric CO_2 concentrations have driven increased ocean CO_2 uptake. Ocean CO_2 sink trends have grown linearly over the past six decades, rising from about $-1.1 \pm 0.4\text{ Gt C year}^{-1}$ in the early 1960s to about $-2.8 \pm 0.4\text{ Gt C year}^{-1}$ in 2022, with a projection to reach $2.9 \pm 0.6\text{ Gt C year}^{-1}$ in 2023 (Friedlingstein et al., 2023). When CO_2 dissolves and absorbs into seawater, CO_2 reacts with seawater to form carbonic acid (H_2CO_3), which then

dissociates, resulting in a reduction of the carbonate ion (CO_3^{2-}) concentration and increases the bicarbonate ion (HCO_3^-) and hydrogen ion (H^+) concentrations (Figure 1.3c), causing a reduction in ocean pH and a profound alteration of ocean carbonate chemistry in a process described as ocean acidification (OA) (Caldeira & Wickett, 2003; Feely et al., 2004). Ocean surface seawater pH has declined about ≈ 0.1 units since the industrial era began, or -0.017 to -0.027 pH units per decade since the late 1980s, which equates to $\approx 26\%$ increase in H^+ concentration (IPCC, 2013, 2021). Furthermore, since the 1980s, there has been a reported decline in pH in the subtropical open oceans ranging from -0.016 to -0.019 pH units per decade, which is equivalent to an increase in H^+ concentration of ca $\approx 4\%$ per decade; meanwhile, the western tropical Pacific showed a slower pH decrease of -0.010 to -0.013 pH units per decade (IPCC, 2021).

Changes in the equilibrium state of the carbonate system in seawater, primarily CO_3^{2-} and HCO_3^- , resulting from increased $p\text{CO}_2$, have direct geochemical implications on the carbonate saturation state (Ω) (Doney et al., 2009). Under the IS92a scenario² in 2100, CO_3^{2-} concentration of tropical surface ocean is projected to decline $\approx 45\%$ relative to preindustrial levels, leading to a reduction in seawater Ω (Orr et al., 2005). From 1750 to 2010, the global average CO_3^{2-} declined by $\approx 16\%$ from 228 to $190 \mu\text{mol kg}^{-1}$ (Jiang et al., 2023). Based on dissolution kinetics, the reduction in seawater Ω (particularly aragonite Ω_{arag} and calcite Ω_{calc}) is assumed to affect the formation and dissolution rate of calcium carbonate (CaCO_3) (Feely et al., 2004; Orr et al., 2005), which is the chemical compound precipitated by most marine organisms for their shells or skeletons.

² The IS92a scenario was one of several emission scenarios developed in the early 1990s by the IPCC to explore different possible pathways of future GHGs emissions. These scenarios were part of the IPCC's Second Assessment Report (SAR) published in 1995. The IS92a scenario falls under the so-called "business-as-usual" category, representing a future with relatively high GHGs emissions if no specific policies or actions are taken to mitigate climate change. The scenario assumes a continuation of historical trends and does not incorporate significant efforts to reduce emissions or address climate change (IPCC, 1996).

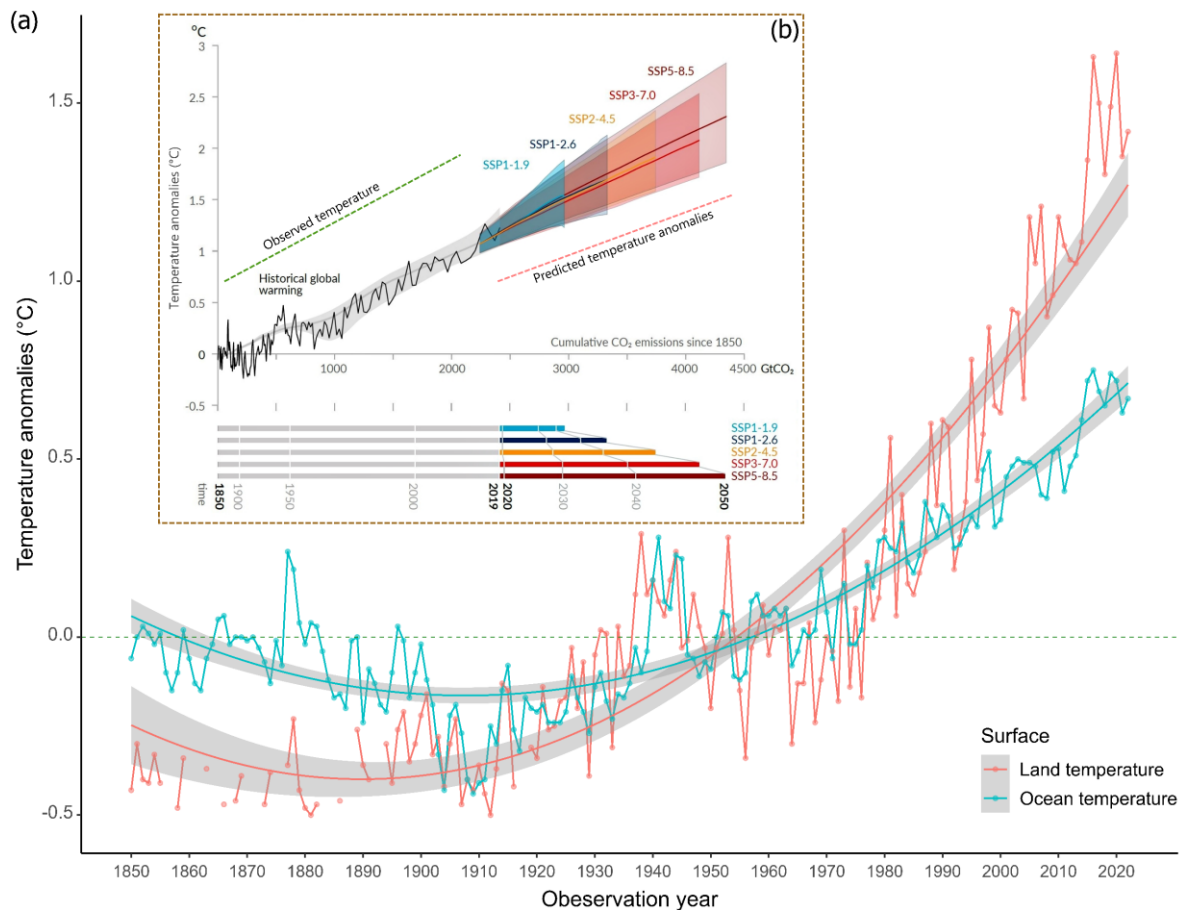


Figure 1.2. Historical and projection of global surface temperature. (a). The annual mean of earth's surface temperature anomalies from 1850 to 2022. The trends of land and ocean surface temperature anomalies are 0.09 °C/decade and 0.04 °C/decade, respectively. Datasets were extracted from NOAA (2023), (b). Cumulative temperature (1850-2019) and projected temperature (2020-2050) of the earth's surface based on GHG CO₂ emissions (modified from IPCC (2021)). The projected temperatures are modeled using cumulative CO₂ emissions under the IPCC-SSPs scenario.

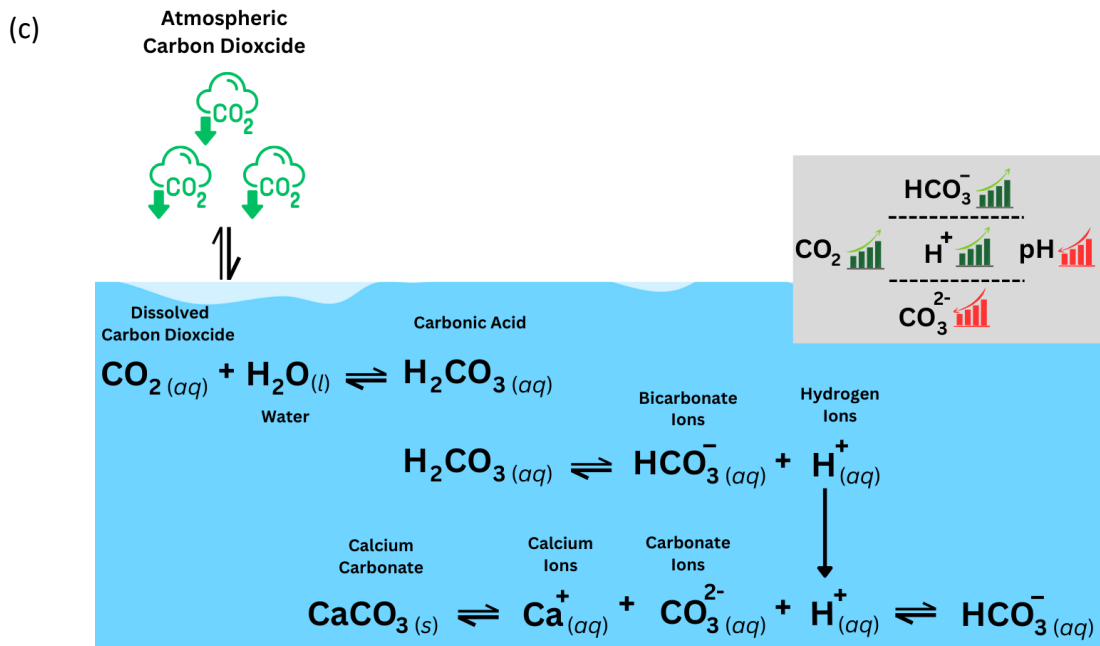
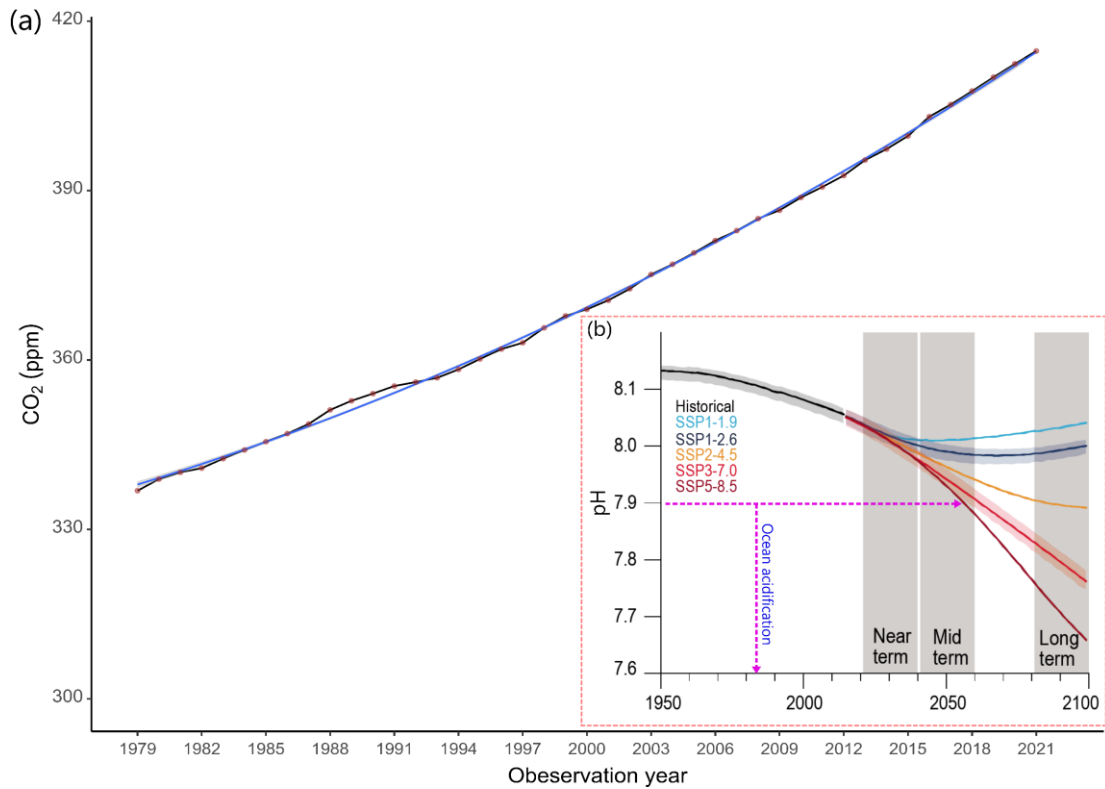


Figure 1.3. Historical and projection of the global surface CO₂-pH trend and the potential for ocean acidification. (a) observed and current global atmospheric CO₂ concentration trend. Datasets were extracted from (Lan et al., 2023), (b) the cumulative ocean pH (1950-2019), and the projected surface ocean pH (2020-2010) based on the GHG CO₂ emissions (modified from IPCC (2021)). The projected surface ocean pH is modeled using cumulative CO₂ emissions under the IPCC-SSPs scenario, (c) schematic diagram of the ocean acidification processes.

1.2. Effect of ocean acidification and ocean warming on marine organisms

Global ocean change is causing significant environmental changes that potentially pose major challenges for marine organisms. Physicochemical changes in the ocean, by rising temperatures and acidification, can directly or indirectly alter several biochemical responses in marine organisms, which cascade at the molecular, individual, population, community, and ecosystem levels, including their adaptive capacity (Brierley & Kingsford, 2009; Doney et al., 2012; Poloczanska et al., 2013). Obtaining insight into the current responses of marine organisms to environmental stressors, together with their adaptive potential to future environmental scenarios, is crucial for predicting the consequences of persistent global change on populations, communities, and ecosystems. Over the past decade, the effects of single and multi-stressors on marine organisms have been extensively studied using various approaches both in the laboratory and in the natural environment at different scales, magnitudes, and durations across a wide range of taxa including cnidaria, crustaceans, mollusks, echinoderms, and marine plants (Bednaršek et al., 2021; Harvey et al., 2013; Hu et al., 2022; Ji & Gao, 2021; Leung et al., 2022; Medeiros & Souza, 2023; Przeslawski et al., 2015; Thomas et al., 2020). The response of organisms to stressors is variable, typically affecting biological performance (e.g., behavior, metabolism, foraging, competitive capability, growth, and reproduction), fitness, and skeletal mineralogy (Gao et al., 2020; Nagelkerken & Munday, 2016). Additionally, the intensity and conditions of stressors have species-specific effects (Kroeker et al., 2013), leading to vastly variable and complex responses in marine organisms depending on taxa (Harvey et al., 2013), stressor exposure, and organismal adaptive potential (Heugens et al., 2001; Parker et al., 1999; Vargas et al., 2017), and biological complexity³ (Harvey et al., 2014), thus making it difficult to accurately predict outcomes for specific species or even ecosystem.

Temperature plays a crucial role in the biological functions and shaping the physiological mechanisms of marine organisms, impacting from embryonic development and biochemical performance to species distribution (Arroyo et al., 2022; Knapp & Huang, 2022; Peck et al., 2009; Sunday et al., 2012). A modest change in temperature can have a significant consequence on the stability, flexibility, and structure of molecules involved in biological processes (Miller & Stillman, 2012; Slein et al., 2023; Somero, 2002). E.g., the structure of enzymes, which are

³ Biological complexity refers to the complex organization and interplay between organisms across different levels of biological organization, including molecular, cellular, organ, organism, population, community, and ecosystem levels. It includes the diversity of life forms, their structural and functional features, and the dynamic mechanisms that regulate their behavior, development, and interactions with the environment (Adami, 2009).

critical for numerous biochemical reactions in echinoderms, may be altered by changes in temperature (Lawrence, 1985); hence, it could affect catalytic activity and efficiency, potentially impairing processes of digestion and metabolism (Klinger et al., 1997; Schulte, 2015). In addition, the thermal sensitivity of structural proteins in echinoderms, particularly involved in skeleton formation (Killian & Wilt, 2008; Livingston et al., 2006; Matranga et al., 2013), could be affected by increased temperature (Dubois, 2014; Magdalena et al., 2012; Zhan et al., 2019) and therefore have implications on the skeletal development and integrity, which are vital for their survival and ecological role in marine ecosystems. Furthermore, elevated temperature (OW) beyond thermal tolerance thresholds leads to rapid deterioration in bio-physiological functions, compromising the biological performances and survivability of marine organisms (see reviews Lang et al. (2023); Nguyen et al. (2011); Smith et al. (2023)). OW has contributed to mass mortality events (Garrabou et al., 2022), altered organism distribution (Lonhart et al., 2019) and migration (Langan et al., 2021), increased incidence of infectious disease outbreaks (Tracy et al., 2019), hypoxia (Earhart et al., 2022), coral bleaching (McManus et al., 2020; Suggett & Smith, 2020), disrupted reproductive biology (Alix et al., 2020), changes in food webs and trophic dynamics (du Pontavice et al., 2020; Maureaud et al., 2017), increased invasive species dispersion (Occhipinti-Ambrogi, 2007), and altered behavior of marine organisms (Joyce et al., 2022).

OA is a stressor that also potentially affects marine organisms and ecosystem functions. The decreased pH and changes in the seawater carbonate system due to elevated concentrations of CO₂ can potentially lead to bioecological implications, affecting a wide range of marine life, including mollusks, corals, pteropods, foraminifera, echinoderm, and other calcifying organisms (Fabry et al., 2008; Kroeker et al., 2010). Related to this context, marine calcareous organisms have a unique susceptibility because of the calcification processes are expected to be hindered by decreased seawater pH (Cyronak et al., 2016), which is essential for forming and preserving calcium carbonate (CaCO₃) skeleton structures, including shells, endoskeletons, and exoskeletons (Orr et al., 2005). Additionally, OA may lead to acidosis⁴, which in turn can disrupt numerous critical physiological processes, including aerobic metabolism (Pörtner, 2008). It can impact the growth, development, abundance, reproduction, settlement, metabolism, sensory functions, and survival of marine organisms, with numerous species being

⁴ Acidosis refers to a physiological condition where there is an imbalance in the internal pH levels of organisms, typically caused by increased acidity in the surrounding seawater due to OA (Melzner et al., 2009).

more vulnerable in their early life stages (Ashur et al., 2017; Hendriks et al., 2010; Kroeker et al., 2010; Przeslawski et al., 2015; Ross et al., 2011). However, the effects of OA are not uniform across taxa and location, and the rate at which it occurs is a determining factor in the extent to which calcifying organisms will be able to adapt (Wittmann & Pörtner, 2013).

In addition to altering the bio-physiological performance of organisms, in some studies, OW and OA (as sole or combined factors) have been found to significantly affect the skeletal microstructure and integrity of calcareous species, i.e., biomineralization (Byrne & Fitzner, 2019; Figuerola et al., 2021). However, other studies observed that effects are highly specific to the taxonomic group, with some showing negative responses, some positive responses, and others remaining unaffected (Byrne et al., 2014; Fabricius et al., 2011; Hofmann & Bischof, 2014; Iglesias-Rodriguez et al., 2008; Ries et al., 2009). This variability in response appears to be intricately linked to the biological formation system of the calcareous skeleton or shell, as well as the delicate balance between calcification (production and deposition of CaCO_3) and dissolution (CaCO_3 dissociates and incorporated into a solution) processes (Clark, 2020). Calcification has been used as a proxy to evaluate the direct effects of CO_2 alteration on various taxa since OA is recognized to increase the vulnerability of CaCO_3 shell or skeleton-building organisms to biomineralization processes and promote dissolution (Levin et al., 2015). The impacts on the calcification rates of calcifying organisms by OA are attributable to decreases in pH (i.e., increasing proton concentrations, $[\text{H}^+]$) and saturation state (Ω) (Cyronak et al., 2016). Decreases in pH might affect calcification in two fashions: directly, by decreasing concentrations and rates of CO_3^{2-} formation within the extracellular calcifying medium (ECM), and indirectly, by altering the metabolism (Erez et al., 2011).

Among marine invertebrates, various taxa precipitate different forms of CaCO_3 (polymorphs) with different solubilities, thus, potentially different sensitivities to OA and OW (Adkins et al., 2021; Andersson et al., 2008). The CaCO_3 skeleton consists of one or a combination of calcite with subgroup low Mg calcite (LMC) and high Mg calcite (HMC) (Long et al., 2014), aragonite, and the rare mineral vaterite (Skinner & Ehrlich, 2014). No chemical boundary clearly separates pure calcite from MgCO_3 . In general, pure calcite is categorized as a crystalline form of CaCO_3 that is composed solely of calcite minerals without any significant impurities or other mineral phases, and it contains 56.03% CaO and 43.97% CO_2 (Haldar, 2020). Further, calcites with >4 wt% (4 wt% ~ 10 mol%) MgCO_3 are conventionally defined as HMC (Chave, 1962; Ries et al.,

2009; Stanley et al., 2002; Tucker & Wright, 1990), although this boundaries is not universally acknowledged, e.g., Smith et al. (2006) divides MgCO_3 into three groups: LMC (0 wt% to 4 wt% MgCO_3), intermediate Mg calcite (IMC; 4 wt% to 8 wt% MgCO_3), and HMC (>8 wt% MgCO_3), while Andersson and Mackenzie (2011) recommends a threshold between IMC and HMC is 12 wt% MgCO_3 . Mineral solubility in seawater varies, with vaterite being the most thermodynamically unstable and having highest solubility among CaCO_3 polymorphs (Addadi et al., 2003), Mg-calcite being the most soluble than aragonite and pure calcite, and aragonite being more soluble than pure calcite (Andersson et al., 2008; Morse et al., 2006; Raz et al., 2000; Walter, 1984). The solubility of calcite increases with increasing Mg content (Davis et al., 2000). This could lead shells or skeletons with high Mg calcite (e.g., bryozoans, echinoderms, calcareous red algae, and some foraminifera) to become more soluble, thus rendering those marine organisms with such mineral phases more susceptible to OA (Figuerola et al., 2021; Lebrato et al., 2016). Furthermore, increased ocean temperatures (OW) were found to exacerbate the effects of OA in species with Mg-calcite or aragonite shells or skeletons, as the Mg content in calcite typically enhanced with increased seawater temperature (Burton & Walter, 1987; Mucci, 1987; Oomori et al., 1987), therefore, potentially increasing the solubility of the skeleton with temperature. In addition, such conditions are also found in aragonite crystal-producing organisms (e.g., corals, mollusks, pteropods, and most extant fish species), in which reduced pH and aragonite saturation state (Ω_{ar}) due to OA decreases the rate of aragonite precipitation in CaCO_3 skeleton structure (Byrne & Fitzner, 2019; Cohen & Holcomb, 2009; Gazeau et al., 2013).

Although OW and OA have first been studied as distinct stressors on marine organisms, recent studies have demonstrated that their interactions lead to non-linear and synergistic effects (Table 1.1) due to complex interactions between physiological, ecological, and biogeochemical processes (Boyd & Hutchins, 2012; Gao et al., 2020; Gruber, 2011) through additive effects (combined stressor effects equal the sum of stressor's individual effects; no additional stress), antagonistic effects (one stressor offsets the effect of the other; decreased stress), and synergistic effects (the interplay of stressors results in a combined effect that is greater than the sum of their individual effects; amplified stress) (Folt et al., 1999; Todgham & Stillman, 2013; Figure 1.4). Ultimately, the sensitivity of marine organisms to OA and OW correlates with

life stage, mobility, acclimatization and adaptation⁵, thermal windows of species, habitat and ecological niche, genetic diversity, trophic interactions, and geographic location (Andersson et al., 2015; Breitbart et al., 2015; Byrne & Przeslawski, 2013; Donelson et al., 2019; Harvey et al., 2013; Hillebrand et al., 2018; Hu et al., 2024; Przeslawski et al., 2015; Wittmann & Pörtner, 2013).

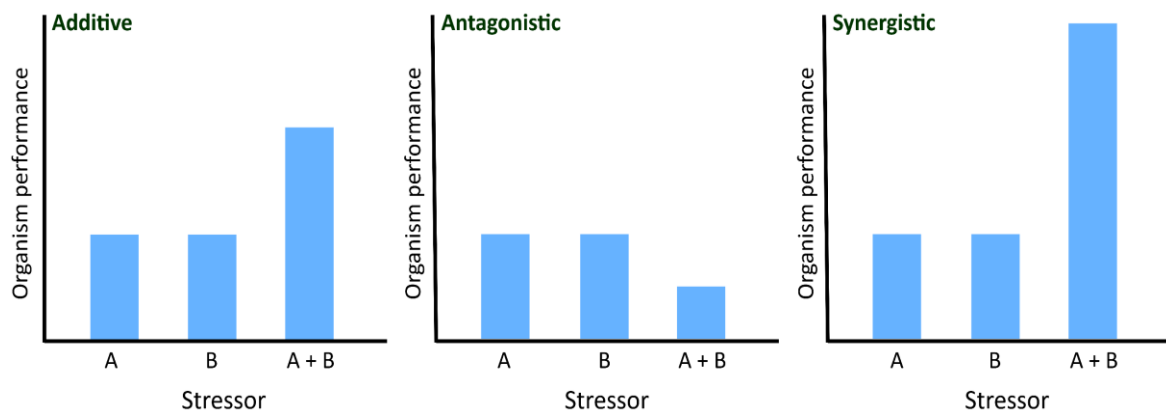


Figure 1.4. Conceptual approach of stressor interactive effects on organismal performance. Multiple stressors may independently affect performance (additive interactive effect), interact to decrease performance (antagonistic interactive effect), or interact to increase performance (synergistic interactive effect) in a non-linear and unpredictable manner (modified from Todgham and Stillman (2013)).

⁵ Acclimatization refers to physio-biochemical modifications or controlled phenotypic responses by an individual organism to multiple simultaneous stressors in the natural environment at a specific timeframe. Acclimatization serves to enhance the fitness and life performance of organisms in the environment and is a prerequisite for the adaptation process. Acclimatization chronic changes are reversible. Adaptation refers to the process whereby an organism undergoes a physical, behavioral, biochemical, or physiological modification in order to better acclimate to its environment, enhancing the ability to withstand, reproduce, and evolve, which usually proceeds very slowly. Adaptation may involve genetic modification when adverse environments endure over multiple generations of a species (Hill et al., 2012; Randall et al., 1997; Willmer et al., 2004).

Table 1.1. Studies on the impacts of ocean acidification and ocean warming as combined stressors (OW*OA) on marine invertebrates. The studies involved factorial experimental design, level of OA (pH/ $p\text{CO}_2$), and OW (Temperature, °C). This study contains only descriptive statistics. OA*OW refers to the effects of combined stressors, which are statistically significant ($p < 0.05$). The pH levels are listed as published on the total scale (pH_T^a), NBS scale (pH_{NBS}^b), or no scale (pH^c) if not indicated. $p\text{CO}_2$ levels ($\mu\text{atm/ppm}$) indicated next to pH. Abbreviations, OA: ocean acidification; OW: ocean warming; OA*OW: ocean acidification + ocean warming (combined stressor effect); NS: not specified.

Taxon	Species (life stage)	pH/ $p\text{CO}_2$ level	Temperature level	Exposure duration	Interactive effect of ocean acidification and ocean warming	References
Starfish	<i>Aquilonastra yairi</i> (adult)	8.00 ^a /455 μatm , 7.74 ^a /1052 μatm , 7.47 ^a /2066 μatm	27 °C, 32 °C	90 days	OA*OW altered Ca-ATPase and Mg-ATPase activities	Khalil et al. (2024c)
Starfish	<i>Aquilonastra yairi</i> (adult)	8.00 ^a /455 μatm , 7.74 ^a /1052 μatm , 7.47 ^a /2066 μatm	27 °C, 32 °C	90 days	OA*OW increased metabolic rates, 32 °C : 2066 μatm generated a stable-low calcification rate	Khalil et al. (2023)
Starfish	<i>Aquilonastra yairi</i> (adult)	8.00 ^a /455 μatm , 7.74 ^a /1052 μatm , 7.47 ^a /2066 μatm	27 °C, 32 °C	90 days	OA*OW altered skeletal Mg/Ca ratio and degraded skeleton structures	Khalil et al. (2022)
Starfish	<i>Asterias rubens</i> (adult)	8.1 ^b /400 ppm, 7.9 ^b /760 ppm	20 °C, 24 °C	70 days	OA*OW reduced growth rate and calcified mass	Keppel et al. (2014)
Starfish	<i>Parvulastra exigua</i> (adult)	8.2 ^b /356-366 ppm, 7.8 ^b /1022-1075 ppm,	18 °C, 21 °C, 24 °C	1 day	OA*OW increased O ₂ consumption	McElroy et al. (2012)

		7.6 ^b /1679–1778 ppm				
Starfish	<i>Pisaster ochraceus</i> (juvenile)	7.9 ^b /380 μ atm, 7.8 ^b /780 μ atm	12 °C, 15 °C	70 days	OA*OW increased the feeding rate and reduced the calcified material	Gooding et al. (2009)
crown-of-thorns starfish	<i>Acanthaster spp.</i> (larvae)	8.01 ^b /548.4 μ atm, 8.00 ^b /555.2 μ atm, 7.74 ^b /989.2 μ atm, 7.72 ^b /1022.7 μ atm	Ambient, +2°C	21 days	OA*OW delayed larvae development	Hue et al. (2022)
Mussel	<i>Mytilus coruscus</i> (adult)	8.1 ^b , 7.8 ^b , 7.4 ^b	23 °C, 28 °C	28 days	OA*OW reduced clearance rates, oxygen consumption rates, ammonia excretion rates, oxygen-to-nitrogen (O:N) ratios, ATP content, and pyruvate kinase activities	Tang et al. (2022)
Pteropods	<i>Limacina spp.</i> (juvenile)	8.0 ^a /400 μ atm, 7.9 ^a /750 μ atm, 7.7 ^a /1100 μ atm	3.5 °C, 5.5 °C	7 days	OA*OW reduced PUFA compound	Lischka et al. (2022)
Pteropod (Antarctic)	<i>Limacina helicina antarctica</i> (adult)	8.2 ^a / 264 μ atm, 7.95 ^a /500 μ atm, 7.7 ^a /920 μ atm	-0.8 °C, 4 °C	16 days	OA*OW increased metabolic rate	Hoshijima et al. (2017)
Giant clam	<i>Tridacna squamosa</i> (juvenile)	8.1 ^b /450 μ atm, 7.8 ^b / 950 μ atm	28.5 °C, 30.5 °C	60 days	OA*OW increased interindividual variation in mineral concentrations and reduced shell nitrogen content	Armstrong et al. (2022)

Foraminifera	<i>Amphistegina lobifera</i> (adult)	8.16 ^b /492 ppm, 7.97 ^b /963 ppm, 7.50 ^b /3182 ppm	28 °C, 31 °C	2 months	OA*OW reduced foraminifera pore sizes, putative decreases in test stability, and increased microenvironmental pH gradients	Stuhr et al. (2021)
Coral	<i>Pocillopora damicornis</i> (adult)	8.1 ^a /400 ppm, 7.9 ^a /1000 ppm, 7.5 ^a /2800 ppm	28 °C, 31 °C	8 weeks	OA*OW decreased $\delta^{11}\text{B}$, $[\text{CO}_3^{2-}]_{\text{cf}}$, Ω_{cf} , and DIC_{cf}	Guillermic et al. (2021)
Coral	<i>Stylophora pistillata</i> (adult)	8.1 ^a /400 ppm, 7.9 ^a /1000 ppm, 7.5 ^a /2800 ppm	28 °C, 31 °C	8 weeks	OA*OW decreased $\delta^{11}\text{B}$, $[\text{CO}_3^{2-}]_{\text{cf}}$, Ω_{cf} , and DIC_{cf}	Guillermic et al. (2021)
Coral	<i>Acropora hyacinthus</i> (adult)	8.00 ^a /410 μatm , 7.85 ^a /652 μatm , 7.71 ^a /934 μatm	26 °C, 28.5 °C, 31 °C	12 weeks	OA*OW increased dark respiration rate and calcification rate	Anderson et al. (2019)
Coral	<i>Pocillopora damicornis</i> (larvae)	8.0 ^a /500 μatm , 7.7 ^a /1100 μatm	29 °C, 30.8 °C	21 days	OA*OW decreased photochemical efficiency (F_v/F_m) and budding rate	Jiang et al. (2017)
Sponge	<i>Spherospongia vesparium</i> (adult)	8.1 ^a , 7.7 ^a	26 °C, 32 °C	6 days	OA* OW interfered with the sponge microbiome; combined OA and OW permanently destabilized the structure and function of the sponge microbial community	Chai et al. (2024)
Sea urchin	<i>Echinometra lucunter</i> (Embryo-larvae)	8.2 ^c , 7.5 ^c	26 °C, 28 °C	NS	OA*OW decreased embryo-larval development	Caetano et al. (2021)

Sea urchin	<i>Echinometra lucunter</i> (larvae)	8.0 ^b , 7.7 ^b , 7.4 ^b	26 °C, 28 °C, 30 °C, 34 °C, 38 °C	3 months	OA*OW decreased the pluteus larvae development rate	Pereira et al. (2020)
Sea urchin	<i>Loxechinus albus</i> (juvenile)	7.7 ^b /500 µatm, 7.4 ^b /1400 µatm	15 °C, 20 °C	30 days	OA*OW increased <i>HSP70</i> transcription level	Manriquez et al. (2019)
Sea urchin	<i>Lytechinus variegatus</i> (larvae)	8.1 ^b , 7.8 ^b	28 °C, 31 °C	13 days	OA*OW reduced body length and rod length; increased asymmetrical rod form	Lenz et al. (2019)
Sea urchin	<i>Paracentrotus lividus</i> (adult)	7.9 ^a /634 µatm, 7.7 ^a /990 µatm, 7.4 ^a /1756 µatm	17 °C, 21 °C	81 days	OA*OW reduced growth	Cohen-Rengifo et al. (2019)
Sea urchin	<i>Tripneustes gratilla</i> (juvenile-adult)	8.1 ^b , 7.8 ^b , 7.6 ^b	22 °C, 25 °C, 28 °C	146 days	OA*OW reduced gonad index	Dworjanyn and Byrne (2018)
Sea urchin	<i>Loxechinus albus</i> (juvenile)	7.8 ^a /400 µatm, 7.6 ^a /1200 µatm	16 °C, 19 °C	7 months	OA*OW fasted foraging speed (horizontal)	Manriquez et al. (2017)
Sea urchin (Antarctic)	<i>Sterechinus neumayeri</i> (adult)	8.0 ^b /419 µatm, 7.7 ^b /834 µatm, 7.5 ^b /1361 µatm	-0.3 °C, 1.9 °C, 2.2 °C	40 months	OA*OW reduced energy consumed and energy absorbed from food	Morley et al. (2016)
Sea urchin	<i>Paracentrotus lividus</i> (larvae)	8.1 ^b /310 µatm, 7.7 ^b /895 µatm, 7.4 ^b /1862 µatm	19 °C, 20.5 °C, 22.5 °C	30 days	OA*OW increased mortality rate, shorted body, and arm length	Garcia et al. (2015)

Gastropod	<i>Austrocochlea concamerata</i> (adult)	8.1 ^b /400 ppm, 7.8 ^b /940 ppm	21 °C, 24 °C	8 weeks	OA*OW reduced assimilation efficiency, absorption rate, the scope for growth (energy budget), and shell weight (strength); increased respiration rate	Leung et al. (2020)
Gastropod	<i>Tritia reticulata</i> (veliger)	8.1 ^b , 7.9 ^b	18 °C, 20 °C, 22 °C	14 days	OA*OW increased larval mortality; slowed swimming activities	Fonseca et al. (2020)
Gastropod	<i>Dicathais orbita</i> (adult)	380 ppm, 750 ppm	23 °C, 25 °C	35 days	OA*OW reduced PUFAs concentration	Valles-Regino et al. (2015)
Gastropod	<i>Tegula atra</i> (Adult)	7.9 ^b /500 µatm, 7.5 ^b /1600 µatm	12 °C, 20 °C	60 days	OA*OW exhibited an antagonistic interactive effect; when the pCO ₂ level was increased, the positive effect of OW on oxygen uptake decreased	Benitez et al. (2024)
Mussel	<i>Mytilus edulis</i> (adult)	8.0 ^b /380 ppm, 7.8 ^b /1000 ppm	17 °C, 20 °C	8 weeks	OA*OW reduced mussel body volume, shell width and length	Knights et al. (2020)
Mussel	<i>Mytilus edulis</i> (adult)	8.1 ^b , 7.8 ^b	19 °C, 22 °C, 25 °C	2 months	OA*OW reduced calcification rate and Ca/Mg ratio	Li et al. (2015)
Mussel	<i>Mytilus coruscus</i> (adult)	8.1 ^b , 7.7 ^b	20 °C, 30 °C	30 days	OA*OW reduced digestive enzyme activities	Khan et al. (2020)
Mussel	<i>Mytilus galloprovincialis</i> (adult)	8.0 ^c , 7.65 ^c	16 °C, 21 °C	22 days	OA*OW reduced condition index, growth rate and organic matter; increased respiration rate	Gestoso et al. (2016)

Mussel	<i>Mytilus edulis</i> (adult)	380 μ atm, 550 μ atm, 750 μ atm, 1000 μ atm	12 °C, 14 °C	9 months	OA*OW reduced the aragonite/calcite ratio and shell thickness	Fitzer et al. (2015)
Copepod	<i>Acartia tonsa</i> (adult)	500 μ atm, 1000 μ atm, 1500 μ atm, 2000 μ atm, 2500 μ atm, 3000 μ atm	13 °C, 19 °C	26 days	OA*OW increased the developmental rate and produced an antagonistic effect on instantaneous mortality rates.	Garzke et al. (2020)
Sea hares	<i>Stylocheilus striatus</i> (adult)	8.10 ^b , 7.85 ^b , 7.65 ^b	28 °C, 31 °C	2 weeks	OA*OW increased the time to foraging choice and metabolic rate; reduced foraging choice and locomotion speed	Horwitz et al. (2020)
Oyster	<i>Magallana gigas</i> (adult)	7.8 ^b /400 ppm, 7.7 ^b /750 ppm, 7.6 ^b /1000 ppm	16.8 °C, 20 °C	12 weeks	OA*OW reduced protein, lipid, carbohydrate, and caloric content; increased accumulation of copper	Lemasson et al. (2019)
Oyster	<i>Ostrea edulis</i> (adult)	8.0 ^b /400 ppm, 7.8 ^b /750 ppm, 7.7 ^b /1000 ppm	16.8 °C, 20 °C	12 weeks	OA*OW reduced lipid content	Lemasson et al. (2019)
Lobster	<i>Homarus americanus</i> (adult)	8.1 ^b /47 Pa, 7.1 ^b /948 Pa	16 °C, 20 °C	16 days	OA*OW reduced hemolymph pH; increased hemolymph $p\text{CO}_2$ (Pa), HCO_3^- , and ammonia concentration; increased oxygen consumption and ammonia excretion; reduced citrate synthase enzyme activities	Klymasz-Swartz et al. (2019)

Scallop	<i>Pecten maximus</i> (adult)	8.05 ^b /362 ppm, 8.09 ^b /454 ppm, 7.82 ^b /860 ppm, 7.85 ^b /946 ppm, 7.41 ^b /2639 ppm, 7.42 ^b /2750 ppm	9.0 °C, 12 °C	74 days	OA*OW increased condition factor (Fulton's <i>K</i>)	Cameron et al. (2019)
Scallop	<i>Argopecten irradians</i> (juvenile)	7.9 ^a , 7.2 ^a	24 °C, 31 °C	4 weeks	OA*OW reduced survival rate	Stevens and Gobler (2018)
Scallop	<i>Argopecten purpuratus</i> (juvenile)	8.0 ^b /400 µatm, 7.7 ^b /1000 µatm	14 °C, 18 °C	18 days	OA*OW increased ingestion rate,	Lardies et al. (2017)
Clams	<i>Mercenaria mercenaria</i> (juvenile)	7.9 ^a , 7.2 ^a	24 °C, 31 °C	4 weeks	OA*OW reduced respiration rate and growth rate; Increased survival rate	Stevens and Gobler (2018)
Cockle	<i>Cerastoderma edule</i> (adult)	8.2 ^b /335 µatm, 8.11 ^b /325 µatm, 7.82 ^b /870 µatm, 7.75 ^b /746 µatm	15 °C, 18 °C	50 days	OA*OW reduced condition index	Ong et al. (2017)
Seahorses	<i>Hippocampus guttulatus</i> (adult)	8.0 ^a /400 µatm, 7.5 ^a /1400 µatm	18 °C, 26 °C, 30 °C	NS	OA*OW increased respiration and ventilation rate; reduced swinging behavior	Faleiro et al. (2015)
Brittle star	<i>Microphiopholis gracillima</i> (adult)	8.1 ^b /177 µatm, 7.8 ^b /420 µatm, 7.6 ^b /713 µatm	25 °C, 28 °C, 32 °C	6 weeks	OA*OW increased respiration rate and increased mortality	Christensen et al. (2017)

Brittle star	<i>Hemipholis cordifera</i> (adult)	8.1 ^b /177 μatm , 7.8 ^b /420 μatm , 7.6 ^b /713 μatm	25 °C, 28 °C, 32 °C	6 weeks	OA*OW increased respiration rate and increased mortality	Christensen et al. (2017)
Brittle star	<i>Ophionereis schayeri</i> (adult)	8.0 ^b /327 μatm , 7.7 ^b /1080 μatm , 7.3 ^b /2316 μatm ,	19 °C, 25 °C,	5 weeks	OA*OW increased O ₂ uptake	Christensen et al. (2011)
Brittle star (Arctic)	<i>Ophiecten sericeum</i> (adult)	8.3 ^b /265 μatm , 7.7 ^b /733 μatm , 7.3 ^b /1836 μatm ,	5 °C, 8.5 °C	20 days	OA*OW reduced arm regeneration and differentiation (functional recovery)	Wood et al. (2011)
Brittle star	<i>Ophiura ophiura</i> (adult)	8.0 ^b /573 μatm , 7.7 ^b /1341 μatm , 7.3 ^b /2411 μatm ,	10.5 °C, 15 °C	40 days	OA*OW increased O ₂ uptake rate	Wood et al. (2010)

1.3. The adaptive potential of marine organisms to global ocean change

The adaptive capacity is the potential of individual species or population(s) to respond, tolerate, or adapt to climate change through various ecophysiological mechanisms (Dawson et al., 2011), which are influenced by the ecosystem's capacities, community-population structures and Interspecies connectivity (Bernhardt & Leslie, 2013; Côté & Darling, 2010). Marine organisms under changing environments are predicted to experience various combinations of phenotypic plasticity⁶ (i.e., behavioral, morphological, and physiological) through acclimatization, phenological shift⁷, biogeographical movement, and/or genetically based adaptation or microevolution to altered environments (i.e., OA and OW); species unable to rapidly perform these adaptive responses could face potential extinction (Donelson et al., 2019; Fuller et al., 2010; Hoffmann & Sgro, 2011; Kelly et al., 2013; Ross et al., 2023; Somero, 2010; Staudinger et al., 2013; Sydeman & Bograd, 2009).

Acclimatization facilitates an adaptive response to a changing environment within the lifetime of an individual organism. This process depends on phenotypic plasticity, where physiological, morphological, and behavioral changes induced by environmental conditions generate a phenotypic spectrum from single genotypes (Chown et al., 2010; Donelson et al., 2019; Kelly, 2019). Consequently, phenotypic plasticity serves as a potential short-term resilience mechanism against stressors associated with climate change, with the potential for further propagation through transgenerational transmission, involving stressor-induced epigenetic effects (Donelson et al., 2018; Lee et al., 2020; McCaw et al., 2020). However, it requires trade-offs between these pathways and energy, where excessive energy is needed, causing less energy to be devoted to other bio-physiological processes and functions (Kelly et al., 2013; Sokolova et al., 2012). On the other side, long-term adaptive processes are preceded by modifications in the genetic material of the organism through evolution (Kelley et al., 2016).

The initial adaptive response through phenotypic plasticity of marine species to changing environmental conditions is characterized by behavioral adjustments directly derived from the

⁶ Phenotypic plasticity is the intrinsic capability of a marine organism and its genotype to generate multiple phenotypes (the anatomical or morphological attributes exhibited by an organism) and modulate their behavioral or physiological responses in the presence of diverse environmental conditions (Pigliucci et al., 2006). Plasticity may manifest as adaptive, wherein the organism demonstrates persistence in a novel environment, or as nonadaptive, signifying a departure from the optimal state (Ghalambor et al., 2007).

⁷ Phenological shift is temporal adjustments observed in the occurrence of biological events or phases in the life cycles of organisms (e.g., molting, migration, and reproduction), a phenomenon attributed to fluctuations in climatic conditions or habitat-related factors (Lieth, 1974; Thackeray et al., 2016).

regulation of physiological and biochemical processes that allow organisms to withstand adverse environmental stressors, ensuring the maintenance of fitness and population success (Wong & Candolin, 2015). Furthermore, behavioral changes have been proposed as an important biomarker⁸ to determine the existence of potentially significant bioeffects of natural or anthropogenic pollution in the marine environment (Galloway et al., 2004). In recent years, an increasing number of studies have indicated that behavioral change could play an essential role in allowing marine organisms to cope with the environmental changes induced by OA-OW and help explain why certain species are able to survive or even thrive, while others falter (Beaugrand & Kirby, 2018; Briffa et al., 2012; Clements & Hunt, 2015; Nagelkerken & Munday, 2016; Padilla & Savedo, 2013).

Morphological modifications of marine organisms, defined as the adjustment of physical (phenotypic) characteristics to changing environmental conditions, have been identified as adaptive mechanisms in response to climate change (Hellberg et al., 2001; Munday et al., 2013). These alterations can manifest rapidly as short-term responses (acclimation/acclimatization) as a trade-off pathway to mitigate the adverse impact of stressors on other physiological factors within an ecosystem/niche or develop gradually over an extended timeframe, constituting an adaptation process (Chan et al., 2011; Ross et al., 2023). For instance, in ectothermic⁹ species, morphological acclimatization is evident in changes such as altered body size (Gardner et al., 2011; Kaustuv et al., 2001), coloration (Kronstadt et al., 2013), structural modifications in the shells and exoskeletons (Todd, 2008), or dormancy (Chevin & Hoffmann, 2017). These adjustments often contribute to thermal biology and energetic regulation, enabling organisms to better cope with temperature fluctuations and maintain optimal physiological functions.

Physiological phenotypic plasticity in marine organisms in response to global ocean change refers to their ability to adapt and modify physiological traits to cope with unfavorable and changing environmental conditions. This plasticity allows them to maintain essential functions

⁸ Biomarker is a functional measure of stressor exposure manifested at the sub-organismal (biochemical and cellular), physiological, or behavioral level and impacts occurring at higher levels of the biological organization, e.g., population level (Mouneyrac & Amiard-Triquet, 2013).

⁹ Ectothermic, so-called cold-blooded animal, is an animal that acquires its body heat primarily from its surroundings environment, e.g., most invertebrates, fish, amphibians, and reptiles (Schulte, 2011).

such as metabolism, thermoregulation¹⁰, and reproduction (Morley et al., 2019). The ability of marine organisms to demonstrate adaptive phenotypic plasticity manifests itself through complex mechanisms spanning across multiple physiological levels and systems, including various adjustments on molecular, cellular, tissue, and organismal levels to mitigate and respond to changes in their environment (Evans & Hofmann, 2012; Seebacher et al., 2014; Somero, 2012). Growing empirical data highlight that elevated temperatures (OW) may enhance the fitness of marine organisms within physiological constraints, therefore, potentially enhancing their adaptive capacities to cope with climate change (Foo & Byrne, 2016; Leung et al., 2021; Leung et al., 2019). Apparently, the physiological adaptive potential of marine organisms is largely dependent on species-specific, time-scale exposure of organisms to stressors and environmental conditions encountered by parent generations (Donelson et al., 2018). Numerous marine species may exhibit a higher adaptive capacity to gradual warming beyond the scope delineated by short-term experimental investigations. Rapid elevated experimental temperatures, characterized by quick or acute warming, possess the potential to amplify measurable physiological effects and simultaneously hinder the manifestation of adaptive responses (Munday et al., 2013; Seebacher et al., 2014). In particular, global ocean change represents a long-term process that unfolds across generations of diverse marine organisms (IPCC, 2023), fostering the potential evolution of resistance to gradual temperature rise. Insight into the physiological adaptive capabilities of organisms in response to climate change is important for predicting future species distributions and population dynamics, as well as implementing effective conservation strategies (Wikelski & Cooke, 2006).

1.4. Bioindicator species for assessing the effects of ocean warming and ocean acidification

Bioindicators are organisms or biological systems that provide valuable information about the health and quality of the environment and how it changes, attributed to anthropogenic perturbations (e.g., pollution and habitat degradation) or natural stressors (e.g., cyclones, currents, and waves) through time (Holt & Miller, 2010; Markert et al., 2003). The use of bioindicators for pollutant impact assessment in both terrestrial and marine ecosystems has been widely and intensely applied through *in-situ* (direct field assessment) and *ex-situ* (laboratory-based experimental) approaches (da Costa Filho et al., 2022; Parmar et al., 2016).

¹⁰ Thermoregulation refers to the ability of an organism to maintain its internal body temperature within a restricted range utilizing autonomic control mechanisms through various physiological mechanisms to maintain thermal homeostasis (Tattersall et al., 2012).

In the marine environment, various organisms and biological processes are employed to monitor and understand the impacts of anthropological activities, climate change, and pollution on marine habitats. To serve as a bioindicator for pollution-environment stressors, an organism must satisfy specific criteria; in general, the candidate organism should possess ecological and societal significance, exhibit suitable distribution and accessibility, preferably possess longevity, and demonstrate sensitivity to stressors (Gerhardt, 2009). One prominent group of marine bioindicators includes benthic invertebrates, e.g., echinoderms, mollusks, and crustaceans, organisms that play a crucial role in marine trophic dynamic (Heymans et al., 2014).

Over the past decades, members of the phylum Echinodermata have been broadly used to evaluate the effects of increased GHG-CO₂ (OA) and temperature (OW) on marine organisms, particularly on calcifying marine animals (Bednaršek et al., 2021; Dupont et al., 2010; Lang et al., 2023). Echinoderms constitute a heterogeneous assemblage of deuterostome division, encompassing a total of 20550 species including 13000 extinct species and 7550 extant species (Zhang, 2013), categorized into five distinct classes: Crinoidea (sea lilies and feather stars), Asteroidea (sea stars or starfishes), Ophiuroidea (brittle stars), Echinoidea (sea urchins), and Holothuroidea (sea cucumbers) (Pawson, 2007). The widespread distribution and bio-ecological significance in marine habitats (some are considered as keystone species, e.g., Asteroidea (Gaymer & Himmelman, 2008; Paine, 1966), along with the understanding of their fundamental bio-physiological profiles and high sensitivity to many types of contaminants or stressors, establish this phylum as an ideal model for the investigation of ocean stressors (Garcês & Pires, 2023).

Echinodermata are considered highly sensitive to CO₂/pH changes due to their comparatively low metabolic rate and temperature-dependent metabolism (Hughes et al., 2011), weak pH regulation abilities (Stumpp & Hu, 2017), and calcified skeletal structure (Gorzela, 2021). The echinoderm skeleton is composed of high Mg calcite, which is susceptible to dissolution under OA conditions (Andersson et al., 2008). Furthermore, as an ectotherm animal, echinoderms demonstrate high sensitivity to environmental warming, with physiological responses dependent on temperature fluctuations within their thermal tolerance range (Sampaio et al., 2021). It renders echinoderms become a suitable bio-model species to examine the effect of elevated ocean temperatures. However, multiple studies have indicated that certain species of

echinoderm do not experience adverse effects under exposure to OA and OW, neither as sole nor combined stressors (Byrne & Fitzer, 2019; Leung et al., 2022; Medeiros & Souza, 2023; Ross et al., 2023; Venegas et al., 2023). This substantiates the proposition that the impacts of OA and OW are predominantly dependent on the species-specific attributes and the intensities of stressor exposures.

Assays of the effects of OA and OW as sole or combined factors on Echinodermata as bioindicators have generated a significant number of studies (262 articles¹¹; see Lang et al. (2023); Medeiros and Souza (2023) for reviews) mainly focused on species of the class Echinoidea (sea urchins, 198 articles¹¹). However, it is noteworthy that there is currently an absence of investigations on the effects of OA and OW on crinoids, while starfish is a moderately studied class (i.e., Asteroidea, 47 articles¹¹). Investigations examining the impact of elevated CO₂ and temperature levels on responses of echinoderm have delved into physiological effects on growth, feeding, survival, reproduction, acid-base regulation, metabolism, calcification, and skeletal mineralogy.

1.5. Research aim and approach

1.5.1. Study objective and hypothesis

The objectives of this thesis focus on assessing the interactive effects of current and projected near-future global ocean change (OA and OW) on the physio-chemical processes of tropical-subtropical asterinid starfish species and to recognize the mechanisms used by them to tolerate (acclimation potential) future global changes. For this, we undertook long-term controlled laboratory experiments, comparing observations between current ocean physics-chemical states and manipulated temperature, carbonate chemistry, and pH conditions, simulating predictions for future oceans. Furthermore, to the best of our knowledge, this study addresses for the first time the interactive effects of two stressors on aspects of micro-physiology, i.e., calcification, metabolic lipid-fatty acids, and enzyme activity in a tropical-subtropical starfish species.

¹¹ Search using the Google Scholar platform was performed on 31 January 2024

This dissertation addresses the following specific aims:

1. Evaluate the biomineralization parameters on the tropical-subtropical asterinid starfish *Aquilonastra yairi* under OA and OW conditions, e.g., skeletal mineralogy and microstructures (Chapter 2)

Hypothesis: Elevated seawater temperature and decreased seawater pH will negatively affect the biomineralization parameters of asterinid starfish, exhibiting alterations in skeletal mineralogy and microstructure relative to ambient conditions.

2. Investigate how future predictions of OA and OW affect the life development of *A. yairi*, namely survivability, metabolic rate, righting behavior, and calcification rate (Chapter 3).

Hypothesis: Under projected OA and OW scenarios, asterinid starfish will undergo decreased survival rates due to increased physiochemical stress triggered by environmental changes. Furthermore, metabolic rates of asterinid starfish will increase in response to elevated temperatures caused by altered energetic expenditure and physiological stress. Then, the righting behavior of asterinid starfish will be negatively affected; become slower, potentially impairing their locomotion abilities. Calcification rates will decrease under OA conditions, which mirrors the challenge of maintaining skeletal integrity.

3. Evaluate the micro-physiological responses of *A. yairi* when OA and OW stressors are added in terms of their lipid-fatty acids (FAs) biochemistry and enzyme activity (Chapter 4).

Hypothesis: Simultaneous OA and OW will significantly modify asterinid starfish lipid-FAs biochemistry and enzyme activities. Starfish will exhibit alterations in lipid and FAs composition, including modifications of FA profiles in response to environmental stress. Meanwhile, the enzyme activities involved in the calcification process will be significantly reduced under OA and OW stress.

1.5.2. Model species: asterinid starfish

Asteroids (starfish or sea stars; class: Asterozoa) are among the largest diversified classes of the phylum Echinodermata with distinctive and varied body shapes, comprising 1962 different species that are grouped into 40 families and 366 different genera (taxonomic status: accepted; Mah (2024); WoRMS Editorial Board (2024)). Starfish are dispersed at all ocean depth gradients ranging from intertidal to abyssal zones (~6000 m) and are present throughout the world's

oceans; however, they are most abundant in tropical Atlantic and Indo-Pacific regions (Blake, 1990; Clark & Downey, 1992). Starfish have multifaceted ecological roles, impacting marine ecosystems through predation activities, bioturbation¹² (functioning as habitat engineers), organic matter decomposition, and fostering nutrient recycling (Belaústegui et al., 2017; Menge & Sanford, 2013; Rahman et al., 2018). Certain starfish species function as keystone organisms and as integral components of trophic interactions (Menge et al., 2013; Paine, 1966).

Within the class Asteroidea, the family Asterinidae (asterinid starfish) is the largest constituent group comprising 35 genera and 172 species (taxonomic status: accepted; WoRMS Editorial Board (2024)). Asterinid are typically small starfish that exhibit distinctive anatomical characteristics, including a flattened dorsal side, very short arms, and radial body symmetry manifesting as a penta-radial arrangement in which five arms radiate symmetrically from a central disk; however, there is variation within the group (O'Loughlin & Waters, 2004). Besides playing pivotal ecological roles owing to their adaptations and interactions within marine ecosystems, asterinid starfish are particularly suitable as bioindicator species to observe environmental disturbances (Mah & Blake, 2012; Rahman et al., 2018) due to their unique planktonic juvenile and subsequent benthic life history stages and evolution (Byrne, 2006), and as they encompass diversified species and thus perform an ecological structuring role in their habitat (Moreau et al., 2021; Saier, 2001). Also, they are relatively moderate-tolerant to habitat changes caused by environmental stressors (Holt & Miller, 2010; McElroy et al., 2012; Nguyen & Byrne, 2014). Some species in this group are considered keystone species due to their role at the trophic level in benthic communities (Menge & Sanford, 2013), where changes in their populations influence the entire community and the stability of the habitat, making them beneficial in early detection and timely mitigation of environmental disruptions (Byrne & Przeslawski, 2013).

To investigate the effect of OA and OW on asterinid starfish, *A. yairi* (Figure 1.4) was studied under a controlled laboratory setup. In addition to general attributes underlying the use of asterinid starfish as bioindicators, as described in the paragraph above, the use of this asterinid

¹² Bioturbation is the disturbance and alteration of sediment or soil by living organisms (e.g., benthic invertebrates), primarily through activities like burrowing, tunneling, and movement. This process affects the physical, chemical, and biological aspects of the substrate, including mechanical mixing, nutrient redistribution, sediment oxygenation, and the creation of diverse microhabitats. Bioturbation plays a vital role in nutrient cycling and overall ecosystem functioning (Arya et al., 2022; Kristensen et al., 2012).

species as a bioindicator is based on their geographically widespread distribution and their life history as an intertidal species (Ebert, 2021) that are frequently subjected to high environmental variability and susceptible to terrestrial and oceanic disturbances. These rapid changes in environmental regimes, primarily temperature, are decisive factors affecting the bio-physiology of intertidal species (Helmuth et al., 2005; Helmuth & Hofmann, 2001). Starfish are ectothermic animals that respond to environmental change more rapidly compared to terrestrial species; the fact that they are slow-moving inhibits them from escaping from environmental regime alterations, hence qualifying them as reliable bioindicators (Mieszkowska, 2021; Pincebourde et al., 2009). *A. yairi* has been reported to occur from tropical to subtropical regions, mainly across the Mediterranean Sea, Red Sea, and Gulf of Suez (Al-Rshaidat et al., 2016; Ebert, 2021; O'Loughlin & Rowe, 2006). The biological aspects of this species remain poorly described, but *A. yairi* is recognized as a tiny and cryptic nocturnal starfish species that lives under rocks, reef structures, and within rubble zones (intertidal areas); body size reaches a radius of up to ≈ 7 mm (body length measurement from the disk's center to the longest arm's tip) with the number of arms up to eight, but usually six arms, often forming asymmetrical post-fissiparity, and reproduces by fission (Ebert, 2021; O'Loughlin & Rowe, 2006).

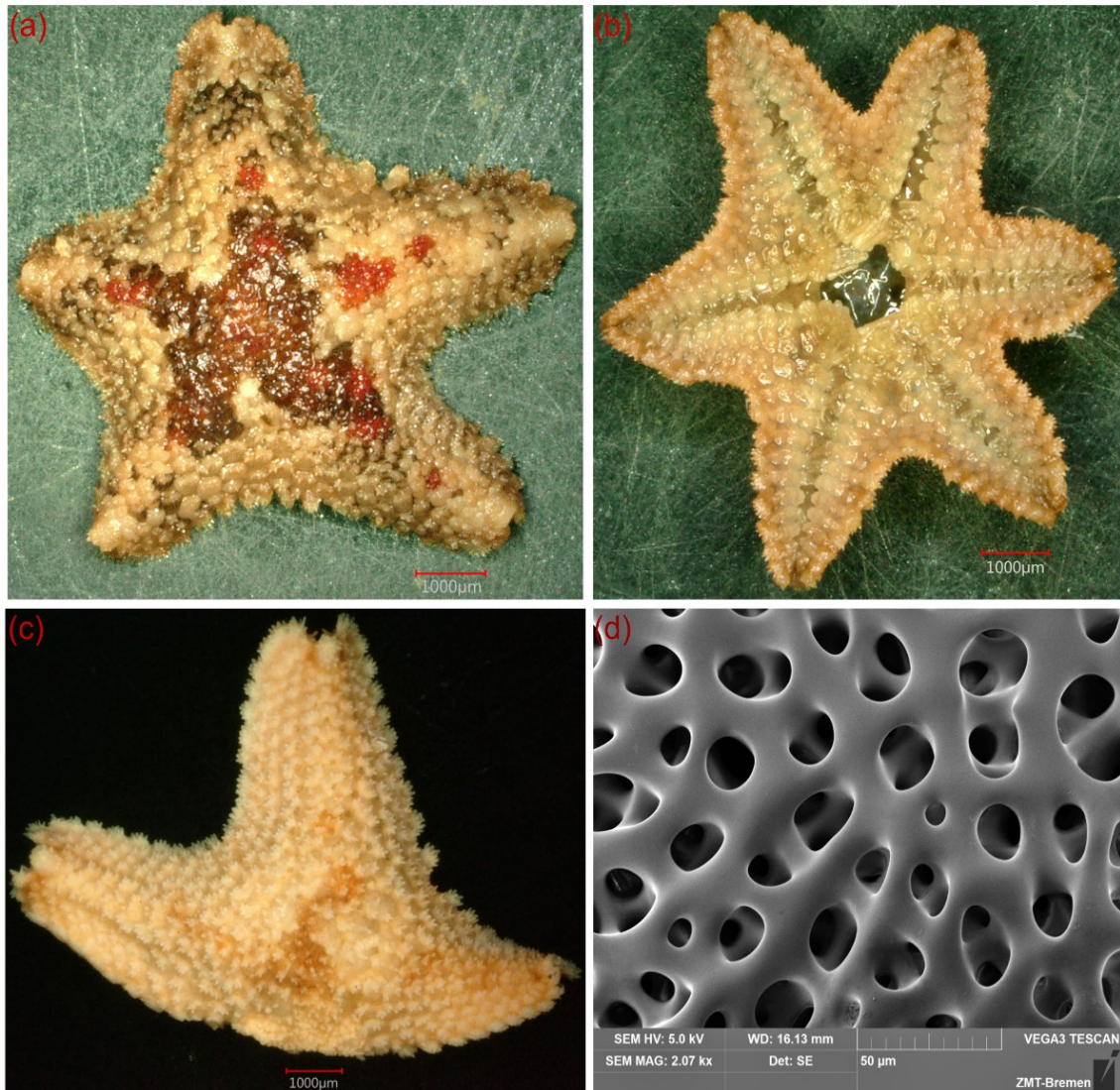


Figure 1.4. The studied asternid starfish *Aquilonastra yairi*. (a) dorsal (upper) part, (b) ventral (bottom) part, (c) fissiparous-asexual reproduction (fission) fragment, (d) skeleton microstructure appearance (stereom pore).

1.5.3. Experimental design and procedures

The long-term starfish culture experiment aimed to address the defined research objectives (see Subchapter 1.5.1). Here, the general setup is given. Detailed information relevant for the different chapters is provided in the methodology section of each of those chapters. To investigate the physiochemical alteration of starfish induced by elevated seawater $p\text{CO}_2$ and temperature, starfish of the species *A. yairi* were reared in aquaria system under controlled experimental environment conditions at the Marine Experimental Ecology (MAREE) - Leibniz Center for Tropical Marine Research (ZMT), Bremen (Figure 1.4. and Supplementary Figure

S2.1). The species of *A. yairi* used in this experiment originated from the culture stock of the MAREE-ZMT.

Elevated temperature and pCO₂ experiment in an aquaria setup

In total, 342 specimens (size 3-11 mm in diameter) of adult *A. yairi* were prepared for the test, cleaned of the adhering external material, and allowed to acclimate in a communal tank with a recirculating water system at an ambient temperature of 27 °C for seven days. After an additional seven-day acclimation phase, individuals ($n = 19$) were randomly distributed into 18 experimental aquaria (25 liters), which were illuminated with LED lights (Aquaillumination® Hydra 52 HD) with 25-30 $\mu\text{mol photons m}^{-2} \text{s}^{-1}$. The starfish were reared for 90 days in one of six treatments (three replicate tanks per treatment), where two temperature levels were crossed with three regimes of $p\text{CO}_2$: (T1) 27 °C: 455 μatm , (T2) 27 °C: 1052 μatm , (T3) 27 °C: 2066 μatm , (T4) 32 °C: 455 μatm , (T5) 32 °C: 1052 μatm , and (T6) 32 °C: 2066 μatm , which represent factorial combinations of ambient conditions and future levels of temperature and CO_2 change. The targeted temperature levels and $p\text{CO}_2$ concentrations were gradually increased over ten days to prevent physiological shock.

Treatment tank temperatures ($\pm\text{SE}$) were kept at 27 (± 0.05) and 32 (± 0.08) °C, independently, using a closed-circle heating system (Heaters Titanium Tube 600 W, Shego, Germany) managed by a programmable thermostat. The $p\text{CO}_2$ of the pumped gas was regulated by mixing compressed CO_2 -free air and compressed CO_2 using an electronic solenoid valve mass flow controller (HTK Hamburg, Germany; pure CO_2 provided by Linde GmbH, Pullach, Germany) to produce a gas mixture formulated to the target $p\text{CO}_2$ condition according to standard operating procedures (SOPs) for CO_2 measurements in the ocean (Dickson et al., 2007). Temperature, salinity, and pH_{NBS} were measured three times per week using a multielectrode portable probe (WTW Multiline 3630 IDS, Xylem Analytics, Germany). The $\text{pH}_{\text{total scale}}$ was measured weekly through the spectrophotometric method following SOP 6b (Dickson et al., 2007) using the indicator dye meta, *m*-cresol purple as the chromogenic reagent. Seawater samples for total alkalinity (A_T) and dissolved inorganic carbon (DIC or C_T) analysis were collected weekly and measured following the protocols described in Dickson et al. (2007). A_T was measured by open-cell potentiometric Gran titration (precision, $\pm 10 \mu\text{mol kg}^{-1}$), and DIC was determined by the colorimetric analytical method using a Shimadzu DIC analyzer (precision, $\pm 10 \mu\text{mol kg}^{-1}$). The seawater carbonate system parameters $p\text{CO}_2$, carbonate ion concentration [CO_3^{2-}], bicarbonate

ion concentration $[\text{HCO}_3^-]$, aqueous CO_2 , calcite saturation state (Ω_{Ca}), and aragonite saturation state (Ω_{Ar}) were calculated with the program CO_2SYS software for MS Excel (Pelletier et al., 2007b), using Hansson (1973) and Mehrbach et al. (1973) refitted by Dickson and Millero (1987) for K_1 and K_2 carbonic acid constants; Dickson (1990) for K_{HSO_4} equilibrium constant; Dickson and Riley (1979) for K_{HF} dissociation constant; Uppström (1974) for the boric acid constant ($[\text{B}]_{\text{T}}$); and Mucci (1983) for the stoichiometric calcite solubility constant.

Determination of the physio-chemical parameters

The methods used in this study to evaluate the effects of OW and OA on the physiochemical aspects of starfish are described in detail in individual chapters. A concise overview of the methodology is presented in Table 1.2.

Table 1.2. Observed parameters and methodology applied to examine the effect of OW and OA on the starfish *A. yairi*.

Chapter	Physiochemical parameter	Methodology description
Chap. 2	Skeletal mineralogy composition	The concentration of skeletal minerals (Ca, Mg, and Sr) was analyzed using plasma optical emission spectroscopy (ICP-OES).
Chap. 2	Skeleton microstructure	Starfish specimens were cut into thin sections, rinsed to remove organic matter, and subsequently air-dried. Skeleton plates were then mounted on stubs and observed under a scanning electron microscope (SEM) to characterize and compare the skeleton microstructure between treatments.
Chap. 3	Metabolic rates	Metabolic rates were estimated as rates of oxygen consumption (M_{O_2}). Real-time M_{O_2} was measured biweekly using optical fluorescence-based oxygen respirometry. The O_2 consumption rate was then calculated using the equation from Sinclair et al. (2006)

Chap. 3	Mortality	Dead starfish were identified by the distinctive loss of color (e.g., whitening) on the dorsal side (aboral surface) or by the absence of tube feet (podia) movement. These parameters were observed daily.
Chap. 3	Righting behavior	The righting response refers to the starfish's ability, when positioned on the ventral side, to flip over into the normal position on the dorsal side. The righting activity coefficient (RAC) was calculated using the formula from Watts and Lawrence (1990).
Chap. 3	Calcification rate	Starfish calcification rate (GTA) was quantified using the modified alkalinity anomaly technique proposed by Gazeau et al. (2015).
Chap. 4	Total lipid	Total lipid (ΣL_C) was extracted and purified according to the methods described by Bligh and Dyer (1959).
Chap. 4	Fatty acids (SFAs, MUFAs, and PUFAs)	The fatty acids (FAs) of the starfish were determined as fatty acid methyl esters (FAMES) in accordance with methods from Christie (1998).
Chap. 4	Enzyme activities (Ca-ATPase and Mg-ATPase activities)	Assessment of enzyme activity is initiated by measuring protein concentration using the Bradford assay method (Bradford, 1976). Furthermore, Ca-ATPase and Mg-ATPase activities were measured according to protocols initially developed by Chan et al. (1986), Busacker and Chavin (1981) and modified by Prazeres et al. (2015)

1.5.4. Outline of the thesis

This dissertation uses a multifaceted approach to examine and assist in better predicting the effects of global ocean change (OA and OW) on the physio-chemical aspects of tropical-subtropical asterinid starfish and to address the knowledge gaps outlined above (Figure 1.5).

Chapter 1: General overview of global ocean change, particularly ocean warming and ocean acidification, and the research related to the effects of this global ocean change on biological aspects of marine organisms. Furthermore, it identified existing knowledge gaps that need to be overcome in order to enhance our understanding of the future responses of marine organisms to global ocean change.

Chapter 2: Ocean warming amplifies the effects of ocean acidification on skeletal mineralogy and microstructure in the asterinid starfish *A. yairi*. This chapter focuses on evaluating the alterations in the mineral composition and microstructure of starfish skeletons exposed to high temperatures and elevated $p\text{CO}_2$. Starfish specimens from six combinations of temperature (27 °C and 32 °C) and $p\text{CO}_2$ (455 μatm , 1052 μatm , 2066 μatm) treatments within two incubation times, 45 days and 90 days, were collected to compare the quantity of skeleton constituent minerals as well as skeletal microstructure differences. The study provides valuable insights into biomineralization capacities in calcifying organisms, specifically echinoderm, within the context of projected global oceanic changes. The outcomes of this research have been published in the *Journal of Marine Science and Engineering*.

Chapter 3: Long-term physiological responses to combined ocean acidification and warming show energetic trade-offs in an asterinid starfish. This chapter assesses the combined effects of elevated $p\text{CO}_2$ and temperature on organismal metabolism, mortality, righting behavior, and calcification of the coral reef-associated starfish *A. yairi*. Specimens were incubated at two temperature levels (27 °C and 32 °C) crossed with three $p\text{CO}_2$ regimes (455 μatm , 1052 μatm , and 2066 μatm). Subsequently, the predetermined observation indicators were frequently analyzed and compared between treatments, offering insight into the performance of essential physiological functions and behaviors of marine organisms under OA and OW pressure and potential acclimation pathways. The outcomes of this research have been published in the scientific journal *Coral Reefs*.

Chapter 4: Simultaneous ocean acidification and warming do not alter the lipid-associated biochemistry but induce enzyme activities in an asterinid starfish. This chapter delves into a comprehensive examination of lipid and associated fatty acids (FAs) biochemistry, alongside the assessment of enzyme activities pivotal in the biomineralization pathway of the tropical-

subtropical asterinid starfish, *A. yairi*, in response to current and future global ocean change scenarios. Starfish used in our experiments were acclimatized at two temperature levels (27 °C, 32 °C) crossed with three $p\text{CO}_2$ concentrations (455 μatm , 1052 μatm , 2066 μatm) over 90 days. Predetermined biochemical factors were analyzed at 30-day intervals to gain insight into the micro-physiochemical profile and its alterations due to exposure to elevated temperatures and $p\text{CO}_2$. The compelling findings of this study have been peer-reviewed and disseminated through publication in *Science of The Total Environment*.

Following the preceding chapters, the general discussion in Chapter 5 provides an extensive and in-depth discussion that integrates previous studies, addresses subsidiary aspects, evaluates and elaborates on findings, and helps to understand the importance of the research.

Chapter 6: Conclusion and future research provides a comprehensive summary of the main findings of this dissertation, then outlines emerging research questions and suggests potential future research directions in this field. To enhance both intelligibility and accessibility, a comprehensive list of references for each chapter is presented at the end of this dissertation. This consolidated reference section allows for easy access and browsing of the sources cited for each chapter.

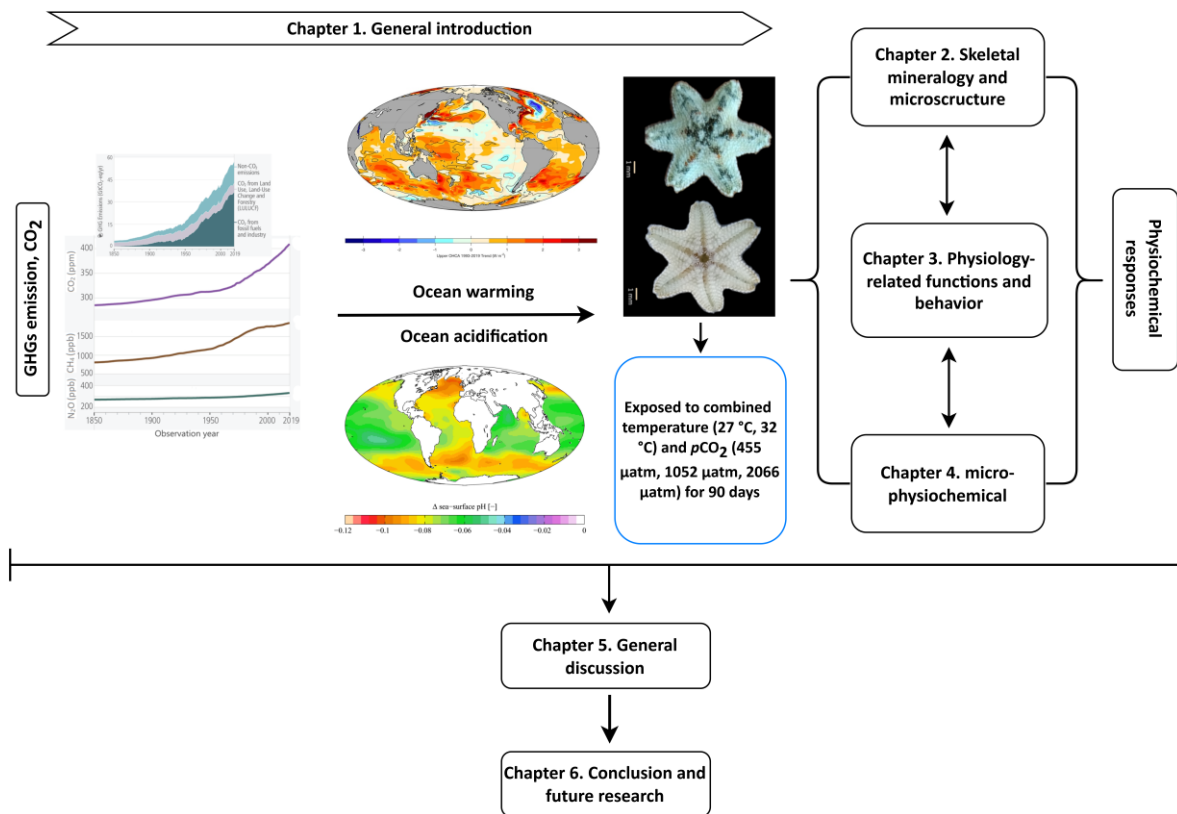


Figure 1.5. Schematic outline of the chapter-specific objectives and overarching approach of the dissertation. The background context of ocean warming and acidification caused by GHGs-CO₂ and its ramifications on marine life (Chapter 1), the interactive effects of OA/OW on the biomineralization process of starfish *A. yairi* which is reflected in their skeletal mineralization and microstructure (Chapter 2), potential alterations in important physiological factors and behaviour of starfish under OA/OW environment (Chapter 3), starfish micro-physiochemical profiles of lipid-FAs and its enzyme activities under OA/OW conditions (Chapter 4), the previous chapters are further synthesized (Chapter 5), general conclusion and questions that may remain unaddressed in this dissertation are highlighted for future studies (Chapter 6).

Chapter 2. Ocean warming amplifies the effects of ocean acidification on skeletal mineralogy and microstructure in the asterinid starfish *Aquilonastra yairi*

This work has been *published* in the *Journal of Marine Science and Engineering*, 10(8), <https://doi.org/10.3390/jmse10081065>.

Munawar Khalil^{1,2,3,*}, **Steve S. Doo**^{1,4}, **Marleen Stuhr**¹, and **Hildegard Westphal**^{1,2,4}

¹ Leibniz Centre for Tropical Marine Research (ZMT), 28359 Bremen, Germany

² Faculty of Geosciences, University of Bremen, 28359 Bremen, Germany

³ Department of Marine Science, Faculty of Agriculture, Universitas Malikussaleh, Reuleut Main Campus, Aceh 24355, Indonesia

⁴ Physical Science and Engineering (PSE) and Red Sea Research Center (RSRC), King Abdullah University of Science and Technology (KAUST), Thuwal 23955-6900, Saudi Arabia

Article

Ocean Warming Amplifies the Effects of Ocean Acidification on Skeletal Mineralogy and Microstructure in the Asterinid Starfish *Aquilonastra yairi*

Munawar Khalil ^{1,2,3,*}, Steve S. Doo ^{1,4}, Marleen Stuhr ¹ and Hildegard Westphal ^{1,2,4}

¹ Leibniz Centre for Tropical Marine Research (ZMT), 28359 Bremen, Germany; steve.doo@leibniz-zmt.de (S.S.D.); marleen.stuhr@leibniz-zmt.de (M.S.); hildegard.westphal@kaust.edu.sa (H.W.)

² Faculty of Geosciences, University of Bremen, 28359 Bremen, Germany

³ Department of Marine Science, Faculty of Agriculture, Universitas Malikussaleh, Reuleut Main Campus, Aceh 24355, Indonesia

⁴ Physical Science and Engineering (PSE), Red Sea Research Center (RSRC), King Abdullah University of Science and Technology (KAUST), Thuwal 23955-6900, Saudi Arabia

* Correspondence: munawar.khalil@leibniz-zmt.de



Citation: Khalil, M.; Doo, S.S.; Stuhr, M.; Westphal, H. Ocean Warming Amplifies the Effects of Ocean Acidification on Skeletal Mineralogy and Microstructure in the Asterinid Starfish *Aquilonastra yairi*. *J. Mar. Sci. Eng.* **2022**, *10*, 1065. <https://doi.org/10.3390/jmse10081065>

Academic Editor: Markes E. Johnson

Received: 31 May 2022

Accepted: 1 July 2022

Published: 3 August 2022

Publisher's Note: MDPI stays neutral with regard to jurisdictional claims in published maps and institutional affiliations.



Copyright: © 2022 by the authors. Licensee MDPI, Basel, Switzerland. This article is an open access article distributed under the terms and conditions of the Creative Commons Attribution (CC BY) license (<https://creativecommons.org/licenses/by/4.0/>).

Abstract: Ocean acidification and ocean warming compromise the capacity of calcifying marine organisms to generate and maintain their skeletons. While many marine calcifying organisms precipitate low-Mg calcite or aragonite, the skeleton of echinoderms consists of more soluble Mg-calcite. To assess the impact of exposure to elevated temperature and increased $p\text{CO}_2$ on the skeleton of echinoderms, in particular the mineralogy and microstructure, the starfish *Aquilonastra yairi* (Echinodermata: Asteroidea) was exposed for 90 days to simulated ocean warming (27 °C and 32 °C) and ocean acidification (455 μatm , 1052 μatm , 2066 μatm) conditions. The results indicate that temperature is the major factor controlling the skeletal Mg (Mg/Ca ratio and Mg_{norm} ratio), but not for skeletal Sr (Sr/Ca ratio and Sr_{norm} ratio) and skeletal Ca (Ca_{norm} ratio) in *A. yairi*. Nevertheless, inter-individual variability in skeletal Sr and Ca ratios increased with higher temperature. Elevated $p\text{CO}_2$ did not induce any statistically significant element alterations of the skeleton in all treatments over the incubation time, but increased $p\text{CO}_2$ concentrations might possess an indirect effect on skeletal mineral ratio alteration. The influence of increased $p\text{CO}_2$ was more relevant than that of increased temperature on skeletal microstructures. $p\text{CO}_2$ as a sole stressor caused alterations on stereom structure and degradation on the skeletal structure of *A. yairi*, whereas temperature did not; however, skeletons exposed to elevated $p\text{CO}_2$ and high temperature show a strongly altered skeleton structure compared to ambient temperature. These results indicate that ocean warming might exacerbate the skeletal maintaining mechanisms of the starfish in a high $p\text{CO}_2$ environment and could potentially modify the morphology and functions of the starfish skeleton.

Keywords: ocean acidification; ocean warming; echinoderm; starfish; mineralogy; skeleton; biomineralization

1. Introduction

The oceans are estimated to take up ~31% of the CO_2 increase that is currently observed [1]. This is known to lead to lowered pH values of the seawater, resulting in a reduced carbonate saturation state (Ω), and changes in carbonate–bicarbonate ion balance, recognized as ocean acidification (OA) [2,3]. These changes in seawater chemistry lead to measurable reactions of marine species and ecosystems, and are known to have negative repercussions for many calcifying organisms [4–7], including certain scleractinian corals, bryozoans, molluscs, and echinoderms. Decreased carbonate ion concentration [CO_3^{2-}] can disrupt the physiologically regulated biomineralization mechanism that generates, preserves and maintains calcium carbonate (CaCO_3) structures, e.g., exoskeleton, test,

Statement of contribution

Idea and concept: Personal contribution 85%. M. Khalil developed the idea to focus on the skeletal mineral composition and skeletal structure of starfish under ocean acidification and ocean warming, with contributions on methods from H. Westphal, S.S. Doo, and M. Stuhr. The research project was supervised by H. Westphal.

Research: Personal contribution 90%. M. Khalil carried out laboratory experiments, conducted skeletal mineralogy analysis, worked with a scanning electron microscope (SEM) for skeletal images, analyzed the data, created figures and tables, and interpreted the data.

Manuscript writing: Personal contribution 90%. M. Khalil wrote the initial manuscript, with contributions and improvements from H. Westphal, S.S. Doo, and M. Stuhr.

Abstract

Ocean acidification and ocean warming compromise the capacity of calcifying marine organisms to generate and maintain their skeletons. While many marine calcifying organisms precipitate low-Mg calcite or aragonite, the skeleton of echinoderms consists of more soluble Mg-calcite. To assess the impact of exposure to elevated temperature and increased $p\text{CO}_2$ on the skeleton of echinoderms, in particular the mineralogy and microstructure, the starfish *Aquilonastra yairi* (Echinodermata: Asteroidea) was exposed for 90 days to simulated ocean warming (27 °C and 32 °C) and ocean acidification (455 μatm , 1052 μatm , 2066 μatm) conditions. The results indicate that temperature is the major factor controlling the skeletal Mg (Mg/Ca ratio and Mg_{norm} ratio), but not for skeletal Sr (Sr/Ca ratio and Sr_{norm} ratio) and skeletal Ca (Ca_{norm} ratio) in *A. yairi*. Nevertheless, inter-individual variability in skeletal Sr and Ca ratios increased with higher temperature. Elevated $p\text{CO}_2$ did not induce any statistically significant element alterations of the skeleton in all treatments over the incubation time, but increased $p\text{CO}_2$ concentrations might possess an indirect effect on skeletal mineral ratio alteration. The influence of increased $p\text{CO}_2$ was more relevant than that of increased temperature on skeletal microstructures. $p\text{CO}_2$ as a sole stressor caused alterations on stereom structure and degradation on the skeletal structure of *A. yairi*, whereas temperature did not; however, skeletons exposed to elevated $p\text{CO}_2$ and high temperature show a strongly altered skeleton structure compared to ambient temperature. These results indicate that ocean warming might exacerbate the skeletal maintaining mechanisms of the starfish in a high $p\text{CO}_2$ environment and could potentially modify the morphology and functions of the starfish skeleton.

Keywords: ocean acidification, ocean warming, echinoderm, starfish, mineralogy, skeleton, biomineralization

2.1. Introduction

The oceans are estimated to take up $\approx 31\%$ of the CO_2 increase that is currently observed (Watson et al., 2020). This is known to lead to lowered pH values of the seawater, resulting in a reduced carbonate saturation state (Ω), and changes in carbonate–bicarbonate ion balance, recognized as ocean acidification (OA) (Feely et al., 2004; Sabine et al., 2004). These changes in seawater chemistry lead to measurable reactions of marine species and ecosystems, and are known to have negative repercussions for many calcifying organisms (Dupont et al., 2010; Hoegh-Guldberg & Bruno, 2010; Orr et al., 2005; Rodolfo-Metalpa et al., 2010), including certain scleractinian corals, bryozoans, mollusks, and echinoderms. Decreased carbonate ion concentration $[\text{CO}_3^{2-}]$ can disrupt the physiologically regulated biomineralization mechanism that generates, preserves, and maintains calcium carbonate (CaCO_3) structures, e.g., exoskeleton, test, spine, tube feet, teeth, pedicellariae and spicules (Killian & Wilt, 2008; Mann, 1983; Matranga et al., 2011; Orr et al., 2005). This mechanism involves mineral formation, characteristics, morphogenesis, and organic molecules (Feng, 2011; Gilbert & Wilt, 2011; Gorzelak, 2021; Mann, 1983). This is particularly the case for organisms precipitating a skeleton composed of high Mg-calcite (HMC), i.e., with a significant concentration of magnesium carbonate (MgCO_3) in the carbonate ($>4 \text{ mol}\% \text{MgCO}_3$) (Kawahata et al., 2019; Ries et al., 2016). HMC is the most soluble of the polymorphs of crystalline CaCO_3 and is thermodynamically metastable (Morse et al., 2006; Ries et al., 2016). Furthermore, previous studies have shown that OA significantly affects the size and weight of shells or skeletons of many marine calcifiers (Anand et al., 2021; Duquette et al., 2017; Watson et al., 2012). In contrast, some calcifiers, mainly photosynthesizing or photosymbiotic ones, including some corals and algae, show positive responses in calcification and growth values as they benefit from increased CO_2 concentrations by an enhanced photosynthesis rate, which provides additional potential energy for the calcification process (Ries et al., 2009).

At the same time, seawater temperature (ocean warming, OW) influences the ecophysiology of marine organisms (Pörtner, 2008), skeletal mineralogy (Chave, 1954; Duquette et al., 2018; Gorzelak, 2021; Hermans et al., 2010; Lowenstam & Weiner, 1989; Ries et al., 2016; Weber, 1973; Weiner & Dove, 2003), growth rate (Gazeau et al., 2013), and mineral growth control mechanisms (Olson et al., 2012). Previous studies have found inconsistent reactions to increased temperature exposure, ranging from no effect to significant changes in skeletal mineralogy. For example, the skeletal Mg/Ca ratios of the scleractinian coral *Acropora* sp.

(Reynaud et al., 2007), the sea urchin *Paracentrotus lividus* (Hermans et al., 2010), the foraminifera *Planoglabratella operculari*, *Quinqueloculina yabei* (Toyofuku et al., 2000) and *Ammonia tepida* (Dissard et al., 2010) increase with temperature; conversely, the skeletal Mg/Ca ratios of the sea urchin *Lytechinus variegatus* was significantly lower in individuals kept at high temperature (~30 °C) compared to the ambient temperature (~26 °C) (Duquette et al., 2018). Skeletal Sr/Ca ratios decreases with increasing temperature in the scleractinian coral *Acropora* sp. (Bell et al., 2017; Reynaud et al., 2007), Sr/Ca ratios increases with increasing temperature in the foraminifera *A. tepida* (Dissard et al., 2010) or *Globigerinoides ruber* (Kisakürek et al., 2008), and is not significantly affected by temperature in the foraminifera *Trifarina angulosa* (Rathburn & De Deckker, 1997). However, the effects of temperature on skeletal mineralogy and structure are still largely unclear and are likely influenced by phylogenetic factors, growth rate (Dodd, 1967; Weber, 1973; Weiner & Dove, 2003), latitude (Chave, 1954), biological 'vital effects' (Kolbuk et al., 2020), and stage or species-specific differences (LaVigne et al., 2013).

The effects of combined OA and OW on marine calcifier organisms are thought to be additive, antagonistic, or synergistic (Todgham & Stillman, 2013). Previous meta-studies observed complex responses of calcifying marine organisms to combined OW and OA that vary from a significant negative effect to no effect on the organism (Harvey et al., 2013). Moreover, there is a trend toward enhanced sensitivity (i.e., the capability to sense and respond to environmental alterations) of biomineralization, growth, survival, and life stages development to OA in corals, echinoderm, and mollusks when being concurrently exposed to elevated temperatures (Kroeker et al., 2013). Besides, there is growing evidence that elevated temperatures can exacerbate microstructure disruption caused by elevated $p\text{CO}_2$ in ectotherm species, e.g., in some mollusks such as the giant clam *Tridacna maxima* (Brahmi et al., 2021) and the mussel *Mytilus edulis* (Knights et al., 2020; Li et al., 2015), and echinoderms such as the sea urchin *Tripneustes gratilla* (Byrne et al., 2014). However, these synergistic effects of OA and OW seem to be complex, and the magnitude of effect sizes and organism response varies between taxa groups, trophic level, habitat, and life stages (Byrne, 2011; Harvey et al., 2013; Kroeker et al., 2013).

Echinoderms comprise a wide variety of taxa, with a complex calcium carbonate biomineralization. Their skeleton is formed within the syncytium by progressive crystallization

of a transient amorphous calcium carbonate phase (ACC) (Politi et al., 2004), through a biologically controlled intracellular mechanism within vesicles or vacuoles formed by fused cell membranes inside cells (Feng, 2011; Gorzelak, 2021; Kokorin et al., 2015). The echinoderm endoskeleton is composed of a complex three-dimensional porous microstructure (stereom) with connecting trabeculae (i.e., mesh-like interconnecting matrix rod of calcite skeleton) (Gorzelak, 2021), which are composed of 99.8–99.9% weight/weight (w/w) HMC with Sr as the primary trace element (Borremans et al., 2009; Dubois, 2014), and the other 0.1–0.2% (w/w) of the skeleton being organic components consisting of proteins and glycoproteins, called the intrastereomic organic matrix (IOM) (Killian & Wilt, 1996; Weiner, 1985). The IOM has critical functions in the biomineralization process during the transient ACC phase by stabilizing the skeleton, controlling mineral incorporation into the skeleton, and controlling the nucleation and morphology of the skeletal crystals (Addadi & Weiner, 1992; Hermans et al., 2011). The trace element concentration of biogenic CaCO₃ is affected by biological factors, e.g., phylogeny, life stage, food supply, as well as by physical-chemical factors, e.g., temperature, salinity, seawater carbonate chemistry, concentration of Mg²⁺ and Ca²⁺ ions in the seawater, light, and hydrostatic pressure (Borremans et al., 2009; Kolbuk et al., 2020; Lowenstam & Weiner, 1989; Mackenzie et al., 1983; Ries, 2011; Ries et al., 2016). Seawater chemistry influences the mineralogy of the echinoderm skeleton by changing the physiological cost of sustaining the biological control of intracellular chemistry (Knoll, 2003). For echinoderms with their skeletons being composed of HMC (MgCO₃ between 2.5% and 39% (Matranga et al., 2011)), their skeletons become more soluble under OA conditions (Andersson et al., 2008; Byrne & Fitzer, 2019; Dubois, 2014; Morse et al., 2006).

To gain a better understanding of the effects of combined OA and OW on biomineralization, systematic comparative studies across a phylogenetically diverse spectrum of taxa are needed (Knoll, 2003). The present study contributes to this goal by investigating the mineral composition and skeleton microstructure of *Aquilonastra yairi* (phylum Echinodermata, class Asteroidea, family Asterinidae) under controlled OA and OW conditions. This asterinid starfish thrives in the marine intertidal and coral reefs of the Red Sea and the Mediterranean Sea, where it lives in crevices and beneath corals or rocks (O'Loughlin & Rowe, 2006). It has an important ecological function as a grazer of marine algae, bacterial mats, detritus, and other fragments of food (Menge & Sanford, 2013). Previous studies have indicated deleterious effects of combined OA and OW on the physiological performances of asterinid starfish (Balogh &

Byrne, 2020; Khalil et al., 2023; McElroy et al., 2012; Nguyen & Byrne, 2014), while the effects of each stressor and their potential synergetic effects on skeletal mineral ratio and microstructure are currently still poorly understood.

2.2. Materials and methods

2.2.1. Experimental design and control of seawater chemistry

In this study, starfish *A. yairi* was used as a model organism to investigate the combined effects of OW and OA. A total of 342 specimens of *A. yairi* (size 3–11 mm) from the cultivated stock of the MAREE (Marine Experimental Ecology facility) of ZMT, Bremen, Germany, were studied in the present experiment. Following acclimation procedures (see Supplementary Materials), the starfish were cultured for 90 days in six different treatments, namely at two different temperatures (ambient temperature: 27 °C, and high temperature: 32 °C) crossed with three levels of $p\text{CO}_2$ (low $p\text{CO}_2$: 455 μatm , medium $p\text{CO}_2$: 1052 μatm , and high $p\text{CO}_2$: 2066 μatm). All six treatments were replicated in three aquaria (Supplementary Materials Figure S2.1).

Target temperature and $p\text{CO}_2$ levels were ramped up gradually over the first ten days to avoid physiological shock. Then the temperature (mean \pm SE) in the treatment tanks was maintained at 27 ± 0.05 °C and 32 ± 0.08 °C, respectively, using a closed circle heating system (Heaters Titanium Tube 600 W, Schego Schemel & Goetz, Offenbach, Germany), controlled with a programmable thermostat. The mixture of the gas bubbled into the seawater in the bottom storage compartment sump was reached by blending compressed CO_2 -free air and compressed CO_2 (pure CO_2 provided by Linde GmbH, Pullach, Germany) using electronic solenoid-valve mass-flow controllers (HTK Hamburg GmbH, Hamburg, Germany) in accordance with the standard operating procedure (SOP) for ocean CO_2 measurements (Dickson et al., 2007). Details of the seawater chemistry control and manipulation are provided in the Supplementary Materials. The seawater parameters and carbonate chemistry for the experimental exposures are given in Table 2.1.

Table 2.1. Seawater chemistry values measured during a 90-day experimental period for *Aquilonastra yairi* reared under two temperature levels (27 °C and 32 °C) crossed with three levels of $p\text{CO}_2$ (455 μatm , 1052 μatm , and 2066 μatm). Data are presented as mean values \pm SE. A_T , total alkalinity; DIC, dissolved inorganic carbon; $p\text{CO}_2$, partial pressure of CO_2 ; $[\text{CO}_3^{2-}]$, carbonate ion concentration; $[\text{HCO}_3^-]$, bicarbonate ion concentration; $[\text{CO}_2]$, dissolved CO_2 ; Ω_{Ca} , calcite saturation state; Ω_{Ar} , aragonite saturation state.

Treatment	Measured parameters					
	Salinity (PSU)	Temperature (°C)	pH _(NBS scale)	pH _(total scale)	A_T ($\mu\text{mol/kg-SW}$)	DIC ($\mu\text{mol/kg-SW}$)
27 °C: 455 μatm	34.56 \pm 0.12	27.48 \pm 0.06	8.13 \pm 0.00	8.00 \pm 0.00	2504.42 \pm 15.33	2168.86 \pm 15.23
27 °C: 1052 μatm	34.73 \pm 0.06	27.23 \pm 0.04	7.87 \pm 0.01	7.74 \pm 0.01	2514.45 \pm 16.78	2340.99 \pm 11.62
27 °C: 2066 μatm	34.75 \pm 0.05	27.34 \pm 0.03	7.60 \pm 0.01	7.47 \pm 0.01	2539.83 \pm 38.86	2479.40 \pm 36.58
32 °C: 455 μatm	34.65 \pm 0.08	32.03 \pm 0.05	8.13 \pm 0.00	8.00 \pm 0.00	2510.27 \pm 47.18	2134.38 \pm 38.40
32 °C: 1052 μatm	34.78 \pm 0.05	32.10 \pm 0.04	7.87 \pm 0.00	7.74 \pm 0.00	2532.19 \pm 40.05	2325.20 \pm 40.02
32 °C: 2066 μatm	34.76 \pm 0.02	32.20 \pm 0.08	7.60 \pm 0.01	7.47 \pm 0.01	2584.38 \pm 41.93	2493.30 \pm 37.87
Treatment	Calculated parameters					
	$p\text{CO}_2$ (μatm)	$[\text{CO}_3^{2-}]$ ($\mu\text{mol/kg-SW}$)	$[\text{HCO}_3^-]$ ($\mu\text{mol/kg-SW}$)	$[\text{CO}_2]$ ($\mu\text{mol/kg-SW}$)	Ω_{Ca}	Ω_{Ar}
27 °C: 455 μatm	456.13 \pm 8.24	245.64 \pm 2.52	1911.05 \pm 14.94	12.17 \pm 0.22	5.96 \pm 0.06	3.96 \pm 0.04
27 °C: 1052 μatm	1059.58 \pm 32.04	138.12 \pm 4.64	2178.74 \pm 9.58	28.42 \pm 0.86	3.35 \pm 0.11	2.22 \pm 0.07
27 °C: 2066 μatm	2075.40 \pm 30.99	81.18 \pm 2.35	2342.71 \pm 34.29	55.51 \pm 0.82	1.97 \pm 0.06	1.31 \pm 0.04
32 °C: 455 μatm	453.78 \pm 6.51	273.82 \pm 8.23	1849.66 \pm 30.77	10.90 \pm 0.16	6.71 \pm 0.20	4.52 \pm 0.14
32 °C: 1052 μatm	1045.15 \pm 44.00	162.68 \pm 4.67	2147.47 \pm 38.59	25.05 \pm 1.06	3.98 \pm 0.11	2.69 \pm 0.08
32 °C: 2066 μatm	2057.31 \pm 74.42	99.46 \pm 4.64	2344.63 \pm 34.94	49.20 \pm 1.78	2.44 \pm 0.11	1.64 \pm 0.08

2.2.2. Skeletal mineral composition analysis

On days 45 and 90 of the experimental treatment, six specimens from each replicate tank (i.e., 36 in total on each of those days) were randomly collected and rinsed in Milli-Q (18.2 M Ω) water before drying for ~48 h at 40 °C. In preparation for trace element analysis, to remove organic material from the skeletal matrix, dried starfish were soaked in hydrogen peroxide (H₂O₂) (Bray et al., 2014; Ehrlich et al., 2011; Russell et al., 2004) for 24 h and subsequently cleaned mechanically, i.e., residual organic material was removed by forceps, and further potential contaminations were removed with deionized water in an ultrasonic bath. Then, the sample material was manually ground using a mortar and pestle. The powdered samples were kept at room temperature in sealed vials until analysis.

The element concentration of Ca, Mg, and Sr in the skeleton was determined with a Spectro CIROS Vision (SPECTRO Analytical Instruments GmbH, Kleve, Germany) inductively coupled plasma optical emission spectroscope (ICP-OES). The samples (weighing 0.02–0.1 mg) were digested with concentrated nitric acid (HNO₃) and H₂O₂ (high-purity of trace metal grade reagent). The solutions were then diluted to the acidity of 0.5 M HNO₃ with aliquots of 0.1 mL and weighed again. Instrument calibration solutions (Inorganic Ventures™ 1000 ppm standard stock solution) were prepared using single-element standards in proportion to the *A. yairi* skeleton concentrations. Measurements of all starfish samples were done routinely against the international reference standard JLS⁻¹, a coral in-house working standard (ZMT-CM₁), and HNO₃ blanks. Mg and Sr mineral elements are reported as a ratio over calcium (Ca), i.e., Mg/Ca, and Sr/Ca and over total skeletal material, i.e., Ca_{norm}, Mg_{norm}, and Sr_{norm}, to account for minor organic material still present on or within the carbonate skeleton.

2.2.3. Analysis of the skeleton microstructure

One specimen from the 45-day and 90-day incubations from each treatment tank was randomly selected ($n = 12$), washed, and prepared for the SEM analysis. Each starfish was cut with dissecting scissors around the part of arms and cleaned of soft tissue. Organic material was dissolved using a 30% H₂O₂ solution buffered in NaOH (0.1 N) at room temperature for 24 h. Skeletons were then rinsed with distilled water repeatedly to remove any remaining organic material and then air-dried for 48 h at room temperature. Skeleton plates were then mounted on a stub with carbon-based tape and gold-sputtered (Cressington Sputter Coater 108 auto, Cressington Scientific Instruments, Watford, UK) for 30 s. Secondary electron images (SE) were

generated with a scanning electron microscope (SEM; Tescan Vega3 XMU, Brno – Kohoutovice, Czech Republic) to characterize the skeleton microstructure, using a beam voltage of 5 kV for a magnification of up to 3000×. All SEM micrographs were examined for any visible differences between treatments, including signs of dissolution, surface smoothness, the shape of stereom pores, and the shape of inner matrix aperture pores.

2.2.4. Statistical analysis

Statistical analysis was performed using the software R, version 4.1.3 (R Core Team, 2022). Normality of data distribution and homogeneity of variance was tested with the Shapiro–Wilk statistic W test ($\alpha = 0.05$) (Shapiro & Wilk, 1965) and Levene’s test ($\alpha = 0.05$) (Levene, 1960), respectively, and indicated that all data of skeletal mineral ratios were normally distributed and the homoscedasticity assumption for the data was equal. The effects of temperature, $p\text{CO}_2$, incubation time, and their interactions on skeletal mineral element to calcium ratios (Mg/Ca and Sr/Ca) and skeletal mineral element to total skeletal material ratios (Ca_{norm} , Mg_{norm} , and Sr_{norm}) were examined using three-way analysis of variance (ANOVA), and Tukey HSD post hoc analyses were conducted using agricolae R-package 1.3–5 (de Mendiburu, 2021). Temperature, $p\text{CO}_2$, and incubation time were fixed factors, while skeletal mineral ratios were used as response variables. All statistics were evaluated with a significance level of $\alpha = 0.05$.

2.3. Result

Over the duration of the experiment (90 days), the starfish mortality rate was low and only found in the high-temperature treatment. In general, the results indicate that elevated temperature and $p\text{CO}_2$ changed the skeletal mineral composition, whereas elevated $p\text{CO}_2$ affected skeletal microstructure in *A. yairi*.

2.3.1. Elemental composition of skeletal carbonate

Overall, a relatively small range of Mg/Ca ratio values were observed across all our treatments (181.95–204.26 mmol/mol). The starfish had consistently higher Mg/Ca ratios in the 32 °C treatments (190.90 ± 1.41 mmol/mol, mean \pm SE) than those held at 27 °C (187.59 ± 0.83 mmol/mol, mean \pm SE) throughout all $p\text{CO}_2$ concentration levels. Both incubation time and temperature had a main effect on skeletal Mg/Ca ratio ($p = 0.049$ and $p = 0.033$, respectively; Table 2.2). Inter-individual variability in skeletal Mg/Ca ratios was substantially higher in starfish subjected to high temperatures (32 °C) compared to those exposed to ambient

temperatures (27 °C) in all $p\text{CO}_2$ combined treatments (Figure 2.1A). No consistent $p\text{CO}_2$ effect as the sole factor was found, and the Mg/Ca ratio displayed the typical parabolic responses to $p\text{CO}_2$ (Figure 2.1A). Elevated $p\text{CO}_2$ as the sole stressor did not significantly affect skeletal Mg/Ca ratios ($p = 0.414$, Table 2.2). The interaction of temperature: $p\text{CO}_2$: incubation time on starfish skeletal Mg/Ca ratios was significant ($p = 0.014$, Table 2.2). However, Tukey's HSD post hoc analysis did not reveal any significant interactions in Mg/Ca ratios (Table 2.2 and Supplementary Materials Table S2.1).

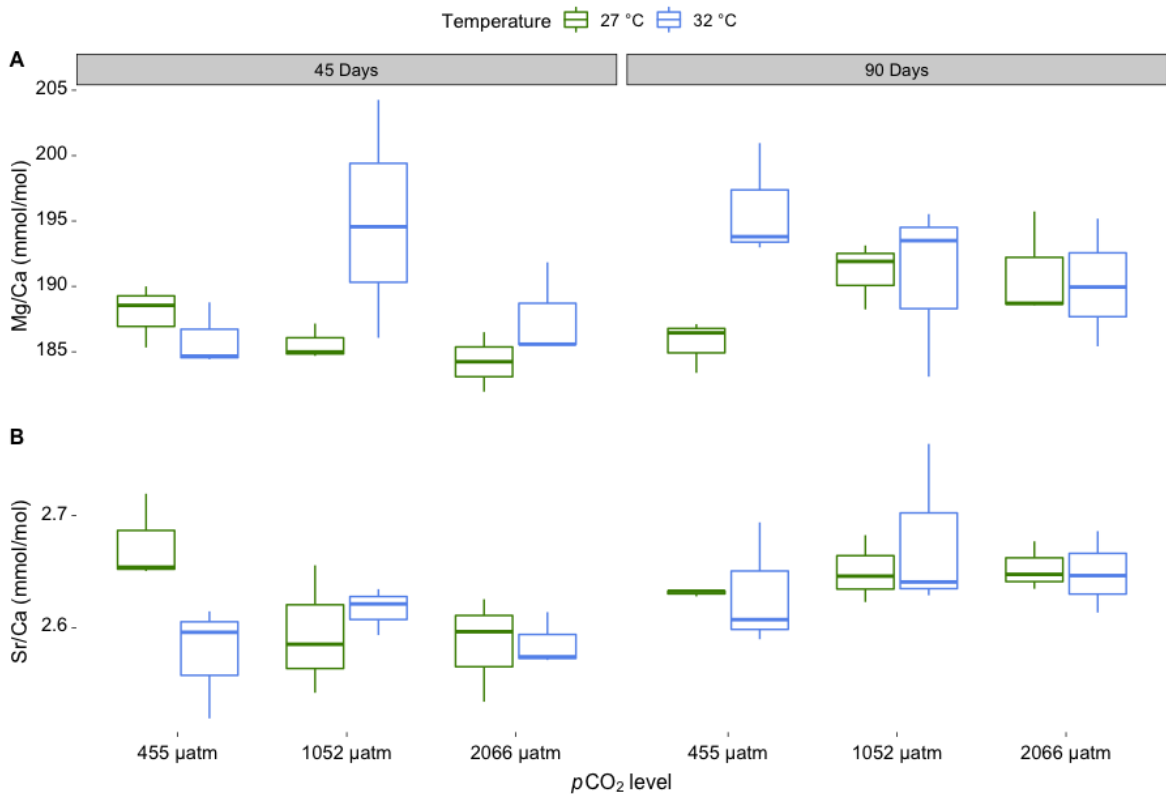


Figure 2.1. Changes in skeletal properties (A) Mg/Ca ratios (mmol/mol) and (B) Sr/Ca ratios (mmol/mol) of skeletal carbonate in *A. yairi* exposed to different temperatures (27 °C and 32 °C) crossed with different $p\text{CO}_2$ concentrations (455 μatm , 1052 μatm , and 2066 μatm) measured after 45 and 90 days of incubation ($n = 36$).

Sr/Ca ratios ranged from 2.52 mmol/mol to 2.76 mmol/mol across treatments (Figure 2.1B). The Sr/Ca ratio at 32 °C had the highest fluctuation in values compared to 27 °C, where Sr/Ca ratios at 27 °C treatments (2.63 ± 0.01 mmol/mol, mean \pm SE) were slightly higher than for the 32 °C treatments (2.62 ± 0.01 mmol/mol, mean \pm SE) (Figure 2.1B). Inter-individual variability

of Sr/Ca ratios were substantially higher for medium and high $p\text{CO}_2$ treatments (1052 μatm , 2066 μatm) compared to low $p\text{CO}_2$ (455 μatm) treatments; this was the case at both temperature levels (Figure 2.1B). No significant response of Sr/Ca ratio to differences in the $p\text{CO}_2$ and temperature as combined or as sole stressors (Table 2.2). However, skeletal Sr/Ca ratios were significantly altered over incubation time ($p = 0.006$, Table 2.2), with increasing values from samples taken after 45 days compared to those collected after 90 days.

Ca_{norm} ratios showed relatively variable values, which ranged between 647.74 mg/g and 755.30 mg/g across all treatments (Figure 2.2A). Ca_{norm} ratios were changed over the incubation time ($p = 0.036$, Table 2.2). The Ca_{norm} ratios at 27 °C rose from 699.73 ± 5.41 mg/g (mean \pm SE) at 45 days to 709.02 ± 4.33 mg/g (mean \pm SE) at 90 days incubation time (enhanced 1.33%), whereas the Ca_{norm} ratios at 32 °C rose from 693.51 ± 8.93 mg/g (mean \pm SE) at 45 days to 712.60 ± 7.48 mg/g (mean \pm SE) at 90 days incubation time (enhanced 2.74%). Ca_{norm} ratios were not significantly affected by temperature ($p = 0.838$, Table 2.2) or $p\text{CO}_2$ ($p = 0.307$, Table 2.2) as a single factor, nor as a combined factor ($p = 0.250$, Table 2.2).

Mg_{norm} ratios from the skeleton of *A. yairi* were significantly altered by incubation time ($p = 0.001$, Table 2.2). Mg_{norm} ratios increased from 45 days to 90 days in both temperature treatment conditions (Figure 2.2B). At 27 °C, the Mg_{norm} ratios increased from 109.57 ± 0.94 mg/g (mean \pm SE) at 45 days to 112.98 ± 0.57 mg/g (mean \pm SE) at 90 days incubation time (i.e., 3.11% increase), while at 32 °C, the Mg_{norm} ratios increased from 110.61 ± 1.04 mg/g (mean \pm SE) at 45 days to 115.31 ± 0.63 mg/g (mean \pm SE) at 90 days incubation time (4.25% increase). There was no significant effect of $p\text{CO}_2$ nor any combined effect of the factors (Table 2.2). However, temperature led to a marginal increase in the Mg_{norm} ratios ($p = 0.051$, Table 2.2).

Sr_{norm} ratios were altered over incubation time ($p = 0.005$, Table 2) at both temperature treatments (Figure 2.2C). The mean value of the Sr_{norm} ratio at 27 °C increased by 2.38% from day 45 (3.36 ± 0.04 mg/g, mean \pm SE) to day 90 (3.44 ± 0.02 mg/g, mean \pm SD). Similarly, the mean value of Sr_{norm} ratio at 32 °C increased from 45 days (mean \pm SD, 3.30 ± 0.04 mg/g) to 90 days (3.47 ± 0.06 mg/g, mean \pm SD) incubation time (5.15% increase). However, there was no significant effect of combined stressor factors nor solely stressor factors on Sr_{norm} ratios (Table 2.2).

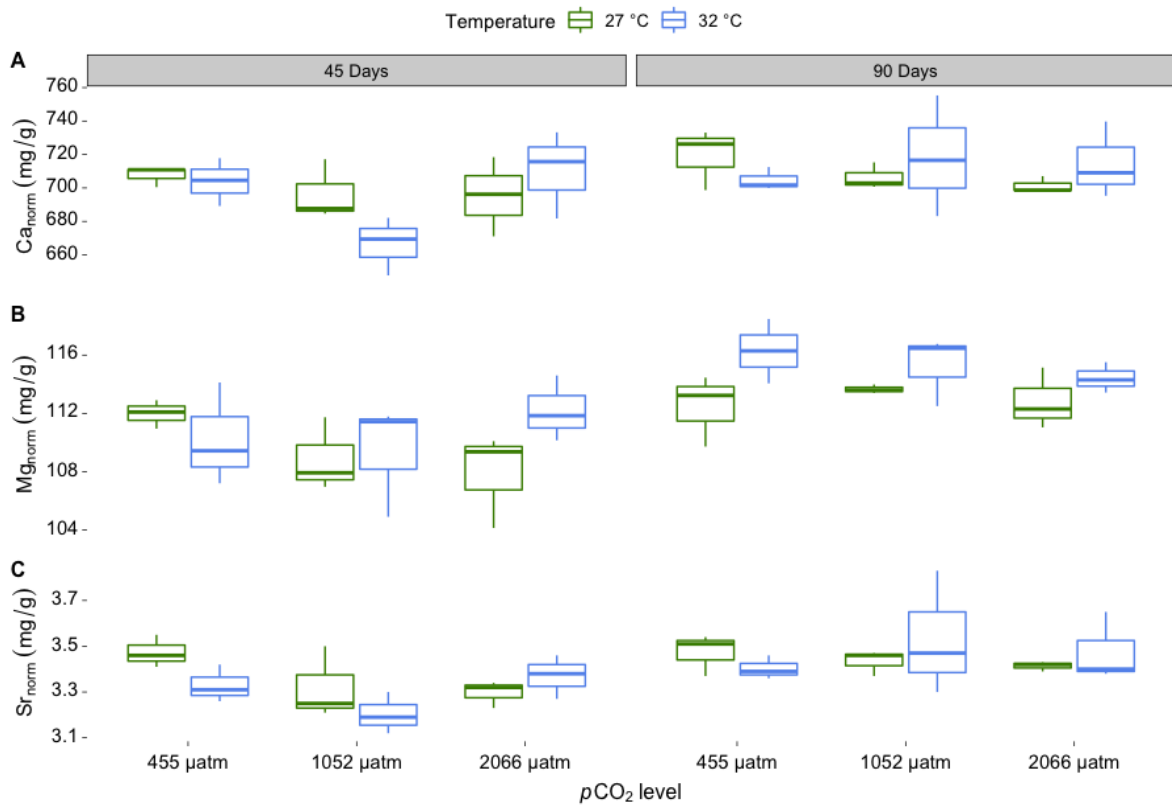


Figure 2.2. Ratios between skeletal mineral element to total skeletal material (**A**) Ca_{norm} ratios (mg/g), (**B**) Mg_{norm} ratios (mg/g), and (**C**) Sr_{norm} ratios (mg/g) in *A. yairi* exposed to elevated temperatures levels (27 °C and 32 °C) crossed with increased $p\text{CO}_2$ concentrations (455 μatm , 1052 μatm and 2066 μatm) measured after 45 and 90 days of incubation ($n = 36$).

Table 2.2. Summary of three-way ANOVA results for the skeletal mineral ratios of *A. yairi* exposed to temperature (27 °C, 32 °C) crossed with elevated $p\text{CO}_2$ (455 μatm , 1052 μatm , 2066 μatm) treatments for 45 and 90 days incubation time. Bold terms indicate a significant difference ($p < 0.05$).

Skeletal mineral ratio	df	F	Pr (<F)	Post-hoc test result*
Mg/Ca ratio				
Incubation time	1	4.319	0.049	90 days > 45 days
$p\text{CO}_2$	2	0.915	0.414	
Temperature	1	5.144	0.033	32 °C > 27 °C
Incubation time: $p\text{CO}_2$	2	0.715	0.500	
Incubation time: temperature	1	0.039	0.845	
$p\text{CO}_2$: temperature	2	0.478	0.626	
Incubation time: $p\text{CO}_2$: temperature	2	5.143	0.014	n.s., Supplementary Materials Table S2.1
Residuals	24			
Sr/Ca ratio				
Incubation time	1	9.027	0.006	90 days > 45 days
$p\text{CO}_2$	2	0.405	0.671	
Temperature	1	0.481	0.495	
Incubation time: $p\text{CO}_2$	2	1.794	0.188	
Incubation time: temperature	1	1.519	0.230	
$p\text{CO}_2$: temperature	2	2.016	0.155	
Incubation time: $p\text{CO}_2$: temperature	2	1.132	0.339	
Residuals	24			
Ca_{norm} ratio				
Incubation time	1	4.951	0.036	90 days > 45 days
$p\text{CO}_2$	2	1.242	0.307	
Temperature	1	0.043	0.838	
Incubation time: $p\text{CO}_2$	2	1.711	0.202	
Incubation time: temperature	1	0.59	0.450	
$p\text{CO}_2$: temperature	2	1.471	0.250	
Incubation time: $p\text{CO}_2$: temperature	2	1.65	0.213	
Residuals	24			

Mg _{norm} ratio				
Incubation time	1	24.523	0.001	90 days > 45 days
$p\text{CO}_2$	2	0.582	0.566	
Temperature	1	4.206	0.051	32 °C > 27 °C
Incubation time: $p\text{CO}_2$	2	0.616	0.548	
Incubation time: temperature	1	0.621	0.438	
$p\text{CO}_2$: temperature	2	0.609	0.552	
Incubation time: $p\text{CO}_2$: temperature	2	2.133	0.140	
Residuals	24			
Sr _{norm} ratio				
Incubation time	1	9.814	0.005	90 days > 45 days
$p\text{CO}_2$	2	0.500	0.613	
Temperature	1	0.156	0.696	
Incubation time: $p\text{CO}_2$	2	1.862	0.177	
Incubation time: temperature	1	1.405	0.248	
$p\text{CO}_2$: temperature	2	1.655	0.212	
Incubation time: $p\text{CO}_2$: temperature	2	0.707	0.503	
Residuals	24			

* Tukey HSD post hoc tests were performed where ANOVA results indicated significant effects of one or several factors (incubation time, $p\text{CO}_2$, temperature) with p-values adjusted for multiple testing (p_{adj}).

2.3.2. Skeletal microstructure

High magnification SEM micrographs showed marked differences in skeletal structure between low $p\text{CO}_2$ (455 μatm) compared to medium and high $p\text{CO}_2$ treatments (1052 μatm , 2066 μatm , respectively) at both ambient and high temperatures (27 °C, 32 °C, respectively). The skeletal structure in low $p\text{CO}_2$ crossed with ambient (27 °C: 455 μatm) and high temperatures (32 °C: 455 μatm) revealed no remarkable differences between 45-day and 90-day incubation time. The stereom pores were arranged equally in shape and the aperture pores of the inner matrix were relatively equal in shape, while the trabecular surface was smooth (Figure 2.3A,B,G,H and Table 2.3).

In contrast, after 45-day and 90-day incubation times, the skeleton from medium and high $p\text{CO}_2$ treatments at ambient temperatures showed stereom structures that were more variable in shape compared to the control treatment, and signs of degradation, i.e., dissolution, were observed on the surface of the trabeculae (Figure 2.3C–F and Table 2.3). Furthermore, under high temperatures, these medium and high $p\text{CO}_2$ treatments in addition result in signs of skeletal degradation observed at the trabeculae surface, while the apertures of the inner matrix pores were wider (i.e., un-equal in shape) compared to the control treatment and the ambient temperature crossed with medium and high $p\text{CO}_2$ treatments (Figure 2.3I–L and Table 2.3).

Table 2.3. Skeletal microstructure characteristics of *A. yairi* under crossed temperatures and $p\text{CO}_2$ conditions at different incubation times as observed with scanning electron microscopy (SEM).

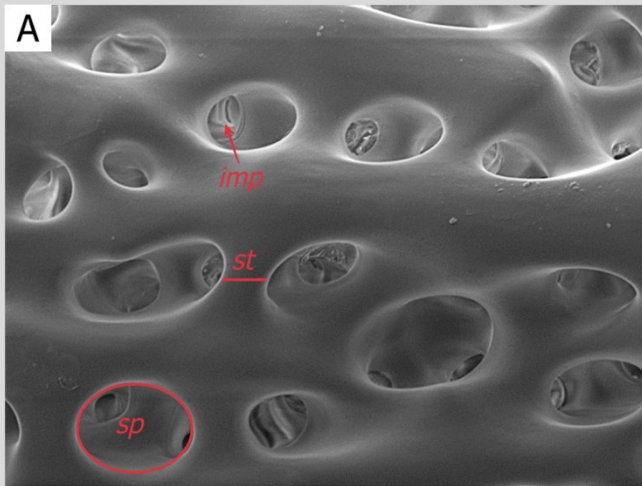
Incubation time	Temperature	$p\text{CO}_2$	Skeletal surface	Stereom pores	Inner matrix pores
45 days	27 °C	455 μatm	ND	ES	EP
		1052 μatm	DS	US	EP
		2066 μatm	DS	US	UP
	32 °C	455 μatm	ND	ES	EP
		1052 μatm	DS	US	UP
		2066 μatm	HD	HU	UP
90 days	27 °C	455 μatm	ND	ES	EP
		1052 μatm	DS	US	EP
		2066 μatm	DS	US	UP
	32 °C	455 μatm	ND	ES	EP
		1052 μatm	DS	US	UP
		2066 μatm	HD	HU	UP

Note: ND: the skeleton surface is smooth and has no signs of degradation; DS: the skeleton surface had degradation signs; HD: the skeleton surface had high degradation signs; ES: the stereom pores were equal in shape; US: the stereom pores were un-equal in shape; HU: the stereom pores were highly un-equal in shape; EP: the inner matrix aperture pores were relatively equal in shape; UP: the inner matrix aperture pores were relatively un-equal in shape (wider). $n = 12$.

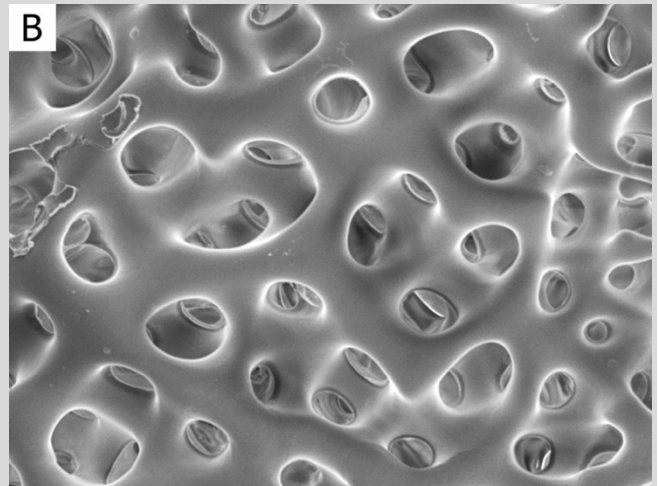
45 days

90 days

27 °C: 455 µatm

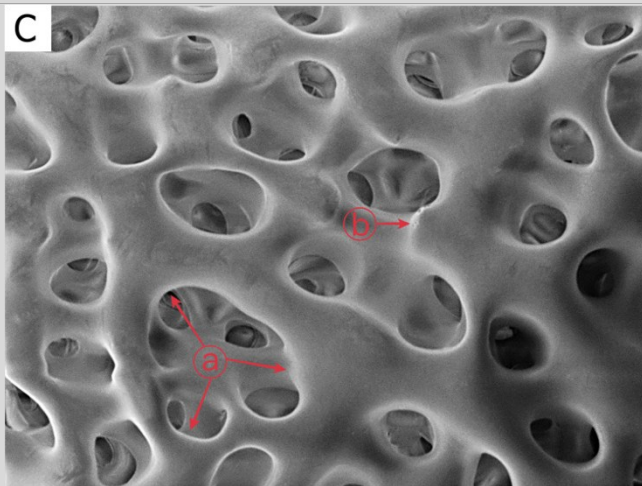


SEM HV: 5.0 kV WD: 16.28 mm
 SEM MAG: 3.00 kx Det: SE 20 µm
 VEGA3 TESCAN
 ZMT-Bremen

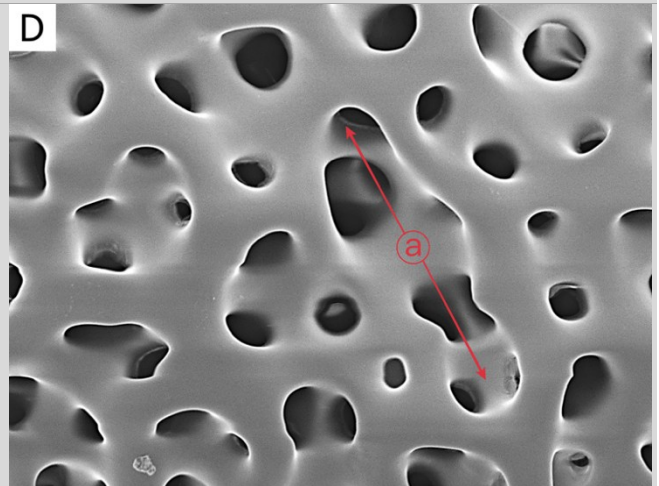


SEM HV: 5.0 kV WD: 16.20 mm
 SEM MAG: 3.00 kx Det: SE 20 µm
 VEGA3 TESCAN
 ZMT-Bremen

27 °C: 1052 µatm

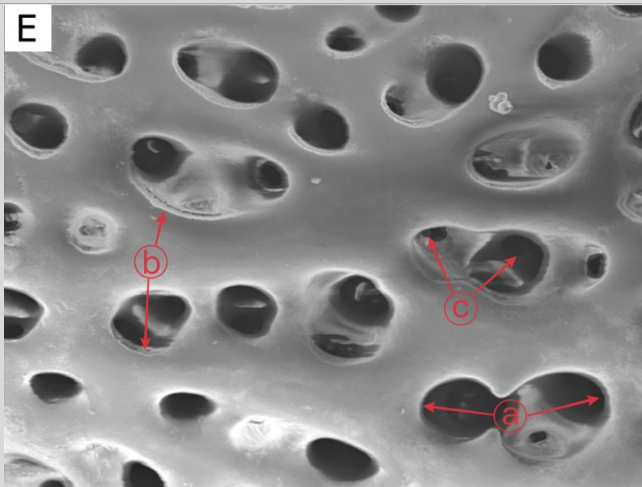


SEM HV: 5.0 kV WD: 16.30 mm
 SEM MAG: 3.00 kx Det: SE 20 µm
 VEGA3 TESCAN
 ZMT-Bremen

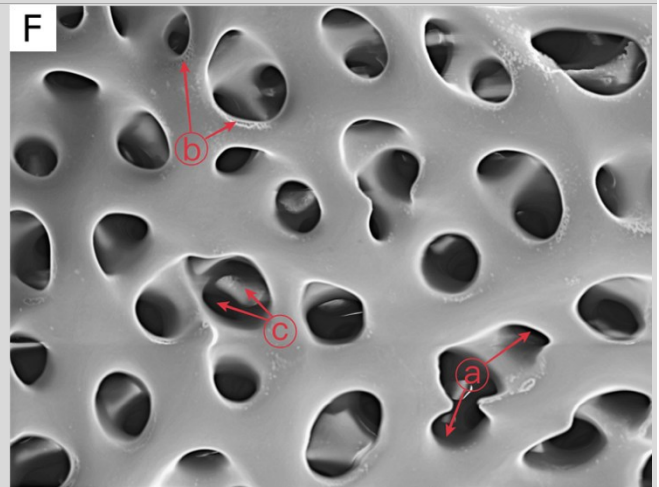


SEM HV: 5.0 kV WD: 16.33 mm
 SEM MAG: 3.00 kx Det: SE 20 µm
 VEGA3 TESCAN
 ZMT-Bremen

27 °C: 2066 µatm



SEM HV: 5.0 kV WD: 16.44 mm
 SEM MAG: 3.00 kx Det: SE 20 µm
 VEGA3 TESCAN
 ZMT-Bremen



SEM HV: 5.0 kV WD: 16.30 mm
 SEM MAG: 3.00 kx Det: SE 20 µm
 VEGA3 TESCAN
 ZMT-Bremen

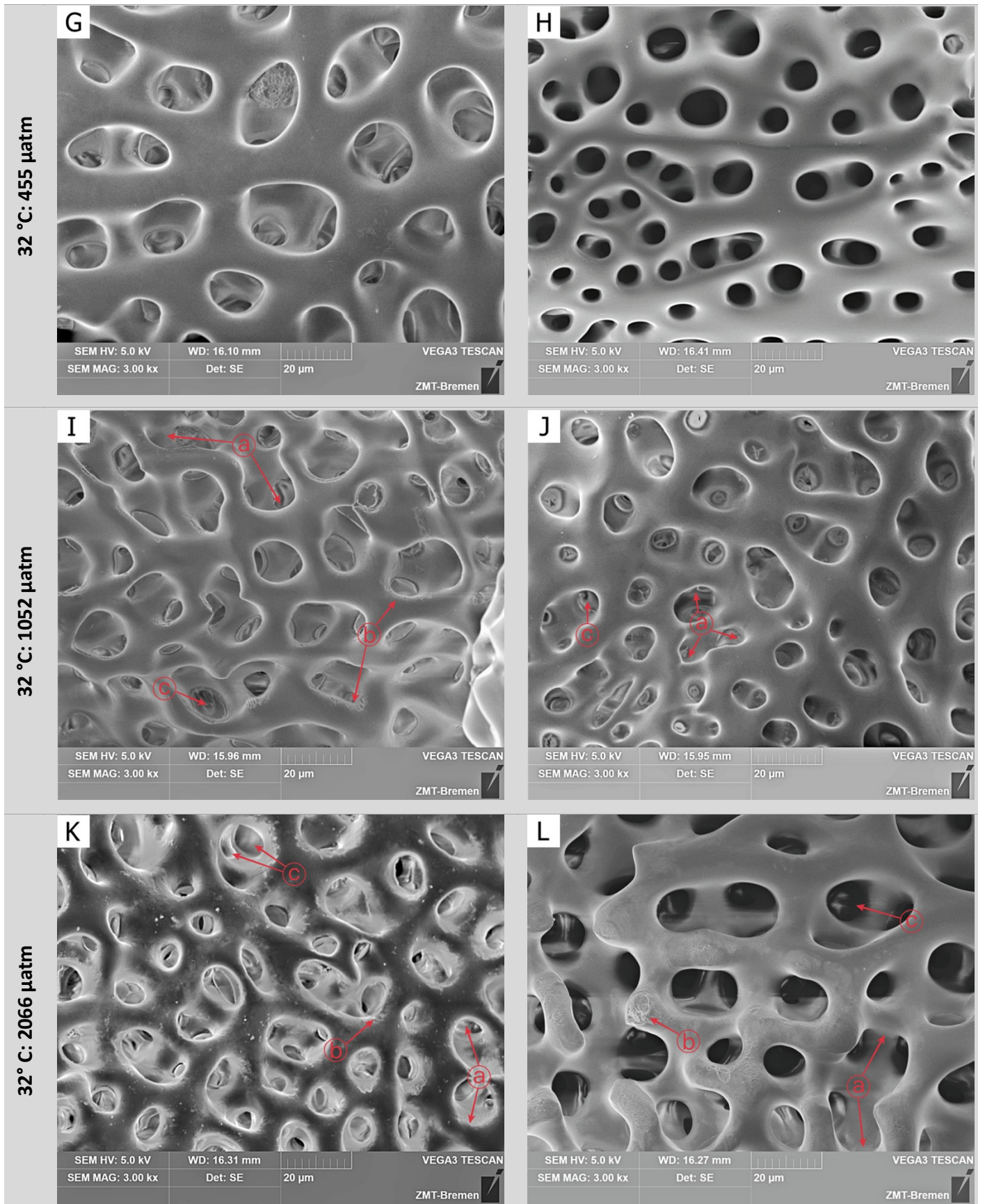


Figure 2.3. SEM micrographs of the skeletal microstructure of *A. yairi* cultured under two temperature levels (27 °C and 32 °C) crossed with three $p\text{CO}_2$ concentrations (455 µatm, 1052 µatm and 2066 µatm).

Stereom microstructure after 45 (A,C,E,G,I,K) and 90 days (B,D,F,H,J,L) of incubation time. *sp*: stereom pore; *st*: skeleton trabeculae; *imp*: stereom inner matrix pore; ① the galleries stereom pores are less-equal in shape; ② dissolution in calcium carbonate skeleton; ③ increased size of inner matrix aperture pores. Technical image acquisition, SEM mode: SE, SEM HV: 5.0 kV, SEM magnification: 3000×.

2.4. Discussion

Our results imply that temperature plays a primary regulatory role in Mg concentration in the skeletal carbonate of *A. yairi*, where the Mg/Ca ratios increase under high-temperatures. This corroborates results from previous studies that found higher Mg concentrations associated with higher temperatures in echinoid and asteroid species (Chave, 1954; Weber, 1969; Weber, 1973). This temperature association was previously attributed to kinetic factors affecting ion discrimination (Weber, 1973) and also to the physiological mechanisms that control Mg absorption in cells (Rosenthal et al., 1997) during the biomineralization process. The increased Mg content of HMC was connected to an amorphous calcium magnesium carbonate (ACMC) precursor (Purgstaller et al., 2021; Radha et al., 2012). At high temperatures, the aqueous Mg²⁺ solvation energy barrier becomes lower (Di Lorenzo et al., 2018); hence this condition might favor more Mg²⁺ to be incorporated into the calcite lattice, encouraging the formation of ACMC, which later transforms into HMC.

Echinoderms are generally considered relatively poor regulators of internal acid–base balance, where the range of regulatory capacities is species-specific (Stumpp & Hu, 2017). In hypercapnic conditions (high *p*CO₂, low pH), echinoderms increase the bicarbonate concentration in their coelomic fluid and practice passive skeletal dissolution to support internal acid–base regulatory functions due to acidosis (Miles et al., 2007). Higher Mg concentrations in the skeleton in conjunction with a degradation in the inner skeleton (see Section 2.3.2) due to skeletal dissolution, as documented in the current studies, support the assumption of a trade-off mechanism (Asnaghi et al., 2014; Khalil et al., 2023). The released HMC mineral is then used as an active buffering mechanism to compensate for changes in internal pH that may help to avoid or reduce physiological impacts.

We noticed that no single (temperature or *p*CO₂) nor combined stressor treatment affected skeletal Sr (Sr/Ca and Sr_{norm}) in *A. yairi*. This contrasts with previous studies on the starfish

Asterias rubens (Borremans et al., 2009) and the sea urchin *P. lividus* (Hermans et al., 2010), which reported that the Sr/Ca ratio depended on temperature. These contrasting results indicate a species-specific skeletal Sr control mechanism in the echinoderm group that may respond to the stressors. The calcification rates might play an important role in skeletal Sr precipitation rather than direct dependence on temperature. It is difficult to discriminate the effects of temperature and $p\text{CO}_2$ on skeletal Sr. Our data indicated that the skeletal Sr was increased over incubation time in all treatment combinations (Supplementary Materials Figure S2.2) except the 27 °C: 455 μatm treatment, assuming that temperature and $p\text{CO}_2$ might have an indirect effect on skeletal Sr through their control over the calcification process (Kısakürek et al., 2008; Lorens, 1981; Russell et al., 2004; Weiner & Dove, 2003), which are common in biogenic calcites (Lea et al., 1999; Stoll et al., 2002). However, the incorporation pathways of Sr into the echinoderm ACC are still poorly understood, so further studies are needed.

We found a strong correlation between skeletal Sr and skeletal Mg ($R^2 = 0.04$, $p < 0.001$, Supplementary Materials Figure S2.3), as Sr_{norm} increases with increasing Mg_{norm} ratio. Hence, Mg might play a role in affecting the Sr precipitation. Sr ions cannot easily substitute for Ca ions due to differences in cations ions size and weight (Sr^{2+} ionic radius of 1.18 Å: Ca^{2+} ionic radius of 1.00 Å (Shannon, 1976)), which makes them incompatible in calcite (Tesoriero & Pankow, 1996). High concentrations of Mg^{2+} (ionic radius of 0.72 Å (Shannon, 1976)) that are incorporated in inorganic calcite can distort the crystal lattice (i.e., lattice deformation), which increases the size of calcium lattice positions and thus allows for increased incorporation of Sr^{2+} (Mucci & Morse, 1983).

Similar to skeletal Sr, we found no direct influence of temperature or $p\text{CO}_2$ on the Ca_{norm} ratio (Table 2.2). However, the highest inter-individual variability of Ca_{norm} indicates that temperature and/or $p\text{CO}_2$ considerably alter the production of skeletal Ca in *A. yairi*, where Ca_{norm} ratios exhibited an increase with incubation time, except for the treatment of 27 °C: 455 μatm (~703 mg/g) where the ratio was relatively unchanged (Supplementary Materials Figure S2.4). CaCO_3 is more soluble at lower temperatures (Zeebe & Wolf-Gladrow, 2001) and high $p\text{CO}_2$ (Ries et al., 2009). Under OW conditions, starfish seem to be able to boost their capacity to control calcification through the modulation of the intracellular calcifying fluids pH to produce CaCO_3 . This might provide them with higher resistance and resilience towards the effects of OA. The increased energetic costs of this physiological response are indicated by

elevated respiration rates (Khalil et al., 2023). Hence, in the long term, this phenotypic plasticity and biocalcification control mechanism might have further physiological implications for the starfish.

The hypercapnic conditions of the high $p\text{CO}_2$ treatment in our experiment have resulted in visible adverse effects on the skeletal structures in both ambient as well as elevated temperatures (Figure 2.3, Table 2.3). We detected changes in the stereom pores, the inner matrix pores and degradation of the skeleton surface through reduced deposition or dissolution, which increased over incubation time in the starfish that were exposed to medium and high $p\text{CO}_2$. These skeletal alterations might be due to the thin layer of epithelial tissue covering the starfish body wall (Dubois & Chen, 1989), which acts as a protective membrane between the skeleton and the seawater (Melzner et al., 2020). Furthermore, the degradation of the epithelial tissue could also explain why the combination of OW with OA enhances the degradation of the skeletal structure that was observed in the high $p\text{CO}_2$ treatment (32 °C: 2066 μatm). We hypothesize that the epithelial tissue might become weaker in its function due to degradation of the epithelium cells during long-term experiments. Epithelial tightness is controlled by a protein series that molds a seal among epithelial cells (Melzner et al., 2020), which are sensitive to elevated temperature.

The seawater chemistry factor, which was underlying the altered skeletal structure in *A. yairi* might involve calcium carbonate saturation state (Ω). Skeletal degradation provides evidence that the skeleton of *A. yairi* was negatively affected by lowered calcite saturation state (Ω_{ca}) as a function of increasing $p\text{CO}_2$ (Table 2.1), which directly affects the biomineralization and dissolution of the CaCO_3 in skeletal structures (Feely et al., 2009; Watson et al., 2012). Near $\Omega_{\text{ca}} \sim 3$, we found stereom alteration and degradation signs in trabeculae, which indicates that *A. yairi* was facing difficulty in producing and maintaining their skeleton compared to low $p\text{CO}_2$ treatments ($\Omega_{\text{ca}} > 5$). Previous studies found that the skeletal morphometric development of echinoid (e.g., sea urchin *L. variegatus*) was significantly affected by $\Omega_{\text{ca}} 2.53$ (Challener et al., 2013). Furthermore, increased susceptibility of the skeleton to dissolution through OA was suggested to be due to the skeleton composed of HMC, which is 30 times more soluble than pure calcite (McClintock et al., 2011; Politi et al., 2004). When the qualitative approach depicts changes in the skeleton micro-morphology because of exposure to elevated $p\text{CO}_2$ and temperature (Table 2.3, Figure 2.3), further investigation using quantitative analysis (e.g.,

stereom and inner matrix pore size) is required to quantify the alteration magnitude in skeleton microstructure as the deleterious impact of OA and OW (Hazan et al., 2014; Johnson et al., 2020).

Under OW and OA scenarios, calcifying marine organisms are expected to face unfavorable conditions to produce and maintain their skeletal HMC in order to sustain their biomechanical functions. Phenotypic plasticity requires re-allocation of energy as a trade-off and may represent a potential key mechanism for species viability (Gibbin et al., 2017). For *A. yairi*, this mechanism might reflect strategies to maintain their skeletal HMC in a low pH environment by modulating their cellular chemistry to create isolated microenvironments of deposition, producing the specific mineral they necessitate, which involves significant energy re-allocation (Stumpp et al., 2012). Since the asterinid starfish produces HMC, which is more soluble than calcite and aragonite, it signifies that more energy will be required to preserve the calcification process as the mechanism in both constructing and maintaining their skeletal components, leading to energy trade-offs against other physiological processes (Khalil et al., 2023; Wood et al., 2008).

Changes in the shape of the stereom pores and degradation of the starfish skeleton potentially have implications for skeletal strength, stiffness, and function. Weakening of the structure possibly will reduce locomotion performance and result in a lower ability to resist predators and to face ocean currents, which then conveys consequences to the benthic community structure.

2.5. Acknowledgements

We would like to thank Andreas Kunzmann (ZMT, Bremen, Germany) for his advice on the starfish *A. yairi* as a model organism. Many thanks are due to the ZMT laboratory staff, namely Jule Mawick, Sebastian Flotow, Silvia Hardenberg, José Garcia, Nico Steinel, Matthias Birkicht and Fabian Hüge. This research project was supported by the Academy Doctoral Research—Grant Leibniz Centre for Tropical Marine Research (ZMT), Germany and the Ministry of Education, Culture, Research, and Technology (MoECRT), Republic of Indonesia—Asian Development Bank (ADB) AKSI Project [grant number L3749-INO].

2.6. Supplementary materials

Animal collection and acclimation

To prepare the *Aquilonastra yairi* specimens for the experiment, they were cleansed from externally attached materials, thoroughly rinsed with flowing seawater repeatedly and small forceps to lift the attached debris, and allowed to acclimate in a communal tank with a recirculating water system at the ambient temperature of ≈ 27 °C for seven days. Afterwards, they were randomly distributed into 18 experimental aquaria (25 litres), illuminated with LED lamps (Aquaillumination® Hydra 52 HD) at 25–30 $\mu\text{mol photons m}^{-2} \text{s}^{-1}$. After an additional seven-day acclimation phase, the main experiment was started. No visual sign of stress (i.e., discoloration and erratic flipping) was observed during the acclimation period. During acclimation and experimental exposure, the starfish *A. yairi* were able to feed on living diatoms that naturally grow at the aquaria walls and deposited detritus flocs.

Seawater chemistry control and manipulation

Temperature, salinity, and pH_{NBS} (pH electrodes calibrated in diluted National Bureau of Standards buffers) were measured three times per week using a calibrated multielectrode portable probe (WTW Multiline 3630 IDS, Xylem Analytics, Weilheim, Germany). The $\text{pH}_{\text{total scale}}$ was measured weekly via spectrophotometry (Shimadzu UV-1700 Pharma Spec UV-Vis Spectrophotometer) following SOP 6b [1] using the indicator dye *m*-cresol purple (Sigma-Aldrich). Seawater samples for total alkalinity (A_T) and dissolved inorganic carbon (DIC) analysis were collected weekly in 500-mL borosilicate glass vials, poisoned with 200- μL of saturated mercuric chloride (HgCl_2) solution and refrigerated until analysis. A_T and DIC were measured according to the best practice of ocean acidification seawater measurement protocols (Dickson et al., 2007). A_T was measured by open-cell potentiometric Gran titration (precision, $\pm 10 \mu\text{mol kg}^{-1}$), and DIC was determined by the colorimetric analytical method using a Shimadzu DIC analyser (precision, $\pm 10 \mu\text{mol kg}^{-1}$). The seawater carbonate system parameters $p\text{CO}_2$, carbonate ion concentration $[\text{CO}_3^{2-}]$, bicarbonate ion concentration $[\text{HCO}_3^-]$, aqueous CO_2 , calcite saturation state (Ω_{Ca}), aragonite saturation state (Ω_{Ar}) were calculated with the program CO_2SYS for Microsoft Excel (Pelletier et al., 2007b), using Hansson (1973) and Mehrbach et al. (1973) refitted by Dickson and Millero (1987) for K_1 and K_2 carbonic acid constants; Dickson (1990) for K_{HSO_4} equilibrium constant; Dickson and Riley (1979) for K_{HF} dissociation constant; Upström (1974) for the boric acid constant ($[\text{B}]_T$); and Mucci (1983) for the stoichiometric calcite solubility constant.

Table S2.1. Tukey HSD post hoc test for the interactive effects of incubation time (45 and 90 days), $p\text{CO}_2$ (455 μatm , 1052 μatm , 2066 μatm) and temperature (27 °C, 32 °C) on skeletal Mg/Ca ratio of *A. yairi* using the ‘agricolae R-package’ for multiple comparisons to interrogate the main effects of incubation time, temperature and $p\text{CO}_2$ (incubation time: $p\text{CO}_2$: temperature, $p = 0.014$, Table 2.2).

Condition	diff.	lwr.	upr.	p_{adj}
90 days:1052 μatm :27 °C vs 45 days:1052 μatm :27 °C	5.4800	-7.3920	18.3520	0.9156
45 days:2066 μatm :27 °C vs 45 days:1052 μatm :27 °C	-1.3833	-14.2553	11.4887	1.0000
90 days:2066 μatm :27 °C vs 45 days:1052 μatm :27 °C	5.3933	-7.4787	18.2653	0.9233
45 days:455 μatm :27 °C vs 45 days:1052 μatm :27 °C	2.3467	-10.5253	15.2187	0.9999
90 days:455 μatm :27 °C vs 45 days:1052 μatm :27 °C	0.0400	-12.8320	12.9120	1.0000
45 days:1052 μatm :32 °C vs 45 days:1052 μatm :27 °C	9.3533	-3.5187	22.2253	0.3220
90 days:1052 μatm :32 °C vs 45 days:1052 μatm :27 °C	5.0967	-7.7753	17.9687	0.9460
45 days:2066 μatm :32 °C vs 45 days:1052 μatm :27 °C	2.0433	-10.8287	14.9153	1.0000
90 days:2066 μatm :32 °C vs 45 days:1052 μatm :27 °C	4.5700	-8.3020	17.4420	0.9741
45 days:455 μatm :32 °C vs 45 days:1052 μatm :27 °C	0.3467	-12.5253	13.2187	1.0000
90 days:455 μatm :32 °C vs 45 days:1052 μatm :27 °C	10.3000	-2.5720	23.1720	0.2077
45 days:2066 μatm :27 °C vs 90 days:1052 μatm :27 °C	-6.8633	-19.7353	6.0087	0.7355
90 days:2066 μatm :27 °C vs 90 days:1052 μatm :27 °C	-0.0867	-12.9587	12.7853	1.0000
45 days:455 μatm :27 °C vs 90 days:1052 μatm :27 °C	-3.1333	-16.0053	9.7387	0.9988
90 days:455 μatm :27 °C vs 90 days:1052 μatm :27 °C	-5.4400	-18.3120	7.4320	0.9192
45 days:1052 μatm :32 °C vs 90 days:1052 μatm :27 °C	3.8733	-8.9987	16.7453	0.9926
90 days:1052 μatm :32 °C vs 90 days:1052 μatm :27 °C	-0.3833	-13.2553	12.4887	1.0000
45 days:2066 μatm :32 °C vs 90 days:1052 μatm :27 °C	-3.4367	-16.3087	9.4353	0.9972
90 days:2066 μatm :32 °C vs 90 days:1052 μatm :27 °C	-0.9100	-13.7820	11.9620	1.0000
45 days:455 μatm :32 °C vs 90 days:1052 μatm :27 °C	-5.1333	-18.0053	7.7387	0.9435
90 days:455 μatm :32 °C vs 90 days:1052 μatm :27 °C	4.8200	-8.0520	17.6920	0.9626
90 days:2066 μatm :27 °C vs 45 days:2066 μatm :27 °C	6.7767	-6.0953	19.6487	0.7494
45 days:455 μatm :27 °C vs 45 days:2066 μatm :27 °C	3.7300	-9.1420	16.6020	0.9945
90 days:455 μatm :27 °C vs 45 days:2066 μatm :27 °C	1.4233	-11.4487	14.2953	1.0000
45 days:1052 μatm :32 °C vs 45 days:2066 μatm :27 °C	10.7367	-2.1353	23.6087	0.1667
90 days:1052 μatm :32 °C vs 45 days:2066 μatm :27 °C	6.4800	-6.3920	19.3520	0.7951
45 days:2066 μatm :32 °C vs 45 days:2066 μatm :27 °C	3.4267	-9.4453	16.2987	0.9973
90 days:2066 μatm :32 °C vs 45 days:2066 μatm :27 °C	5.9533	-6.9187	18.8253	0.8657
45 days:455 μatm :32 °C vs 45 days:2066 μatm :27 °C	1.7300	-11.1420	14.6020	1.0000
90 days:455 μatm :32 °C vs 45 days:2066 μatm :27 °C	11.6833	-1.1887	24.5553	0.1000

45 days:455 μ atm:27 °C vs 90 days:2066 μ atm:27 °C	-3.0467	-15.9187	9.8253	0.9990
90 days:455 μ atm:27 °C vs 90 days:2066 μ atm:27 °C	-5.3533	-18.2253	7.5187	0.9266
45 days:1052 μ atm:32 °C vs 90 days:2066 μ atm:27 °C	3.9600	-8.9120	16.8320	0.9912
90 days:1052 μ atm:32 °C vs 90 days:2066 μ atm:27 °C	-0.2967	-13.1687	12.5753	1.0000
45 days:2066 μ atm:32 °C vs 90 days:2066 μ atm:27 °C	-3.3500	-16.2220	9.5220	0.9978
90 days:2066 μ atm:32 °C vs 90 days:2066 μ atm:27 °C	-0.8233	-13.6953	12.0487	1.0000
45 days:455 μ atm:32 °C vs 90 days:2066 μ atm:27 °C	-5.0467	-17.9187	7.8253	0.9493
90 days:455 μ atm:32 °C vs 90 days:2066 μ atm:27 °C	4.9067	-7.9653	17.7787	0.9578
90 days:455 μ atm:27 °C vs 45 days:455 μ atm:27 °C	-2.3067	-15.1787	10.5653	0.9999
45 days:1052 μ atm:32 °C vs 45 days:455 μ atm:27 °C	7.0067	-5.8653	19.8787	0.7118
90 days:1052 μ atm:32 °C vs 45 days:455 μ atm:27 °C	2.7500	-10.1220	15.6220	0.9996
45 days:2066 μ atm:32 °C vs 45 days:455 μ atm:27 °C	-0.3033	-13.1753	12.5687	1.0000
90 days:2066 μ atm:32 °C vs 45 days:455 μ atm:27 °C	2.2233	-10.6487	15.0953	1.0000
45 days:455 μ atm:32 °C vs 45 days:455 μ atm:27 °C	-2.0000	-14.8720	10.8720	1.0000
90 days:455 μ atm:32 °C vs 45 days:455 μ atm:27 °C	7.9533	-4.9187	20.8253	0.5470
45 days:1052 μ atm:32 °C vs 90 days:455 μ atm:27 °C	9.3133	-3.5587	22.1853	0.3276
90 days:1052 μ atm:32 °C vs 90 days:455 μ atm:27 °C	5.0567	-7.8153	17.9287	0.9487
45 days:2066 μ atm:32 °C vs 90 days:455 μ atm:27 °C	2.0033	-10.8687	14.8753	1.0000
90 days:2066 μ atm:32 °C vs 90 days:455 μ atm:27 °C	4.5300	-8.3420	17.4020	0.9757
45 days:455 μ atm:32 °C vs 90 days:455 μ atm:27 °C	0.3067	-12.5653	13.1787	1.0000
90 days:455 μ atm:32 °C vs 90 days:455 μ atm:27 °C	10.2600	-2.6120	23.1320	0.2119
90 days:1052 μ atm:32 °C vs 45 days:1052 μ atm:32 °C	-4.2567	-17.1287	8.6153	0.9846
45 days:2066 μ atm:32 °C vs 45 days:1052 μ atm:32 °C	-7.3100	-20.1820	5.5620	0.6601
90 days:2066 μ atm:32 °C vs 45 days:1052 μ atm:32 °C	-4.7833	-17.6553	8.0887	0.9645
45 days:455 μ atm:32 °C vs 45 days:1052 μ atm:32 °C	-9.0067	-21.8787	3.8653	0.3724
90 days:455 μ atm:32 °C vs 45 days:1052 μ atm:32 °C	0.9467	-11.9253	13.8187	1.0000
45 days:2066 μ atm:32 °C vs 90 days:1052 μ atm:32 °C	-3.0533	-15.9253	9.8187	0.9990
90 days:2066 μ atm:32 °C vs 90 days:1052 μ atm:32 °C	-0.5267	-13.3987	12.3453	1.0000
45 days:455 μ atm:32 °C vs 90 days:1052 μ atm:32 °C	-4.7500	-17.6220	8.1220	0.9661
90 days:455 μ atm:32 °C vs 90 days:1052 μ atm:32 °C	5.2033	-7.6687	18.0753	0.9384
90 days:2066 μ atm:32 °C vs 45 days:2066 μ atm:32 °C	2.5267	-10.3453	15.3987	0.9998
45 days:455 μ atm:32 °C vs 45 days:2066 μ atm:32 °C	-1.6967	-14.5687	11.1753	1.0000
90 days:455 μ atm:32 °C vs 45 days:2066 μ atm:32 °C	8.2567	-4.6153	21.1287	0.4943
45 days:455 μ atm:32 °C vs 90 days:2066 μ atm:32 °C	-4.2233	-17.0953	8.6487	0.9855
90 days:455 μ atm:32 °C vs 90 days:2066 μ atm:32 °C	5.7300	-7.1420	18.6020	0.8910
90 days:455 μ atm:32 °C vs 45 days:455 μ atm:32 °C	9.9533	-2.9187	22.8253	0.2455

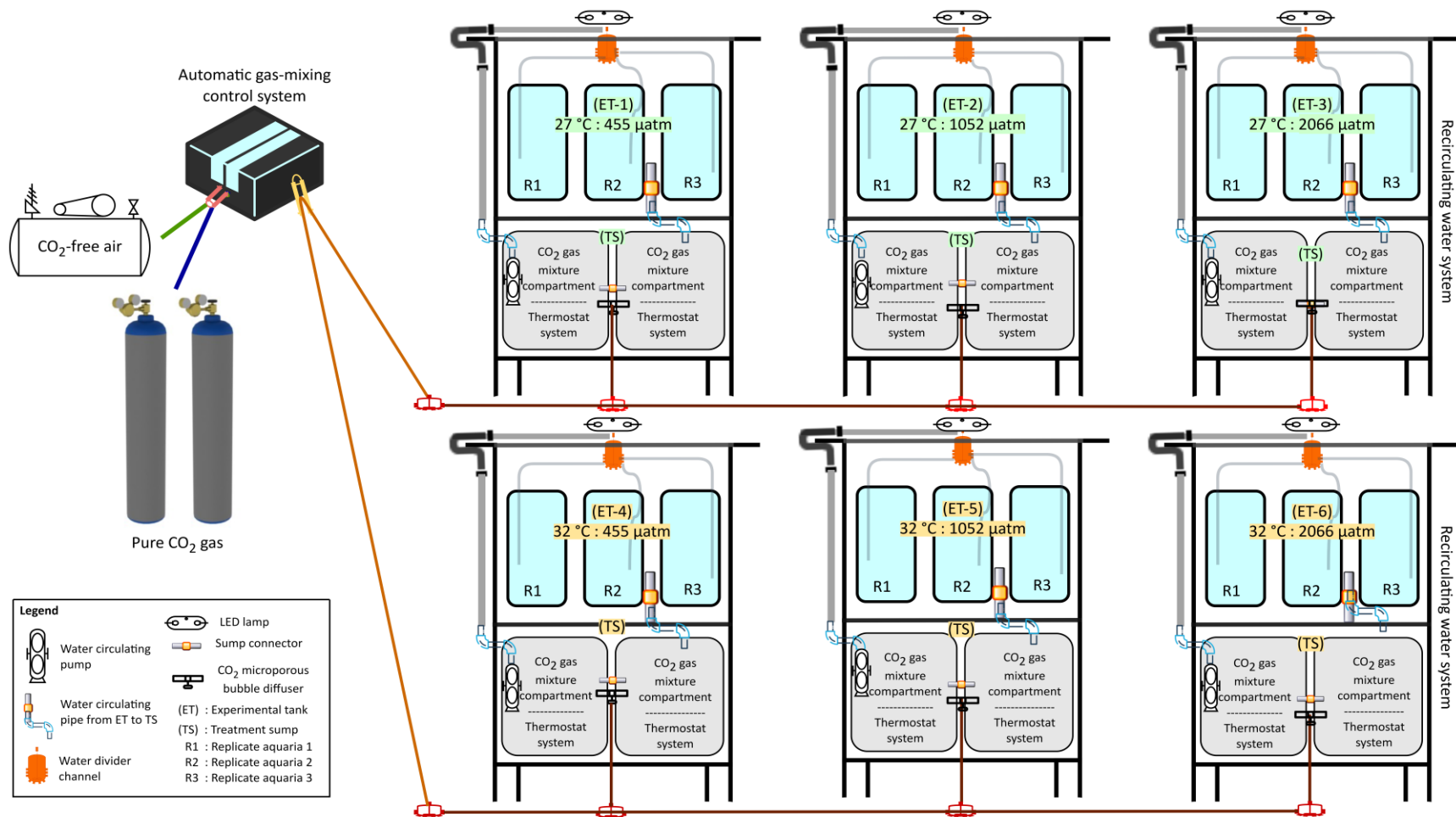


Figure S2.1. Schematic of ocean acidification and ocean warming experimental design with a fully factorial combination of low $p\text{CO}_2$ (455 μatm), moderate $p\text{CO}_2$ (1052 μatm), and high $p\text{CO}_2$ (2066 μatm) treatments with ambient temperature (27 °C) and high temperature (32 °C) treatments.

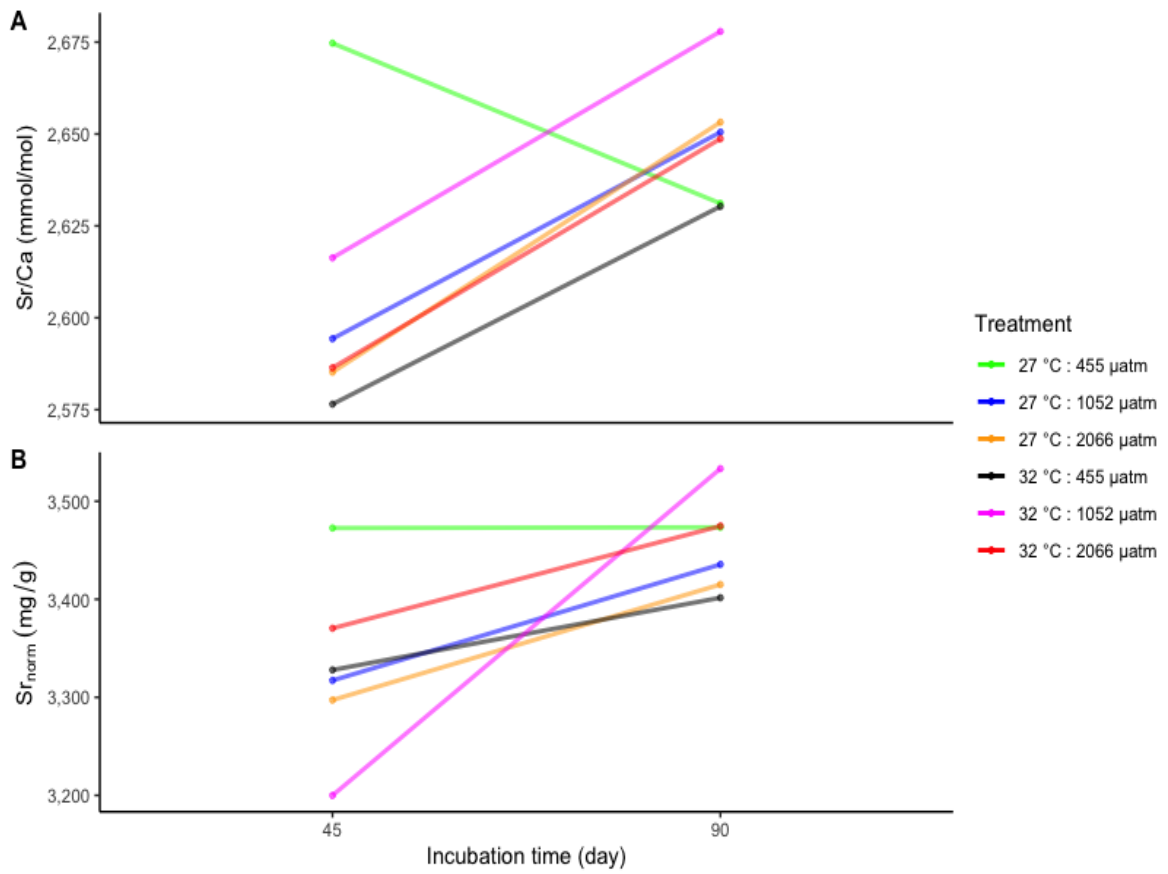


Figure S2.2. Skeletal Sr values over incubation time in *A. yairi* exposed to elevated temperatures levels (27 °C and 32 °C) crossed with increased pCO₂ concentrations (455 µatm, 1052 µatm, and 2066 µatm). **(A)** Sr/Ca ratio (mmol/mol), **(B)** Sr_{norm} ratio (mg/g). Data were presented as mean ($n = 36$).

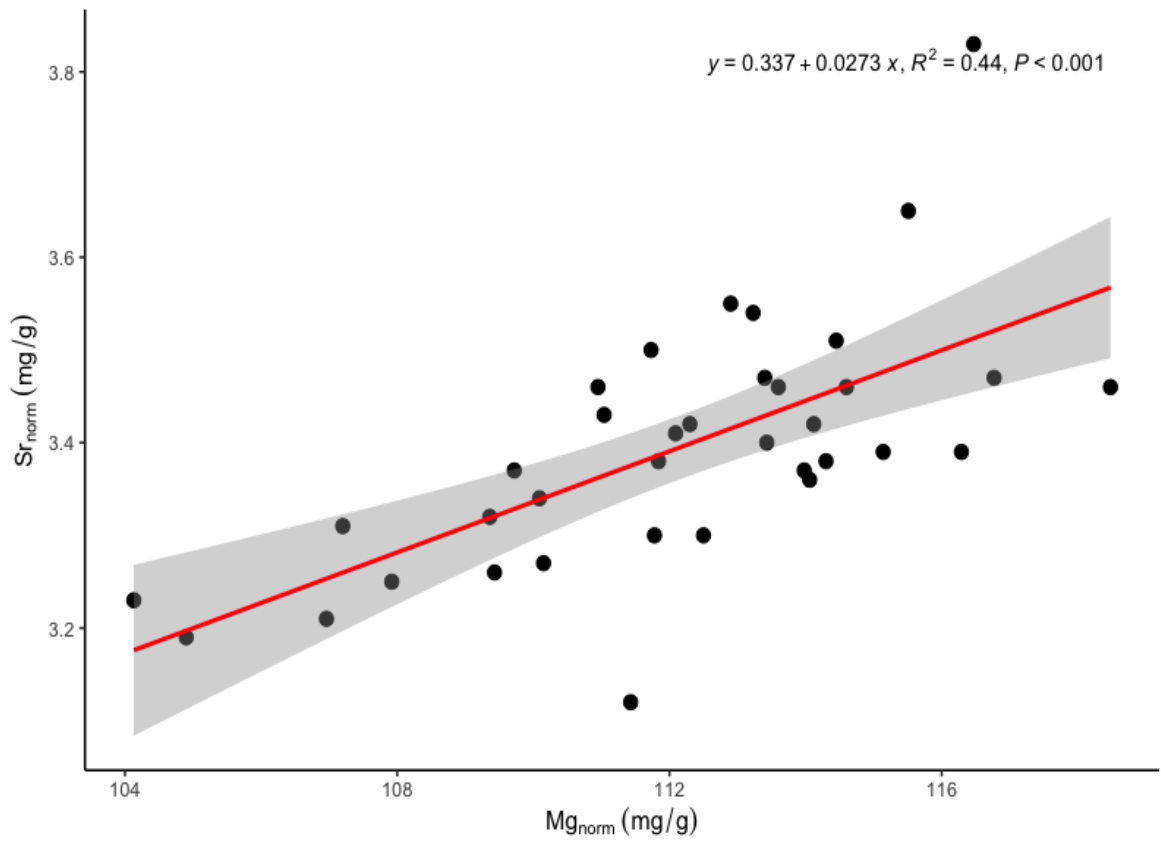


Figure S2.3. Correlation of Sr_{norm} ratios (mg/g) against Mg_{norm} ratios (mg/g) ($R^2 = 0.44$, $F_{1, 34} = 26.78$, $p = 1.019 \times 10^{-5}$) in *A. yairi* exposed to elevated temperatures levels (27 °C and 32 °C) crossed with increased $p\text{CO}_2$ concentrations (455 μatm , 1052 μatm , and 2066 μatm). $n = 36$.

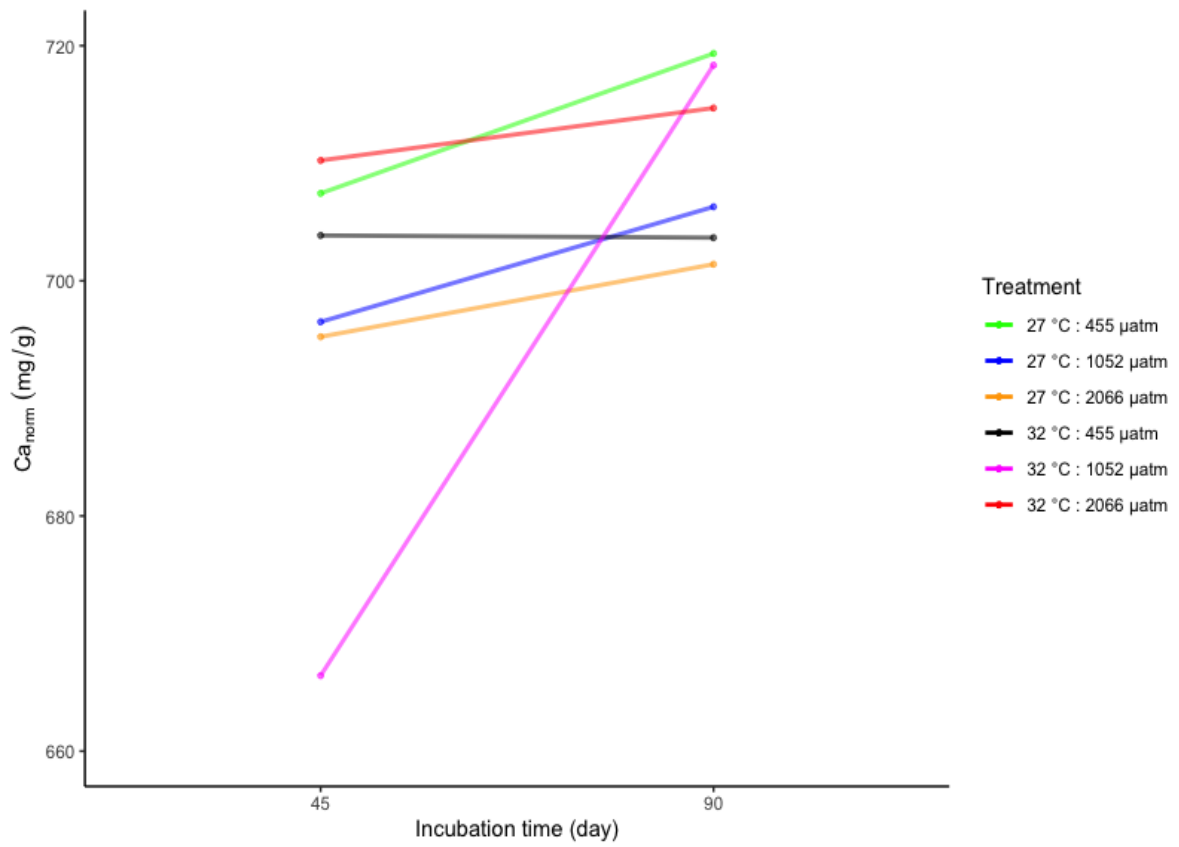


Figure S2.4. Skeletal Ca_{norm} (mg/g) ratio over incubation time in *A. yairi* exposed to elevated temperatures levels (27 °C and 32 °C) crossed with increased pCO_2 concentrations (455 μatm , 1052 μatm , and 2066 μatm). Data were presented as mean ($n = 36$).

Chapter 3. Long-term physiological responses to combined ocean acidification and warming show energetic trade-offs in an asterinid starfish

This work has been *published* in *Coral Reefs* 42, 845–858, <https://doi.org/10.1007/s00338-023-02388-2>.

Munawar Khalil^{1,2,3,*}, **Steve S. Doo**^{1,4}, **Marleen Stuhr**¹, and **Hildegard Westphal**^{1,2,4}

¹ Leibniz Centre for Tropical Marine Research (ZMT), 28359 Bremen, Germany;

² Faculty of Geosciences, University of Bremen, 28359 Bremen, Germany

³ Department of Marine Science, Faculty of Agriculture, Universitas Malikussaleh, Reuleut Main Campus, Aceh 24355, Indonesia

⁴ Physical Science and Engineering (PSE) and Red Sea Research Center (RSRC), King Abdullah University of Science and Technology (KAUST), Thuwal 23955-6900, Saudi Arabia



REPORT

Long-term physiological responses to combined ocean acidification and warming show energetic trade-offs in an asterinid starfish

Munawar Khalil^{1,2,3} · Steve S. Doo^{1,4} · Marleen Stuhr¹ · Hildegard Westphal^{1,2,4}

Received: 3 November 2022 / Accepted: 26 April 2023 / Published online: 16 May 2023
© The Author(s), under exclusive licence to International Coral Reef Society (ICRS) 2023

Abstract While organismal responses to climate change and ocean acidification are increasingly documented, longer-term (> a few weeks) experiments with marine organisms are still sparse. However, such experiments are crucial for assessing potential acclimatization mechanisms, as well as predicting species-specific responses to environmental change. Here, we assess the combined effects of elevated $p\text{CO}_2$ and temperature on organismal metabolism, mortality, righting activity, and calcification of the coral reef-associated starfish *Aquilonastra yairi*. Specimens were incubated at two temperature levels (27 °C and 32 °C) crossed with three $p\text{CO}_2$ regimes (455 μatm , 1052 μatm , and 2066 μatm)

for 90 days. At the end of the experiment, mortality was not altered by temperature and $p\text{CO}_2$ treatments. Elevated temperature alone increased metabolic rate, accelerated righting activity, and caused a decline in calcification rate, while high $p\text{CO}_2$ increased metabolic rate and reduced calcification rate, but did not affect the righting activity. We document that temperature is the main stressor regulating starfish physiology. However, the combination of high temperature and high $p\text{CO}_2$ showed nonlinear and potentially synergistic effects on organismal physiology (e.g., metabolic rate), where the elevated temperature allowed the starfish to better cope with the adverse effect of high $p\text{CO}_2$ concentration (low pH) on calcification and reduced skeletal dissolution (antagonistic interactive effects) interpreted as a result of energetic trade-offs.

Supplementary Information The online version contains supplementary material available at <https://doi.org/10.1007/s00338-023-02388-2>.

✉ Munawar Khalil
munawar.khalil@leibniz-zmt.de
Steve S. Doo
steve.doo@leibniz-zmt.de
Marleen Stuhr
marleen.stuhr@leibniz-zmt.de
Hildegard Westphal
hildegard.westphal@kaust.edu.sa

- ¹ Leibniz Centre for Tropical Marine Research (ZMT), Fahrenheitstraße 6, 28359 Bremen, Germany
- ² Faculty of Geosciences, University of Bremen, Klagenfurter Str. 2-4, 28359 Bremen, Germany
- ³ Department of Marine Science, Faculty of Agriculture, Universitas Malikussaleh, Reuleut Main Campus, North Aceh 2435, Indonesia
- ⁴ Physical Science and Engineering (PSE) and Red Sea Research Center (RSRC), King Abdullah University of Science and Technology (KAUST), Thuwal 23955-6900, Saudi Arabia

Keywords Starfish *Aquilonastra yairi* · Multiple stressors · Interactive effect · Physiological response · Calcification · Climate change acclimatization

Introduction

Rising CO_2 concentration in the oceans has led to lowered seawater pH, referred to as ocean acidification (OA), while simultaneous ocean warming (OW) and changes in circulation, stratification, nutrient, salinity, and oxygen levels result in complex changes in environmental conditions (Doney et al. 2012). Many marine calcifiers such as foraminifera, mollusks, echinoderms, corals, and coralline algae are expected to be negatively impacted by OA (Kawahata et al. 2019; Figuerola et al. 2021), whereas those organisms that have photosynthesizing or photosymbiotic capabilities (e.g., algae; zooxanthellate corals) also exhibit increased growth (Ries et al. 2009; Cornwall et al. 2017). Generally,

Statement of Contribution

Idea and concept: Personal contribution 95%. M. Khalil developed the idea to focus on the physiochemistry aspect of starfish under ocean acidification and ocean warming, with contributions on method from H. Westphal, S.S. Doo, and M. Stuhr. The research project was supervised by H. Westphal.

Research: Personal contribution 90%. M. Khalil carried out laboratory experiments, conducted starfish respiration measurement, mortality examination, righting behavior observation, quantified the calcification rate of the starfish, analyzed the data, created figures and tables, and interpreted the data.

Manuscript writing: Personal contribution 90%. M. Khalil wrote the initial manuscript, with contributions and improvements from H. Westphal, S.S. Doo, and M. Stuhr.

Abstract

While organismal responses to climate change and ocean acidification are increasingly documented, longer-term (> a few weeks) experiments with marine organisms are still sparse. However, such experiments are crucial for assessing potential acclimatization mechanisms, as well as predicting species-specific responses to environmental change. Here, we assess the combined effects of elevated $p\text{CO}_2$ and temperature on organismal metabolism, mortality, righting activity, and calcification of the coral reef-associated starfish *Aquilonastra yairi*. Specimens were incubated at two temperature levels (27 °C and 32 °C) crossed with three $p\text{CO}_2$ regimes (455 μatm , 1052 μatm , and 2066 μatm) for 90 days. At the end of the experiment, mortality was not altered by temperature and $p\text{CO}_2$ treatments. Elevated temperature alone increased metabolic rate, accelerated righting activity, and caused a decline in calcification rate, while high $p\text{CO}_2$ increased metabolic rate and reduced calcification rate, but did not affect the righting activity. We document that temperature is the main stressor regulating starfish physiology. However, the combination of high temperature and high $p\text{CO}_2$ showed non-linear and potentially synergistic effects on organismal physiology (e.g., metabolic rate), where the elevated temperature allowed the starfish to better cope with the adverse effect of high $p\text{CO}_2$ concentration (low pH) on calcification and reduced skeletal dissolution (antagonistic interactive effects) interpreted as a result of energetic tradeoffs.

Keywords: starfish *Aquilonastra yairi*, multiple stressors, interactive effect, physiological response, calcification, climate change acclimatization

3.1. Introduction

Rising CO₂ concentration in the oceans has led to lowered seawater pH, referred to as ocean acidification (OA), while simultaneous ocean warming (OW) and changes in circulation, stratification, nutrient, salinity, and oxygen levels result in complex changes in environmental conditions (Doney et al., 2012). Many marine calcifiers such as foraminifera, mollusks, echinoderms, corals, and coralline algae are expected to be negatively impacted by OA (Figuerola et al., 2021; Kawahata et al., 2019), whereas those organisms that have photosynthesizing or photosymbiotic capabilities (e.g., algae; zooxanthellate corals) also exhibit increased growth (Cornwall et al., 2017; Ries et al., 2009). Generally, physiology-related processes such as the skeleton formation of marine organisms are impacted by OA (Gazeau et al., 2007; Wittmann & Pörtner, 2013). Moreover, OA potentially affects ecological processes influencing the performance of marine organisms, with consequences in shaping community structure, disrupting population dynamics, and altering ecosystem function (Hale et al., 2011; Hall-Spencer & Harvey, 2019; Widdicombe & Spicer, 2008). Concurrently, OW is a critical driver of physiological mechanisms defining the thermal tolerance window of marine ectotherm species (Pörtner, 2012), with tropical species commonly being more sensitive relative to temperature (Tewksbury et al., 2008). Ecological processes such as species distribution, life history, community assemblage, and marine ecosystem structure are all influenced by OW (Doo et al., 2020; Hillebrand et al., 2018; Hoegh-Guldberg & Bruno, 2010). On the organismal level, OW has been shown to negatively affect overall physiological performance, immune defense, feeding, reproductive biology (Pörtner & Farrell, 2008; Stuhr et al., 2021; Yao & Somero, 2014), and metabolic processes (Hoegh-Guldberg & Bruno, 2010).

While studies on the impacts of climate change on marine life have focused mainly on ocean acidification or ocean warming as individual/sole stressors (Bednaršek et al., 2021; Dupont & Pörtner, 2013; Wittmann & Pörtner, 2013; Yao & Somero, 2014), recently, more studies on combined stressors have been undertaken. Previous meta-analyses identify trends towards increased sensitivity to OA when marine species are simultaneously exposed to OW (Bednaršek et al., 2019; Kroeker et al., 2013), associated with effects on adaptation capacity, thermal tolerance, activity level, mobility, life stages, and life history (Byrne & Przeslawski, 2013; Pörtner & Farrell, 2008). Other studies found that marine organisms that are adapted to high fluctuations in temperature and pH are possibly more resistant to future environmental

changes due to their preadapted physiological capacities (acclimation) and phenotypic plasticity (Ericson et al., 2018; Leung et al., 2022; Melzner et al., 2009; Whiteley, 2011).

For echinoderms, earlier studies show varied reactions (Byrne & Hernández, 2020). In echinoids, the combination of OW (+5°C) and OA (-0.5 pH units) leads to an increased metabolism rate (Carey et al., 2016), decreased growth rate in +3°C warming and -0.2 pH units (Uthicke et al., 2014), reduced thermal tolerance at +5°C warming and -0.3 pH units (Manriquez et al., 2019), and significantly impacted reproductive potential at +6°C warming and -0.5 pH units (Dworjanyn & Byrne, 2018); in brittle stars to metabolic upregulation at +6°C warming and -0.6 pH units (Christensen et al., 2011) and slowed arm regeneration at +3.5°C warming and 1.0 pH units (Wood et al., 2011); and in crown-of-thorns starfish (COTS) to either decreased larval size at +4°C warming and -0.5 pH units (Kamya et al., 2014) or beneficial effects on growth and feeding at +4°C warming and -0.4 pH units (Kamya et al., 2018). In general, early life stages were more sensitive to OA and OW; however, OW of +3°C seems to mitigate the negative effects of OA (-0.3 pH units) in certain species of echinoderms (Brennand et al., 2010).

Studies on starfish (phylum Echinodermata, class Asteroidea), specifically, have shown that the impacts of OW and OA as sole or combined stressors widely range from strongly depressed metabolic rates reaching below the normal resting value (Collard et al., 2013) to non-significant effects (McElroy et al., 2012). OW elicits increased metabolic rates in starfish, similar to other ectotherms (Peck et al., 2008), while elevated seawater $p\text{CO}_2$ in conjunction with increased temperature generally results in increased mortality rates (Byrne et al., 2013). OW is further documented to increase the righting rate (Ardor Bellucci & Smith, 2019; Kleitman, 1941; Peck et al., 2008; Watts & Lawrence, 1986; Watts & Lawrence, 1990), while righting behavior was not significantly modulated by decreased pH (McCarthy et al., 2020). For small-sized starfish such as asterinids (family Asterinidae), the combined stressors of OA and OW have been found to induce metabolic depression (McElroy et al., 2012) and increased larvae and juvenile mortality (Byrne et al., 2013; Nguyen & Byrne, 2014). However, we are unaware of other studies that document and quantify the calcification processes of asterinid starfish, neither in an ambient environment nor under predicted climate change conditions (i.e., combined OW and OA). Moreover, the acclimatization potential of tropical asterinid starfish to prolonged periods of changes in pH and temperature is largely unknown. To address this knowledge gap, we performed a controlled laboratory experiment to examine the long-term integrative effects

of ocean acidification and warming on metabolic rate, mortality, righting response, and calcification rate for 90 days on the cryptic tropical asterinid starfish *Aquilonastra yairi*. Ecologically, the starfish *A. yairi* is a nocturnal species inhabiting underwater rocks, reef structures, and intertidal rubble areas in the Red Sea, Mediterranean Sea, and Gulf of Suez (Ebert, 2021; O'Loughlin & Rowe, 2006). Although this starfish species inhabits shallow intertidal waters, its bioecology remains poorly known.

3.2. Material and methods

3.2.1. Experimental design and seawater chemistry control and measurement

A total of 342 specimens (size 3-11 mm) of adult *A. yairi* (Supplementary Figure S3.1) were collected from stock cultures in the MAREE (Marine Experimental Ecology) of ZMT, Bremen (Germany). Following acclimation (see Supplementary Text), the starfish were held for 90 days in one of six treatments (three replicate tanks each) where two temperature levels were crossed with three $p\text{CO}_2$ regimes: (T1) 27 °C : 455 μatm , (T2) 27 °C : 1052 μatm , (T3) 27 °C : 2066 μatm , (T4) 32 °C : 455 μatm , (T5) 32 °C : 1052 μatm , and (T6) 32 °C : 2066 μatm , which represent factorial combinations of ambient conditions and future levels of CO_2 and temperature change according to the IPCC-Representative Concentration Pathways (RCPs) 8.5 greenhouse gas emission scenario for the year 2100 (IPCC, 2014). Moreover, the ambient temperature (27 °C) represents the average sea surface temperature (SST) in summer (June-October) in natural habitats of *A. yairi* (e.g., Gulf of Suez). To avoid physiological shock, targeted $p\text{CO}_2$ and temperature levels were slowly ramped up over ten days. In short, to generate gas mixtures formulated to the target $p\text{CO}_2$ conditions, CO_2 -free air and pure CO_2 gas were mixed with solenoid-valve mass flow controllers and bubbled via flexible microporous air stones into the seawater reservoirs of each treatment group, then continuously pumped into replicate tanks. Treatment tank temperatures were maintained using a closed-circle heating system controlled with a programmable thermostat (Supplementary Figure S3.2). Details of the water chemistry control and manipulation are provided in the Supplementary Text and Khalil et al. (2022). Aquarium water samples were obtained during experiments for carbonate chemistry assessment. The water parameters and carbonate chemistry for the treatment tanks are given in Supplementary Table S3.1.

3.2.2. Metabolic rate

Metabolic rates of *A. yairi* under each of the six treatment groups ($n = 6$ individuals per treatment) were estimated as rates of oxygen consumption (M_{O_2}). Real-time M_{O_2} was measured bi-weekly throughout the experiment using optical fluorescence-based oxygen respirometry (24-channel oxygen meter – SDR SensorDish Reader, PreSens, Germany). Subsequently, the individual starfish specimen was weighed for damp-dry wet body mass (see Supplementary Text). The rate of O_2 consumption was calculated using the equation by Sinclair et al. (2006):

$$M_{O_2} (\mu\text{mol g}^{-1} \text{h}^{-1}) = (([C]_i - [C]_f - [C]_{\text{blank}} (\mu\text{mol L}^{-1}) * V (\text{L})) / (\text{WBM} (\text{g}) * t (\text{h})),$$

where $[C]_i$ is the initial $[O_2]$ concentration vials ($\mu\text{mol L}^{-1}$), $[C]_f$ is the final $[O_2]$ concentration in the sample vial for specimen i ($\mu\text{mol L}^{-1}$) after time t (h), $[C]_{\text{blank}}$ is the difference between the initial $[O_2]$ concentration in the blank vial minus the final $[O_2]$ concentration in the blank vial ($\mu\text{mol L}^{-1}$) over time t , V is the volume of the vial (minus the displacement of the starfish) (L), and WBM is the damp-dry wet body mass of the specimen i (g).

3.2.3. Mortality

During the 90-day exposure, every 24 hours, the treatments were checked for mortality of individuals. Dead *A. yairi* were identified by a characteristic loss in color (e.g., whitening) on the dorsal side (aboral surface) or by the absence of tube feet (podia) movement. Dead starfish were removed from the experimental tanks. Mortality rates were assessed from the cumulative mortality per 30-day experimental period (i.e., after 30, 60, and 90 days, respectively) and compared between treatments after 90 days. The mortality rate was calculated by the following equation: Mortality (%) = dead individuals per treatment / total individuals per treatment $\times 100\%$

3.2.3. Righting behaviour

Righting behavior of starfish *A. yairi* ($n = 6$ individuals per treatment) was measured periodically (six times) during the incubation time (see Supplementary Text). The righting response refers to the ability of a starfish when positioned on the ventral side (oral surface), to turn over into the normal position on the dorsal side (aboral surface). The righting activity coefficient (RAC) is used to indicate the organismal intensity of activity patterns (Stickle & Diehl, 1987) and reflects the level of stress and well-being (Lawrence & Cowell, 1996). RAC was counted as $\text{RAC} = 1.000 / \text{righting time response (s)}$ (Watts & Lawrence, 1990). The increased RAC rate indicates that

the starfish need less time to return to their natural position, thus being related to higher stress levels and vice versa (Sonnenholzner et al., 2010).

3.2.5. Calcification rate

The alkalinity anomaly technique was used to determine the calcification rate (G_{TA}) of the starfish *A. yairi* ($n = 3$ individuals per treatment). This procedure has been widely used for short-term incubation as it is a non-destructive and precise technique (see Supplementary Text). Changes of A_T throughout the incubations were corrected for the discharge of inorganic nutrients follows the modified equation from Gazeau et al. (2015):

$$G_{TA} = \Delta NH_4^+ - \Delta A_T - \Delta(NO_3^- + NO_2^-) - \Delta PO_4^{3-} / 2 * dw * t$$

Where G_{TA} is the calcification rate of the starfish ($\mu\text{mol CaCO}_3 \text{ g dw}^{-1} \text{ h}^{-1}$); and ΔNH_4^+ , ΔA_T , $\Delta(NO_3^- + NO_2^-)$, ΔPO_4^{3-} ($\mu\text{mol kg}^{-1}$) refer to the variations in concentrations of ammonium, total alkalinity, nitrate + nitrite, and phosphate, between the beginning and the end of the experiment, respectively; dw is the damp-dry wet weigh (g) of the starfish; t represents time (h) of incubation.

3.2.6. Statistical analysis

All statistical analyses were performed with the software R version 4.2.2 (R Core Team, 2023), complemented with R-package 'car' v.3.1-0 (Fox & Weisberg, 2019). The Shapiro-Wilk statistic W test (Shapiro & Wilk, 1965) was used to test the data for normality, while Levene's test was applied to check the homogeneity of variance (Levene, 1960), before ANCOVA and ANOVA model statistical analysis was performed. When data were not normally distributed or indicated heteroscedasticity, a logarithmic transformation ($\text{Log}(x)$) was carried out following Sokal and Rohlf (2012). The effect of OA and OW on the metabolic rate and righting behavior of the starfish were analyzed by using multifactorial analysis of covariance (ANCOVA) with $p\text{CO}_2$ concentration and temperature as fixed factors, while incubation time was treated as a continuous covariate. Then, a two-factor analysis of variance (ANOVA) was used to determine whether $p\text{CO}_2$ concentration and temperature (treated as fixed factors) and the combination of the factors had an effect on the starfish calcification rate. Tukey's honestly significant difference (HSD) post hoc comparisons were used to detect significant differences among treatments. All statistics were evaluated with a significance level of $\alpha = 0.05$.

The OA and OW effects on physiological parameters were visualized using the R-package 'ggplot2' v.3.3.6 (Wickham, 2016). Linear polynomial interpolation analyses (formula: $y \sim \text{poly}(x, 2)$) were conducted to determine the best-fit shape of fixed factor ($p\text{CO}_2$ and temperature) and continuous covariate (incubation time) relationship on the metabolic rates (Supplementary Figure S3.3) and the RAC (Supplementary Figure S3.4).

3.3. Results

3.3.1. Metabolic rate

The metabolic rate M_{O_2} (measured as O_2 consumption) was lower at 27 °C compared to 32 °C throughout the entire experiment (Figure 3.1; Supplementary Table S3.2 and Figure S3.3). Metabolic rate was lowest at ambient temperature crossed with low $p\text{CO}_2$ concentration (27 °C : 455 μatm , $0.820 \pm 0.047 \mu\text{mol g}^{-1} \text{h}^{-1}$; mean \pm SE), whereas the highest M_{O_2} was found at high temperature and low $p\text{CO}_2$ concentration (32 °C : 455 μatm , $1.459 \pm 0.086 \mu\text{mol g}^{-1} \text{h}^{-1}$; mean \pm SE). The O_2 consumption of the individual starfish was strongly elevated, i.e. by ~46%, with increased temperature compared to ambient temperature treatments (from $0.979 \pm 0.042 \mu\text{mol g}^{-1} \text{h}^{-1}$ to $1.431 \pm 0.091 \mu\text{mol g}^{-1} \text{h}^{-1}$; mean \pm SE, $F_{1, 240} = 61.023$, $p = 0.001$; Table 3.1).

As the sole factor, $p\text{CO}_2$ was found to significantly affect M_{O_2} , where increased $p\text{CO}_2$ linearly increased O_2 consumption at ambient temperature (from $0.820 \pm 0.047 \mu\text{mol g}^{-1} \text{h}^{-1}$ to $1.130 \pm 0.066 \mu\text{mol g}^{-1} \text{h}^{-1}$; mean \pm SE, equal to 37.80% on average; $F_{2, 240} = 3.264$, $p = 0.040$; Table 3.1 and Supplementary Table S3.4). Respiration was significantly affected by combined factors of temperature and $p\text{CO}_2$ ($F_{2, 240} = 4.315$, $p = 0.014$; Table 3.1 and Supplementary Tables S3.4), implying that the major influence of temperature on O_2 consumption was notably diminished by high $p\text{CO}_2$ (decreased from $1.459 \pm 0.091 \mu\text{mol g}^{-1} \text{h}^{-1}$ to $1.419 \pm 0.066 \mu\text{mol g}^{-1} \text{h}^{-1}$; mean \pm SE, equal to -2.74% on average; Supplementary Table S3.2). Exposure time significantly influenced O_2 consumption and exhibited parabolic M_{O_2} responses to the stressors in all treatments ($F_{6, 240} = 3.027$, $p = 0.007$; Table 3.1 and Supplementary Figure S3.3).

3.3.2. Mortality

In total, four specimens died throughout the experiment. All of these mortalities occurred within the last 30 days of the experiment, which means that from day 1 to 60 of exposure, survival in all treatment groups was at 100%. No mortality was observed for any of the 27 °C temperature treatment groups (i.e., 27 °C combined with 455 μatm , 1052 μatm , and 2066

μatm). At 32 °C, one specimen, which equals to 1.56%, died in 455 μatm treatment (day 84) as well as in 1052 μatm treatment (day 71), and two specimens (3.17%) died at 2066 μatm treatment (days 67 and 79).

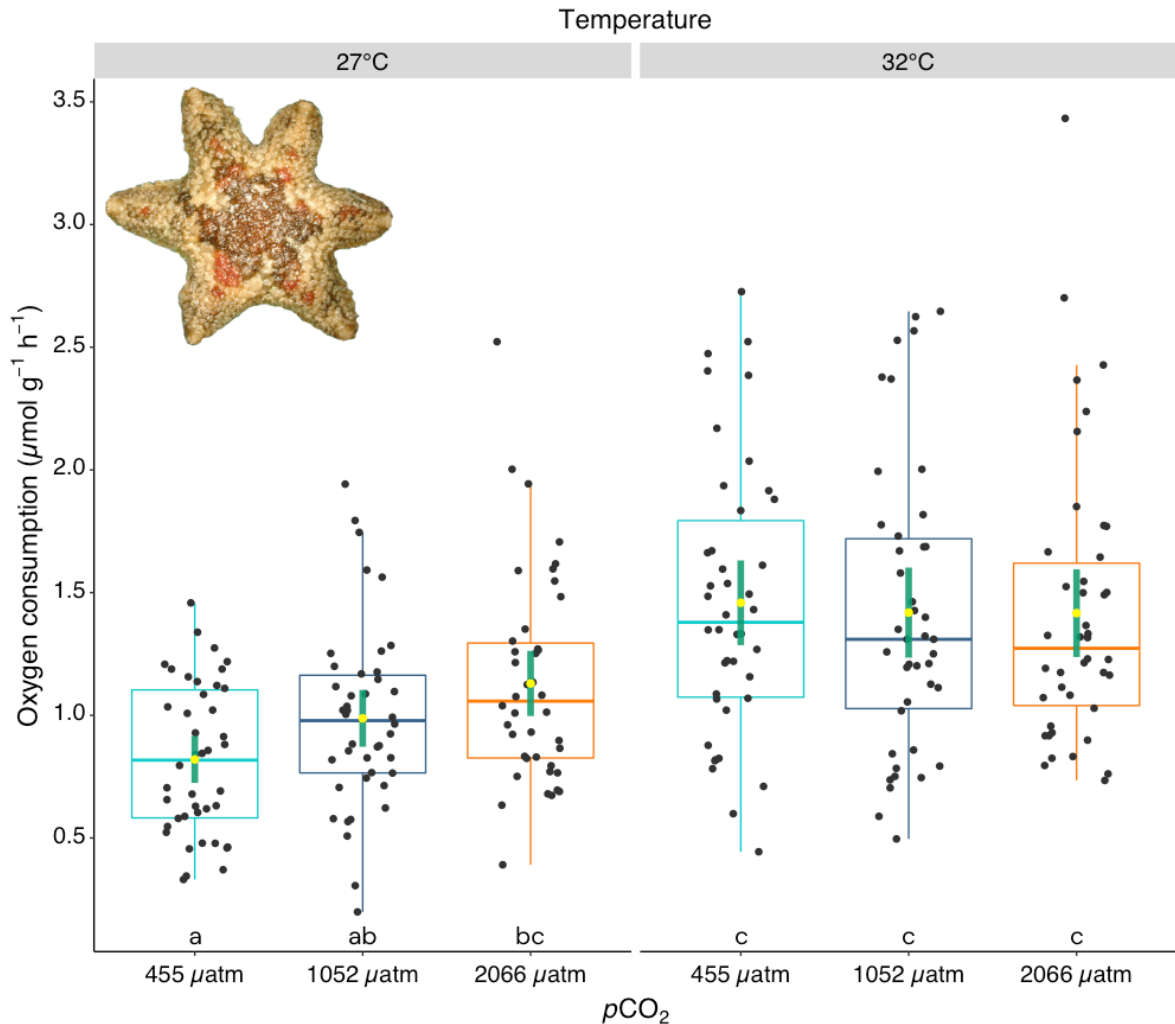


Figure 3.1. The metabolic rate (M_{O_2}) responses, measured as oxygen consumption of *A. yairi* (shown in the upper left corner) reared under different $p\text{CO}_2$ levels (455 μatm , 1052 μatm , and 2066 μatm) and temperatures (27 °C and 32 °C). $n = 42$ individuals per treatment group. The yellow dots indicate the mean effect in each treatment, and green vertical bars indicate 95% confidence intervals. Dots represent individual M_{O_2} values, displayed with jitter to avoid overlap. Different letters designate significant differences between treatments ($p \leq 0.05$) based on Tukey's HSD post hoc comparison.

3.3.3. Righting activity

All individuals were capable of righting in less than 10 min after inversion. The fastest righting activity coefficient (RAC) was observed at high temperature crossed with medium $p\text{CO}_2$ concentration (32 °C: 1052 μatm , 21.042 ± 1.393 ; mean \pm SE), while the lowest RAC was observed at ambient temperature and high $p\text{CO}_2$ concentration (27 °C : 2066 μatm , 13.745 ± 0.815 ; mean \pm SE). Righting time was significantly faster at a temperature of 32 °C compared to 27 °C ($F_{2, 205} = 45.473$, $p = 0.001$; Figure 3.2; Supplementary Table S3.3), i.e., the elevated temperature increased RAC by ~39% (from 14.616 ± 0.076 to 20.263 ± 1.324 ; mean \pm SE; $F_{1, 205} = 45.473$, $p = 0.001$; Table 3.1). RAC declined linearly with incubation time in all treatments ($F_{5, 205} = 2.255$, $p = 0.050$; Table 3.1 and Supplementary Figure S3.4). Moreover, the ANCOVA model analysis indicated that the RAC was neither affected by $p\text{CO}_2$ as sole factor ($F_{2, 205} = 0.784$, $p = 0.458$; Table 3.1), nor by a combination of both factors ($F_{2, 205} = 0.401$, $p = 0.671$; Table 3.1).

3.3.4. Calcification rate

In general, the calcification rate (G_{TA}) of *A. yairi* was significantly affected by $p\text{CO}_2$ as a sole factor ($F_{2, 12} = 59.431$, $p = 0.001$; Table 3.1 and Supplementary Table S3.4), with reduced G_{TA} at 2066 μatm compared to 455 and 1052 μatm . Moreover, statistical analysis confirmed that the G_{TA} on *A. yairi* indicated a significant interaction of the effects of temperature: $p\text{CO}_2$ ($F_{2, 12} = 44.506$, $p = 0.001$; Figure 3.3a, Table 3.1 and Supplementary Table S3.4). Calcification rate decreased significantly in response to increasing $p\text{CO}_2$ under both temperature treatments (Table 3.1, Supplementary Table S3.4). As a sole factor, temperature did not affect the G_{TA} of *A. yairi* ($F_{2, 12} = 4.326$, $p = 0.060$; Table 3.1).

A negative linear trend in G_{TA} was found at ambient temperatures (27 °C), where individuals exposed to high $p\text{CO}_2$ (2066 μatm , $\text{pH}_{\text{sw (total scale)}} = 7.47 \pm 0.01$; mean \pm SE: $G_{\text{TA}} = -1.506 \pm 0.476$ $\mu\text{mol CaCO}_3 \text{ g dw}^{-1} \text{ h}^{-1}$; mean \pm SD) showed 258.94% reduction in mean G_{TA} compare to individuals reared at low $p\text{CO}_2$ (455 μatm , $\text{pH}_{\text{sw (total scale)}} = 8.00 \pm 0.00$; mean \pm SE: $G_{\text{TA}} = 0.947 \pm 0.206$ $\mu\text{mol CaCO}_3 \text{ g dw}^{-1} \text{ h}^{-1}$; mean \pm SD). In contrast to the ambient temperature treatment, the G_{TA} at elevated temperature treatment (32 °C) showed stable-lower trends, ranging between -0.194 and 0.255 $\mu\text{mol CaCO}_3 \text{ g dw}^{-1} \text{ h}^{-1}$ (0.096 ± 0.127 $\mu\text{mol CaCO}_3 \text{ g dw}^{-1} \text{ h}^{-1}$; mean \pm SD). However, in the 32 °C treatments, the starfish exposed to higher $p\text{CO}_2$ (2066 μatm , $\text{pH}_{\text{sw (total scale)}} = 7.47 \pm 0.01$; mean \pm SE: $G_{\text{TA}} = -0.011 \pm 0.164$ $\mu\text{mol CaCO}_3 \text{ g dw}^{-1} \text{ h}^{-1}$; mean \pm SD) revealed a 107.69% decline in mean compared to starfish exposed at low $p\text{CO}_2$ (455 μatm , pH_{sw}

(total scale) = 8.00 ± 0.00 ; mean \pm SE: $G_{TA} = 0.147 \pm 0.010 \mu\text{mol CaCO}_3 \text{ g dw}^{-1} \text{ h}^{-1}$; mean \pm SD) (Figure 3.3a and 3.3b).

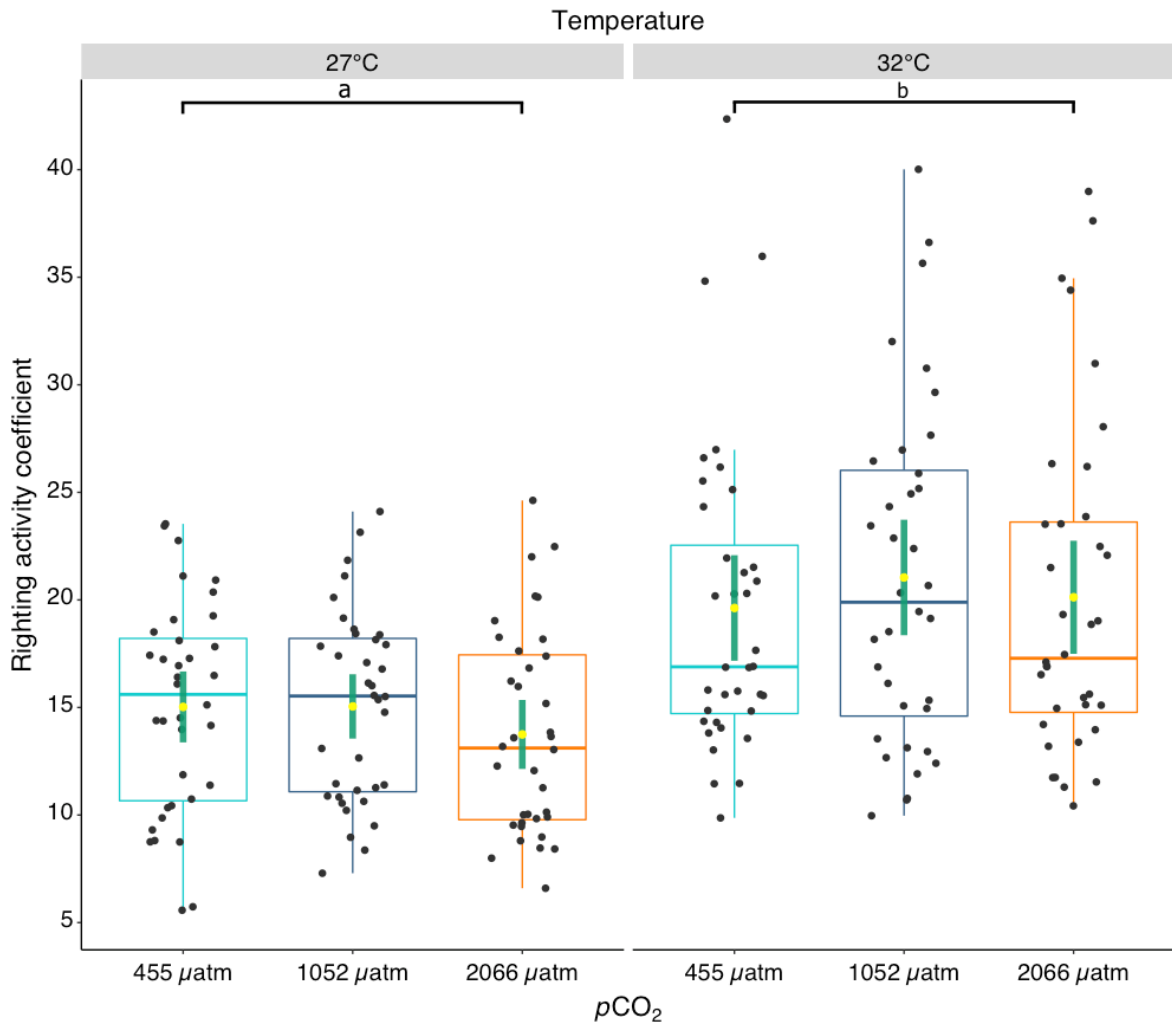


Figure 3.2. Righting activity coefficient (RAC) of *A. yairi* exposed under different $p\text{CO}_2$ concentrations (455 μatm , 1052 μatm , 2066 μatm) and temperatures (27 °C, 32 °C). High RAC values indicate low righting times (s), and vice versa ($n = 36$ individuals per treatment group). Relatively higher RAC values are associated with higher levels of stress. The green vertical bar indicates 95% confidence intervals, yellow dots indicate the mean effect in each treatment. Dots represent individual RAC values, displayed with jitter to avoid overlap. Different letters designate significant differences between treatment groups ($p \leq 0.05$).

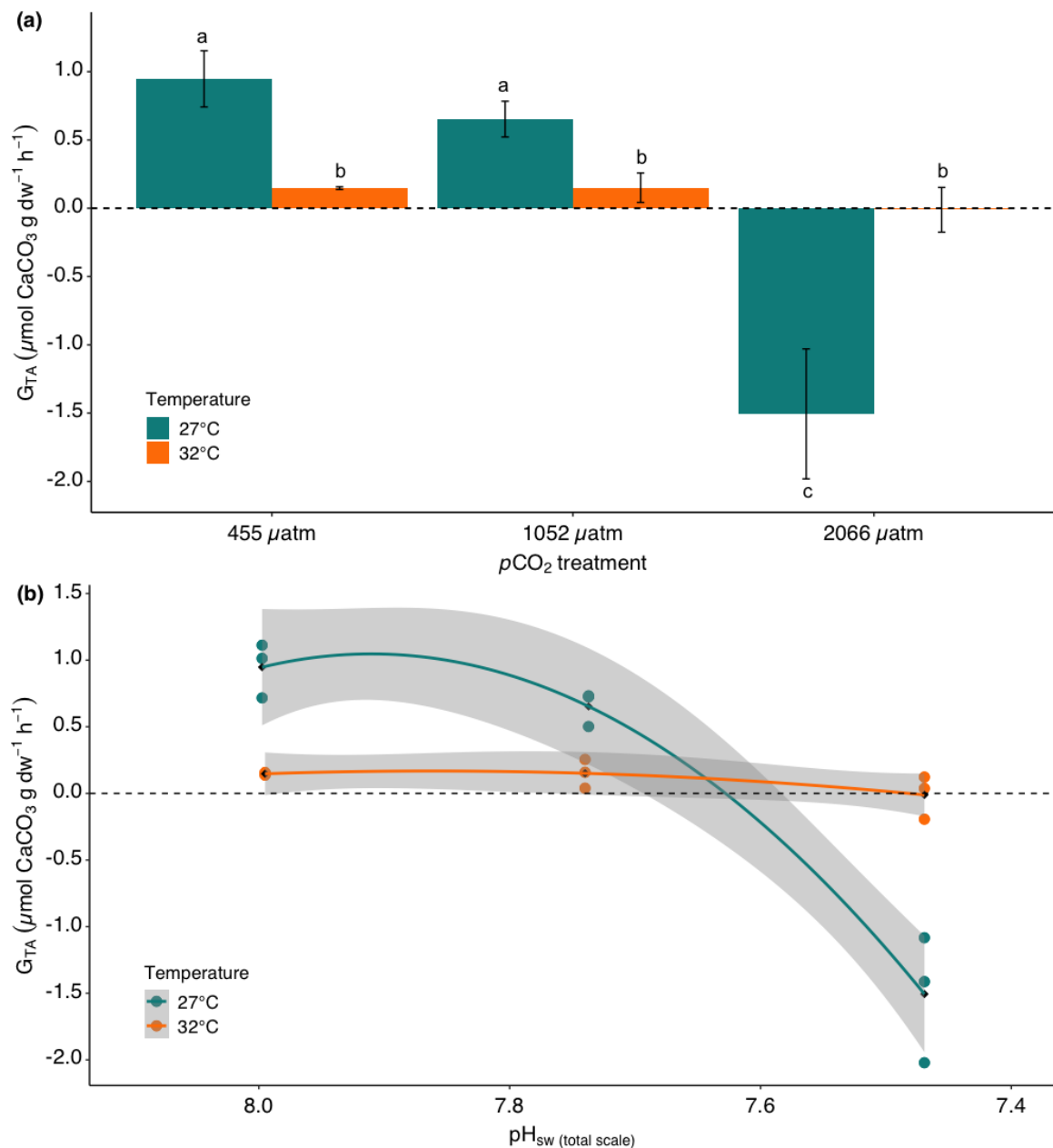


Figure 3.3. Calcification rate (G_{TA}) of *A. yairi* reared under different $p\text{CO}_2$ concentrations (455 μatm , 1052 μatm , 2066 μatm) and temperatures (27 °C, 32 °C). Horizontal dotted lines indicate zero G_{TA} . **(a)** shows the relationship between mean calcification rate, temperature, and $p\text{CO}_2$ concentration. Error bars indicate standard deviation and different letters designate significant differences between treatments ($p \leq 0.05$) based on Tukey's HSD post hoc comparison. **(b)** shows the pH_{sw} (total scale)-dependence of *A. yairi* calcification rate at 27 °C and 32 °C. The symbols (cyan and orange cycles) indicate the calcification rate for the starfish in each replicate, and black symbols represent the mean effect for the starfish in each treatment. Shaded areas represent the 95% confidence interval; $n = 18$ (three samples per treatment).

Table 3.1. Results of the multifactorial statistical analysis on metabolic rate, righting activity, and calcification rate of the starfish *A. yairi* reared under different $p\text{CO}_2$ concentrations (455 μatm , 1052 μatm , 2066 μatm) and temperatures (27 °C, 32 °C) for 90 days of incubation time. Significant effects ($p \leq 0.05$) are in bold.

Effect	df	Sum Sq.	Mean Sq.	F	Pr (>F)	Post hoc summary (Tukey HSD)
Metabolic rate (ANCOVA)						
Incubation time	6	2.779	0.463	3.027	0.007	day-60 > day-1, day-45, day-75, day-90 (Supplementary Table S3.4)
Temperature	1	9.338	9.338	61.023	0.001	32 °C > 27 °C
$p\text{CO}_2$	2	0.999	0.500	3.264	0.040	2066 μatm > 455 μatm (Supplementary Table S3.4)
Temperature: $p\text{CO}_2$	2	1.321	0.660	4.315	0.014	32 °C:455 μatm > 27 °C:455 μatm ; 27 °C:2066 μatm > 27 °C:455 μatm ; 27 °C:1052 μatm > 32 °C:455 μatm ; 32 °C:1052 μatm > 27 °C:455 μatm , 27 °C:1052 μatm ; 32 °C:2066 μatm > 27 °C:455 μatm , 27 °C:1052 μatm (Supplementary Table S3.4)
Residuals	240	36.726	0.153			
Righting activity (ANCOVA)						
Incubation time	5	1.350	0.270	2.255	0.050	day-90 < day-37 (Supplementary Table S3.4)
Temperature	1	5.444	5.444	45.473	0.001	32 °C > 27 °C
$p\text{CO}_2$	2	0.188	0.094	0.784	0.458	
Temperature: $p\text{CO}_2$	2	0.096	0.048	0.401	0.671	
Residuals	205	24.542	0.120			
Calcification rate (two-way ANOVA)						
Temperature	1	0.045	0.045	4.326	0.060	
$p\text{CO}_2$	2	1.246	0.623	59.431	0.001	2066 μatm < 455 μatm , 1052 μatm (Supplementary Table S3.4)

						27 °C:455 µatm > 27 °C:2066 µatm, 32 °C:455 µatm, 32 °C:1052 µatm, 32 °C:2066 µatm;
Temperature:pCO ₂	2	0.933	0.467	44.506	0.001	27 °C:1052 > 32 °C:455 µatm, 32 °C:1052 µatm, 27 °C:2066 µatm, 32 °C:2066 µatm; 27 °C:2066 µatm > 32 °C:455 µatm, 32 °C:1052 µatm, 32 °C:2066 µatm (Supplementary Table S3.4)
Residuals	12	0.126	0.011			

3.4. Discussion

3.4.1. Metabolic response under multiple stressors

In our study, the metabolism of *A. yairi* was significantly impacted by elevated seawater $p\text{CO}_2$, temperature, and incubation time. Respiration rates (M_{O_2} , as a proxy for organismal metabolism) varied significantly with temperature, $p\text{CO}_2$, and combined $p\text{CO}_2$ and temperature. Mean M_{O_2} values increase over time as acclimation temperature capacity increases (from 27 °C to 32 °C), indicating rising thermal sensitivity. At a temperature of 32 °C, *A. yairi* consumed 46.16 % (on average) more oxygen compared to the specimens kept at 27 °C, suggesting increased metabolic activity as a stress response through the physiological adjustment over time to the elevated temperature (Lenz et al., 2019). This was followed by a continued rise in metabolism to a new steady-state condition as the starfish adapted their physiology to the new environment (i.e., acclimation to increased temperature condition), demonstrating physiological adaptability (Piersma & Drent, 2003). Concurrent exposure to lowered pH and warmer seawater conditions could lead *A. yairi* to undergo metabolic suppression, which is an effective adaptation mechanism that enables organisms to survive acute short-term stress by temporarily reducing energy-intensive processes in order to increase the time-span of tolerance (Guppy & Withers, 2007; Pörtner & Farrell, 2008; Pörtner et al., 2004). Increased metabolism is thought to be a response to an amplified energy requirement associated with elevated temperature levels and $p\text{CO}_2$, hence reducing the energy available for other energy-intensive processes for example, the increased energy used for basal maintenance and intra-extracellular acid-base balance (Sokolova 2013). We suspect that *A.*

yairi might suppress physiological processes in order to maintain homeostasis function and fitness, thus modifying the mechanism for energy assimilation, hormone regulatory processes, enzyme activities, membrane composition, ion and gas transport, and mitochondrial abundance or mitochondrial capacity as has previously been described for a range of organisms (Hazel, 1995; Hochachka & Somero, 2002; Sokolova et al., 2012; Willmer et al., 2004); however, this is as yet to be proven. Increasing metabolic rate as a response to increasing temperature has also been found in the sea urchins *Lytechinus variegatus* (Lenz et al., 2019), brittle stars *Ophionereis schayeri* (Christensen et al., 2011) and *Ophiura ophiura* (Wood et al., 2010). Since *A. yairi* demonstrated an increase in metabolic rate along with increasing temperature, indicating the relationship between physiological performance, body temperature, and environmental temperature, it is necessary to evaluate the mechanistic relation using the thermal performance curve models in further studies.

Although temperature is known to be the main factor for metabolism, $p\text{CO}_2$ also influences metabolic rates through its effects on changing seawater pH and, afterwards regulating cellular acid-base balance and ion transport (Kaniewska et al., 2012). When the external pH is highly variable, acid-base control includes proton generation, transport, consumption, and intracellular compartment buffering, demanding a higher energy supply (Seibel & Walsh, 2001; Seibel & Walsh, 2003). The mechanisms by which decreased seawater pH alter metabolic rates in marine invertebrates are complex, species-specific, and vary depending on the metabolic pathway component that is impacted (Pan et al., 2015). In asterinid starfish, the effect of elevated $p\text{CO}_2$ concentrations as an individual stressor on the metabolic rate might be negligible at the organismal level (McElroy et al., 2012). Markedly, we observed that the metabolic rate increased with rising $p\text{CO}_2$ concentration in the 27 °C treatments, but conversely, acclimation to the high temperature (32 °C) caused a narrow and non-significant decrease in metabolic rate along with rising $p\text{CO}_2$ concentration. These results indicate that the combined changes of temperature and $p\text{CO}_2$ produce a complex pattern of non-linear (synergistic) responses in the metabolic rate, unpredictably affecting physiological performance (Folt et al., 1999; Todgham & Stillman, 2013). Similar complex metabolic responses to elevated $p\text{CO}_2$ and temperature have been reported before from other marine invertebrates (Harvey et al., 2013; Przeslawski et al., 2015), e.g., the decapod *Metapenaeus joyneri* (Dissanayake & Ishimatsu, 2011), the porcelain crabs *Petrolisthes cinctipes* (Paganini et al., 2014), the sea urchin *L. variegatus* (Lenz et al., 2019), and the sea hare *Stylocheilus striatus*

(Horwitz et al., 2020). However, our report here is the first to show that high temperatures can reduce the negative effect of increased $p\text{CO}_2$ concentration on starfish metabolism.

3.4.2. Ocean warming and $p\text{CO}_2$ impact on mortality

High resilience of *A. yairi* was observed to the ranges of future $p\text{CO}_2$ and temperature levels simulated in this study. In fact, we observed no negative effect of OW or OA as a single stressor or their interaction to their mortality rate. Our findings are consistent with earlier studies exposing adult starfish *Leptasterias polaris* (Dupont & Thorndyke, 2012) to elevated temperature and $p\text{CO}_2$ conditions as single or combined stressors. In contrast, a high mortality rate was commonly found in the early life stages of echinoderms species when exposed to ocean acidification and warming, such as the starfish *Meridiastra calcar* (Nguyen et al., 2012), and *Patiriella regularis* (Byrne et al., 2013). While the adult *A. yairi* studied here did not show any such effect, data on the early life stages of this starfish are as yet lacking.

The resilience of *A. yairi* to elevated temperatures and $p\text{CO}_2$ levels observed here regarding their mortality rate may be attributed to several factors. (i) Sensitivity to stressors varies across life stages (Kroeker et al., 2013), where the adult stage has more capability to cope with stressors due to their structure and functional size of organs (Piersma & Lindström, 1997), including mechanisms to surge M_{O_2} and suppress un-substantial physiology processes to increase biological performance and fitness. It implies that there might be a regulatory tradeoff between metabolic physiology and other physiological functions when exposed to high temperatures and $p\text{CO}_2$ in order to maintain an acceptable level of fitness and thus reduce the mortality rate. (ii) When the organism is capable of acclimating its temperatures and $p\text{CO}_2$ threshold to the new level that falls within the thermo-pH tolerance limits, the fitness of the organism is maintained, yielding decreases in their mortality rate (Pörtner, 2008; Pörtner, 2012; Tomanek, 2010). (iii) *A. yairi* as a marine intertidal organism is adapted to habitats that experience high fluctuations in temperature and pH and seems to have preadapted physiological capacities and plasticity (Ericson et al., 2018; Melzner et al., 2009; Whiteley, 2011; Widdicombe & Spicer, 2008). While this study focused on chronic heat stress of +5°C, further acute heat stress in the form of marine heat waves or thermal pulse in shallow-water habitats could elicit deleterious effects (Balogh & Byrne, 2020; Vinagre et al., 2018), and should be addressed in future studies.

3.4.3. Ocean warming influence on righting response

Righting reflexes are regularly used as a proxy of health, fitness, and stress in echinoderms (Lawrence & Cowell, 1996), where delayed righting duration may heighten predation risk (Gutowsky et al., 2016). Our results show that *A. yairi* successfully performed functional behavior (righting performance) at both temperatures, 27 °C and 32 °C, combined with elevated $p\text{CO}_2$ concentration levels (455 μatm , 1052 μatm , and 2066 μatm). This implies that the experimental conditions were within the thermal and $p\text{CO}_2$ tolerance range of *A. yairi*. Our results show that the elevated temperature was the primary influence on the righting response. We interpret the observation that RAC was significantly higher at 32 °C compared to 27 °C to indicate that temperature induced an increased metabolic rate (as the source of energy supply) and stimulated neuronal systems to actuate muscle kinetics, thus rising locomotion speed (Young et al., 2006a, 2006b). Ectothermic animals, including echinoderms, generally exhibit a positive correlation between environmental temperature, body temperature and metabolic rate (Carey et al., 2016; Ulbricht, 1973). Similar to this current study, faster righting responses after exposure to maximum tolerance temperatures were observed in other echinoderms species, including *Luidia clathrate* (Watts & Lawrence, 1986; Watts & Lawrence, 1990), and *Echinaster (Othilia) graminicola* (Ardor Bellucci & Smith, 2019).

In this study, we found that increased $p\text{CO}_2$ did not influence the righting response of *A. yairi* at either of the temperatures (27 °C and 32 °C). Similar observations have been reported for the sea urchin *L. variegatus* (Challener & McClintock, 2013), and *Paracentrotus lividus* (Marceta et al., 2020). The increasing of the metabolism as a response to temperature changes provides excess energy that allows the starfish to control their homeostatic mechanisms, including cellular acid-base regulation (Pörtner et al., 2004) to avert acidosis, so that the effect of $p\text{CO}_2$ (hypercapnia) is minimized. Consequently, neuromuscular function to coordinate between tube feet and spine in righting activities occurs with minimum disruption. Besides, the experimental time span of exposure to elevated $p\text{CO}_2$ would have been insufficient to trigger physiological alterations associated with behavior and sensory impairment. In our experiment, exposure time significantly influenced the righting activity of *A. yairi*, with RAC getting lower with the time of exposure in all treatment groups (Supplementary Figure S3.4). A recent study on the sea urchin *P. lividus* found a similar behavior where righting time variability was significantly affected by exposure time (Asnicar et al., 2021). We speculate that *A. yairi* might experience musculoskeletal fatigue due to continuous and prolonged exposure to stressors,

resulting in gradual interferences in the nervous system and neurotransmission (Heuer et al., 2019), followed by weakening muscle contractions and decreased locomotion speed that produces slackness in righting time behavior. Clearly, the timescale of exposure is critical such that animals might not respond to elevated $p\text{CO}_2$ on a timescale typical for experiments, but may do so after prolonged exposure.

3.4.4. Potential antagonistic effect of elevated temperature and $p\text{CO}_2$ on calcification

The capability of *A. yairi* observed here to calcify in an environment with lowered pH is a threshold-negative trend (i.e., narrow change on calcification rate under medium $p\text{CO}_2$ concentration (G_{TA} : positive); negative G_{TA} value under highest $p\text{CO}_2$ concentration) when the ambient temperature is crossed with elevated $p\text{CO}_2$ (Ries, 2011; Ries et al., 2009). We here observe the dissolution of CaCO_3 and loss of calcified substance in *A. yairi* exposed to a high $p\text{CO}_2$ concentration (2066 μatm) at 27 °C temperature environments ($G_{\text{TA}} = -1.51 \pm 0.48 \mu\text{mol CaCO}_3 \text{ g dw}^{-1} \text{ h}^{-1}$). This corroborates earlier studies on echinoderms that found decreased calcification under high- $p\text{CO}_2$ (low pH) conditions in the sea star *Pisaster ochraceus* (Gooding et al., 2009), the urchins *Echinometra mathaei* (Shirayama, 2005), and *E. viridis* (Courtney et al., 2013).

Conversely, *A. yairi* exhibited a depressed but low-positive net calcification rate at 32 °C under low and medium $p\text{CO}_2$ treatments; low-negative G_{TA} (in mean) at 32 °C under high $p\text{CO}_2$ treatment. Similar temperature-related effects in calcification rate have been reported for several calcifying marine species, for example, the Pacific starfish *P. ochraceus* (Gooding et al., 2009). This can possibly be explained by these starfish allocating their energy supplies towards maintaining a positive calcification rate in an elevated CO_2 environment. Energy is required to regulate the pH at the site of calcification through maintaining an H^+ -gradient between the external seawater and the internal membrane-bound calcifying fluid (Ries 2011). This elevated energy allocation for calcification could be met by the increase in metabolic rate observed at higher temperature (see Subchapter 3.3.1), potentially providing more metabolic energy. Thus, energy reallocation to calcification and other *physiologically*-mediated or physiological processes (D'Olivo and McCulloch 2017; Glazier et al. 2020), could be a potential acclimation to changing environmental conditions (Stuhr et al. 2021). However, as calcification is an energetically costly process, it is expected that an energetic tradeoff mechanism occurs between constructing and maintaining the skeleton with other physiological processes. In the

long term, this mechanism might have further adverse physiological repercussions for the starfish. Corroborating our interpretation, a positive increase in calcification rate coinciding with an increase in metabolic rates was also found in the brittlestar *O. ophiura* (Wood et al. 2010).

Our study shows that, besides seawater carbonate chemistry, temperature acts as an indirect determinant in regulating the calcification and dissolution rate of *A. yairi*, because temperature influences the physiological and biochemical processes that are contingent on the thermal tolerance capacity of organisms (Pörtner 2012). Our findings indicate that elevated temperature might alleviate the effect of ocean acidification on calcification performance in *A. yairi* and thereby mitigate the impacts of decreases in carbonate saturation in the seawater (Ω ; Supplementary Table S3.1). Additionally, increased temperatures are potentially advantageous to calcifying organisms as precipitation of CaCO_3 is enhanced by higher temperatures (Manno et al. 2012; Pinsonneault et al. 2012), while reducing the solubility of seawater CO_2 , thus decreasing the dissolution rate (Ries et al. 2016). A positive calcification response to increasing temperatures at high $p\text{CO}_2$ has been described before for organisms where the temperature is beneath the thermal optimum and depending on their potential adaptability to increasing temperatures (Karelitz et al. 2017; Manríquez et al. 2017), and here we observe an analogous behavior for *A. yairi*.

We interpret the combined effects of increasing temperature and $p\text{CO}_2$ on the calcification rate of *A. yairi* as an antagonistic response, with OW reducing the negative effects of OA. The term antagonistic effect describes the situation when the combined effect of multiple stressors is less than the sum of effects elicited by single stressors, in which one stressor offsets the effect of the other (Folt et al. 1999), influenced by different responsible parameters including organism phyla, genetics, life stages, feeding, disturbance history, stressors magnitude, exposure duration, and light (Kroeker et al. 2013; Przeslawski et al. 2015; Guillermic et al. 2021). This suggests that a lowered calcification rate or even dissolution at higher $p\text{CO}_2$ concentrations (lowered pH) can be partially compensated by elevated temperature. Previous studies on the sea star *P. ochraceus* (Gooding et al., 2009), and the sea urchin *Tripneustes gratilla* (Brennand et al. 2010), and *E. viridis* (Courtney et al. 2013) have shown a similar antagonistic interactive reaction to OA and OW with respect to calcification. For the starfish *A. yairi* studied here, the calcification response to OA is resilient under the higher temperature (32 °C), even though at a

low-positive calcification rate. However, we documented that for long-term exposure, low calcification rate (G_{TA} close to $0 \mu\text{mol CaCO}_3 \text{ g dw}^{-1} \text{ h}^{-1}$) in high temperature ($32 \text{ }^\circ\text{C}$) under elevated $p\text{CO}_2$ treatments altered to the microstructure and mineral composition of the starfish skeleton (Khalil et al. 2022), which means that calcification rate might not compensate for the dissolution rate in the longer perspective.

3.5. Conclusion

Our study gives novel insights into the potential response of the starfish *A. yairi* to future OA and OW. The parameters $p\text{CO}_2$ and temperature as sole or combined stressors had little effect on starfish mortality, but temperature acted as a primary regulator of increased metabolic and accelerated righting activity, whereas $p\text{CO}_2$ leads to a decreased calcification rate. Notably, *A. yairi* might benefit from increased temperatures to mitigate the negative effect of increased $p\text{CO}_2$ on their calcification. Seemingly, an accelerated metabolic rate in response to elevated temperatures is a functional factor that provides sufficient energy for starfish to endure low seawater pH. Energetic trade-offs and reallocation among physiological processes are exhibited to maintain starfish performance and survivability throughout the duration of exposure. Sufficient food availability is required to sustain a higher energetic demand. Increasing feeding activities could alter the feeding behavior of the starfish and potentially increase the risk of predation, even though faster righting activity is thought to decrease predation risk. However, such ecological consequences are as yet unknown. Clearly, understanding how environmental stressors affect the physiology and performance of marine organisms is essential in predicting species-specific responses to climate change, with implications to the ecosystem context.

3.6. Acknowledgements

We are grateful to MoECRT, Republic of Indonesia - ADB AKSI Project for a doctoral scholarship granted to MK. We thank Silvia Hardenberg, José Garcia, Nico Steinel of the ZMT Marine Experimental Ecology Facility (MAREE) for providing advice, support, and technical assistance, and ZMT laboratory staff Matthias Birkicht, Fabian Hüge, and Stefanie Bröhl for assistance in the chemistry and biology laboratories. The authors thank the reviewers for their comments, which greatly improved the article.

3.7. Supplementary materials

Supplementary text

Animal collection and acclimation

Aquilonastra yairi (342 specimens, size 3-11 mm) were collected from stock cultured in the MAREE (Marine Experimental Ecology) of ZMT. The specimens were cleaned from epibionts and debris and allowed to acclimate in a tank with a recirculating system to the temperature of ≈ 27 °C. After seven days of acclimation, the starfish were randomly distributed to the 18 treatment tanks (19 specimens in each tank) for a further 7-day acclimation period (see Khalil et al. (2022)).

Seawater chemistry control and manipulation

The $p\text{CO}_2$ of the bubbled gases were regulated by blending compressed CO_2 -free air and compressed CO_2 using electronic solenoid-valve mass flow controllers (HTK Hamburg, Germany; pure CO_2 provided by Linde GmbH, Pullach, Germany) to generate gas mixtures formulated to the target $p\text{CO}_2$ conditions in accordance with the standard operating procedure (SOP) for ocean CO_2 measurements (Dickson et al., 2007), and bubbled through microporous air stones into the lower water reservoirs of each treatment group. Water was continuously pumped from the lower reservoir to the three replicate tanks contained within the upper reservoir of each treatment group. Water overflowed the replicate tanks into the upper reservoir, then streamed down into the lower reservoir. Dead coral fragments and activated charcoal were used to filter the water in the lower reservoir. Furthermore, an aquarium pump circulates the aquarium water continuously from the lower reservoir to the replicate tanks in the upper reservoir. The treatment group and replicate tank were covered with a transparent Plexiglas lid to avert in-/outgassing and minimize evaporation. Treatment tank temperatures ($\pm\text{SE}$) were maintained at $27 (\pm 0.05)$ °C and $32 (\pm 0.08)$ °C, separately using a closed circle heating system (Heaters Titanium Tube 600 W, Shego, Germany) controlled with a programmable thermostat (Supplementary Figure S3.2).

Temperature, salinity, and pH_{NBS} were measured three times per week using a multielectrode portable probe (WTW Multiline 3630 IDS, Xylem Analytics, Germany). National Bureau of Standard (NBS) buffers pH 4.00 and 7.00 were used to calibrate the pH electrode probe, while the salinity-conductivity probe was calibrated with certified seawater reference material (Dickson CRM batch #154) of salinity 33.347. The $\text{pH}_{\text{total scale}}$ was measured weekly through the

spectrophotometric (Shimadzu UV-1700 Pharma Spec UV-Vis Spectrophotometer) method following SOP 6b (Dickson et al., 2007) using the indicator dye meta, *m*-cresol purple (Sigma-Aldrich) as the chromogenic reagent. Seawater samples for total alkalinity (A_T) and dissolved inorganic carbon (C_T) analysis were collected weekly in 500-mL borosilicate glass vials and poisoned with 200 μ L of saturated mercuric chloride (HgCl_2) solution and refrigerated until analysis. Measurements of A_T and C_T followed the protocols described in Dickson et al. (2007). A_T was measured by open-cell potentiometric Gran titration (to a precision of 10 $\mu\text{mol/kg}$), and C_T was determined by the colorimetric analytical method using a Shimadzu DIC analyzer (to a precision of 10 $\mu\text{mol/kg}$). The seawater carbonate system parameters $p\text{CO}_2$, carbonate ion concentration [CO_3^{2-}], bicarbonate ion concentration [HCO_3^-], aqueous CO_2 , calcite saturation state (Ω_{Ca}), and aragonite saturation state (Ω_{Ar}) were calculated with the program CO_2SYS software for MS Excel (Pelletier et al., 2007b), using Hansson (1973) and Mehrbach et al. (1973) refitted by Dickson and Millero (1987) for K_1 and K_2 carbonic acid constants; Dickson (1990) for K_{HSO_4} equilibrium constant; Dickson and Riley (1979) for K_{HF} dissociation constant; Uppström (1974) for the boric acid constant ($[\text{B}]_{\text{T}}$); and Mucci (1983) for the stoichiometric calcite solubility constant (supplementary material, Table S1). The full description of seawater chemistry control and manipulation is presented in Khalil et al. (2022)

Metabolic rate measurement

Oxygen consumption rate (M_{O_2}) was measured seven times throughout the experiment, namely on days 1, 15, 30, 45, 60, 75, and 90 of incubation time. Any epibionts were identified and removed prior to the measurement to prevent competition for oxygen consumption. During each of the seven measuring campaigns, six starfish per treatment (in total $n = 36$) were continuously observed for 60 minutes in 2-mL respiration glass vials equipped with integrated planar oxygen sensors (5 mm diameter, optical isolation, type SV-PSt5-NAU-D5-YOP, PreSens, Germany). For the measurements, the individuals were transferred into respiration glass vials that were filled with seawater of the same $p\text{CO}_2$ and temperature as the starfish had been exposed to throughout the experiment, along with two controls per treatment to correct for microorganism respiration (blank vials containing seawater from experimental tanks but no starfish).

The starfish were placed in the respiration glass vials in the experimental seawater tanks when immersed to avoid air bubbles and placed sequentially on the sensor disk surface. The

respiration glass vials were then closed tightly and sealed. The starfish were acclimated to the respiration vials for 30 minutes prior to the 60 minutes incubation in which M_{O_2} was measured. M_{O_2} measurements were performed under dark condition by using an incubator (temperature accuracy ± 0.1 °C) equipped with an orbital shaker. The glass vials were constantly stirred during the measuring period with a rotating plate at a speed of 50 rpm to ensure homogeneous oxygen measurements (Clark et al., 2013). Respiration data were obtained at three-minute time intervals using the digital software SDR v4.0.0 (PreSens, Germany). Following the respiration measurements, the individual starfish were patted dry, and damp-dry wet fresh body mass was weighed using an analytical balance with an accuracy of 0.0001 g. The starfish were returned back to their aquaria immediately after the testing.

Righting activity coefficient measurement

Righting activity coefficient (RAC) was measured six times throughout the experiment (on days 1, 19, 37, 55, 73, and 90 of exposure). To measure righting activity time, individual starfish were gently placed inside a petri dish with the dorsal side inverted in the experimental tanks at the corresponding treatment scenario. The righting activity was considered completed when the ventral side of the disc and the ambulacra were laid entirely on the bottom floor of the experimental tank (Lawrence & Cowell, 1996; McCarthy et al., 2020). The time taken by the starfish to invert the ventral side to the bottom substrate was recorded (in seconds) and observed for a total of 10 min. Individuals that did not exhibit any righting action within ten minutes were assigned a value of 0 (Watts & Lawrence, 1990). The righting time response of the starfish individuals ($n = 6$ per treatment, 36 in total per time interval) for all treatments were recorded every 19 days over the 90 days of the experimental period.

Calcification rate measurement

Calcification was estimated by using the relationship: $Ca^{2+} + 2HCO_3^- \rightleftharpoons CaCO_3 + CO_2 + H_2O$, based on the assumption that the precipitation of 1 mole of $CaCO_3$ consumes 2 moles of HCO_3^- (Gazeau et al., 2007; Martin et al., 2006). However, other biogeochemical mechanisms, e.g., changes in inorganic nutrient concentration, might also have an influence on total alkalinity A_T (Wolf-Gladrow et al., 2007). Consequently, the starfish calcification rate (G_{TA}) was estimated using the modified alkalinity anomaly technique proposed by Gazeau et al. (2015) to correct for other processes (e.g., remineralization and assimilation) that can affect A_T independent from calcification. Calcification rates were determined by conducting short-term incubations

(48 hours) on individual starfish in a closed system. One individual from each replicate ($n = 18$) was chosen randomly and placed in separate 300-mL polyethylene beakers containing 50 ml of filtered seawater (0.45 μm) from the respective treatment tanks. The beakers were then placed in an incubator to maintain a consistent temperature (27 ± 0.1 °C and 32 ± 0.1 °C, respectively), and the seawater was constantly mixed in each beaker via a stir-plate (30 rpm) during the incubation. Before and after incubation, samples were taken from all beakers for determining total alkalinity (A_T), ammonium (NH_4^+), nitrate + nitrite ($\text{NO}_3^- + \text{NO}_2^-$), and phosphate (PO_4^{3-}). Samples were immediately fixated with 100 μL of a saturated solution of mercuric chloride (HgCl_2) and refrigerated (4 °C) for further analysis. A_T was determined by open-cell potentiometric Gran titration (accuracy ± 10 $\mu\text{mol kg}^{-1}$).

Supplementary table

Table S3.1. Seawater parameters (mean \pm SE) from treatment tanks of *A. yairi*. A_T , total alkalinity; C_T , dissolved inorganic carbon (DIC); $p\text{CO}_2$, partial pressure of CO_2 ; $[\text{CO}_3^{2-}]$, carbonate ion; $[\text{HCO}_3^-]$, bicarbonate ion; $[\text{CO}_2]$, dissolved CO_2 ; Ω_{ca} , calcite saturation state; Ω_{Ar} , aragonite saturation state; SW, seawater.

Measured parameters	Treatment					
	T1 (27 °C : 455 μatm)	T2 (27 °C : 1052 μatm)	T3 (27 °C : 2066 μatm)	T4 (32 °C : 455 μatm)	T5 (32 °C : 1052 μatm)	T6 (32 °C : 2066 μatm)
Salinity (PSU)	34.56 \pm 0.12	34.73 \pm 0.06	34.75 \pm 0.05	34.65 \pm 0.08	34.78 \pm 0.05	34.76 \pm 0.02
Temperature (°C)	27.48 \pm 0.06	27.23 \pm 0.04	27.34 \pm 0.03	32.03 \pm 0.05	32.10 \pm 0.04	32.20 \pm 0.08
pH_T (NBS scale)	8.13 \pm 0.00	7.87 \pm 0.01	7.60 \pm 0.01	8.13 \pm 0.00	7.87 \pm 0.00	7.60 \pm 0.01
pH_T (total scale)	8.00 \pm 0.00	7.74 \pm 0.01	7.47 \pm 0.01	8.00 \pm 0.00	7.74 \pm 0.00	7.47 \pm 0.01
A_T ($\mu\text{mol/kg-SW}$)	2504.42 \pm 15.33	2514.45 \pm 16.78	2539.83 \pm 38.86	2510.27 \pm 47.18	2532.19 \pm 40.05	2584.38 \pm 41.93
C_T ($\mu\text{mol/kg-SW}$)	2168.86 \pm 15.23	2340.99 \pm 11.62	2479.40 \pm 36.58	2134.38 \pm 38.40	2325.20 \pm 40.02	2493.30 \pm 37.87

Calculated parameters	Treatment					
	T1 (27 °C : 455 μatm)	T2 (27 °C : 1052 μatm)	T3 (27 °C : 2066 μatm)	T4 (32 °C : 455 μatm)	T5 (32 °C : 1052 μatm)	T6 (32 °C : 2066 μatm)
$p\text{CO}_2$ (μatm)	456.13 \pm 8.24	1059.58 \pm 32.04	2075.40 \pm 30.99	453.78 \pm 6.51	1045.15 \pm 44.00	2057.31 \pm 74.42
$[\text{CO}_3^{2-}]$ ($\mu\text{mol/kg-SW}$)	245.64 \pm 2.52	138.12 \pm 4.64	81.18 \pm 2.35	273.82 \pm 8.23	162.68 \pm 4.67	99.46 \pm 4.64
$[\text{HCO}_3^-]$ ($\mu\text{mol/kg-SW}$)	1911.05 \pm 14.94	2178.74 \pm 9.58	2342.71 \pm 34.29	1849.66 \pm 30.77	2147.47 \pm 38.59	2344.63 \pm 34.94
$[\text{CO}_2]$ ($\mu\text{mol/kg-SW}$)	12.17 \pm 0.22	28.42 \pm 0.86	55.51 \pm 0.82	10.90 \pm 0.16	25.05 \pm 1.06	49.20 \pm 1.78
Ω_{ca}	5.96 \pm 0.06	3.35 \pm 0.11	1.97 \pm 0.06	6.71 \pm 0.20	3.98 \pm 0.11	2.44 \pm 0.11
Ω_{Ar}	3.96 \pm 0.04	2.22 \pm 0.07	1.31 \pm 0.04	4.52 \pm 0.14	2.69 \pm 0.08	1.64 \pm 0.08

Table S3.2. The effect of temperature (27 °C, 32 °C) and $p\text{CO}_2$ (455 μatm , 1052 μatm , and 2066 μatm) on the starfish *A. yairi* metabolic rate for 90 days of incubation time.

Treatment	Oxygen consumption (mean \pm SE)
T1, 27 °C : 455 μatm ($n = 42$)	0.820 \pm 0.047 $\mu\text{mol g}^{-1} \text{h}^{-1}$
T2, 27 °C : 1052 μatm ($n = 42$)	0.988 \pm 0.057 $\mu\text{mol g}^{-1} \text{h}^{-1}$
T3, 27 °C : 2066 μatm ($n = 42$)	1.130 \pm 0.066 $\mu\text{mol g}^{-1} \text{h}^{-1}$
T4, 32 °C : 455 μatm ($n = 42$)	1.459 \pm 0.086 $\mu\text{mol g}^{-1} \text{h}^{-1}$
T5, 32 °C : 1052 μatm ($n = 42$)	1.419 \pm 0.091 $\mu\text{mol g}^{-1} \text{h}^{-1}$
T6, 32 °C : 2066 μatm ($n = 42$)	1.416 \pm 0.089 $\mu\text{mol g}^{-1} \text{h}^{-1}$

Table S3.3. The effect of temperature (27 °C, 32 °C) and $p\text{CO}_2$ (455 μatm , 1052 μatm , and 2066 μatm) on the starfish *A. yairi* righting activity coefficient (RAC) for 90 days of incubation time.

Treatment	RAC (mean \pm SE)
T1, 27 °C : 455 μatm ($n = 36$)	15.025 \pm 0.774
T2, 27 °C : 1052 μatm ($n = 36$)	15.048 \pm 0.709
T3, 27 °C : 2066 μatm ($n = 36$)	13.745 \pm 0.815
T4, 32 °C : 455 μatm ($n = 36$)	19.624 \pm 1.227
T5, 32 °C : 1052 μatm ($n = 36$)	21.042 \pm 1.393
T6, 32 °C : 2066 μatm ($n = 36$)	20.122 \pm 1.353

Table S3.4. Tukey HSD post hoc test results for the sole and interactive effects of temperature (27 °C and 32 °C), and $p\text{CO}_2$ (455 μatm , 1052 μatm , and 2066 μatm) on the starfish *A. yairi* metabolic rate and calcification rate (Table 3.1) for 90 days of incubation time. Significant effects ($p < 0.05$) are in bold.

Condition	diff.	lwr.	upr.	p_{adj}
<i>Metabolic rate (Mo_2)</i>				
<i>Incubation time</i>				
day15 vs day1	0.128	-0.146	0.402	0.806
day30 vs day1	0.107	-0.168	0.381	0.910
day45 vs day1	0.054	0.220	0.328	0.997
day60 vs day1	0.331	0.057	0.605	0.007
day75 vs day1	0.014	-0.260	0.288	1.000
day90 vs day1	0.040	-0.234	0.314	0.999
day30 vs day15	-0.022	-0.296	0.252	1.000
day45 vs day15	-0.074	-0.349	0.200	0.984
day60 vs day15	0.203	-0.071	0.477	0.300
day75 vs day15	-0.114	-0.388	0.160	0.879
day90 vs day15	-0.088	-0.363	0.186	0.962
day45 vs day30	-0.053	-0.327	0.221	0.998
day60 vs day30	0.224	-0.050	0.499	0.189
day75 vs day30	-0.092	-0.367	0.182	0.953
day90 vs day30	-0.067	-0.341	0.208	0.991
day60 vs day45	0.277	0.003	0.551	0.046
day75 vs day45	-0.040	-0.314	0.235	1.000
day90 vs day45	-0.014	-0.288	0.260	1.000
day75 vs day60	-0.317	-0.591	-0.043	0.012
day90 vs day60	-0.291	-0.565	-0.017	0.029
day90 vs day75	0.026	-0.248	0.300	1.000
<i>$p\text{CO}_2$</i>				
1052 μatm vs 455 μatm	0.071	-0.071	0.214	0.465
2066 μatm vs 455 μatm	0.154	0.012	0.296	0.030
2066 μatm vs 1052 μatm	0.083	-0.060	0.225	0.358
<i>Temperature:$p\text{CO}_2$</i>				
32 °C : 455 μatm vs 27 °C : 455 μatm	0.575	0.330	0.820	0.000

27 °C : 1052 μ atm vs 27 °C : 455 μ atm	0.181	-0.065	0.426	0.282
32 °C : 1052 μ atm vs 27 °C : 455 μ atm	0.537	0.292	0.782	0.000
27 °C : 2066 μ atm vs 27 °C : 455 μ atm	0.330	0.084	0.575	0.002
32 °C : 2066 μ atm vs 27 °C : 455 μ atm	0.553	0.308	0.799	0.000
27 °C : 1052 μ atm vs 32 °C : 455 μ atm	-0.394	-0.639	-0.149	0.000
32 °C : 1052 μ atm vs 32 °C : 455 μ atm	-0.038	-0.283	0.207	0.998
27 °C : 2066 μ atm vs 32 °C : 455 μ atm	-0.245	-0.491	0.000	0.050
32 °C : 2066 μ atm vs 32 °C : 455 μ atm	-0.021	-0.267	0.224	1.000
32 °C : 1052 μ atm vs 27 °C : 1052 μ atm	0.356	0.111	0.602	0.001
27 °C : 2066 μ atm vs 27 °C : 1052 μ atm	0.149	-0.096	0.394	0.503
32 °C : 2066 μ atm vs 27 °C : 1052 μ atm	0.373	0.128	0.618	0.000
27 °C : 2066 μ atm vs 32 °C : 1052 μ atm	-0.207	-0.453	0.038	0.151
32 °C : 2066 μ atm vs 32 °C : 1052 μ atm	0.016	-0.229	0.262	1.000
32 °C : 2066 μ atm vs 27 °C : 2066 μ atm	0.224	-0.021	0.469	0.096

Righting activity (RAC)

Incubation time

day19 vs day1	0.075	-0.159	0.310	0.940
day37 vs day1	0.091	-0.143	0.326	0.872
day55 vs day1	-0.046	-0.280	0.189	0.993
day73 vs day1	-0.040	-0.274	0.195	0.997
day90 vs day1	-0.143	-0.378	0.092	0.499
day37 vs day19	0.016	-0.219	0.251	1.000
day55 vs day19	-0.121	-0.356	0.114	0.675
day73 vs day19	-0.115	-0.350	0.120	0.721
day90 vs day19	-0.218	-0.453	0.016	0.085
day55 vs day37	-0.137	-0.372	0.098	0.546
day73 vs day37	-0.131	-0.366	0.103	0.594
day90 vs day37	-0.234	-0.469	0.000	0.050
day73 vs day55	0.006	-0.229	0.241	1.000
day90 vs day55	-0.097	-0.332	0.137	0.840
day90 vs day73	-0.103	-0.338	0.131	0.804

Calcification rate (G_{TA})

pCO₂

1052 μ atm vs 455 μ atm	0.115	-0.043	0.273	0.168
2066 μ atm vs 455 μ atm	0.607	0.449	0.764	0.000

2066 μatm vs 1052 μatm	0.492	0.334	0.649	0.000
<i>Temperature:pCO₂</i>				
32 °C : 455 μatm vs 27 °C : 455 μatm	0.533	0.252	0.814	0.000
27 °C : 1052 μatm vs 27 °C : 455 μatm	0.233	-0.048	0.514	0.128
32 °C : 1052 μatm vs 27 °C : 455 μatm	0.530	0.249	0.811	0.000
27 °C : 2066 μatm vs 27 °C : 455 μatm	1.138	0.857	1.419	0.000
32 °C : 2066 μatm vs 27 °C : 455 μatm	0.609	0.328	0.889	0.000
27 °C : 1052 μatm vs 32 °C : 455 μatm	-0.300	-0.581	-0.019	0.034
32 °C : 1052 μatm vs 32 °C : 455 μatm	-0.003	-0.284	0.278	1.000
27 °C : 2066 μatm vs 32 °C : 455 μatm	0.605	0.324	0.886	0.000
32 °C : 2066 μatm vs 32 °C : 455 μatm	0.076	-0.205	0.357	0.938
32 °C : 1052 μatm vs 27 °C : 1052 μatm	0.297	0.017	0.578	0.036
27 °C : 2066 μatm vs 27 °C : 1052 μatm	0.905	0.624	1.186	0.000
32 °C : 2066 μatm vs 27 °C : 1052 μatm	0.376	0.095	0.657	0.007
27 °C : 2066 μatm vs 32 °C : 1052 μatm	0.608	0.327	0.888	0.000
32 °C : 2066 μatm vs 32 °C : 1052 μatm	0.078	-0.202	0.359	0.929
32 °C : 2066 μatm vs 27 °C : 2066 μatm	-0.529	-0.810	-0.248	0.000

Supplementary figure

(a)



(b)



Figure S3.1. Asterinid starfish *A. yairi*, **(a)** dorsal view, **(b)** ventral view.

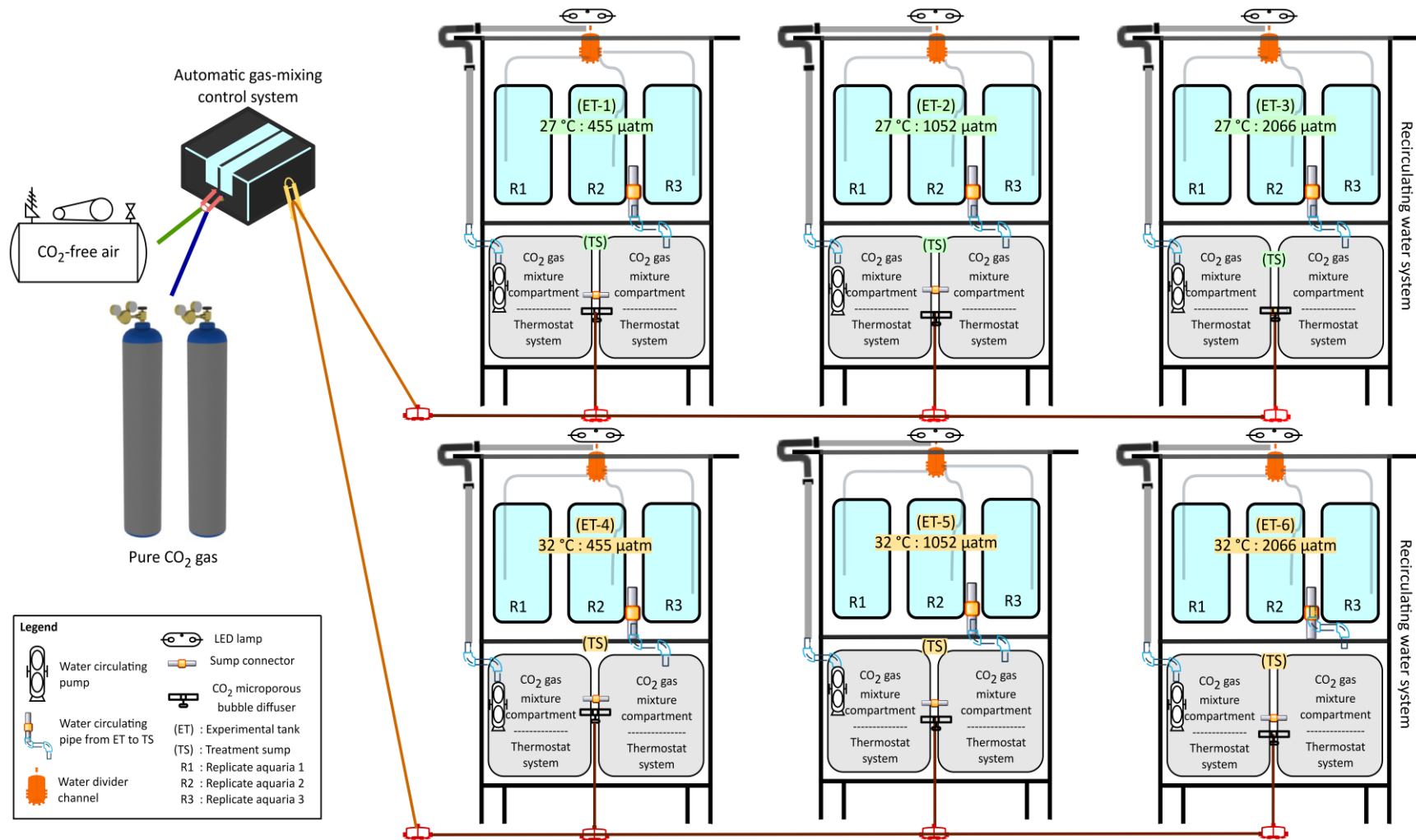


Figure S3.2. Schematic of experimental design to determine the impact of ocean acidification and warming on the tropical asterinid starfish *A. yairi* (unmodified from Khalil et al. (2022)).

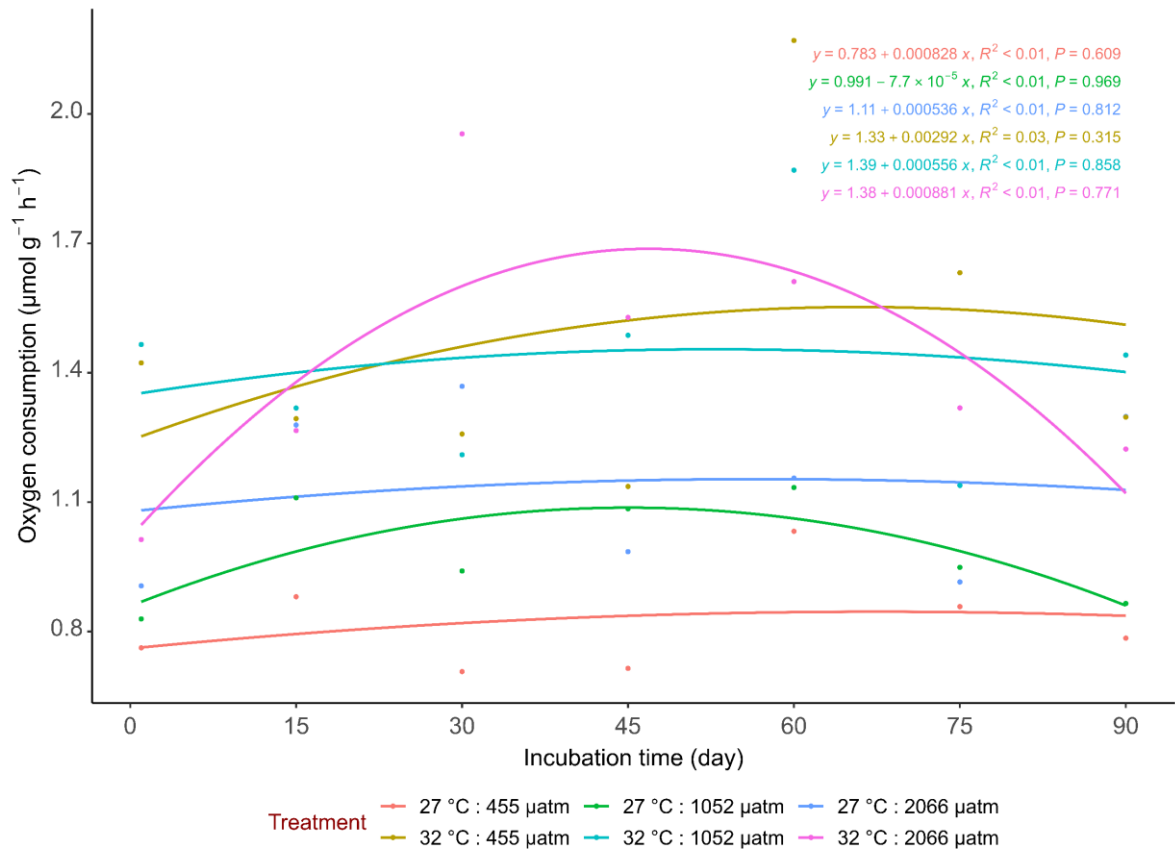


Figure S3.3. Linear polynomial interpolation model for the metabolic rate (M_{O_2}) responses of *A. yairi* reared under different $p\text{CO}_2$ concentrations (455 μatm , 1052 μatm , and 2066 μatm) and temperatures (27 °C, 32 °C) for 90 days of incubation time. Colored dots indicate the mean effect on M_{O_2} in each treatment.

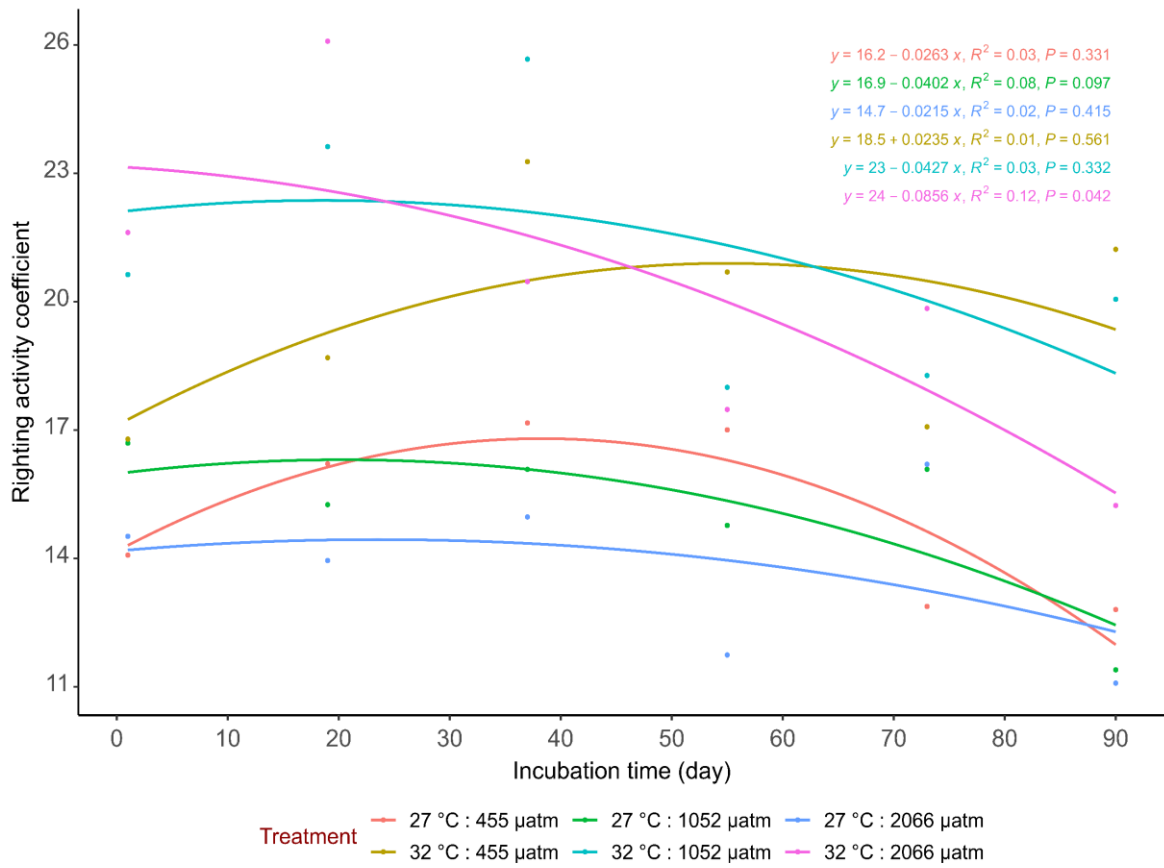


Figure S3.4. Linear polynomial interpolation model for the righting activity coefficient (RAC) of *A. yairi* reared under different pCO₂ concentrations (455 μatm, 1052 μatm, and 2066 μatm) and temperatures (27 °C, 32 °C) for 90 days of incubation time. Colored dots indicate the mean effect on RAC in each treatment.

Chapter 4. Simultaneous ocean acidification and warming do not alter the lipid-associated biochemistry but induce enzyme activities in an asterinid starfish

This work has been published in Science of The Total Environment 932, 173000, <https://doi.org/10.1016/j.scitotenv.2024.173000>.

Munawar Khalil^{1,2,3,*}, Marleen Stuhr¹, Andreas Kunzmann¹, and Hildegard Westphal^{1,2}

¹ Leibniz Centre for Tropical Marine Research (ZMT), 28359 Bremen, Germany;

² Faculty of Geosciences, University of Bremen, 28359 Bremen, Germany

³ Department of Marine Science, Faculty of Agriculture, Universitas Malikussaleh, Reuleut Main Campus, Aceh 24355, Indonesia



Simultaneous ocean acidification and warming do not alter the lipid-associated biochemistry but induce enzyme activities in an asterinid starfish

Munawar Khalil^{a,b,c,*}, Marleen Stuhr^a, Andreas Kunzmann^a, Hildegard Westphal^{a,b}

^a Leibniz Centre for Tropical Marine Research (ZMT), Fahrenheitstraße 6, 28359 Bremen, Germany

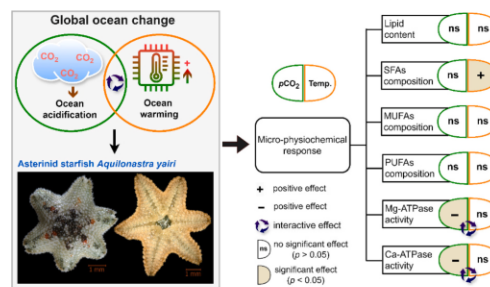
^b Faculty of Geosciences, University of Bremen, Klagenfurter Str. 2-4, 28359 Bremen, Germany

^c Department of Marine Science, Faculty of Agriculture, Universitas Malikussaleh, Reuleut Main Campus, 24355 North Aceh, Indonesia

HIGHLIGHTS

- Ocean acidification and warming impacts on tropical-subtropical asterinid starfish were investigated.
- Combined stressors did not affect starfish lipid and fatty acids.
- Ocean warming increased starfish total lipid, SFAs, and PUFAs but reduced MUFAs concentration.
- Elevated temperature allowed starfish to cope with the negative effect of increased pCO₂ on enzyme activities.

GRAPHICAL ABSTRACT



ARTICLE INFO

Editor: Olga Pantos

Keywords:

Global ocean change
Multiple stressors
Asteroid
Lipid content
Fatty acid
Calcification-related enzyme

ABSTRACT

Ocean acidification and warming affect marine ecosystems from the molecular scale in organismal physiology to broad alterations of ecosystem functions. However, knowledge of their combined effects on tropical-subtropical intertidal species remains limited. Pushing the environmental range of marine species away from the optimum initiates stress impacting biochemical metabolic characteristics, with consequences on lipid-associated and enzyme biochemistry. This study investigates lipid-associated fatty acids (FAs) and enzyme activities involved in biomineralization of the tropical-subtropical starfish *Asterionaster yairi* in response to projected near-future global change. The starfish were acclimatized to two temperature levels (27 °C, 32 °C) crossed with three pCO₂ concentrations (455 μatm, 1052 μatm, 2066 μatm). Total lipid (ΣL_C) and FAs composition were unaffected by combined elevated temperature and pCO₂, but at elevated temperature, there was an increase in ΣL_C, SFAs (saturated FAs) and PUFAs (polyunsaturated FAs), and a decrease in MUFAs (monounsaturated FAs). However, temperature was the sole factor to significantly alter SFAs composition. Positive parabolic responses of Ca-ATPase and Mg-ATPase enzyme activities were detected at 27 °C with elevated pCO₂, while stable enzyme activities were observed at 32 °C with elevated pCO₂. Our results indicate that the lipid-associated biochemistry of *A. yairi* is resilient and capable of coping with near-future ocean acidification and warming. However, the

* Corresponding author at: Leibniz Centre for Tropical Marine Research (ZMT), Fahrenheitstraße 6, 28359 Bremen, Germany.
E-mail address: munawar.khalil@leibniz-zmt.de (M. Khalil).

<https://doi.org/10.1016/j.scitotenv.2024.173000>

Received 18 December 2023; Received in revised form 30 April 2024; Accepted 3 May 2024

Available online 6 May 2024

0048-9697/© 2024 The Authors. Published by Elsevier B.V. This is an open access article under the CC BY license (<http://creativecommons.org/licenses/by/4.0/>).

Statement of Contribution

Idea and concept: Personal contribution 95%. M. Khalil developed the idea to focus on the biochemical metabolic characteristic of asterinid starfish under ocean acidification and ocean warming projection, with contributions on method from H. Westphal, and M. Stuhr. The research project was supervised by H. Westphal.

Research: Personal contribution 85%. M. Khalil carried out laboratory experiments, analyzed the data, created figures and tables, and interpreted the data.

Manuscript writing: Personal contribution 95%. M. Khalil wrote the initial manuscript, with contributions and improvements from H. Westphal, M. Stuhr, and A. Kunzmann.

Abstract

Ocean acidification and warming affect marine ecosystems from the molecular scale in organismal physiology to broad alterations of ecosystem functions. However, knowledge of their combined effects on tropical-subtropical intertidal species remains limited. Pushing the environmental range of marine species away from the optimum initiates stress impacting biochemical metabolic characteristics, with consequences on lipid-associated and enzyme biochemistry. This study investigates lipid-associated fatty acids (FAs) and enzyme activities involved in biomineralization of the tropical-subtropical starfish *Aquilonastra yairi* in response to projected near-future global change. The starfish were acclimatized to two temperature levels (27 °C, 32 °C) crossed with three $p\text{CO}_2$ concentrations (455 μatm , 1052 μatm , 2066 μatm). Total lipid (ΣL_c) and FAs composition were unaffected by combined elevated temperature and $p\text{CO}_2$, but at elevated temperature, there was an increase in ΣL_c , SFAs (saturated FAs) and PUFAs (polyunsaturated FAs), and a decrease in MUFAs (monounsaturated FAs). However, temperature was the sole factor to significantly alter SFAs composition. Positive parabolic responses of Ca-ATPase and Mg-ATPase enzyme activities were detected at 27 °C with elevated $p\text{CO}_2$, while stable enzyme activities were observed at 32 °C with elevated $p\text{CO}_2$. Our results indicate that the lipid-associated biochemistry of *A. yairi* is resilient and capable of coping with near-future ocean acidification and warming. However, the calcification-related enzymes Ca-ATPase and Mg-ATPase activity appear to be more sensitive to $p\text{CO}_2$ /pH changes, leading to vulnerability concerning the skeletal structure.

Keywords: global ocean change, multiple stressors, asteroid, lipid content, fatty acid, calcification-related enzyme

4.1. Introduction

Approximately $\approx 25\%$ (mean uptake of -2.7 ± 0.3 Pg C per year⁻¹, 1 Pg = 10^{15} g) of the annual CO₂ emissions are directly absorbed by the oceans (Gruber et al., 2023) and significantly alter seawater chemistry (i.e., reductions in pH and re-equilibration of carbonate systems), termed ocean acidification (OA) (Zeebe, 2012). These alterations leave an imprint on oceanic and coastal environments with potential impacts on the eco-physiology of marine organisms, especially calcifying species (Doney et al., 2012; Feely et al., 2004; Leung et al., 2022). Previous studies have shown that OA impacts physio-chemical aspects (i.e., behavior, reproduction, growth, development, survival, fitness, and metabolism) and skeletal mineralogical structures (i.e., biomineralization) of marine organisms (Byrne & Fitzner, 2019; Dubois, 2014; Figuerola et al., 2021; Kroeker et al., 2013; Leung et al., 2022; Melzner et al., 2020). Furthermore, the effects of OA on marine organisms can interact, often non-intuitively, with those of other environmental stressors, including ocean warming (OW) (Gao et al., 2020). OW alone is recognized to elicit detrimental consequences on vital biological processes of a wide range of marine organisms, with cascading effects on habitat structure and ecosystem functioning (Smale et al., 2019).

Among marine ecosystems, intertidal regions are predicted to experience the most significant impacts of OA and OW due to their exposure to high variability in temperature, pH, and direct anthropogenic drivers (Harley et al., 2006). This environmental volatility could expose marine intertidal organisms (e.g., anthozoa, asteroidea, bivalvia, and gastropoda) to conditions beyond the limits of their tolerance range, which may substantially impact their biological performance metrics (Byrne, 2011; Gao et al., 2020; Melzner et al., 2020). OA and OW can affect cellular and molecular processes that are physically reflected by an organism (Pörtner, 2008). Furthermore, OA and OW have been recognized to influence the intracellular ionic balance in calcifying organisms (Ramesh et al., 2017). Consequently, major reductions in biological performance and shifts in the organismal mode of life (i.e., active vs. passive) can follow, subsequently disrupting the trophic levels and causing further shifts in the food web system (Guinotte & Fabry, 2008; Pörtner, 2008).

As slow-moving intertidal echinoderms, asteroids (common name: starfish or sea stars, class asteroidea) are highly susceptible to abiotic and biotic changes in their habitat. Owing to their capacity as ectothermic animals with narrow tolerable to temperature alterations, asteroids

are considered useful model organisms for global change studies focusing on the effects of OW and OA (Lang et al., 2023; Nguyen & Byrne, 2014). OA can narrow the thermal tolerance range, resulting in a higher susceptibility to extreme temperatures and reducing an organism's performance metrics, altering morphological structures, behavioral responses, and physiological processes (Pörtner, 2008; Schalkhauser et al., 2012; Walther et al., 2009). Furthermore, the asteroid endoskeleton is composed of high Mg-calcite (>4 wt% MgCO₃ (Dickson, 2002; Weber, 1969)); hence, it is more susceptible to dissolution under OA conditions (Dubois, 2014; Figuerola et al., 2021). Previous research has shown that interactive effects (additive or synergistic) of OA and OW in the asteroid class elevated the metabolic rate (Khalil et al., 2023), increased larval mortality (Byrne et al., 2013), and produced larval developmental delay (Hue et al., 2022), behavioral modifications (McLaren & Byrne, 2022), modified coelomic fluid and coelomocytes (Wahlteiz et al., 2023) and altered skeletal mineralogy (Khalil et al., 2022). On the contrary, other studies have found that some asteroids could benefit from combined OA and OW, showing increased growth (Gooding et al., 2009), and feeding enhancement (Kamya et al., 2016). However, the biochemical and physiological mechanisms underlying the phenotypic response of asteroids to lower pH (high $p\text{CO}_2$) and increased temperature remain unknown.

Understanding how organisms might respond to combined OA and OW can be gained through laboratory experiments that expose organisms to manipulated levels of seawater $p\text{CO}_2$ and temperature. While in recent years, abundant experiments have been carried out studying the effects of future environmental changes (e.g., elevated temperature, reduced pH, hypoxia, and changes in seawater Mg²⁺/Ca²⁺ ratio as a sole or combined stressor) on the physiological processes and skeletal production of echinoderm species (Azcarate-Garcia et al., 2024; Byrne & Fitzer, 2019; Hu et al., 2022; Lang et al., 2023; Sampaio et al., 2021; Smith et al., 2016), we here examine how a tropical-subtropical asterinid starfish regulates its physiological performance in response to environmental stressors (OA and OW) by analyzing the composition of lipid-associated fatty acids (FAs) and the activities of enzymes typically involved in the calcification process. Lipids and associated FAs play a critical role in maintaining the functions of growth, metabolism, and buoyancy control; lipid-FAs are not only an essential factor for the fluidity of the plasma membrane but also a carrier for the preservation of material and energy in marine animals and serve as indicators of an organism's dietary pattern and bio-physiological condition (Dalsgaard et al., 2003; Zhukova, 2022). Marine organisms also utilize

their lipids as a defense mechanism against the influence of environmental stressors or lipid peroxidation by restructuring FAs and sterols (isoprenoid-derived lipids, e.g., cholesterol in animals) of the lipid bilayer to preserve the physical characteristics of biological membranes (Hazel & Williams, 1990; Parrish, 2013). FAs indicate biochemical alterations in response to organismal physiological stress conditions (Bennett et al., 2018; Filimonova et al., 2016), immunity (Gao et al., 2018), and inflammation (Calder, 2010). FAs contain carboxylic acids with long hydrocarbon chains of different lengths and saturation grades (classified by the number of double bonds), generally classified into saturated fatty acids (SFAs, no double bonds), monounsaturated fatty acids (MUFAs, one double bond per molecule) and polyunsaturated fatty acids (PUFAs, two or more double bonds per molecule) (IUPAC-IUB, 1977). Among these FA chains, PUFAs such as eicosapentaenoic acid (EPA; C₂₀:5 ω 3) and docosahexaenoic acid (DHA; C₂₂:6 ω 3) are FA compounds essential for growth, reproduction, and survival (Kattner et al., 2007), and are involved in maintaining cell structures and functions in marine organism (Filimonova et al., 2016).

It is well known from marine animals that FA compounds and membranes are influenced by environmental factors (Dalsgaard et al., 2003; Hazel, 1995; Hazel & Williams, 1990; Yoon et al., 2022), including temperature (e.g., elevated temperature significantly reduced PUFAs and increased SFAs concentration) (Garzke et al., 2016; Valles-Regino et al., 2015) and *p*CO₂ (e.g., high levels of *p*CO₂ increase SFAs and reduced PUFAs concentrations) (Rossoll et al., 2012). Increased ratios of PUFAs (ω 6: ω 3) in animals indicate inflammation and physiological unhealth (Calder, 2010; Safuan et al., 2021). However, ectothermic animals are recognized to have the ability to counteract the effects of environmental stressors through an organism-specific physiological response termed homeoviscous adaptation (HVA) (Ernst et al., 2016; Sinensky, 1974). This adaptation process allows organisms to strengthen their cell membrane structure (i.e., PUFAs formation alters membrane fluidity and SFAs formation increases membrane stability) to avert membrane destabilization and maintain the functional state of cell membranes (Ernst et al., 2016; Hazel, 1995; Sinensky, 1974).

Enzymes play the main role as protein catalysts in most physiological processes to accelerate and regulate biochemical reactions (Hill et al., 2012). They are fundamental in the FA synthesis pathway (e.g., desaturation and elongation of FAs carbon chain) (Zhuang et al., 2022). Furthermore, enzymes are the principal agents of physiological transformation in that they are

responses to alterations in the external environment (Hill et al., 2012). Changes in enzyme activity under OA/OW are reliable proxies to determine the resulting physiological-related process disruption (Donachy et al., 1989; Prazeres & Pandolfi, 2016), including biomineralization processes in calcifying organisms (Chave, 1984; Ivanina et al., 2020). Moreover, alterations in membrane-bound enzymes (e.g., Ca-ATPase and Mg-ATPase) are biomarker indicators of organismal stress, where the level of enzyme variation mirrors the impairment of physiological function that entails these enzyme systems (Vijayavel et al., 2007). Although studies have shown that OA or OW as sole stressors can significantly alter Ca-ATPase and Mg-ATPase activities in coral (Jiang et al., 2019) and foraminifera (Prazeres & Pandolfi, 2016; Prazeres et al., 2015), the interactive combined effects of OA and OW on asteroids remain largely unknown.

To address these knowledge gaps on FAs biochemical composition and enzyme activities (Ca-ATPase and Mg-ATPase) in asteroids, we performed a controlled laboratory experiment and investigated the long-term interactive effects of OA and OW for 90 days in the small asterinid starfish *Aquilonastra yairi* (Echinodermata: Asteroidea: Asterinidae). *A. yairi* is a nocturnal species that lives under rocks, reef structures, and in rubble areas; distributed from tropical to subtropical regions particularly in the eastern Mediterranean Sea, the Red Sea, and the Gulf of Suez (Ebert, 2021; O'Loughlin & Rowe, 2006). Our study provides insights into the physiological tolerance and resilience of *A. yairi* when exposed to near-future combined OA/OW conditions and supports our understanding of the consequences on their biological performance.

4.2. Methods

4.2.1. Experimental design and exposure conditions

Adult specimens of *A. yairi* were taken from stock cultured in the MAREE (Marine Experimental Ecology) facility of ZMT, Bremen, Germany (342 specimens: size 3-11 mm) and were cleaned from debris. They were allowed to acclimate in a communal tank with recirculating artificial seawater (Red Sea Salt, Germany) to a temperature of ≈ 27 °C for seven days. Then, asteroids were randomly assigned to 18 experimental tanks (19 specimens in each tank) for a further seven-day acclimation period. During the acclimation period, no visible signs of stress were observed (i.e., discoloration and erratic flipping). Following acclimation, asteroids were exposed for 90 days to one of the six combinations of two temperature levels (27 °C and 32 °C) crossed with three concentrations of $p\text{CO}_2$ (455 μatm , 1052 μatm , and 2066 μatm), which

represent factorial combinations of ambient environments and the forthcoming levels of changes in the temperature and $p\text{CO}_2$ regime according to the IPCC-Representative Concentration Pathways (RCPs) 8.5 emission scenario for year 2100 (IPCC, 2014). Moreover, the ambient temperature (27 °C) represents the summer mean sea surface temperature (SST) (June to October) in natural habitats of *A. yairi* (e.g., in the Gulf of Suez). Three replicate experimental tanks were set up for each treatment. Each experimental tank was independent of the others, with isolated chillers, heaters, and CO_2 systems. To prevent physiological shock, temperature, and $p\text{CO}_2$ concentration levels were ramped up over ten days. During experimental exposure, *A. yairi* was feeding on living diatoms that were allowed to grow on the walls of aquaria and deposited detritus flocs. The experimental conditions and design are described in detail in Khalil et al. (2022).

Seawater samples were periodically taken during experiments to assess the carbonate chemistry of the seawater. Briefly, CO_2 -free air and pure CO_2 gas were mixed with solenoid-valve mass flow controllers to generate gas mixtures that were formulated to the target $p\text{CO}_2$ conditions, in compliance with the standard operating procedure (SOP) for ocean CO_2 measurements (Dickson et al., 2007). The resulting gas mixtures were then bubbled into each treatment group's seawater reservoirs using flexible microporous air stones and repeatedly pumped into replicate tanks. A programmed thermostat was used to regulate a closed-circle heating system that maintained treatment tank temperatures. Water parameters (i.e., temperature, salinity, pH_T (total scale), and pH_{NBS} scale) and water carbonate chemistries (total alkalinity (A_T) and dissolved inorganic carbon (C_T)) were measured periodically, which were subsequently used to calculate the water carbonate system. Details of the seawater chemistry control and manipulation, seawater parameters, and carbonate chemistry for the experimental tanks are provided in Supplementary material (Supplementary text and Table S4.1) and Khalil et al. (2022).

4.2.2. Total lipid and fatty acids analysis

Three specimens from each of the six treatment tanks were collected after 30, 60, and 90 days. The specimens were snap-frozen by submerging them in liquid nitrogen, freeze-dried, and stored at -80 °C until further analysis. Total lipid (ΣLC) was extracted and purified according to the methods described by Bligh and Dyer (1959). Briefly, to separate the lower chloroform phase containing lipids from the rest of the tissue, two purification cycles of a 2:1

chloroform/methanol solution and ultrapure water were performed. The upper phase of the homogenates was discarded after centrifugation (3500 rpm for 5 min). ΣL_c was determined gravimetrically by drying and weighing a subsample and expressed in mg lipid per g asteroids dry weight. The fatty acids of the asteroids were determined as fatty acid methyl esters (FAMES) at the end of the experiment. The relative composition of 14–24 carbon chain FAs of each individual was determined by transmethylation of dry asteroids lipid samples by acid-catalyzed esterification with 1% sulfuric acid in methanol, incubated at 50 °C for 16 h, and extracted into FAMES in accordance with methods from Christie (1998). FAMES were analyzed and quantified using a flame ionization detector gas chromatograph (GC) (Agilent 7890B MSD 5977 GC-FID, USA), and the output chromatograph peaks were identified using an FA standard mixture (37-component FAME, Supelco, Bellefonte PA) (Galloway et al., 2015). The FA profile of an individual was interpreted using a printed output chromatograph. To calculate the absolute concentration of each FA, the area of each FA was divided by the area of the internal FA standard. This value was multiplied by the internal FA standard concentration added at the beginning and normalized to their dry weight. Final concentrations of FA are expressed as $\mu\text{g mg}^{-1}$ of dry weight (DW).

4.2.3. Ca-ATPase and Mg-ATPase activity assays

For Ca-ATPase and Mg-ATPase activity assays, nine *A. yairi* specimens were collected from each of the treatment groups after 30, 60, and 90 days of incubation time. As for the lipid analysis, the specimens were snap-frozen, freeze-dried, and stored at -80 °C. The samples were thawed on ice and homogenized in 200 μL Tris buffer (500 mM sucrose, 150 mM KCl, 20 mM Tris, 1 mM dithiothreitol, and 0.1 mM phenylmethylsulphonyl, pH 7.6). Homogenates were then centrifuged at 12,600 *g* for 15 min at 4 °C. The supernatants were transferred to a new tube, and an aliquot of 50 μL was preserved for the determination of protein concentration determination using the Bradford assay (Bradford, 1976). Briefly, BioRad's Bradford micro-assays set on a 96-well flat bottom plate was adapted with a standard protein solution prepared using bovine γ -globulin (1 mg mL^{-1}). In each well of the microplate, 10 μL of each sample was added along with 290 μL of Bradford reagent (Sigma-Aldrich, USA). After 15 min of agitation at 150 revs min^{-1} , the absorbance was read at 600 nm using an Absorbance Microplate Reader (Tecan, Switzerland). Protein concentrations were expressed in mg of protein mL^{-1} .

Ca-ATPase and Mg-ATPase activities were measured according to protocols initially developed by Busacker and Chavin (1981), Chan et al. (1986), and modified by Prazeres et al. (2015). The working buffer for Ca-ATPase contained 80 mM NaCl, 20 mM Tris-Base, 15 mM KCl, and 15 mM CaCl₂. Mg-ATPase was measured using a similar working buffer, where MgCl₂ replaced CaCl₂ at the same concentration, while the pH was adjusted to 8.1. The sample homogenates (20 µL) were mixed with 250 µL of working buffer containing 1 mM ouabain. The reaction started with the addition of 30 µL ATP stock solution (3 mM). Subsequently, the mixture was incubated at 30 °C for 30 min. The reaction was stopped by adding Malachite Green Reagent in a Phosphate Assay Kit (Sigma-Aldrich, USA). Three technical replicates were measured for each sample. The inorganic phosphate (Pi) released by enzyme activity was determined based on a colorimetric method (Fiske & Subbarow, 1925) using the Phosphate Assay Kit (Sigma-Aldrich, USA) and calculated using a standard curve constructed with 1 mM Pi standards (Sigma-Aldrich, USA). The Pi concentration in the reaction mixture on 96-well microplates (Greiner Bio-One, Germany) was quantified at 620 nm by using an Absorbance Microplate Reader (Tecan, Switzerland). Homogenization buffer was used as a blank control. Ca-ATPase and Mg-ATPase activities were normalized to the total protein content and are expressed as µmoles Pi mg protein⁻¹ min⁻¹.

4.2.4. Statistical analysis

All data manipulation, visualization, and statistical analysis were performed using the R programming language v. 4.3.2 (R Core Team, 2023). The Shapiro-Wilk statistic *W* test (Shapiro & Wilk, 1965) combined with visual Q-Q plots and histograms was used to test the data for normality, while Levene's test was applied to check the homogeneity of variance (Levene, 1960), before statistical analysis was performed. When data were not normally distributed or indicated heteroskedasticity, we transformed our predictor variables to improve normality assumptions using 'bestNormalize' v.1.9.1 in the R-statistical package (Peterson, 2021). The effects of elevated temperature and *p*CO₂ and their interaction on ΣL_c and enzyme activities (i.e., Ca-ATPase and Mg-ATPase) were analyzed using a two-way multifactorial analysis of covariance (ANCOVA) using 'car' v.3.1-2 R-statistical package (Fox & Weisberg, 2019), with temperature and *p*CO₂ as fixed factors, while incubation time was treated as a continuous covariate. Subsequently, Tukey's honest significant difference (HSD) post hoc comparisons were used to detect the origin of variation for significant interactions. The magnitude of the effect sizes of the statistical models expressed as partial eta squared (ηp^2), are also specified.

OA/OW and their interaction effects on the saturated fatty acids class (i.e., SFAs, MUFAs, and PUFAs) were analyzed using a two-way multivariate analysis of covariance (MANCOVA) in 'MASS' v.7.3-60 R-statistical package (Venables & Ripley, 2002) complemented with 'car' v.3.1-2 R-statistical package (Fox & Weisberg, 2019). Temperature levels and $p\text{CO}_2$ concentrations (solely and combined) were treated as fixed factors, and incubation time was a covariate in this initial MANCOVA test. Following the MANCOVA test, a series of two-way ANCOVAs were performed on each of the response variables of the FA classes and continued with post hoc comparisons of Tukey's HSD to distinguish significant differences among treatments. In addition, principal component analysis (PCA) was performed to explore differences in FA classes between treatment groups and to identify those FAs that explain most of the variability in the data set, carried out using base R functions combined with the 'ggbiplot' v.0.55 R-package (Wickham, 2016) to visualize the PCA result. The results were considered statistically significant (moderate evidence of an effect) at alpha values of $p \leq 0.05$. All functional response figures were plotted using 'ggplot2' v. 3.4.4 (Wickham, 2016).

4.3. Results

4.3.1. Total lipid

Total lipid (ΣL_c) exhibited a linear decrease with increasing levels of $p\text{CO}_2$ at ambient temperature (27 °C). In contrast, at high temperature (32 °C), elevated $p\text{CO}_2$ concentrations resulted in a parabolic trend in lipid content (Figure 4.1). Under elevated $p\text{CO}_2$, ΣL_c in 27 °C treatments (mean \pm SE; $0.739 \pm 0.040 \text{ mg g}^{-1} \text{ DW}$) was 20.08% higher than in 32 °C treatments ($0.591 \pm 0.102 \text{ mg g}^{-1} \text{ DW}$). The highest lipid content occurred at 32 °C and medium $p\text{CO}_2$ concentration (1052 μatm ; $1.327 \pm 0.562 \text{ mg g}^{-1} \text{ DW}$), while low $p\text{CO}_2$ concentration (455 μatm) at 32 °C treatment produces the lowest lipid content ($0.652 \pm 0.096 \text{ mg g}^{-1} \text{ DW}$). The quantities of lipid content in *A. yairi* were not significantly affected by either elevated temperature (ANCOVA, $p > 0.05$; Supplementary Table S4.2) or $p\text{CO}_2$ (ANCOVA, $p > 0.05$; Supplementary Table S4.2) as sole factor neither combined factors (ANCOVA, $p > 0.05$; Supplementary Table S2), but showed differences between incubation time with higher lipid contents on day 90 compared to day 30 (ANCOVA, $F_{2,43} = 4.85$, $p = 0.02$, $\eta p^2 = 0.18$; Supplementary Table S4.2 and Table S4.4). ΣL_c exhibited a linear increase with incubation time, except for the 32 °C : 2066 μatm treatment where ΣL_c changed in a negative parabolic pattern (Supplementary Figure S4.1).

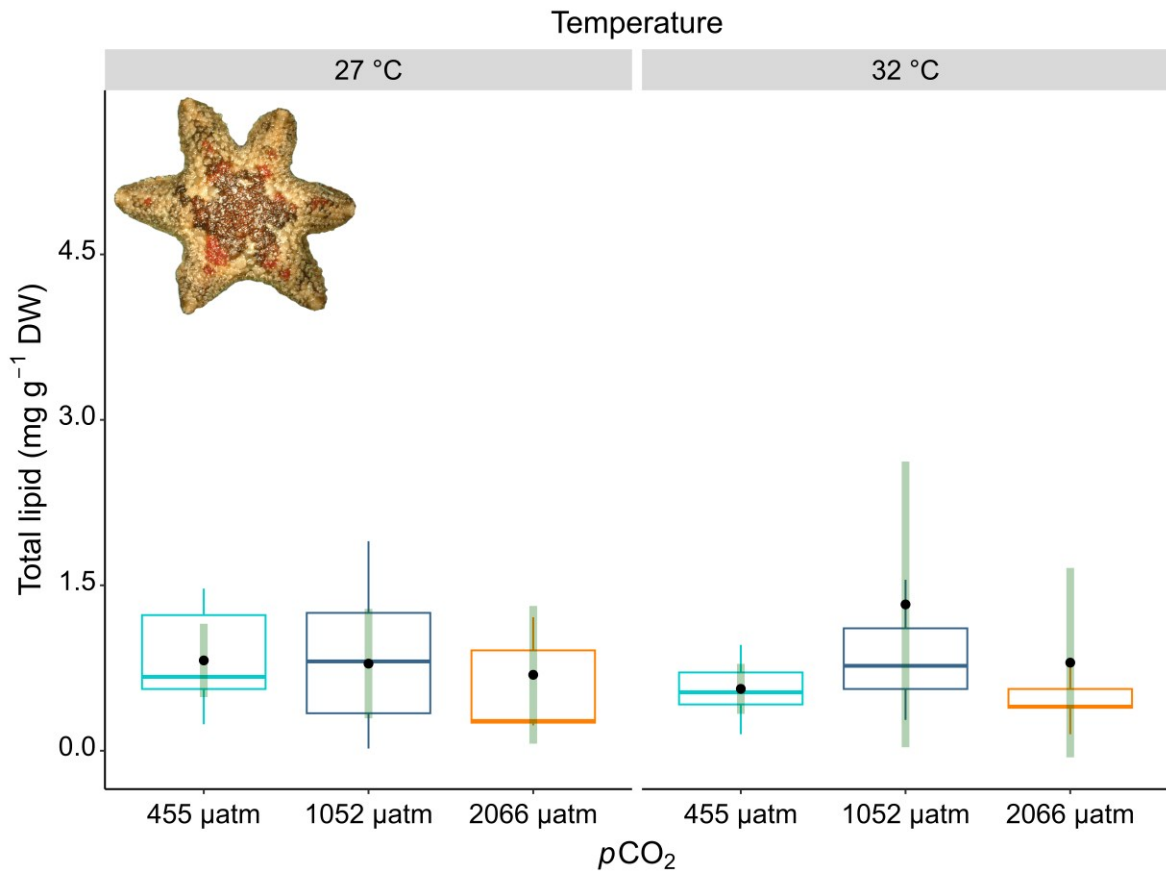


Figure 4.1. Total lipid (mg g^{-1} DW) of *A. yairi* (shown in the upper left corner) for 90 days of exposure to different temperature levels (27 °C, 32 °C) and $p\text{CO}_2$ concentrations (455 μatm , 1052 μatm , and 2066 μatm). Boxplots display the mean effect in each treatment (black dots), median (horizontal solid bar inside the box), interquartile (upper and lower horizontal lines of the box), and 1.5x interquartile ranges (whiskers). Vertical dark-green bars denote 95% confidence intervals of ΣL_c values; $n = 54$.

4.3.2. Fatty acids composition

Saturated FAs (% $\Sigma\text{SFAs} = 43.50\%$ of total detected FAs ($\Sigma_d\text{FAs}$)) were the most abundant components in all treatment groups (Table 4.1, Figure 4.2, and Supplementary Figure S4.2), with the exception of the 27 °C : 455 μatm treatment, followed by monounsaturated FAs (% $\Sigma\text{MUFAs} = 31.81\%$ of $\Sigma_d\text{FAs}$), and polyunsaturated FAs (% $\Sigma\text{PUFAs} = 24.62\%$ of $\Sigma_d\text{FAs}$). Furthermore, *A. yairi* contained more omega-3 (ω_3 ; PUFAs C18:3 ω_3 , C20:5 ω_3 , and C22:6 $\omega_3 = 21.24\%$ of $\Sigma_d\text{FAs}$) than omega-6 (ω_6 ; PUFAs C18:2 ω_6 , C20:2 ω_6 , and C20:4 $\omega_6 = 3.38\%$ of $\Sigma_d\text{FAs}$)

in all treatment groups (Table 4.1). Overall, SFAs were the most dominant FA class in *A. yairi*, followed by MUFAs and PUFAs under all treatment conditions.

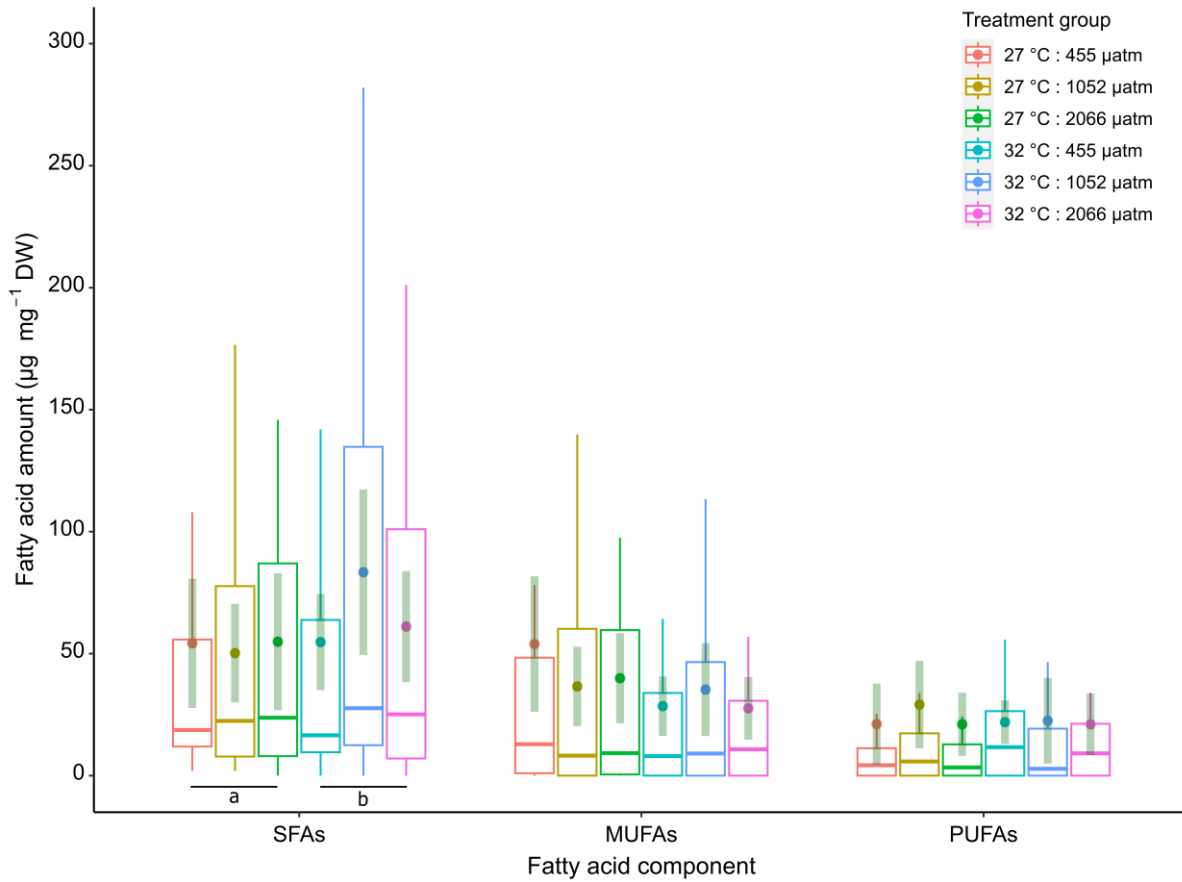


Figure 4.2. Fatty acids composition of asteroid *A. yairi* exposed to different temperature levels (27 °C, 32 °C) and $p\text{CO}_2$ concentrations (455 μatm , 1052 μatm , and 2066 μatm) for 90 days of incubation time. Boxplots display the mean effect in each treatment (color dots), median (horizontal solid bar inside the box), interquartile (upper and lower horizontal lines of the box), and 1.5x interquartile ranges (whiskers). Vertical dark-green bars denote 95% confidence intervals of fatty acids. Letters designate significant differences between the temperature treatment ($p < 0.05$); $n = 54$.

The FA compositions of *A. yairi* exposed to an elevated temperature of 32 °C ($2362.63 \pm 37.41 \mu\text{g mg}^{-1} \text{DW}$) had a higher total FA composition compared to asteroids at an ambient temperature of 27 °C ($2198.67 \pm 22.90 \mu\text{g mg}^{-1} \text{DW}$), reflecting the decrease in MUFAs and PUFAs at 27 °C : 1052 μatm , and 2066 μatm treatments, including a strong decrease in MUFAs C16:1 ω 9 and C18:1 ω 7, and PUFAs C18:2 ω 6 and C20:5 ω 3 (Table 4.1, Figure 4.2, and

Supplementary Figure S4.2). FAs composition at high-temperature treatments increased in a parabolic pattern in response to elevated $p\text{CO}_2$ (Figure 4.2), with the highest intensification observed at 32 °C : 1052 μatm for all FA classes (SFAs, MUFAs, and PUFAs; Table 4.1). Furthermore, SFAs (mean) exhibited an increase at high-temperature and elevated $p\text{CO}_2$ treatments (32 °C : 1052 μatm and 2066 μatm) compared to ambient temperature and low- $p\text{CO}_2$ treatment (27 °C : 455 μatm), whereas MUFAs (mean) reveal a decreased with elevated $p\text{CO}_2$ in all temperature treatment groups (Figure 4.2 and Supplementary Figure S4.2). It is noticed that the concentration of PUFA C18:3 ω 3 (ALA) in high $p\text{CO}_2$ (2066 μatm) at both temperature treatments declined to close to zero (Table 4.1). EPA:DHA ratio decreased with increasing temperature from ca 8.61:1 to 7.47:1 (Table 4.1).

A PCA on the entire FAs composition data set provided a two-dimensional pattern (Figure 4.3), which explained 65.1% of the total variance. Principal component PC1 explained 52.7% of the FAs variability, with the majority of the contribution from SFAs (C20:0, C18:0, C16:0, C14:0, C22:0), MUFAs (C16:1 ω 9, C18:1 ω 7, C18:1 ω 7, C20:1 ω 9), and PUFAs (C20:5 ω 3, C20:2 ω 6). PUFAs C18:2 ω 6, C18:3 ω 3, C20:2 ω 6, and C20:5 ω 3 contributed the most to the principal component PC2, followed by MUFA C22:1 ω 9 and SFA C24:0 which explained 12.4% of the variability in the FAs composition. The 95% confidence interval ellipses of PCA showed no separation between the treatment groups. Furthermore, the PCA showed that there were no notable variations in FAs composition between the six treatment groups.

There was no significant effect of $p\text{CO}_2$ as the sole factor in FA compositions or combined factor with temperature (MANCOVA, $p > 0.05$; Supplementary Table S4.3). Nonetheless, temperature was the only sole factor found to affect SFAs significantly (MANCOVA, $F_{1,6} = 365.84$, $p = 0.04$, Supplementary Table S4.3), but found not significantly to affect other FA classes (MANCOVA, $p > 0.05$; Supplementary Table S4.3). FA classes showed no significant alter by incubation time in all treatment groups (MANCOVA, $p > 0.05$; Supplementary Table S4.3). Subsequent ANCOVA analyses for each of the three FAs classes revealed statistically significant effects of incubation time on SFA C16:0 (ANCOVA, $F_{2,39} = 6.06$, $p = 0.01$, $\eta p^2 = 0.24$; Supplementary Tables S4.2 and S4.4) and PUFA C20:5 ω 3 (ANCOVA, $F_{2,29} = 3.45$, $p = 0.05$, $\eta p^2 = 0.19$; Supplementary Tables S4.2 and S4.4), while temperature as the sole factor observed significantly affected SFA C18:0 (ANCOVA, $F_{1,29} = 5.19$, $p = 0.03$, $\eta p^2 = 0.19$; Supplementary Tables S4.2 and S4.4) only. However, $p\text{CO}_2$ as the sole or combined factor with temperature did not affect any FAs profile in all

treatment groups (ANCOVA, $p > 0.05$; Supplementary Table S4.2). Furthermore, the $\omega 3:\omega 6$ ratio was found not to change significantly affect by any factor (ANCOVA, $p > 0.05$; Supplementary Table S4.2).

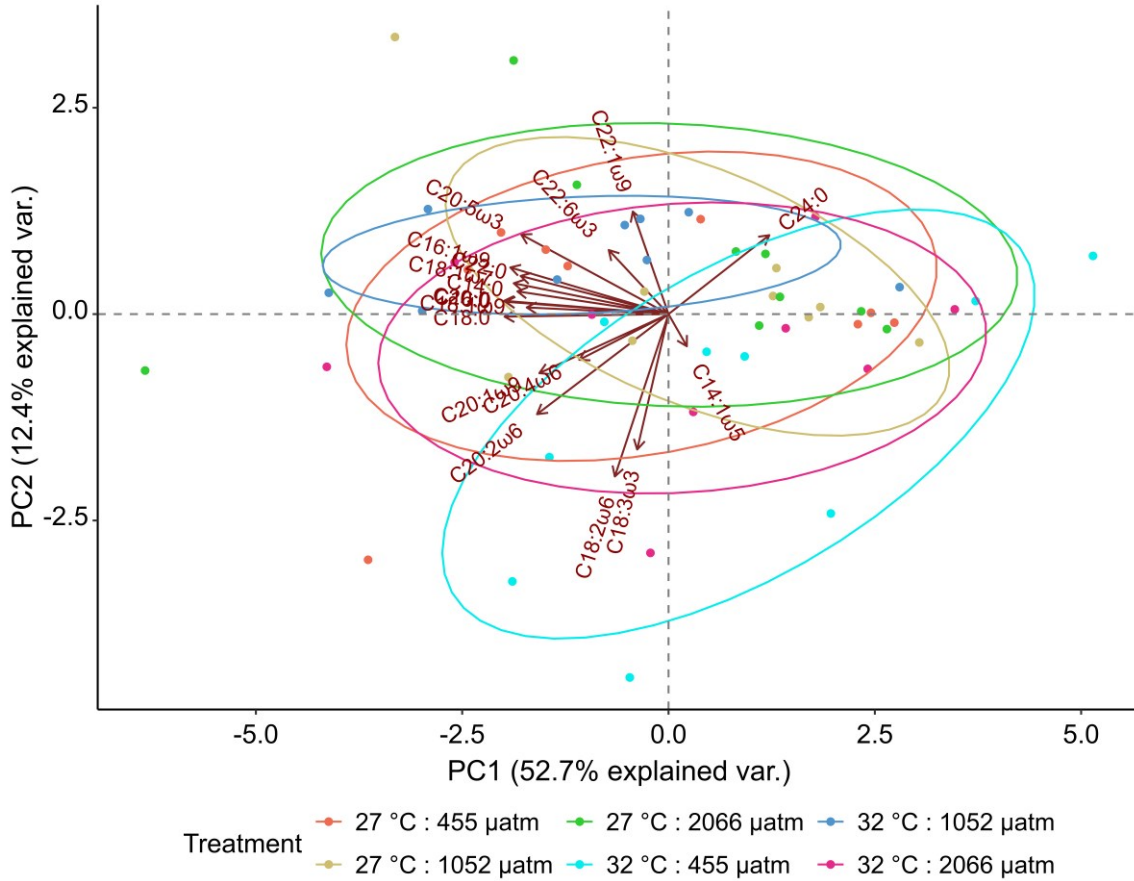


Figure 4.3. Biplot of principal component analysis (PCA) based on fatty acid profiles ($n = 18$ classes) for asteroid *A. yairi* exposed to different temperature levels (27 °C, 32 °C) and $p\text{CO}_2$ concentrations (455 μatm , 1052 μatm , and 2066 μatm) for 90 days of incubation time; $n = 54$. Individual samples are color-coded according to the treatment level. The plot is shown with 95% confidence ellipses.

Table 4.1. Total lipid and fatty acids composition of *A. yairi* reared under different temperature levels (27 °C, 32 °C) and $p\text{CO}_2$ concentrations (455 μatm , 1052 μatm , and 2066 μatm). Total lipid is expressed as mg g^{-1} (mean \pm SE) of asteroids tissue dry weight (DW). FAs are expressed as $\mu\text{g mg}^{-1}$ (mean \pm SE) of asteroids tissue DW. ΣSFAs : sum of SFAs, ΣMUFAs : sum of MUFAs, ΣPUFAs : sum of PUFAs, $\omega 3$: omega-3, $\omega 6$: omega-6, $\Sigma\omega 3:\Sigma\omega 6$: ratio of omega-3 ($\omega 3$) fatty acids to omega-6 ($\omega 6$) fatty acids, EPA:DHA: ratio of eicosapentaenoic acid (EPA) to docosahexaenoic acid (DHA).

Lipid (mg g^{-1} DW) and fatty acids ($\mu\text{g mg}^{-1}$ DW) profile	Temperature: 27 °C			Temperature: 32 °C		
	$p\text{CO}_2$: 455 μatm	$p\text{CO}_2$: 1052 μatm	$p\text{CO}_2$: 2066 μatm	$p\text{CO}_2$: 455 μatm	$p\text{CO}_2$: 1052 μatm	$p\text{CO}_2$: 2066 μatm
<i>Lipid content</i>						
ΣL_c (total lipid)	0.819 \pm 0.144	0.790 \pm 0.215	0.689 \pm 0.255	0.561 \pm 0.096	0.780 \pm 0.146	0.431 \pm 0.067
<i>Saturated fatty acids (SFAs)</i>						
C14:0 (myristic acid)	33.951 \pm 8.349	21.664 \pm 4.777	29.336 \pm 7.308	22.794 \pm 5.978	37.598 \pm 7.772	34.765 \pm 13.073
C16:0 (palmitic acid)	158.177 \pm 42.055	116.436 \pm 26.763	164.601 \pm 58.930	126.428 \pm 26.863	220.231 \pm 38.858	140.754 \pm 27.394
C18:0 (stearic acid)	96.067 \pm 39.108	130.907 \pm 24.849	89.930 \pm 8.192	126.056 \pm 21.900	167.943 \pm 35.030	151.656 \pm 28.139
C20:0 (arachidic acid)	8.166 \pm 1.756	7.110 \pm 1.735	9.409 \pm 3.769	6.460 \pm 1.201	12.793 \pm 2.381	8.335 \pm 1.877
C22:0 (behenic acid)	11.936 \pm 2.672	9.080 \pm 2.461	9.426 \pm 3.768	9.077 \pm 1.772	11.741 \pm 3.650	11.318 \pm 3.124
C24:0 (lignoceric acid)	20.086 \pm 1.894	24.359 \pm 3.796	19.606 \pm 2.111	23.600 \pm 5.575	22.408 \pm 5.374	26.593 \pm 8.162
<i>Monounsaturated fatty acids (MUFAs)</i>						
C14:1 ω 5 (myristoleic acid)	1.273 \pm 0.350	0.410 \pm 0.226	1.057 \pm 0.338	1.275 \pm 0.657	0.489 \pm 0.235	1.372 \pm 0.539
C16:1 ω 9 (palmitoleic acid)	147.920 \pm 52.933	79.149 \pm 24.489	63.579 \pm 10.241	61.512 \pm 21.641	120.378 \pm 34.358	46.091 \pm 12.424
C18:1 ω 9 (oleic acid)	22.467 \pm 8.341	26.892 \pm 12.687	43.533 \pm 19.549	21.538 \pm 4.703	32.295 \pm 5.261	22.141 \pm 4.685
C18:1 ω 7 (vaccenic acid)	163.476 \pm 41.671	90.653 \pm 17.174	110.357 \pm 29.423	78.131 \pm 17.304	134.293 \pm 47.998	96.548 \pm 28.360
C20:1 ω 9 (gondoic acid)	11.605 \pm 2.614	13.559 \pm 5.891	12.744 \pm 7.125	11.294 \pm 2.604	21.905 \pm 8.873	16.205 \pm 3.774

C22:1 ω 9 (erucic acid)	0.054 \pm 0.054	0.195 \pm 0.195	0.211 \pm 0.141	0.000 \pm 0.000	0.000 \pm 0.000	0.000 \pm 0.000
<i>Polyunsaturated fatty acids (PUFAs)</i>						
C18:2 ω 6 (linoleic acid, LA)	4.920 \pm 4.657	2.863 \pm 2.250	0.000 \pm 0.000	15.610 \pm 5.486	3.375 \pm 3.375	8.124 \pm 3.731
C18:3 ω 3 (α -linolenic acid, ALA)	0.929 \pm 0.929	1.450 \pm 0.950	0.000 \pm 0.000	3.185 \pm 1.763	0.000 \pm 0.000	0.000 \pm 0.000
C20:2 ω 6 (eicosadienoic acid)	5.529 \pm 0.938	4.017 \pm 0.667	9.202 \pm 4.425	10.381 \pm 3.112	7.191 \pm 1.968	8.360 \pm 1.498
C20:4 ω 6 (arachidonic acid, AA)	10.370 \pm 3.247	9.563 \pm 3.897	9.090 \pm 5.129	15.184 \pm 4.967	13.884 \pm 4.845	16.522 \pm 7.814
C20:5 ω 3 (eicosapentaenoic acid, EPA)	153.044 \pm 54.857	143.242 \pm 29.017	112.185 \pm 23.199	69.901 \pm 16.069	294.261 \pm 24.507	83.323 \pm 32.343
C22:6 ω 3 (docosahexaenoic acid, DHA)	8.821 \pm 2.640	20.431 \pm 7.753	18.139 \pm 9.174	15.914 \pm 7.676	27.689 \pm 6.617	16.309 \pm 6.696
<i>Fatty acids (FAs) indices</i>						
Σ SFAs	308.297 \pm 28.811	285.196 \pm 27.412	302.703 \pm 29.911	290.815 \pm 27.931	450.306 \pm 43.512	346.827 \pm 31.749
Σ MUFAs	346.741 \pm 31.199	210.664 \pm 16.309	231.270 \pm 17.653	173.750 \pm 13.478	309.360 \pm 24.561	182.356 \pm 14.898
Σ PUFAs	183.613 \pm 24.525	181.567 \pm 22.774	148.617 \pm 17.702	130.174 \pm 9.844	346.400 \pm 47.474	132.638 \pm 11.024
$\Sigma\omega$ 3	226.409 \pm 17.135	209.600 \pm 10.568	157.673 \pm 10.193	108.284 \pm 8.284	321.950 \pm 7.781	99.632 \pm 9.760
$\Sigma\omega$ 6	20.819 \pm 2.947	16.443 \pm 2.271	23.533 \pm 4.932	41.175 \pm 4.522	24.449 \pm 3.396	33.006 \pm 4.348
$\Sigma\omega$ 3: $\Sigma\omega$ 6	7.82:1	10.04:1	7.13:1	2.16:1	13.17:1	3.02:1
EPA:DHA	17.35:1	7.011:1	6.19:1	4.39:1	10.63:1	5.11:1

4.3.3. Ca-ATPase and Mg-ATPase activities

Ca-ATPase and Mg-ATPase activities exhibited a positive parabolic response pattern to increasing $p\text{CO}_2$ at ambient temperature (27 °C) treatment, whereas enzyme activity shows a stable pattern in response to increasing $p\text{CO}_2$ at high temperature (32 °C) (Figure 4.4). The highest Ca-ATPase activity (mean \pm SE; $0.73 \pm 0.03 \mu\text{moles Pi mg protein}^{-1} \text{min}^{-1}$) was observed under ambient temperature and low $p\text{CO}_2$ concentration (455 μatm), and the lowest value ($0.59 \pm 0.02 \mu\text{moles Pi mg protein}^{-1} \text{min}^{-1}$) at ambient temperature and medium $p\text{CO}_2$ concentration (1052 μatm) condition. Ca-ATPase activity was significantly affected by incubation time, where Ca-ATPase activity showed a significant decrease as incubation time progressed with exception of 27 °C : 1055 μatm (ANCOVA, $F_{2,151} = 27.96$, $p = 0.00$, $\eta p^2 = 0.27$; Supplementary Table S4.2, Table S4.4, and Figure S4.3a), $p\text{CO}_2$ concentration (ANCOVA, $F_{2,151} = 4.02$, $p = 0.02$, $\eta p^2 = 0.05$; Figure 4.4a, Supplementary Table S4.2 and Table S4.4) and by the interaction of the factors temperature and $p\text{CO}_2$ (ANCOVA, $F_{2,151} = 6.01$, $p = 0.00$, $\eta p^2 = 0.07$; Supplementary Table S4.2 and Table S4.4), but not by temperature (ANCOVA, $p > 0.05$; Supplementary Table S4.2).

Similarly, Mg-ATPase activity was also significantly affected by the combined factors of temperature and $p\text{CO}_2$ (ANCOVA, $F_{2,151} = 7.75$, $p = 0.00$, $\eta p^2 = 0.09$; Figure 4.4b, Supplementary Table S4.2 and Table S4.4), as well as by the sole factor of $p\text{CO}_2$ (ANCOVA, $F_{2,151} = 3.92$, $p = 0.02$, $\eta p^2 = 0.05$; Supplementary Table S4.2 and Table S4.4) and incubation time (ANCOVA, $F_{2,151} = 25.62$, $p = 0.00$, $\eta p^2 = 0.25$; Supplementary Table S4.2 and Table S4.4). However, temperature as the sole factor was found to not significantly affect Mg-ATPase activity in *A. yairi* (ANCOVA, $p > 0.05$; Supplementary Table S4.2). Furthermore, the highest Mg-ATPase activity was observed in 27 °C : 456 μatm treatment, whereas the lowest was found in 27 °C : 1052 μatm . Apparently, Mg-ATPase activity decreased over incubation time, except for the 27 °C : 1052 μatm treatment with a negative parabolic pattern (Supplementary Figure S4.3b).

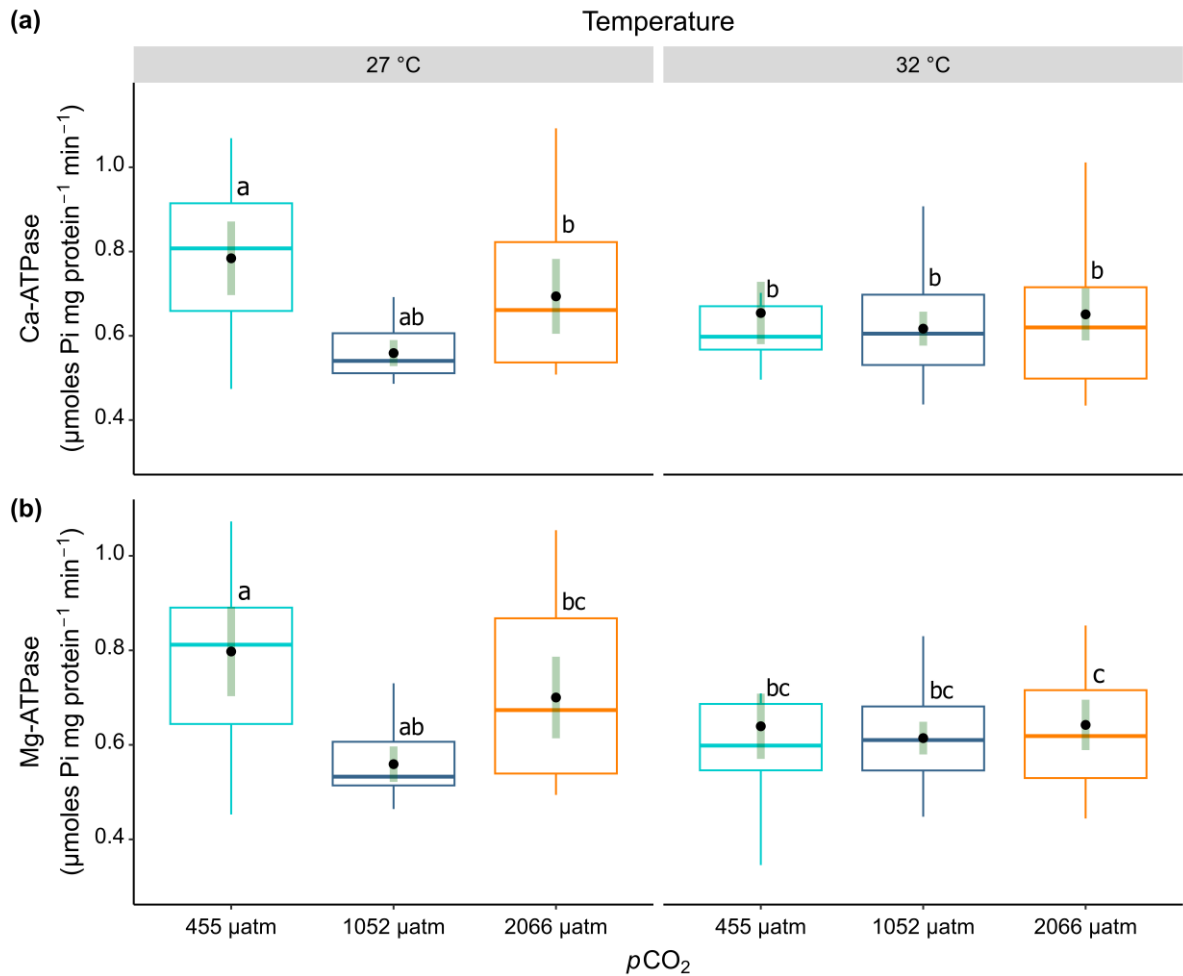


Figure 4.4. Enzyme activities of asteroid *A. yairi* exposed to different temperature levels (27 °C, 32 °C) and $p\text{CO}_2$ concentrations (455 μatm , 1052 μatm , and 2066 μatm) for 90 days of incubation time; **(a)** Ca-ATPase ($\mu\text{moles Pi mg protein}^{-1} \text{min}^{-1}$), and **(b)** Mg-ATPase ($\mu\text{moles Pi mg protein}^{-1} \text{min}^{-1}$). Boxplots display the mean effect in each treatment (black dots), median (horizontal solid bar inside the box), and interquartile (upper and lower horizontal lines of the box) and 1.5x interquartile ranges (whiskers). Vertical dark-green bars denote 95% confidence intervals of enzyme activity values. Letters designate significant differences between the treatment groups (Tukey's HSD, $p < 0.05$); $n = 53$.

4.4. Discussion

4.4.1. Lipid-associated resilience and homeoviscous adaptations

Assessing lipid and associated FAs allows to define the metabolic status, oxidative stress, potential energy provision, cell remediation, developmental potential, and reproductive capacity of an organism (Murphy, 2001; Stanley-Samuelson, 1987). Our results show that increased $p\text{CO}_2$ concentration and temperature level as a sole stressor or combined stressors do not significantly affect the total lipid content (ΣL_c) of *A. yairi*. They imply that this asterinid species is relatively robust against conditions predicted in future global change scenarios. A possible explanation for the absence of significant changes in asteroid ΣL_c in response to elevated temperature and $p\text{CO}_2$ was their retention of foraging capacity and feeding performance under stressful conditions (Gooding et al., 2009); hence, the lipid generation and conservation mechanism could remain functional. Furthermore, tropical-subtropical marine organisms are less exposed to seasonal diet pulses and have faster metabolic rates (Brett et al., 2009), which allows them to control relative lipid levels and subsequently use it rapidly to cope with environmental stressors. Lipids and bioaccumulation of minerals obtained by consuming microalgae (e.g., diatoms and microbial mats) are required continuously throughout the diet to support physiological development and maintain health and fitness (Kainz & Fisk, 2009). Additionally, a higher ΣL_c (in mean) was observed at higher temperatures and medium $p\text{CO}_2$ concentration treatment (32 °C : 1052 μatm), implying that the starfish could have enhanced its biosynthetic capacity to convert non-lipid molecules into lipids in such environmental settings. Future studies should thus verify this in manipulative trials with fully controlled diets.

The lipid sensitivities to OA and OW as sole or combined stressors in marine invertebrates show different scales, varying from functional adaptability (positive effects) to specific physiological losses (negative effects). Our findings concur with earlier research demonstrating that marine invertebrate species exposed to elevated $p\text{CO}_2$ and temperature levels (as sole or combined factors) did not exhibit alterations in their lipids content, e.g., sea urchin *Strongylocentrotus purpuratus* (Matson et al., 2012), sponges *Carteriospongia foliascens*, *Cymbastela coralliophila*, *Rhopaloeides odorabile* and *Stylissa flabelliformis* (Bennett et al., 2018), and the corals *Porites* spp. and *Acropora millepora* (Strahl et al., 2016). In contrast, other studies have found alterations in the organismal lipid content in response to OA and OW, e.g., Caribbean coral *A. cervicornis* ($\Sigma\text{L}_c \uparrow$; OA*) (Towle et al., 2015), scallop *Crassadoma gigantea* ($\Sigma\text{L}_c \uparrow$; OA*) (Alma et al., 2020), blue mussel *Mytilus edulis* ($\Sigma\text{L}_c \uparrow$; OW*) (Matoo et al., 2021), Arctic pteropod

Limacina helicina ($\Sigma L_c \downarrow$; OA:OW*) (Lischka et al., 2022), oyster *Crassostrea virginica* ($\Sigma L_c \downarrow$; OA*) (Schwaner et al., 2023). These differences in responses indicate that the sensitivity is species-specific and probably highly dependent on geographic distribution, habitat, physiological acclimation capacity, stressor intensity, and life history of species.

In addition to their significance in energy conservation, fatty acids are involved in numerous essential cellular functions, most notably through their function as building blocks of cell membranes. Essential FAs are also recognized as key determinants of ecosystem health and stability (Parrish, 2013). Overall, elevated water temperature exerted a larger effect on the FA compositions relative to acidification. Our results showed that under future ocean scenarios, the temperature (as the sole stressor) affects the composition of asteroid FAs, where the FAs composition becomes more saturated during elevated temperature acclimation (i.e., SFAs increase in the negative parabolic pattern). This result is consistent with previous studies in other marine invertebrate species, such as sea cucumber *Apostichopus japonicus* (Yu et al., 2016), copepod *Paracalanus* sp. (Garzke et al., 2016), gastropod *Dicathais orbita* (Valles-Regino et al., 2015), and shrimp *Palaemon elegans* (Maia et al., 2022).

Temperature appears to contribute to increasing the amount of all SFA classes, with SFAs C18:0 alone found to have a statistically significant increase at high temperatures (ANCOVA, $p < 0.05$). However, it seems that the effects of OA might quantitatively modify the impacts of temperature on asteroid SFAs composition. We suggest that the increased concentration of SFA under high-temperature environmental conditions is attributed to the enhanced allocation of SFA to cell membranes to preserve membrane stability and viscosity and is functional in counteracting the reduced internal cell pH due to acidification (Maia et al., 2022); where high temperature often leads to protein degeneration in the lipid bilayer of biomembranes, which generates a preponderance of membrane fluidity and increases membrane permeability (Hazel, 1995). Furthermore, SFA C16:0 is the final major by-product of FAs biosynthesis within the cell cytosol, serving as precursors for long-chain *de novo* biosynthesis of both saturated and unsaturated FAs (Gurr et al., 2002). C16:0 is used as a lipid mediator for cell signaling, neuroprotective, anti-neuroinflammatory, and analgesic activities (Carta et al., 2017). Increases in SFA C16:0 and C18:0 that were found in this study are suggested to represent a response mode to suppress physiological disorders resulting from elevated temperature beyond thermal optima; C16:0 and C18:0 are synthesized on-demand and exert their functions *in loco* during

inflammations and neurodegenerative disorders to counteract inflammation and neuronal lesion. However, drastic increases in C16:0 and C18:0 could have adverse physiological consequences - apoptosis, oxidative stress, and endothelial dysfunction (Carta et al., 2017; Wang et al., 2007). Furthermore, SFAs are categorized as rapid energy resources, and their extraction could accelerate in response to OA/OW conditions to offset the higher energetic expenses associated with survival in a chronic environment (Garzke et al., 2016).

Although neither temperature nor $p\text{CO}_2$ as a sole or combined factor lacked a statistically significant effect on MUFAs (MANCOVA, $p > 0.05$), there was a decreasing trend in the MUFAs abundance as temperature- $p\text{CO}_2$ increased markedly in MUFAs C16:1 ω 9 and C18:1 ω 7. This might indicate thermal-acidity stress responses by the asteroid. MUFAs represent a highly catabolizable energetic resource (Tocher, 2010); thus, asteroid would probably metabolize them to yield energy to offset the energetic deficits that ensue due to increased energy expenditure for cell-physiological processes in parallel with thermoregulation during stressful conditions. Other physiological factors, e.g., development and reproduction under extreme environmental conditions, require immense energy expenditure (Doney et al., 2012), which might also contribute to depletion in MUFA stores. Decreased MUFA levels under warming and acidification conditions were recorded in the sponges *C. foliascens*, *C. coralliophila*, and *S. flabelliformis* (Bennett et al., 2018). Interestingly, however, MUFA palmitoleic acid (C16:1 ω 9) at 32 °C : 1052 μatm was increased compared to 27 °C : 455 μatm . In this context, C16:1 ω 9 enhancement is suggested as a potential acclimation measure to diminish the inflammatory effects caused by elevated temperature, because animal and cell culture studies indicate that C16:1 ω 9 acts as an anti-inflammatory and reduces the adverse effects of higher SFA (de Souza et al., 2018).

Asteroid PUFAs did not significantly alter in response to changes in temperature and/or $p\text{CO}_2$ (i.e., MANCOVA and ANCOVA statistical results). However, individuals reared at 27 °C contained less Σ PUFAs than those reared at 32 °C. All PUFA classes were found to enhance as temperature increased, with a particular major increase observed in C18:2 ω 6 (linoleic acid) and C20:4 ω 6 (arachidonic acid, AA) by $\approx 273\%$ and $\approx 68\%$, respectively. $p\text{CO}_2$ concentrations most likely contributed to modifying the quantitative level of PUFA shifts in response to elevated temperature. These increased levels of PUFAs suggest that tropical-subtropical asteroids are predicted to become more resilient and adaptable to current and future global ocean changes,

where enhancement of PUFAs could be utilized to cope with the adverse physiological effects of stressors (Yoon et al., 2022). Relative enhancement of PUFAs ω_3 and ω_6 with increasing temperature arguably reflects physiological differences that may promote the resistance of this species to environmental stress (i.e., resilience to physiological stress) (Filimonova et al., 2016; Tocher, 2010). Increased PUFAs could be related to acclimation mechanisms to maintain membrane fluidity and permeability and subsequent cell homeostasis, regulate ion flux and thermoregulation in the encounter of environmental changes; besides, PUFAs play important roles in the reproductive process, neurological development, immune system, and serve as essential hormone precursors (i.e., for eicosanoids) (Calder & Grimble, 2002; Stanley-Samuelson, 1987; Zhukova, 2022). Asteroids acquire PUFAs from their diets; therefore, an increase in PUFAs may be related to feeding performances that are not affected by stressors. Moreover, elevated temperatures were found to increase feeding rates in some asteroids species (Gooding et al., 2009), leading to higher nutrition intake. The sources of PUFAs in asteroids diets are unclear, but it has been associated with microorganisms living in benthic habitats, e.g., macroalgae, specific diatom species, protozoa, and microeukaryotes (Howell et al., 2003). Furthermore, some marine invertebrates have the ability to directly synthesize PUFAs (e.g., C20:4 ω_6 , C20:5 ω_3 , and C22:6 ω_3) through the FA desaturation process (Nakamura & Nara, 2004; Yoon et al., 2022). However, further research is required to identify the potential desaturation process in asteroids for generating PUFAs. On the contrary, previous studies have shown that, mostly, marine invertebrates exposed to elevated temperatures as the sole factor or combined with $p\text{CO}_2$ produce a reduction in ΣPUFAs , e.g., sea cucumber *A. japonicus* (Yu et al., 2016), gastropod *D. orbita* (Valles-Regino et al., 2015), scallop *C. gigantea* (Alma et al., 2020), shrimp *P. elegans* (Maia et al., 2022), and hard coral *A. digitifera* (Safuan et al., 2021).

We noted a reduction in PUFA ω_3 along with an enhancement of PUFA ω_6 as temperature increases. This alteration is related to the lipid peroxidation activation mechanism in protecting membranes against oxidation damage induced by stressors. Temperature can modulate cell membrane structure by stimulating the lipid peroxidation pathway that initiates by reactive oxygen species (ROS) (Butow et al., 1998), in which membrane phospholipids (i.e., primarily PUFAs) are exposed to oxidative reactions by ROS. Higher lipid saturation and high O_2 concentration lead to an increase in the velocity of the lipid radical chain reactions (Anacleto et al., 2014). PUFAs ω_3 and ω_6 are further employed to inhibit ROS through increasing macrophage phagocytosis capacity (Ambrozova et al., 2010). Furthermore, the PUFAs $\omega_3:\omega_6$

ratio is well-known to significantly contribute to membrane functions and cellular processes, e.g., cell survivability (Schmitz & Ecker, 2008). Although PUFAs ω 3: ω 6 ratio was marginally significant (ANCOVA, $F_{1,41} = 3.10$, $p = 0.09$, $\eta p^2 = 0.07$; Supplementary Table S4.2) affected by temperature as sole factor, PUFAs ω -3: ω -6 ratio was recoded to decrease from 8.25:1 at ambient temperature (27 °C) to 5.18:1 after being exposed to high-temperature (32 °C) treatment for 90 days. The ratio shift suggests a switch of PUFAs regulation from the anti-inflammatory mode (more PUFAs ω -3) to the pro-inflammatory mode (more PUFAs ω -6) (Schmitz & Ecker, 2008). Inflammation plays an important role in systemic mechanisms of cellular defense and helps protect against harmful stimuli, e.g., immune responses, cell-tissue repair, and warning signals of physiological anomalies; however, prolonged or excessive inflammation can lead to tissue damage, organ dysfunction, and increased risk of various health problems (Calder, 2010; Calder & Grimble, 2002).

The present study reveals a potential acclimation mechanism of cell membrane remodeling homeoviscous adaptation in response to elevated seawater temperature (Hazel, 1995; Hazel & Williams, 1990). An increase in asteroid SFAs and PUFAs followed by a reduction in MUFAs and PUFAs ω -3: ω -6 ratio implied compensatory alterations in fluidity and permeability of cell membrane lipid bilayers to preserve membrane biophysical functions and properties under chronic environmental stress. Still, it remains obscure whether this biochemical acclimation strategy is viable under more prolonged durations and higher intensities of stressors. Moreover, further research is essential to assess the impacts of future ocean scenarios on asteroids larvae (produced by sexual reproductive mode) or 'juvenile' individuals (produced by fissiparous in asexual reproductive mode) since a higher vulnerability at the early developmental stage may pose barriers to species' survival in the continuously changing oceans.

4.4.2. Enzyme activities under multiple stressors and their potential role in calcification

Ca-ATPase and Mg-ATPase activities show susceptibility to changes in $p\text{CO}_2$ and temperature. Statistical analysis indicated that the interaction of OA and OW significantly affected Ca-ATPase and Mg-ATPase activities; enzyme activities decreased with increasing temperature and $p\text{CO}_2$ concentration, suggesting impaired adenosine triphosphate (ATP) production and enzyme function, resulting in reduced energy supplies needed to sustain the metabolic demands of routine maintenance. In addition to serving as energy storage for various physiological cellular

processes (Petersen & Verkhatsky, 2016; Sokolova et al., 2012), ATP is an organic molecule that plays a vital role as a biochemical catalyst in physiological cellular processes, ion transporters or exchangers (e.g., Ca^{2+} and Mg^{2+}) in the calcification process, and in the removal of excess protons (H^+) from the biomineralization site for the skeleton (Ivanina et al., 2020). In ectothermic animals (e.g., echinoids), those bio-cellular processes involve high-energy utilization and intensive catalysts that are provided by ATP (Pan et al., 2015; Stumpp & Hu, 2017). Studies of Ca-ATPase and Mg-ATPase activities under the influence of OA and OW as combined or single factors have yielded different and inconsistent responses. For instance, Ca-ATPase and Mg-ATPase activities of the benthic foraminifera *Amphistegina lessonii* were enhanced after exposure to OA and OW for 30 days; however, *Marginopora vertebralis* had the opposite response (Prazeres et al., 2015). A finding similar to that of the present study was reported in the razor clam *Sinonovacula constricta*, where elevated CO_2 (decreased pH) suppressed Ca-Mg ATPase activity after one week of exposure (Peng et al., 2017). Duration of exposure, stressor intensity, species-specific differences, experimental setups, and methodology appear to contribute to differences in the response of these important enzymes to OA/OW.

Our results showed different Ca-ATPase and Mg-ATPase activities between ambient (27 °C) and high temperature (32 °C) treatments in response to increasing $p\text{CO}_2$ concentrations. Enzyme activity at ambient temperature displayed a positive parabolic curve in response to increased $p\text{CO}_2$ concentrations, indicating a plasticity-physiological acclimation response to balance intracellular acid-base conditions due to changes in pH. Furthermore, lower enzyme activity at medium concentrations of $p\text{CO}_2$ specified stress conditions, where asteroid lost their capacity to accelerate physiological enzyme activities due to disturbances of their energy balance in low-pH environments (Bisswanger, 2017; Khalil et al., 2023). The energy balance could be adversely influenced by OA both directly through the negative effects of lower extracellular and intracellular pH on energy metabolism and indirectly through increased energy expenditure for biomineralization and acid-base regulation processes (Sokolova et al., 2012). On the contrary, at high concentrations of $p\text{CO}_2$ (27 °C : 2066 μatm), asteroid increased enzyme activities to balance extra- and intracellular acid-base conditions to maintain optimal physio-chemical microenvironment conditions, thus ensuring fundamental asteroid component survival (very low mortality, see Khalil et al. (2023)) in these chronic stress environments. Enhanced enzyme activity may allow asteroids to actively pump H^+ to maintain pH homeostasis in the extracellular

calcifying fluid (ECF, pH_{CF}). Consequently, up-regulation of the H^+ pump under high OA renders more metabolic CO_2 produced by cell organelle-mitochondria, which subsequently aggravates calciblastic cell acidosis, making H^+ dissipation more arduous (Laurent et al., 2014; Melzner et al., 2020) and skeletons become more susceptible to dissolution (see Khalil et al. (2022) for the descriptions of skeletal dissolution of asteroids *A. yairi* under OA/OW). We thus suggest that this rapid acceleration would involve a high-energy demand that might result in a trade-off and temporal energy reallocation with other physiological functions (Khalil et al., 2023; Sokolova et al., 2012). Furthermore, increased enzyme activity may indicate increased Ca^{2+} and Mg^{2+} ion provision into the ECF to promote asteroids calcification under OA conditions (Khalil et al., 2022). However, increasing ion supply seems unable to counteract the adverse effects of OA, as evidenced by significantly decreased calcification rates (Khalil et al., 2022).

The opposite condition was observed in the high-temperature regime (32 °C), where Ca-ATPase and Mg-ATPase activities exhibited low-stable responses, although they were significantly reduced compared to the ambient temperature and low pCO_2 concentrations (27 °C : 455 μatm) treatment. Elevated temperature seems to allow *A. yairi* to cope with the negative effect of increased pCO_2 (decreased seawater pH) on enzyme activities (antagonistic interactive effects). High temperatures are likely to stimulate and stabilize enzyme activity by intensifying ATP synthesis and utilization during intracellular acid-base homeostasis. We suggest that elevated temperatures could accelerate enzyme activity by utilizing a high energy supply through optimum-efficiency metabolic pathways to counteract another stressor (i.e., elevated pCO_2) (Somero, 1978), thus alleviating physiological stress and allowing asteroids to maintain other vital physiological-related functions (e.g., biomineralization).

Furthermore, we previously showed that the high-temperature treatment combined with elevated pCO_2 resulted in a low-stable calcification rate in the asteroid *A. yairi* (see Khalil et al. (2023)), which was also reflected in enzyme activity. These identical characteristics represent a strong correlation between enzyme activity and the calcification process, indicating the role of Ca-ATPase and Mg-ATPase as crucial enzymes involved in the biomineralization process in asteroids, in addition to V-type H^+ ATPase (Tresguerres, 2016), carbonic anhydrase (CA), and Na^+/K^+ ATPase (Ivanina et al., 2020; Pan et al., 2015) in echinoderm species. Biomineralization processes (e.g., calcification) are known to be influenced not only by environmental conditions such as pH and temperature or salinity, but also closely related to organic molecules and

biochemical cellular compounds (e.g., protein and enzyme) (Ivanina et al., 2020). The process of Ca^{2+} and Mg^{2+} balance in echinoderm species through intracellular modulation via trans-membrane transporters was described in prior studies (Kolbuk et al., 2020; Stumpp & Hu, 2017); however, the enzymes involved in the process have not been elucidated. The present study has reflected on the roles of enzymes, specifically Ca-ATPase and Mg-ATPase, in the calcification process of echinoids. However, the physio-biochemical mechanisms underlying this process remain unknown; hence, further studies are needed in this direction.

4.5. Conclusions

The impacts of concurrent ocean warming and acidification on lipid content, fatty acids composition, and calcification-related enzyme activities (Ca-ATPase and Mg-ATPase) of the asteroid *A. yairi* were investigated for the first time. Examining total lipid and associated FAs provides insight into how these tropical-subtropical asteroids utilize their energy resources under current and near-future global environmental changes. Under OA/OW conditions, *A. yairi* exhibits acclimation ability to maintain energy homeostasis presumably through efficient lipid-associate regulation and concurrently remodel membrane biophysics (e.g., membrane structure, fluidity, permeability, and functional properties) by adjusting their lipid-FAs biosynthesis, thereby giving them potential compensatory mechanisms to adapt with changes in ocean temperature and pH (i.e., homeoviscous adaptation). Furthermore, elevated temperatures seem to confer a physiological benefit in maintaining enzyme activities that minimize the effects of reduced pH, indicating that Ca-ATPase and Mg-ATPase activities in asteroid species are temperature- and pH-dependent physiological functions. Collectively, the findings of this study provide insight into the potential biochemical adaptation mechanisms utilized by the asteroid species *A. yairi* to cope with ongoing and imminent global changes in ocean conditions, specifically OW and OA. However, it is important to note that different asteroid species may respond differently to OW/OA, depending on the magnitude and rate of environmental change, as well as interactions with other species and ecological processes.

4.6. Acknowledgments

We are grateful to the Ministry of Education, Culture, Research, and Technology (MoECRT), Republic of Indonesia–Asian Development Bank (ADB) AKSI Project for supporting MK with their doctoral scholarship program. We thank Silvia Hardenberg, José Garcia, and Nico Steinel of the ZMT Marine Experimental Ecology Facility (MAREE) for providing support and technical

assistance, and ZMT staff Matthias Birkicht, Fabian Hüge, Raika Himmelsbach, and Constanze von Waldthausen for their assistance in the ZMT chemistry and biology laboratories.

4.7. Data availability

The data that support the findings of this study are available at PANGAEA open access repository; data of total lipid: <https://doi.pangaea.de/10.1594/PANGAEA.965904> (Khalil et al., 2024d), fatty acid compositions: <https://doi.pangaea.de/10.1594/PANGAEA.965902> (Khalil et al., 2024b), and enzyme activities: <https://doi.pangaea.de/10.1594/PANGAEA.965905> (Khalil et al., 2024a).

4.8. Supplementary materials

Supplementary text

Seawater chemistry control and manipulation

Using electronic solenoid valve mass flow controllers (HTK Hamburg, Germany; pure CO₂ provided by Linde GmbH, Pullach, Germany), the $p\text{CO}_2$ of the bubbled gases was regulated by blending compressed CO₂-free air and compressed CO₂ to create gas mixtures that were formulated according to the target $p\text{CO}_2$ conditions in accordance with the standard operating procedure (SOP) for ocean CO₂ measurements (Dickson et al., 2007). Subsequently, the 216-liter treatment sumps were then gradually introduced with the gas stream using a sparging tube. The treatment tank temperatures ($\pm\text{SE}$) were regulated to 27 (± 0.05) °C and 32 (± 0.08) °C, through the utilization of a closed-circulation heating system (Heaters Titanium Tube 600 W, Shego, Germany) that was managed by a programmable thermostat.

Temperature, salinity, and pH_{NBS} (National Bureau of Standards) were measured regularly (three times per week) using a multielectrode portable probe (WTW Multiline 3630 IDS, Xylem Analytics, Germany). The pH electrode probe was calibrated using NBS buffers pH 4.00 and pH 7.00, while the salinity-conductivity probe was calibrated with certified seawater reference material (Dickson CRM batch #154) of salinity 33.347. The $\text{pH}_{\text{total scale}}$ was measured weekly using the spectrophotometric method (Shimadzu UV-1700 Pharma Spec UV-Vis Spectrophotometer) following SOP 6b (Dickson et al., 2007) using the indicator dye meta, *m*-cresol purple (Sigma-Aldrich) as the chromogenic reagent.

Water samples for total alkalinity (A_T) and dissolved inorganic carbon (C_T) analysis were collected weekly in 500-mL borosilicate glass vials. The samples were then poisoned with 200 μ L of saturated mercuric chloride (HgCl_2) solution and refrigerated until further analysis. A_T and C_T measurements were performed according to the protocols described by Dickson et al. (2007). A_T was measured by open cell potentiometric Gran titration (to a precision of 10 μ mol/kg), and C_T was determined by the colorimetric analytical method using a Shimadzu DIC analyzer (to a precision of 10 μ mol/kg). The CO_2SYS software for MS Excel (Pelletier et al., 2007a) was used to calculate the seawater carbonate system parameters $p\text{CO}_2$, carbonate ion concentration [CO_3^{2-}], bicarbonate ion concentration [HCO_3^-], aqueous CO_2 , calcite saturation state (Ω_{Ca}), and aragonite saturation state (Ω_{Ar}): using Hansson (1973) and Mehrbach et al. (1973) refitted by Dickson and Millero (1987) for K_1 and K_2 carbonic acid constants; Dickson (1990) for K_{HSO_4} equilibrium constant; Dickson and Riley (1979) for K_{HF} dissociation constant; Uppström (1974) for the boric acid constant ($[\text{B}]_T$); and Mucci (1983) for the stoichiometric calcite solubility constant. The detail description of water chemistry control and manipulation is provided in Khalil et al. (2022).

Supplementary table

Table S4.1. Summary of water parameters from treatment tanks of *A. yairi*. A_T , total alkalinity; C_T , dissolved inorganic carbon (DIC); $p\text{CO}_2$, partial pressure of CO_2 ; $[\text{CO}_3^{2-}]$, carbonate ion; $[\text{HCO}_3^-]$, bicarbonate ion; $[\text{CO}_2]$, dissolved CO_2 ; Ω_{ca} , calcite saturation state; Ω_{Ar} , aragonite saturation state. Salinity, temperature, $\text{pH}_{\text{NBS scale}}$, $\text{pH}_{\text{T (total scale)}}$, A_T , and C_T were measured in water samples collected during the exposure. Other parameters are calculated using CO_2SYS software. Data are represented as means \pm SE.

Water parameters	Temperature: 27 °C			Temperature: 32 °C		
	$p\text{CO}_2$: 455 μatm	$p\text{CO}_2$: 1052 μatm	$p\text{CO}_2$: 2066 μatm	$p\text{CO}_2$: 455 μatm	$p\text{CO}_2$: 1052 μatm	$p\text{CO}_2$: 2066 μatm
Salinity (PSU)	34.56 \pm 0.12	34.73 \pm 0.06	34.75 \pm 0.05	34.65 \pm 0.08	34.78 \pm 0.05	34.76 \pm 0.02
Temperature (°C)	27.48 \pm 0.06	27.23 \pm 0.04	27.34 \pm 0.03	32.03 \pm 0.05	32.10 \pm 0.04	32.20 \pm 0.08
$\text{pH}_{\text{NBS scale}}$	8.13 \pm 0.00	7.87 \pm 0.01	7.60 \pm 0.01	8.13 \pm 0.00	7.87 \pm 0.00	7.60 \pm 0.01
$\text{pH}_{\text{T (total scale)}}$	8.00 \pm 0.00	7.74 \pm 0.01	7.47 \pm 0.01	8.00 \pm 0.00	7.74 \pm 0.00	7.47 \pm 0.01
A_T ($\mu\text{mol/kg-SW}$)	2504.42 \pm 15.33	2514.45 \pm 16.78	2539.83 \pm 38.86	2510.27 \pm 47.18	2532.19 \pm 40.05	2584.38 \pm 41.93
C_T ($\mu\text{mol/kg-SW}$)	2168.86 \pm 15.23	2340.99 \pm 11.62	2479.40 \pm 36.58	2134.38 \pm 38.40	2325.20 \pm 40.02	2493.30 \pm 37.87
$p\text{CO}_2$ (μatm)	456.13 \pm 8.24	1059.58 \pm 32.04	2075.40 \pm 30.99	453.78 \pm 6.51	1045.15 \pm 44.00	2057.31 \pm 74.42
$[\text{CO}_3^{2-}]$ ($\mu\text{mol/kg-SW}$)	245.64 \pm 2.52	138.12 \pm 4.64	81.18 \pm 2.35	273.82 \pm 8.23	162.68 \pm 4.67	99.46 \pm 4.64
$[\text{HCO}_3^-]$ ($\mu\text{mol/kg-SW}$)	1911.05 \pm 14.94	2178.74 \pm 9.58	2342.71 \pm 34.29	1849.66 \pm 30.77	2147.47 \pm 38.59	2344.63 \pm 34.94
$[\text{CO}_2]$ ($\mu\text{mol/kg-SW}$)	12.17 \pm 0.22	28.42 \pm 0.86	55.51 \pm 0.82	10.90 \pm 0.16	25.05 \pm 1.06	49.20 \pm 1.78
Ω_{ca}	5.96 \pm 0.06	3.35 \pm 0.11	1.97 \pm 0.06	6.71 \pm 0.20	3.98 \pm 0.11	2.44 \pm 0.11
Ω_{Ar}	3.96 \pm 0.04	2.22 \pm 0.07	1.31 \pm 0.04	4.52 \pm 0.14	2.69 \pm 0.08	1.64 \pm 0.08

Table S4.2. Summary of 2-way ANCOVA multifactorial analysis examining the effect of elevated temperature (27 °C, 32 °C) and $p\text{CO}_2$ (455 μatm , 1052 μatm , and 2066 μatm) on the total lipid, fatty acids composition, and enzyme (Ca-ATPase and Mg-ATPase) activities of the asterinid starfish *A. yairi* for 90 days of incubation time. Significant effects ($p < 0.05$) are in bold.

Trait	Trait component	Statistical model: 2-way ANCOVA	df	Sum sq.	Mean sq.	F	Pr (>F)	η^2	Post hoc summary (Tukey HSD)
Lipid content	Total lipid (ΣL_c)	Incubation time	2	0.42	0.21	4.85	0.02	0.18	day 90 > day 30 (Suppl. Table S4.4)
		Temperature	1	0.00	0.00	0.10	0.76	0.00	
		$p\text{CO}_2$	2	0.04	0.05	1.16	0.32	0.05	
		Temperature: $p\text{CO}_2$	2	0.04	0.04	1.01	0.34	0.05	
		Residuals	43	0.65	0.05				
Fatty acids	SFA-C14:0 (myristic acid)	Incubation time	2	8.96	4.48	2.62	0.08	0.24	day 90 < day 60 (Suppl. Table S4.4)
		Temperature	1	0.13	0.13	0.07	0.79	0.02	
		$p\text{CO}_2$	2	0.67	0.34	0.20	0.82	0.02	
		Temperature: $p\text{CO}_2$	2	6.70	3.35	1.96	0.15	0.13	
		Residuals	42	71.74	1.71				
	SFA-C16:0 (palmitic acid)	Incubation time	2	158.20	79.10	6.06	0.01	0.24	
		Temperature	1	12.30	12.31	0.94	0.34	0.02	
		$p\text{CO}_2$	2	9.60	4.82	0.37	0.69	0.02	
		Temperature: $p\text{CO}_2$	2	79.10	39.56	3.03	0.06	0.13	
		Residuals	39	509.30	13.06				
		Incubation time	2	44.95	22.47	3.15	0.06	0.18	

SFA-C18:0 (stearic acid)	Temperature	1	36.96	36.96	5.19	0.03	0.15	27 °C < 32°C
	pCO ₂	2	11.55	5.77	0.81	0.45	0.05	
	Temperature;pCO ₂	2	1.73	0.87	0.12	0.89	0.01	
	Residuals	29	206.62	7.12				
SFA-C20:0 (arachidic acid)	Incubation time	2	2.85	1.42	2.97	0.06	0.13	
	Temperature	1	0.28	0.28	0.58	0.45	0.01	
	pCO ₂	2	0.87	0.43	0.90	0.41	0.04	
	Temperature;pCO ₂	2	1.64	0.82	1.71	0.19	0.08	
SFA-C22:0 (behenic acid)	Residuals	41	19.68	0.48				
	Incubation time	2	4.40	2.20	1.08	0.35	0.06	
	Temperature	1	0.10	0.10	0.05	0.83	0.00	
	pCO ₂	2	0.18	0.09	0.04	0.96	0.00	
SFA-C24:0 (lignoceric acid)	Temperature;pCO ₂	2	1.49	0.75	0.37	0.70	0.02	
	Residuals	36	73.49	2.04				
	Incubation time	2	0.98	0.49	2.17	0.15	0.20	
	Temperature	1	0.10	0.09	0.42	0.53	0.02	
SFA-C24:0 (lignoceric acid)	pCO ₂	2	0.07	0.03	0.14	0.87	0.02	
	Temperature;pCO ₂	2	0.12	0.06	0.27	0.77	0.03	
	Residuals	17	3.86	0.23				
	Incubation time	2	2.76	1.38	2.48	0.10	0.11	
MUFA-C14:1ω5 (myristoleic acid)	Temperature	1	0.01	0.01	0.02	0.88	0.00	
	pCO ₂	2	0.24	0.12	0.22	0.81	0.01	

	Temperature;pCO ₂	2	2.22	1.11	1.99	0.15	0.09
	Residuals	42	23.41	0.56			
MUFA-C16:1ω9 (palmitoleic acid)	Incubation time	2	45.37	22.68	2.08	0.14	0.13
	Temperature	1	10.07	10.07	0.92	0.34	0.03
	pCO ₂	2	8.72	4.36	0.40	0.67	0.03
	Temperature;pCO ₂	2	50.79	25.39	2.33	0.12	0.14
	Residuals	29	316.00	10.90			
MUFA-C18:1ω9 (oleic acid)	Incubation time	2	21.21	10.61	2.08	0.14	0.13
	Temperature	1	5.02	5.02	0.98	0.33	0.03
	pCO ₂	2	2.77	1.39	0.27	0.76	0.02
	Temperature;pCO ₂	2	23.24	11.62	2.27	0.12	0.14
	Residuals	29	148.27	5.11			
MUFA-C18:1ω7 (vaccenic acid)	Incubation time	2	6.50	3.24	0.37	0.69	0.02
	Temperature	1	13.20	13.20	1.51	0.23	0.04
	pCO ₂	2	1.00	0.52	0.06	0.94	0.00
	Temperature;pCO ₂	2	32.90	16.44	1.88	0.17	0.09
	Residuals	39	340.70	8.74			
MUFA-C20:1ω9 (gondoic acid)	Incubation time	2	3.61	1.80	0.54	0.59	0.03
	Temperature	1	1.74	1.74	0.52	0.48	0.02
	pCO ₂	2	4.54	2.27	0.68	0.51	0.04
	Temperature;pCO ₂	2	2.81	1.40	0.42	0.66	0.03
	Residuals	32	106.86	3.34			

MUFA-C22:1 ω 9 (erucic acid)	Incubation time	2	0.76	0.38	0.96	0.39	0.04
	Temperature	1	0.24	0.24	0.59	0.45	0.01
	$p\text{CO}_2$	2	0.46	0.23	0.58	0.56	0.03
	Temperature; $p\text{CO}_2$	2	0.12	0.06	0.15	0.86	0.01
	Residuals	42	16.68	0.40			
PUFA-C18:2 ω 6 (linoleic acid, LA)	Incubation time	2	1.92	0.96	0.66	0.52	0.03
	Temperature	1	5.12	5.12	3.53	0.07	0.08
	$p\text{CO}_2$	2	4.15	2.07	1.43	0.25	0.06
	Temperature; $p\text{CO}_2$	2	5.27	2.64	1.82	0.17	0.08
	Residuals	42	60.88	1.45			
PUFA-C18:3 ω 3 (α - linolenic acid, ALA)	Incubation time	2	1.06	0.53	1.45	0.25	0.06
	Temperature	1	0.01	0.00	0.01	0.91	0.00
	$p\text{CO}_2$	2	1.90	0.95	2.61	0.08	0.10
	Temperature; $p\text{CO}_2$	2	1.78	0.89	2.45	0.10	0.10
	Residuals	45	16.42	0.36			
PUFA-C20:2 ω 6 (eicosadienoic acid)	Incubation time	2	1.36	0.68	1.17	0.32	0.05
	Temperature	1	0.63	0.63	1.08	0.31	0.03
	$p\text{CO}_2$	2	0.75	0.37	0.64	0.53	0.03
	Temperature; $p\text{CO}_2$	2	0.11	0.05	0.09	0.91	0.00
	Residuals	42	24.44	0.58			
PUFA-C20:4 ω 6 (arachidonic acid, AA)	Incubation time	2	0.04	0.02	0.01	0.99	0.00
	Temperature	1	1.01	1.01	0.47	0.50	0.01

	$p\text{CO}_2$	2	0.61	0.30	0.14	0.87	0.01	
	Temperature: $p\text{CO}_2$	2	0.39	0.19	0.09	0.91	0.00	
	Residuals	43	91.50	2.13				
	Incubation time	2	90.70	45.35	3.45	0.05	0.19	day 90 < day 60 (Suppl. Table S4.4)
PUFA-C20:5 ω 3 (eicosapentaenoic acid, EPA)	Temperature	1	28.80	28.78	2.19	0.15	0.07	
	$p\text{CO}_2$	2	49.40	24.72	1.88	0.17	0.11	
	Temperature: $p\text{CO}_2$	2	83.10	41.53	3.16	0.06	0.18	
	Residuals	29	380.70	13.13				
	Incubation time	2	0.58	0.29	0.22	0.81	0.01	
PUFA-C22:6 ω 3 (docosahexaenoic acid, DHA)	Temperature	1	0.37	0.37	0.28	0.60	0.01	
	$p\text{CO}_2$	2	5.36	2.68	2.01	0.15	0.09	
	Temperature: $p\text{CO}_2$	2	1.03	0.51	0.39	0.68	0.02	
	Residuals	40	53.42	1.34				
	Incubation time	2	7.43	3.72	1.48	0.24	0.07	
$\Sigma\omega$ 3: $\Sigma\omega$ 6	Temperature	1	7.78	7.78	3.10	0.09	0.07	
	$p\text{CO}_2$	2	5.50	2.75	1.10	0.34	0.05	
	Temperature: $p\text{CO}_2$	2	1.21	0.61	0.24	0.78	0.01	
	Residuals	41	102.85	2.51				
Enzyme activity	Incubation time	2	0.01	0.01	27.96	0.00	0.27	day 30 > day 60, day 90 (Suppl. Table S4.4)
	Temperature	1	0.00	0.00	0.40	0.53	0.00	

Ca-ATPase	$p\text{CO}_2$	2	0.00	0.00	4.02	0.02	0.05	1052 μatm < 455 μatm (Suppl. Table S4.4)
	Temperature; $p\text{CO}_2$	2	0.00	0.00	6.01	0.00	0.07	27 °C : 455 μatm > 27 °C : 1052 μatm , 32 °C : 1052 μatm (Suppl. Table S4.4)
	Residuals	151	0.03	0.00				
<hr/>								
Mg-ATPase	Incubation time	2	0.02	0.01	25.62	0.00	0.25	day 30 > day 60, day 90 (Suppl. Table S4.4)
	Temperature	1	0.00	0.00	1.68	0.20	0.01	
	$p\text{CO}_2$	2	0.00	0.00	3.92	0.02	0.05	1052 μatm < 455 μatm (Suppl. Table S4.4)
	Temperature; $p\text{CO}_2$	2	0.00	0.00	7.75	0.00	0.09	27 °C : 455 μatm > 32 °C : 455 μatm , 27 °C : 1052 μatm , 32 °C : 1052; 27 °C : 2066 μatm > 27 °C : 1052 μatm (Suppl. Table S4.4)
	Residuals	151	0.05	0.00				

Table S4.3. Summary of 2-way MANCOVA multifactorial analysis examining the effect of elevated temperature (27 °C, 32 °C) and $p\text{CO}_2$ (455 μatm , 1052 μatm , 2066 μatm) on SFAs, MUFAs, and PUFAs of asterinid starfish *A. yairi* for 90 days of incubation time. Significant effects ($p < 0.05$) are in bold.

Statistical Model: 2-way MANCOVA						
	df	Wilks Lambda	approx. F	num. df	den df	Pr (>F)
SFAs						
Incubation time	2	0.00	14.98	12	2	0.06
Temperature	1	0.00	365.87	6	1	0.04
$p\text{CO}_2$	2	0.00	15.74	12	2	0.06
Temperature: $p\text{CO}_2$	1	0.01	22.71	6	1	0.16
Residuals	6					
MUFAs						
Incubation time	2	0.22	1.45	12	16	0.23
Temperature	1	0.29	3.25	6	8	0.06
$p\text{CO}_2$	2	0.52	0.51	12	16	0.88
Temperature: $p\text{CO}_2$	2	0.54	0.47	12	16	0.91
Residuals	13					
PUFAs						
Incubation time	2	0.51	1.35	12	40	0.23
Temperature	1	0.66	1.71	6	20	0.17
$p\text{CO}_2$	2	0.41	1.85	12	40	0.07
Temperature: $p\text{CO}_2$	2	0.49	1.45	12	40	0.18
Residuals	25					

Table S4.4. Tukey HSD post hoc test results for the sole and interactive effects of temperature (27 °C and 32 °C) and $p\text{CO}_2$ (455 μatm , 1052 μatm , and 2066 μatm) on the asterinid starfish *A. yairi* total lipid content (Table S4.1) for 90 days of incubation time. Significant effects ($p \leq 0.05$) are in bold.

Trait	Trait component	Condition	diff.	lwr.	upr.	p_{adj}		
<i>Incubation time</i>								
Lipid content	Total lipid	day 60 vs day 30	0.056	-0.047	0.159	0.390		
		day 90 vs day 30	0.133	0.029	0.237	0.010		
		day 90 vs day 60	0.077	-0.024	0.178	0.168		
<i>Incubation time</i>								
Fatty acids	SFA-C16:0 (Palmitic acid)	day 60 vs day 30	1.946	-1.120	5.013	0.281		
		day 90 vs day 30	-2.592	-5.814	0.630	0.136		
		day 90 vs day 60	-4.538	-7.715	-1.361	0.004		
	<i>Incubation time</i>							
	PUFA-C20:5 ω 3 (Eicosapentaenoic acid, EPA)	day 60 vs day 30	-1.216	-4.599	2.166	0.652		
		day 90 vs day 30	-4.043	-7.866	-0.220	0.037		
day 90 vs day 60		-2.826	-6.650	0.997	0.179			
<i>Incubation time</i>								
Enzyme activity	Ca-ATPase	day 60 vs day 30	-0.017	-0.023	-0.010	0.000		
		day 90 vs day 30	-0.020	-0.027	-0.013	0.000		
		day 90 vs day 60	-0.003	-0.010	0.003	0.471		
		<i>pCO₂</i>						
		1052 μatm vs 455 μatm	-0.008	-0.015	-0.001	0.020		
		2066 μatm vs 455 μatm	-0.002	-0.009	0.005	0.740		
		2066 μatm vs 1052 μatm	0.006	-0.001	0.012	0.112		
		<i>Temperature*pCO₂</i>						
		32 °C : 455 μatm vs 27 °C : 455 μatm	-0.012	-0.024	0.001	0.081		
		27 °C : 1052 μatm vs 27 °C : 455 μatm	-0.022	-0.036	-0.007	0.000		
		32 °C : 1052 μatm vs 27 °C : 455 μatm	-0.012	-0.025	0.000	0.050		
		27 °C : 2066 μatm vs 27 °C : 455 μatm	-0.008	-0.023	0.006	0.519		
32 °C : 2066 μatm vs 27 °C : 455 μatm	-0.010	-0.023	0.002	0.157				
27 °C : 1052 μatm vs 32 °C : 455 μatm	-0.010	-0.023	0.002	0.196				
32 °C : 1052 μatm vs 32 °C : 455 μatm	-0.001	-0.011	0.010	1.000				
27 °C : 2066 μatm vs 32 °C : 455 μatm	0.003	-0.009	0.016	0.976				
32 °C : 2066 μatm vs 32 °C : 455 μatm	0.001	-0.009	0.012	0.999				
32 °C : 1052 μatm vs 27 °C : 1052 μatm	0.009	-0.003	0.022	0.242				

	27 °C : 2066 μ atm vs 27 °C : 1052 μ atm	0.013	-0.001	0.027	0.085
	32 °C : 2066 μ atm vs 27 °C : 1052 μ atm	0.011	-0.001	0.024	0.087
	27 °C : 2066 μ atm vs 32 °C : 1052 μ atm	0.004	-0.008	0.016	0.947
	32 °C : 2066 μ atm vs 32 °C : 1052 μ atm	0.002	-0.008	0.012	0.993
	32 °C : 2066 μ atm vs 27 °C : 2066 μ atm	-0.002	-0.014	0.010	0.998
	<i>Incubation time</i>				
	day 60 vs day 30	-0.018	-0.026	-0.010	0.000
	day 90 vs day 30	-0.023	-0.031	-0.015	0.000
	day 90 vs day 60	-0.005	-0.013	0.003	0.296
	<i>pCO₂</i>				
	1052 μ atm vs 455 μ atm	-0.009	-0.017	-0.001	0.026
	2066 μ atm vs 455 μ atm	-0.002	-0.010	0.006	0.876
	2066 μ atm vs 1052 μ atm	0.007	-0.001	0.015	0.082
	<i>Temperature*pCO₂</i>				
	32 °C : 455 μ atm vs 27 °C : 455 μ atm	-0.017	-0.032	-0.002	0.012
	27 °C : 1052 μ atm vs 27 °C : 455 μ atm	-0.028	-0.044	-0.011	0.000
	32 °C : 1052 μ atm vs 27 °C : 455 μ atm	-0.016	-0.031	-0.002	0.018
	27 °C : 2066 μ atm vs 27 °C : 455 μ atm	-0.010	-0.027	0.007	0.497
	32 °C : 2066 μ atm vs 27 °C : 455 μ atm	-0.014	-0.029	0.000	0.063
	27 °C : 1052 μ atm vs 32 °C : 455 μ atm	-0.010	-0.025	0.005	0.345
	32 °C : 1052 μ atm vs 32 °C : 455 μ atm	0.001	-0.011	0.013	1.000
	27 °C : 2066 μ atm vs 32 °C : 455 μ atm	0.007	-0.008	0.022	0.745
	32 °C : 2066 μ atm vs 32 °C : 455 μ atm	0.003	-0.009	0.015	0.977
	32 °C : 1052 μ atm vs 27 °C : 1052 μ atm	0.011	-0.003	0.026	0.241
	27 °C : 2066 μ atm vs 27 °C : 1052 μ atm	0.017	0.000	0.034	0.040
	32 °C : 2066 μ atm vs 27 °C : 1052 μ atm	0.013	-0.001	0.028	0.092
	27 °C : 2066 μ atm vs 32 °C : 1052 μ atm	0.006	-0.008	0.021	0.828
	32 °C : 2066 μ atm vs 32 °C : 1052 μ atm	0.002	-0.010	0.014	0.994
	32 °C : 2066 μ atm vs 27 °C : 2066 μ atm	-0.004	-0.018	0.011	0.972

Mg-ATPase

Supplementary figure

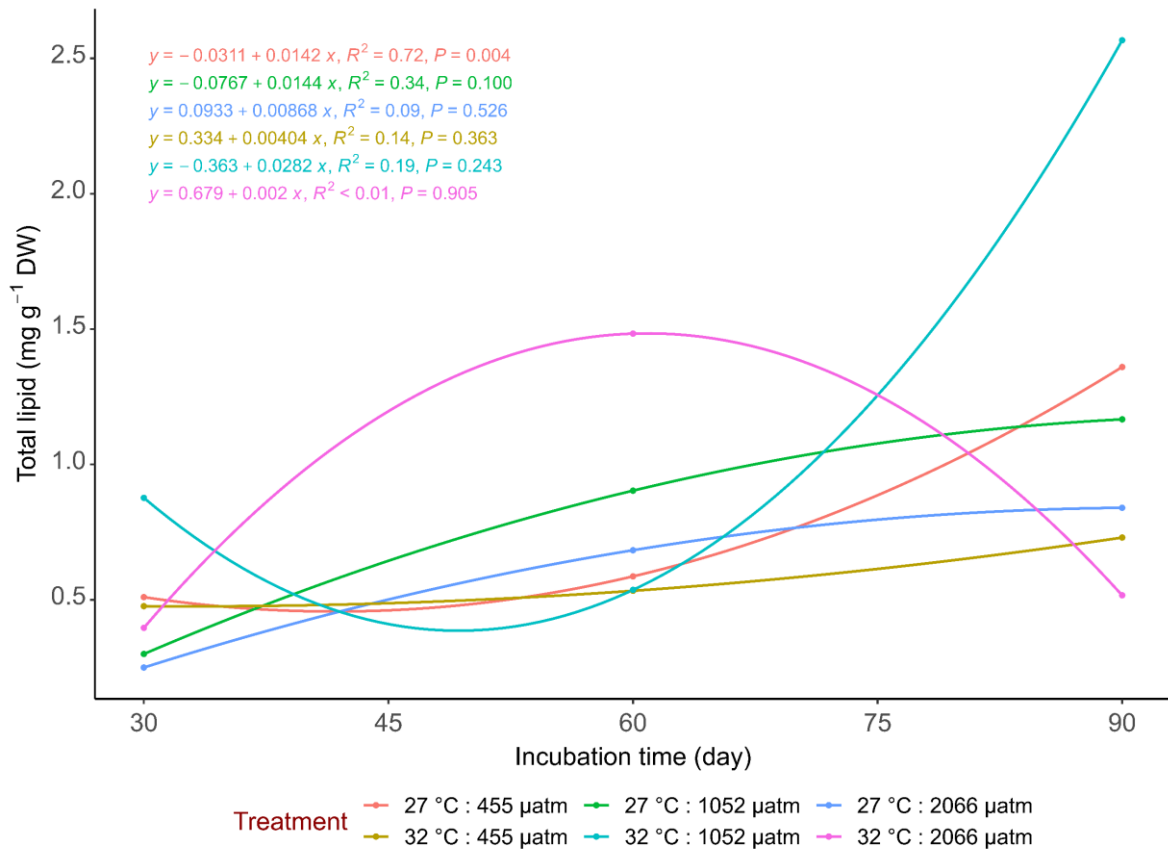


Figure S4.1. Linear polynomial interpolation model for the total lipid content (mg g⁻¹ DW) of *A. yairi* reared under different temperature levels (27 °C, 32 °C) and pCO₂ concentrations (455 μatm, 1052 μatm, and 2066 μatm) for up to 90 days of incubation time. Colored dots indicate the mean total lipid content in each treatment; *n* = 54.

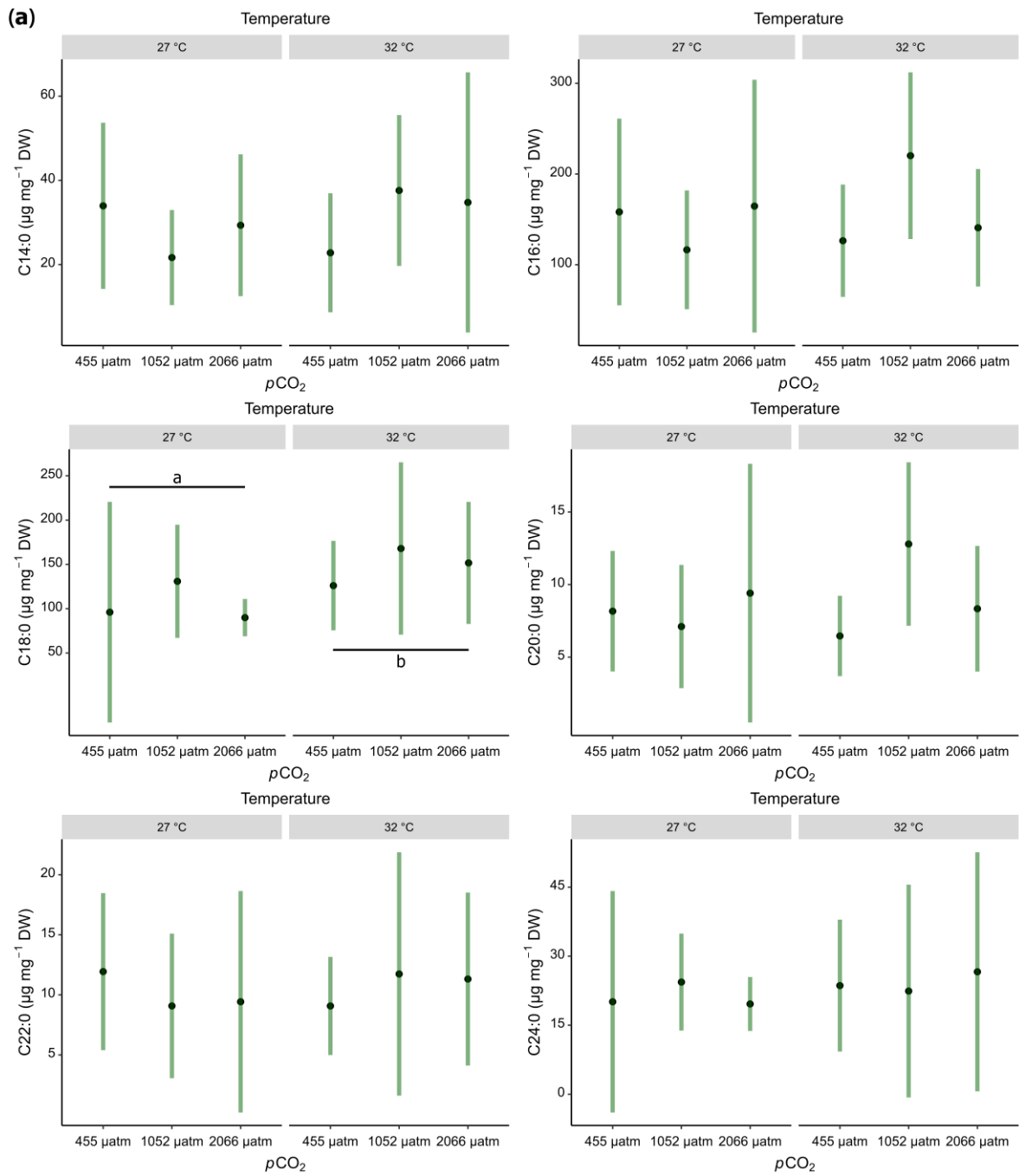


Figure S4.2. Cont.

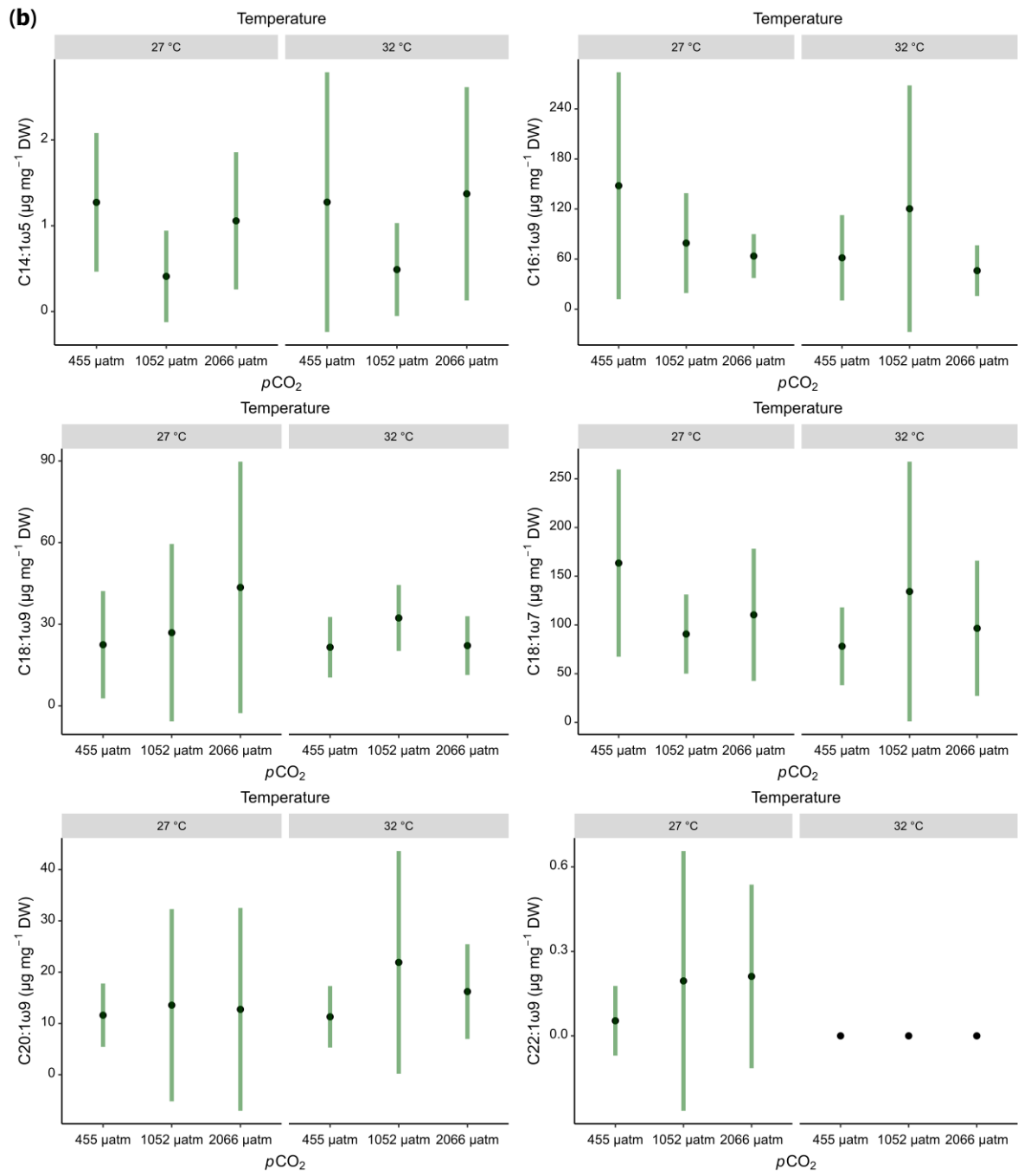


Figure S4.2. Cont.

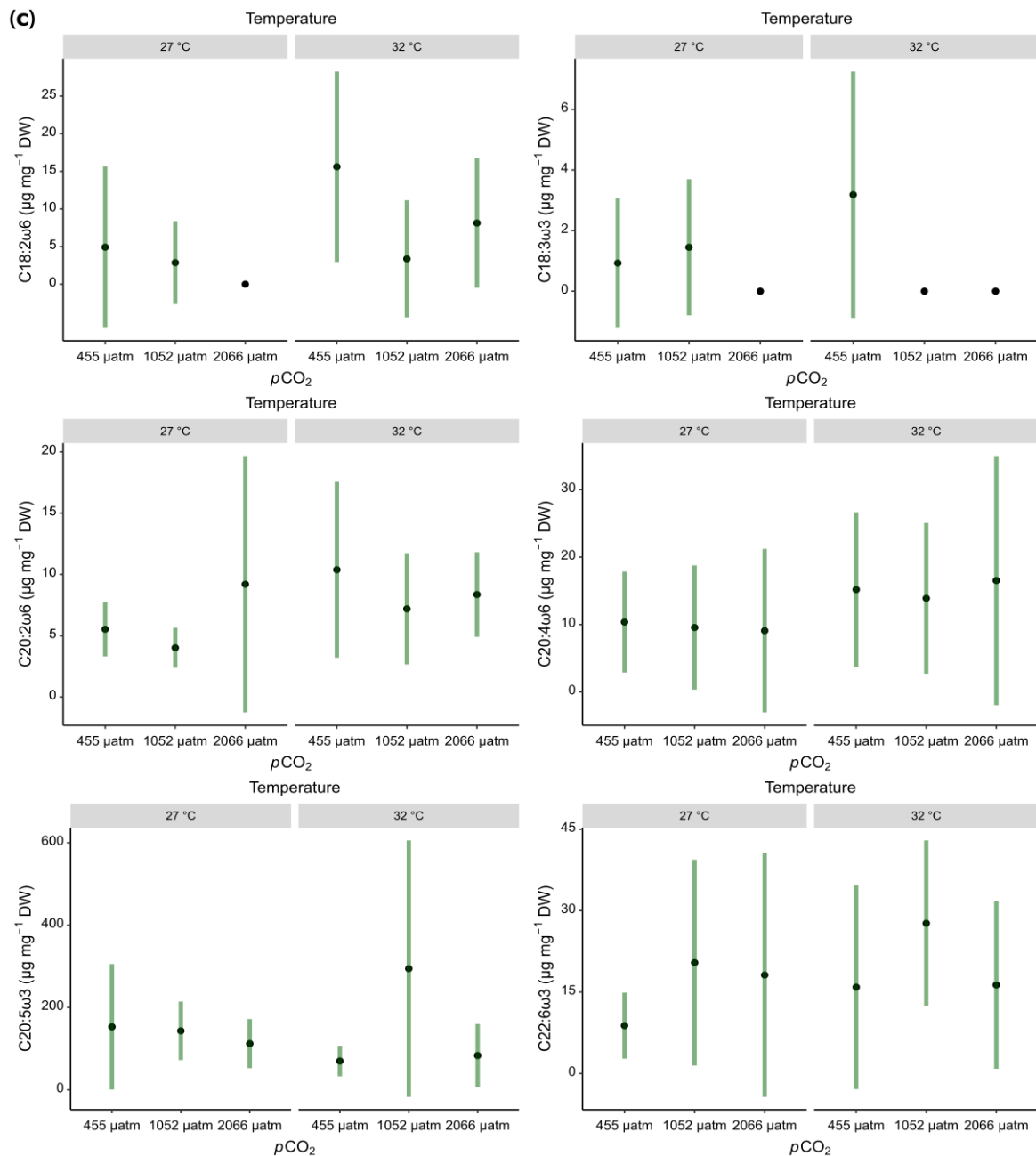


Figure S4.2. Fatty acids (FAs) composition of asteroid *A. yairi* exposed at different temperature levels (27 °C, 32 °C) and $p\text{CO}_2$ concentrations (455 μatm , 1052 μatm , and 2066 μatm) for 90 days. **(a)** Saturated fatty acids (SFAs) composition of *A. yairi*, **(b)** Monounsaturated fatty acids (MUFAs) composition of *A. yairi*, **(c)** Polyunsaturated fatty acids (PUFAs) composition of *A. yairi*. Plots display group mean (black dots). Vertical dark-green bars denote 95% confidence intervals of FAs type values. The letters designate significant differences between treatments; $n = 54$.

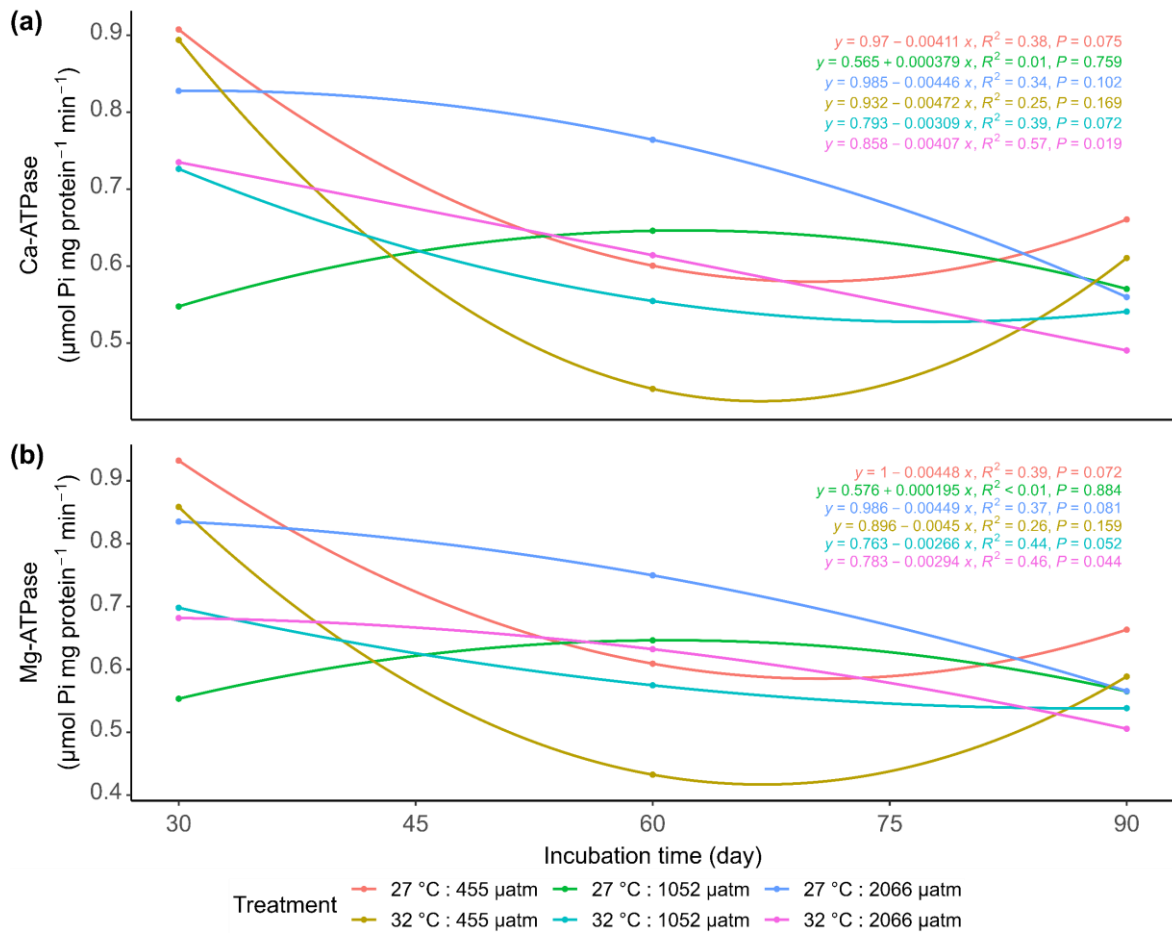


Figure S4.3. Linear polynomial interpolation model for the enzyme activity of starfish *A. yairi* reared under different temperature levels (27 °C, 32 °C) and $p\text{CO}_2$ concentrations (455 μatm , 1052 μatm , and 2066 μatm) for 90 days of incubation time. **(a)** Ca-ATPase ($\mu\text{moles Pi mg protein}^{-1} \text{ min}^{-1}$), and **(b)** Ca-ATPase ($\mu\text{moles Pi mg protein}^{-1} \text{ min}^{-1}$). Colored dots indicate the mean effect on enzyme activity in each treatment; $n = 54$.

Chapter 5. General discussion

Anthropogenic activities have exacerbated global ocean change, triggering the occurrence and intensification of multiple environmental stressors that pose significant challenges to marine organisms and ecosystems (Gissi et al., 2021; IPCC, 2022). These stressors, e.g., elevated temperatures, ocean acidification, ocean deoxygenation, salinity changes, plastic pollution, and coastal hypoxia (Dermawan et al., 2022; Stock et al., 2019); frequently coincide temporally, spatially, and ubiquitous (Halpern et al., 2015; Halpern et al., 2008). Consequently, there is a potential for shifts in species distributions, modified community structures, altered food web dynamics, and diminished ocean productivity (Doney et al., 2012; Hoegh-Guldberg & Bruno, 2010; Pinsky et al., 2020). Therefore, to mitigate the deleterious effects of climate change, it is important to identify stressors that can impair ecosystem resilience.

While the physiological responses of marine species to individual stressors are extensively studied (Leung et al., 2022; Venegas et al., 2023), the cumulative effects of multiple stressors are being continuously investigated (Gunderson et al., 2016; Simeoni et al., 2023). Despite organisms demonstrating relative resilience to individual stressors (Leung et al., 2019; Leung et al., 2022), the introduction of additional stressors can substantially complicate their responses due to potential interactions between stressors or their effects (Carrier-Belleau et al., 2021; Piggott et al., 2015; Ross et al., 2023). Consequently, experiments focusing on a single stressor may not adequately evaluate the sensitivity of organisms to complex environmental changes. Thus, comprehensive investigations involving multiple stressors are necessary for accurately measuring organism responses and predicting ecosystem dynamics in the face of climate change. The primary objective of this thesis was to enhance our comprehension of the collective effects exerted by multiple anthropogenic-caused stressors as sole or combined drivers on the physiochemical characteristics of small-size calcifying marine invertebrates, specifically, the asterinid starfish *Aquilonastra yairi*. Moreover, this thesis also aimed to acquire better insight into the future resilience probability of the species under intensification of OW and OA, their adaptive mechanisms, and potential ecological implications. These species were selected due to their important ecological contributions within ecosystems. Marine organisms living in neritic-intertidal zones are highly susceptible to rapid environmental fluctuations, which can induce physiological stress and alter physiochemical structure when intensity

thresholds are exceeded. It is hypothesized that neritic-intertidal-adapted animals exhibit a wider thermal window than oceanic-adapted animals. These physiological conditions allow them to tolerate short exposures to high temperatures, permitting intertidal organisms to conduct adaptive mechanisms to prevent a reduction of their biological performance (Somero, 2002); however, they might undergo an energy dissipation linked to suboptimal metabolic functions (Ratcliffe et al., 1981).

5.1. Temperature is a key driver affecting physiochemical functions of starfish

Temperature has been recognized as a major physical environmental factor that stimulates various physiological and chemical modifications in marine animals related to organism-level biological performance, e.g., acclimatization and adaptation, fitness, survivability, and development (Kazmi et al., 2022; Nguyen et al., 2011) and is foremost a primary abiotic environmental factor limiting the spatial distribution of marine organisms in thermal-variable habitats (Root et al., 2003; Stuart-Smith et al., 2017). The mechanisms by which temperature alters physiochemical aspects of ectothermic organisms are complex and dependent on taxa, associated with phylogenies, ontogenies, thermal experiences, and geographical-ecology patterns (Bennett et al., 2021; Dahlke et al., 2020; Poloczanska et al., 2016). This present work showed that a temperature shift affects all physiochemical traits evaluated (Chapters 2, 3, and 4); it was found to be the primary driver of alteration in the biomineralization, righting behavior, metabolic rate, FA-SFAs (as a sole factor), and enzyme activity (as a combined factor) of the starfish *A. yairi*. With increased temperature, the higher kinetic energy of biochemical reactions accelerates the rate of the metabolic process and also affects the structural and functional properties of biological macromolecules (i.e., lipid-FAs, protein, and carbohydrate) and enzymatic reaction, which subsequently alters the physiology and behavior (Angilletta Jr., 2009; Hochachka & Somero, 2002). This robust temperature-specific control on physiological traits is also observed in other starfish species, e.g., *Acanthaster cf. solaris* (Lang et al., 2022), *Parvulastra exigua* (Balogh & Byrne, 2020; McElroy et al., 2012), *Echinaster (Othilia) graminicola* (Ardor Bellucci & Smith, 2019), and *Odontaster validus* (Kidawa et al., 2010).

Within the thermal tolerance range, the physiological response of starfish to elevated temperature appears as a causality and cascaded process. As temperature increases, *A. yairi* shows enhanced metabolic activity marked by increased O₂ uptake. This metabolic upregulation may subsequently facilitate the acceleration of macromolecular breakdown (e.g.,

lipid-FAs) through a series of oxidation-reduction reactions (aerobic metabolism pathway). This leads to ATP-synthetizing to sustain energetic supplies and is further distributed into internal physiochemical processes that demand higher amounts of energy. These processes act as thermoregulation mechanisms to maintain internal homeostasis (Hochachka & Somero, 2002) and are essential for sustaining starfish fitness and survivability. Besides, an energetic trade-off is also performed to keep the most crucial physiological processes retained properly (Chapter 3), allowing the starfish to adapt to chronic conditions. Although the energetic trade-off is identifiable, the energetic basis of the trade-off is difficult to quantify (Applebaum et al., 2014). However, when the limit of the thermal tolerance range, i.e., the pejus temperature, is reached, the onset of reduction in O₂ supplies to cells and tissues, indicates the initial threshold for thermal tolerance (Frederich & Portner, 2000). Under this condition, O₂ saturation levels in the cellular fluids and tissue begin to decline, triggering a state of progressive hypoxia (Pörtner, 2002). Subsequently, the capacity of ectothermic organisms for aerobic metabolism starts to decrease due to the failure in the ventilatory and circulatory systems as they have reached the capacity limits and, therefore, are unable to obtain adequate O₂ (Dong et al., 2011; Frederich & Portner, 2000). As a result, the organism transitions into anaerobic metabolism despite sufficient O₂ being available in the environment. The thermal tolerance also becomes more limited over time when animals switch to less efficient anaerobic metabolic pathways, which have a much lower ATP yield relative to aerobic scope, so that eventually, the physiological processes of the organism decline rapidly over time (Schulte, 2015; Schulte et al., 2011), resulting in organ malfunction and subsequent mortality. Nevertheless, the lowest mortality rate recorded in the present study (Chapter 3) suggests that the upper-temperature threshold of 32 °C applied in the present study is still within the thermal tolerance range for starfish *A. yairi* populations.

The experimental results conducted within the framework of this thesis have also demonstrated that temperature as a sole stressor did not significantly affect some other physiochemical traits of the starfish, such as lipid, FA-MUFAs, FA-PUFAs, as well as Ca-ATPase and Mg-ATPase enzyme activities (Chapter 4). Hence, we hypothesize that the optimum temperature varies between each physiochemical trait; it may be related to the multiple performances – multiple optima (MPMO) theory posits that ectotherms have multiple and function-specific physiological thermal optima that contribute to an organism's fitness (Clark et al., 2013). Therefore, although an increase of +5 °C from ambient temperature significantly

affects behavior (e.g., righting behavior), it probably does not constitute the thermal optimum for other performances, such as enzyme activity. However, distinct results apply when a temperature stressor works as a joint stressor (i.e., OA), as explained in the following subchapters.

5.2. Effect of ocean warming and acidification on physiology-related functions of the starfish and their ecological implication

OA and OW as sole or combined factors produced varying impacts on the observed physiochemical traits in asterinid starfish. As a single factor, OW appears to have affected most aspects related to the physiology of the starfish (see Subchapter 5.1), while OA, as a single factor, had significant effects on its metabolic rate, calcification rate, and enzyme activities related to calcification. However, combined stressors were found to alter metabolic rate, calcification rate, and enzyme activities of the starfish. The present study demonstrated that the effects of OA act in an interactive manner with those of OW to modify the physiological traits of starfish. OA and OW effects worked in an additive fashion to elevate the metabolic rate (Chapter 3) and acted antagonistically on the calcification rate (Chapter 3) and enzyme activities (Chapter 4). Therefore, it is evident that the combined stressors have produced variability within the various physiochemical traits of the starfish.

Simultaneous OA and OW exert concurrent stresses on marine animals, amplifying energy requirements to maintain basal physiological processes and acid-base homeostasis (Hu et al., 2024; Kelley & Lunden, 2017; Lang et al., 2023). In response, asterinid starfish exhibit increased oxygen consumption rates (respiration rate, M_{O_2}), a proxy for organismal metabolism (Seibel & Drazen, 2007), suggested as an acclimatization mechanism to mitigate the adverse effects of these combined stressors on their physiochemical traits through increased energy provision; facilitating metabolism adjustments and shifts in energy pathways or energy trade-offs. Achieving this adaptive strategy via altered M_{O_2} results in positive consequences for the biological performance of starfish. In particular, it contributes to very low mortality rates, a maintainable righting capability (behavioral response), and the preservation of calcification processes, although to a lesser extent relative to ambient settings (Chapter 3). Furthermore, increased M_{O_2} combined with the ability of starfish to preserve their lipid-associated FAs content as energy sources are also instrumental in counteracting the effects of OA and OW, either as sole or interplay stressors. However, prolonged high-energy demands to maintain

biological performance under OA and OW stress, respectively, could result in deleterious outcomes, i.e., a reduction in energy availability for reproduction, growth, preservation of calcium carbonate skeletons, and a decrease in foraging ability (Appelhans et al., 2014; Hue et al., 2022; Kamyra et al., 2014). Therefore, under OA and OW stressors, starfish prioritize energetic provision to regulate physiological processes associated with basal survivability instead of other physiological-related processes. Chapter 2 captures the following conditions: increased energy supplies do not indicate a favorable implication for starfish's skeletal structure, where skeletal degradation was observed in starfish exposed to elevated temperatures and $p\text{CO}_2$. Weakened skeletal structures have severe consequences for growth, locomotion, and predator-prey interactions; thereby potentially altering population dynamics and community structure in the future (Byrne & Fitzner, 2019; Kroeker et al., 2014). Hence, energy surplus seems to become crucial for the fitness of marine animals in the near future oceans.

The present work also highlights the importance of the preservation of lipid-FAs in coping with OA and OW stressors (Chapter 4); therefore, the availability of food sources in the environment that might bioconvert into lipid-FAs, which could subsequently synthesize to maintain an energy budget (i.e., the balance between energy income and energy expenditure, see (Davies & Hatcher, 1998), is crucial to sustain biological performance and becomes an essential variable to promote the adaptive capacity of starfish under chronic conditions (Mos et al., 2023; Pörtner, 2012). During treatment in the present study, the starfish population likely had adequate dietary supplies and was further utilized (in the form of energy) to maintain their basal biological performance. However, it is probable that over the longer run, where food availability in the surrounding environment becomes more limited, intra- and interspecies competition for foraging-feeding may yield modifications in the abundance, distribution, and community structure of starfish (Stuckless et al., 2023), potentially leading to cascading impacts on the food web dynamics.

Linear-negative calcification rates were observed in starfish exposed to elevated $p\text{CO}_2$ (Chapter 3); consequently, the calcareous structure of the starfish became more fragile (Chapter 2). However, antagonistic interactive effects were recorded when starfish were exposed to high temperatures, allowing calcification to proceed, although at modest rates (Chapter 3). This suggests that starfish benefited from high temperatures to mitigate the negative effect of

decreasing pH on CaCO_3 incorporation. It should be noted that the calcification process in marine animals is not driven exclusively by seawater carbonate chemistry (Roleda et al., 2012; Toyofuku et al., 2017), but it is also a product of physiological processes that involve energy assimilation-distribution and enzymatic activities (de Goeyse et al., 2021; Findlay et al., 2009; Killian & Wilt, 2008). This explains why, although pH and seawater saturation states (i.e., Ω_{Ar} and Ω_{Cal}) decrease under OA conditions, elevated temperatures accelerate the metabolic activities that may create the optimal alkaline state needed to precipitate CaCO_3 minerals onto the calcification sites. However, increasing temperature leads to an increased Mg:Ca ratio (Chapter 2; Hermans et al. (2010); Morse et al. (1997)). Consequently, increased Mg contents in starfish skeletons could potentially increase their susceptibility to dissolution under OA conditions due to high-Mg CO_3 being more soluble than calcite and aragonite (Dubois, 2014), hence high energetic expenditure is required to maintain calcified skeletons, which in turn compels energetic trade-offs with other physiological processes. Furthermore, increased dissolution of the skeleton could impair the starfish's ability to preserve skeletal structure, which could further affect their locomotion function. Locomotion performance is regarded as an important feature for survival in the majority of starfish species since it determines individuals' capacity to forage, escape predators, disperse, and migrate (Meretta & Ventura, 2021; Montgomery, 2014; Mueller et al., 2011). Thus, this trait can be used as an indicator of the functional integrity and fitness of the species.

Studies assessing the effects of OA concurrent with OW on starfish species, in particular, are still sparse, hence making it challenging to draw comprehensive conclusions on starfish conditions under future ocean scenarios. Despite a number of studies reporting relatively similar results, a range of responses were found among species with different traits. These variations in response are probably due to the bioecological characteristics of the species and subsequent adaptive plasticity, as well as the magnitude and duration of stressor exposure.

Chapter 6. Conclusion and future research

6.1. Conclusion

Increases in GHG-CO₂ since global industrialization have resulted in changes to the physicochemical structure of seawater, notably elevated sea surface temperatures (OW) and OA, with implications on micro-macroscale from altering marine organism's life performances and fitness to broad ecosystem functions and services. The physiochemical effects of OA and OW may be associated with the complex reorganization of cellular functions and molecular processes. Available evidence (see Subchapter 1.2) suggests that the concurrent effects of OA and OW may be more deleterious than the effects of individual stressors. However, organismal responses to abiotic stressors (i.e., OA and OW) are complex and variable, highly dependent on multiple factors, i.e., intensity and combination of stressors, taxa, individual compensatory regulation, organism life history, and biological complexity level; making it difficult to predict the stressor effects on a particular species. Therefore, using various bioindicators to evaluate the effects of stressors provides a comprehensive framework to quantify and predict the magnitude, direction, or manner in which stressors affect the organism's functional and ecosystem function. Furthermore, the effects of elevated ocean temperatures and CO₂ on keystone species and ecosystem engineers (e.g., starfish; see Subchapter 1.4) are of particular concern due to the possibility of disrupting and compromising entire communities. This study contributes to the ongoing discussion over the potential role of physiochemistry on marine ectotherms, especially echinoderm starfish, as coping mechanisms in response to rapid environmental stress. The studies reported in this thesis represent the first research investigating the effects of global ocean change on biomineralization and physiological traits through long-term experiments using small and cryptic asterinid starfish species found in tropical to subtropical regions (Chapter 1).

This thesis revealed that the response of asterinid starfish *A. yairi* to increased temperature and $p\text{CO}_2$ largely relies on their capacity to perform adaptive adjustments, in terms of physiological-related functions or behavioral activities, to these chronic environments (Table 6.1). The key findings of the effects of global ocean change (OA and OW, sole or combined stressors) on asterinid starfish in the present study ranged from population to cellular scales (Figure 6.1), with potential interactive results in several observational variables. This study

found that temperature is the main factor regulating starfish physiological activity, relative to OA, where increased $p\text{CO}_2$ concentration in conjunction with elevated temperature interacts synergistically or antagonistically, depending on the physiologically-related traits of the starfish (Chapter 5). However, starfish seem to harbor adaptive mechanisms that allow them to cope with environmental stress; in the manner of energetic trade-offs and homeostatic pathways, thus allowing them to endure chronic environmental conditions (Chapter 5).

Organismal mortality is a downstream aspect of health that might precede bio-physiological deterioration and dysregulation. The asterinid starfish population studied displayed high resilience to increased intensity of OA and OW (sole or combined stressors) in the scope of survivability (Chapter 3); indicated by low mortality rates (even null at 27 °C temperature treatment groups) throughout 90 days of experimental period and therefore, suggesting high homeostatic capacities. The asterinids were capable of regulating physiological function and utilizing energetic trade-off mechanisms to maintain their fitness (Chapter 3) and routine metabolic biosynthesis (Chapter 4) under sustained elevated temperature and hypercapnic conditions. Moreover, increased metabolic rate in the starfish was interpreted as a strategy for sustaining energy supplies to control starfish homeostatic mechanisms, including regulation of cellular acid-base to prevent acidosis and maintain neuromuscular functions involved in behavioral activities (e.g., righting response) under chronic events.

This thesis provides the first study to measure the calcification rate in starfish species, either at ambient condition or under elevated temperature and hypercapnia regimes (Chapter 3). At ambient temperature (27 °C), the net calcification rate of starfish under reduced pH level (increased $p\text{CO}_2$ concentration) exhibited a negative-threshold curve (Chapter 3; Figure 3.3). However, our findings suggest that increased temperature mitigates the negative effects of OA on calcification performance of the starfish. Antagonistic interactive responses to decreased pH and increased temperature result in a stable-low net calcification rate trend (Chapter 3; Figure 3.3); starfish may continue to sustain a minimum net calcification under chronic conditions. Nevertheless, increasing temperature, on the other side, promotes more Mg^{2+} to incorporate into the calcite lattice, which then transforms into high magnesium calcite (HMC; >4 mol% MgCO_3). HMC is recognized to be more soluble and thermodynamically metastable than low magnesium calcite (LMC) and aragonite; hence, it might make the skeleton more susceptible to dissolution with potential implications on skeletal robustness, rigidity, and

function (Chapter 2). Subsequently, weakened starfish skeleton due to OA and OW could hold detrimental consequences for starfish locomotion, predator defense, and overall fitness, which has potentially broad implications on benthic community structure.

Table 6.1. Overview of the effect of $p\text{CO}_2$, temperature, and combined stressors on the physiochemical traits of asterinid starfish *A. yairi*. Arrows ($\uparrow\downarrow$) indicate the significance and direction of response to elevated stressor levels; (\leftrightarrow) denotes combined stressors acting in a significant and interactive fashion to affect the traits; (-) implies no significant effect was measured, and (\ddagger) indicates an effect of stressor was observed.

Scale	Physiochemical trait	Environmental stressor effect			
		$p\text{CO}_2$	Temperature	$p\text{CO}_2$ * Temperature	
Population-level	Survivability (mortality rate)	-	-	-	
Cellular-level	Mg/Ca ratio	-	\uparrow	-	
	Sr/Ca ratio	-	-	-	
	Mg _{norm}	-	\uparrow	-	
	Sr _{norm}	-	-	-	
	Biom mineralization	Ca _{norm}	-	-	-
	Skeleton structure		\ddagger	\ddagger	\ddagger
	Calcification rate		\downarrow	-	\leftrightarrow
	Metabolic rate		\uparrow	\uparrow	\leftrightarrow
	Righting behavior		-	\uparrow	-
	Lipid	Total lipid	-	-	-
	Fatty acid	SFAs	-	\uparrow	-
		MUFAs	-	-	-
		PUFAs	-	-	-
Enzyme activities	Mg-ATPase	\downarrow	-	\leftrightarrow	
	Ca-ATPase	\downarrow	-	\leftrightarrow	

In the present study, intracellular effects of OA and OW were examined at multiple levels of biological micro-components (e.g., lipid and enzyme) to determine molecular mechanisms potentially involved in the acclimatization process to chronic conditions. The present studies revealed that combined effects of increased temperature and $p\text{CO}_2$ have not significantly modified lipid-associated biochemistry (e.g., total lipid content and FAs profile) of starfish, potentially enabling them to cope with near-future ocean acidification and warming scenarios. Starfish can maintain the amounts and states of lipid-FAs; thus, their functions as energy storage, providing cell insulation (i.e., thermal and electrical insulation for proper cell function), and contributing to membrane structure can be sustained under chronic conditions (Chapter 4). However, temperature as a sole factor was found to alter the amount of SFAs, which then translated as a homeoviscous adaptive mechanism to maintain membrane stability and viscosity; serves to mitigate the impact of decreased internal cell pH resulting from OA. Interestingly, in contrast to lipid-biochemistry, Ca-ATPase and Mg-ATPase enzyme activities were significantly affected by combined temperature and $p\text{CO}_2$. Both Ca-ATPase and Mg-ATPase enzyme activities showed a positive parabolic response at 27 °C with increasing $p\text{CO}_2$, but enzyme activities remained stable at 32 °C with increasing $p\text{CO}_2$ concentration. These enzyme activity characteristics are identical to the calcification patterns of starfish (Chapter 3), indicating a robust correlation between Ca-ATPase and Mg-ATPase enzyme activities and the calcification process on asteroids under OA and OW environments. Therefore, the apparent sensitivity of Ca-ATPase and Mg-ATPase activities to $p\text{CO}_2$ /pH changes raises concerns about potential vulnerabilities in skeletal development and preservation. These enzymes play an important role in Ca^{2+} and Mg^{2+} transport, which are essential for biomineralization. Changes in their activities under combined stressors indicate potential compromises in skeletal integrity, which is consistent with observations reported in Chapter 2 (e.g., skeletal degradation).

Investigating the multifaceted impacts of global ocean change on marine organisms requires a comprehensive research approach. By encompassing diverse biological, chemical, and physical parameters; such investigations may provide a more detailed understanding of organismal responses at different levels of organization. Elucidating the physiological and chemical responses of bioindicator species, such as the asterinid starfish, to combined stressors OA and OW is crucial. This knowledge can inform predictions of their resilience, potential ecological impact within their predominant intertidal habitat, and broader ecosystem implications. Understanding the mechanisms underlying their response to elevated $p\text{CO}_2$ concentrations

(hypercapnia) and rising temperatures will not only explain the starfish's adaptation potential but also elucidate cascading effects on broader ecosystem dynamics.

6.2. Potential further research

This section outlines and explores potential future studies in order to address the research gaps identified in the present study. The present research has highlighted that the upcoming global ocean change has various consequences on the physiological and mineralogical traits of asterinid starfish, from altered skeletal mineralogy and reduced enzyme activity to no significant effect on survivability and lipid biosynthesis of starfish *A. yairi*. It is important to note that the effects of OA and OW (as sole or combined stressors) on the tested traits appear complex and variable, subject to the specific traits and stress response mechanisms regulated by the starfish. The organism's stress response involves a range of physiological, biochemical, and molecular processes that aim to maintain internal homeostasis and mitigate the adverse effects of environmental challenges. This adaptive mechanism often includes the activation of specific genes, stress protein synthesis, immune function, antioxidant responses, and alterations in metabolic pathways to ensure the organism's survival and functionality under adverse conditions (Chevin & Hoffmann, 2017; Migliaccio et al., 2019; Simonetti et al., 2022; Wilson & Matschinsky, 2021). Therefore, a further integrated investigation into the physiochemical instruments of starfish to cope with environmental threats in a broader scope, ranging from genetic expression to cellular defense mechanisms, is needed to develop a comprehensive understanding of specific or combination mechanisms that might be applied in response to multiple and complex environmental stressors.

While this study is concerned with the effect of two major ocean changes in the future, i.e., OA and OW, it is important to highlight that several abiotic factors are projected to contribute to deteriorating future marine ecosystems and biodiversity, including oxygen depletion (deoxygenation) (Deutsch et al., 2023), salinity changes (Rothig et al., 2023), increasing nutrient loading (related to eutrophication) (Wåhlström et al., 2020), and ocean debris and pollution (e.g., plastic debris, chemicals) (Cabral et al., 2019; Thushari & Senevirathna, 2020) may interact synergistically with OA and OW to have negative effects on the life performances of marine organisms (O'Brien et al., 2023; Przeslawski et al., 2015). It is therefore important to examine the potential interactive effect of OW and OA, with other environmental change metrics, on biophysiochemical critical threshold points. This might be particularly important in the context

of resilience to thermal and hypercapnia stresses compromised by additional exposure to hypoxia, salinity changes, or the pollutant load. Furthermore, previous research has indicated that the adverse effect of combined OA and OW on physiochemical aspects of marine animals becomes more pronounced in the presence of additional environmental stressors, e.g., hypoxia (Bernhard et al., 2021; Khan et al., 2021; Khan et al., 2020), salinity shifts (Cole et al., 2016; Ko et al., 2014), and pollutant (Baag & Mandal, 2023), which emphasizes the importance of incorporating multifactorial stressor methods in ecophysiology studies.

Early life stages (i.e., embryo, larvae, juveniles, and asexual fissiparous new individuals) are the most critical phase in the development and survival of echinoderm; therefore, the toxicity assay and abiotic stressor effects assessment are mainly focused on echinoderm gametogenesis and larval development (Bay et al., 1993; Przeslawski et al., 2015). Previous studies suggested that OA and OW are known to exert more significant detrimental effects on early life versus adult stages in echinoderm species (Bednaršek et al., 2021; Byrne & Hernández, 2020; Byrne & Przeslawski, 2013; Leung et al., 2022). As an implication, adaptive potential capacity in early life stages may determine organisms' sustainability and ecological function within an ecosystem. These crucial characteristics suggest the importance of examining the effects of multi-stressors on earlier life stages of starfish, which this present study did not address. Moreover, the effects of environmental stressors during early development may influence the life performances of mature species through potential carryover. Carryover effects (or latent effects) arise when the performance or experience of one life history phase exerts a positive or negative influence on subsequent life history stage performance (Pechenik, 2006), typically carried from larval to juvenile stages and/or from juvenile to adult stages; thus, has potential to confer and enhance resilience under stressed environmental conditions to subsequent lifespans (Parker et al., 2015).

Furthermore, future investigations might focus on exploring the potential of transgenerational effects, examining the capacity and pace of starfish to perform adaptive plasticity (acclimate and adapt) under environmental perturbations across generations. The transgenerational response emerges via nongenetic or epigenetic processes in the parental lifespan, whereby environmental conditions experienced by the parental generation will influence the phenotypic traits of the offspring generation (Mousseau & Fox, 1998). This mechanism, therefore, becomes critical in providing stressor tolerance in the context of global ocean change (Donelson et al.,

2018). Subsequently, in future research, omics-based approaches (e.g., proteomics, transcriptomics, metabolomics, and epigenomics) linked to transgenerational exposure are key to understanding the potential impacts of rapid climate change, including OA and other abiotic environmental stressors on starfish.

Comprehending how ocean climate change affects the physiochemistry of marine organisms provides insights into predictions and mitigations of the impacts of this anthropogenic-induced stressor on ecosystem functions and services. Using multiple taxa and bioindicator/biomarker species, paired with varied analytical approaches, is crucial for evaluating the effects. Therefore, studies on starfish hold significant implications for understanding complex and interconnected threats posed by climate change in the marine environment. Furthermore, investigating the physiochemical responses of starfish to OA and OW has significant implications beyond studying this specific taxon. As an important ecological component of coastal-coral reef ecosystems, understanding the mechanisms by which starfish respond to environmental stressors reflects potential implications for entire ecological communities. Physiochemical adjustments starfish use to mitigate the impacts of OA and OW offers insights into the potential vulnerabilities and resilience of other marine invertebrates, particularly ectothermic species that share similar physiologic pathways in maintaining homeostasis and responding to environmental stresses. Although the effects of OA and OW are species-specific, however, starfish robustness to the OA and OW in some physiochemical traits might mirror the resilience of intertidal animals in other taxa to climate change. Comparative approaches provide insight into mechanisms underlying responses of organisms across different taxonomic groups, which is essential for predicting broader implications on marine biodiversity and ecosystems.

References

- Adami, C. (2009). Biological complexity and biochemical information. In R. A. Meyers (Ed.), *Encyclopedia of complexity and systems science* (pp. 489-511). Springer. https://doi.org/10.1007/978-0-387-30440-3_33.
- Addadi, L., Raz, S., & Weiner, S. (2003). Taking advantage of disorder: Amorphous calcium carbonate and its roles in biomineralization. *Advanced Materials*, *15*(12), 959-970. <https://doi.org/10.1002/adma.200300381>.
- Addadi, L., & Weiner, S. (1992). Control and design principles in biological mineralization. *Angewandte Chemie International Edition in English*, *31*(2), 153-169. <https://doi.org/10.1002/anie.199201531>.
- Adkins, J. F., Naviaux, J. D., Subhas, A. V., Dong, S., & Berelson, W. M. (2021). The dissolution rate of CaCO₃ in the ocean. *Annual Review of Marine Science*, *13*, 57-80. <https://doi.org/10.1146/annurev-marine-041720-092514>.
- Al-Rshaidat, M. M., Snider, A., Rosebraugh, S., Devine, A. M., Devine, T. D., Plaisance, L., Knowlton, N., & Leray, M. (2016). Deep COI sequencing of standardized benthic samples unveils overlooked diversity of Jordanian coral reefs in the northern Red Sea. *Genome*, *59*(9), 724-737. <https://doi.org/10.1139/gen-2015-0208>.
- Alix, M., Kjesbu, O. S., & Anderson, K. C. (2020). From gametogenesis to spawning: How climate-driven warming affects teleost reproductive biology. *Journal of Fish Biology*, *97*(3), 607-632. <https://doi.org/10.1111/jfb.14439>.
- Alma, L., Kram, K. E., Holtgrieve, G. W., Barbarino, A., Fiamengo, C. J., & Padilla-Gamino, J. L. (2020). Ocean acidification and warming effects on the physiology, skeletal properties, and microbiome of the purple-hinge rock scallop. *Comparative Biochemistry and Physiology Part A: Molecular & Integrative Physiology*, *240*, 110579. <https://doi.org/10.1016/j.cbpa.2019.110579>.
- Ambrozova, G., Pekarova, M., & Lojek, A. (2010). Effect of polyunsaturated fatty acids on the reactive oxygen and nitrogen species production by raw 264.7 macrophages. *European Journal of Nutrition*, *49*(3), 133-139. <https://doi.org/10.1007/s00394-009-0057-3>.
- Anacleto, P., Maulvault, A. L., Bandarra, N. M., Repolho, T., Nunes, M. L., Rosa, R., & Marques, A. (2014). Effect of warming on protein, glycogen and fatty acid content of native and invasive clams. *Food Research International*, *64*, 439-445. <https://doi.org/10.1016/j.foodres.2014.07.023>.

- Anand, M., Ranges, K., Maruthupandy, M., Jayanthi, G., Rajeswari, B., & Priya, R. J. (2021). Effect of CO₂ driven ocean acidification on calcification, physiology and ovarian cells of tropical sea urchin *Salmacis virgulata* - A microcosm approach. *Heliyon*, 7(1), e05970. <https://doi.org/10.1016/j.heliyon.2021.e05970>.
- Anderson, K. D., Cantin, N. E., Casey, J. M., & Pratchett, M. S. (2019). Independent effects of ocean warming versus acidification on the growth, survivorship and physiology of two *Acropora* corals. *Coral Reefs*, 38(6), 1225-1240. <https://doi.org/10.1007/s00338-019-01864-y>.
- Andersson, A. J., Kline, D. I., Edmunds, P. J., Archer, S. D., Bednaršek, N., Carpenter, R. C., Chadsey, M., Goldstein, P., Grottoli, A. G., Hurst, T. P., King, A. L., Kübler, J. E., Kuffner, I. B., Mackey, K. R. M., Menge, B. A., Paytan, A., Riebesell, U., Schnetzer, A., Warner, M. E., & Zimmerman, R. C. (2015). Understanding ocean acidification impacts on organismal to ecological scales. *Oceanography*, 28(2), 16-27. <http://www.jstor.org/stable/24861866>.
- Andersson, A. J., & Mackenzie, F. T. (2011). Technical comment on Kroeker et al. (2010) Meta-analysis reveals negative yet variable effects of ocean acidification on marine organisms. *Ecology Letters*, 13, 1419-1434. *Ecology Letters*, 14(8), E1-2. <https://doi.org/10.1111/j.1461-0248.2011.01646.x>.
- Andersson, A. J., Mackenzie, F. T., & Bates, N. R. (2008). Life on the margin: Implications of ocean acidification on Mg-calcite, high latitude and cold-water marine calcifiers. *Marine Ecology Progress Series*, 373, 265-273. <https://doi.org/10.3354/meps07639>.
- Angilletta Jr., M. J. (2009). *Thermal adaptation: A theoretical and empirical synthesis*. Oxford University Press. <https://doi.org/10.1093/acprof:oso/9780198570875.001.1>.
- Appelhans, Y. S., Thomsen, J., Opitz, S., Pansch, C., Melzner, F., & Wahl, M. (2014). Juvenile sea stars exposed to acidification decrease feeding and growth with no acclimation potential. *Marine Ecology Progress Series*, 509, 227-239. <https://doi.org/10.3354/meps10884>.
- Applebaum, S. L., Pan, T. C., Hedgecock, D., & Manahan, D. T. (2014). Separating the nature and nurture of the allocation of energy in response to global change. *Integrative and Comparative Biology*, 54(2), 284-295. <https://doi.org/10.1093/icb/ucu062>.
- Ardor Bellucci, L. M., & Smith, N. F. (2019). Crawling and righting behavior of the subtropical sea star *Echinaster (Othilia) graminicola*: Effects of elevated temperature. *Marine Biology*, 166(11). <https://doi.org/10.1007/s00227-019-3591-4>.
- Armstrong, E. J., Watson, S. A., Stillman, J. H., & Calosi, P. (2022). Elevated temperature and carbon dioxide levels alter growth rates and shell composition in the fluted giant clam, *Tridacna squamosa*. *Scientific Reports*, 12(1), 11034. <https://doi.org/10.1038/s41598-022-14503-4>.

- Arroyo, J. I., Diez, B., Kempes, C. P., West, G. B., & Marquet, P. A. (2022). A general theory for temperature dependence in biology. *Proceedings of the National Academy of Sciences of the United States of America*, *119*(30), e2119872119. <https://doi.org/10.1073/pnas.2119872119>.
- Arya, D. B., Vincent, S. G. T., & Godson, P. S. (2022). Benthic biotopes: Abiotic and biotic factors in the sediment. In P. S. Godson, S. G. T. Vincent, & S. Krishnakumar (Eds.), *Ecology and biodiversity of benthos* (pp. 21-31). Elsevier. <https://doi.org/10.1016/b978-0-12-821161-8.00009-x>.
- Ashur, M. M., Johnston, N. K., & Dixon, D. L. (2017). Impacts of ocean acidification on sensory function in marine organisms. *Integrative and Comparative Biology*, *57*(1), 63-80. <https://doi.org/10.1093/icb/icx010>.
- Asnaghi, V., Mangialajo, L., Gattuso, J. P., Francour, P., Privitera, D., & Chiantore, M. (2014). Effects of ocean acidification and diet on thickness and carbonate elemental composition of the test of juvenile sea urchins. *Marine Environmental Research*, *93*, 78-84. <https://doi.org/10.1016/j.marenvres.2013.08.005>.
- Asnicar, D., Novoa-Abelleira, A., Minichino, R., Badocco, D., Pastore, P., Finos, L., Munari, M., & Marin, M. G. (2021). When site matters: Metabolic and behavioural responses of adult sea urchins from different environments during long-term exposure to seawater acidification. *Marine Environmental Research*, *169*, 105372. <https://doi.org/10.1016/j.marenvres.2021.105372>.
- Azcarate-Garcia, T., Avila, C., & Figuerola, B. (2024). Skeletal Mg content in common echinoderm species from Deception and Livingston Islands (South Shetland Islands, Antarctica) in the context of global change. *Marine Pollution Bulletin*, *199*, 115956. <https://doi.org/10.1016/j.marpolbul.2023.115956>.
- Baag, S., & Mandal, S. (2023). Do global environmental drivers' ocean acidification and warming exacerbate the effects of oil pollution on the physiological energetics of *Scylla serrata*? *Environmental Science and Pollution Research*, *30*(9), 23213-23224. <https://doi.org/10.1007/s11356-022-23849-1>.
- Balogh, R., & Byrne, M. (2020). Developing in a warming intertidal, negative carry over effects of heatwave conditions in development to the pentamerous starfish in *Parvulastra exigua*. *Marine Environmental Research*, *162*, 105083. <https://doi.org/10.1016/j.marenvres.2020.105083>.
- Bay, S., Burgess, R., & Nacci, D. (1993). Status and applications of Echinoid (Phylum Echinodermata) toxicity test methods. In W. G. Landis, J. S. Hugues, & M. A. Lewis (Eds.), *Environmental toxicology and risk assessment* (pp. 281-302). American Society for Testing and Materials.

- Beaugrand, G., & Kirby, R. R. (2018). How Do Marine Pelagic Species Respond to Climate Change? Theories and Observations. *Annual Review of Marine Science*, 10, 169-197. <https://doi.org/10.1146/annurev-marine-121916-063304>.
- Bednaršek, N., Calosi, P., Feely, R. A., Ambrose, R., Byrne, M., Chan, K. Y. K., Dupont, S., Padilla-Gamiño, J. L., Spicer, J. I., Kessouri, F., Roethler, M., Sutula, M., & Weisberg, S. B. (2021). Synthesis of thresholds of ocean acidification impacts on echinoderms. *Frontiers in Marine Science*, 8. <https://doi.org/10.3389/fmars.2021.602601>.
- Bednaršek, N., Feely, R. A., Howes, E. L., Hunt, B. P. V., Kessouri, F., León, P., Lischka, S., Maas, A. E., McLaughlin, K., Nezlin, N. P., Sutula, M., & Weisberg, S. B. (2019). Systematic review and meta-analysis toward synthesis of thresholds of ocean acidification impacts on calcifying pteropods and interactions with warming. *Frontiers in Marine Science*, 6. <https://doi.org/10.3389/fmars.2019.00227>.
- Belaústegui, Z., Muñiz, F., Nebelsick, J. H., Domènech, R., & Martinell, J. (2017). Echinoderm ichnology: bioturbation, bioerosion and related processes. *Journal of Paleontology*, 91(4), 643-661. <https://doi.org/10.1017/jpa.2016.146>.
- Bell, T., Nishida, K., Ishikawa, K., Suzuki, A., Nakamura, T., Sakai, K., Ohno, Y., Iguchi, A., & Yokoyama, Y. (2017). Temperature-controlled culture experiments with primary polyps of coral *Acropora digitifera*: Calcification rate variations and skeletal Sr/Ca, Mg/Ca, and Na/Ca ratios. *Palaeogeography Palaeoclimatology Palaeoecology*, 484, 129-135. <https://doi.org/10.1016/j.palaeo.2017.03.016>.
- Benitez, S., Lagos, N. A., Duarte, C., Cid, M. J., & Navarro, J. M. (2024). Effects of ocean acidification and warming on physiological and behavioural responses of an herbivore snail to waterborne predator cues. *Environmental Pollution*, 340(Pt 1), 122798. <https://doi.org/10.1016/j.envpol.2023.122798>.
- Bennett, H., Bell, J. J., Davy, S. K., Webster, N. S., & Francis, D. S. (2018). Elucidating the sponge stress response; lipids and fatty acids can facilitate survival under future climate scenarios. *Global Change Biology*, 24(7), 3130-3144. <https://doi.org/10.1111/gcb.14116>.
- Bennett, J. M., Sunday, J., Calosi, P., Villalobos, F., Martinez, B., Molina-Venegas, R., Araujo, M. B., Algar, A. C., Clusella-Trullas, S., Hawkins, B. A., Keith, S. A., Kuhn, I., Rahbek, C., Rodriguez, L., Singer, A., Morales-Castilla, I., & Olalla-Tarraga, M. A. (2021). The evolution of critical thermal limits of life on Earth. *Nature Communications*, 12(1), 1198. <https://doi.org/10.1038/s41467-021-21263-8>.
- Bernhard, J. M., Wit, J. C., Starczak, V. R., Beaudoin, D. J., Phalen, W. G., & McCorkle, D. C. (2021). Impacts of multiple stressors on a benthic foraminiferal community: A long-term

- experiment assessing response to ocean acidification, hypoxia and warming. *Frontiers in Marine Science*, 8. <https://doi.org/10.3389/fmars.2021.643339>.
- Bernhardt, J. R., & Leslie, H. M. (2013). Resilience to climate change in coastal marine ecosystems. *Annual Review of Marine Science*, 5(1), 371-392. <https://doi.org/10.1146/annurev-marine-121211-172411>.
- Bisswanger, H. (2017). *Enzyme kinetics: Principles and methods* (3rd ed.). Wiley-VCH Verlag. <https://doi.org/10.1002/9783527806461.ch6>.
- Blake, D. B. (1990). Adaptive zones of the class Asteroidea (Echinodermata). *Bulletin of Marine Science*, 46(3), 701-718.
- Bligh, E. G., & Dyer, W. J. (1959). A rapid method of total lipid extraction and purification. *Canadian Journal of Biochemistry and Physiology*, 37(8), 911-917. <https://doi.org/10.1139/o59-099>.
- Borremans, C., Hermans, J., Baillon, S., André, L., & Dubois, P. (2009). Salinity effects on the Mg/Ca and Sr/Ca in starfish skeletons and the echinoderm relevance for paleoenvironmental reconstructions. *Geology*, 37(4), 351-354. <https://doi.org/10.1130/g25411a.1>.
- Boyd, P. W., Collins, S., Dupont, S., Fabricius, K., Gattuso, J. P., Havenhand, J., Hutchins, D. A., Riebesell, U., Rintoul, M. S., Vichi, M., Biswas, H., Ciotti, A., Gao, K., Gehlen, M., Hurd, C. L., Kurihara, H., McGraw, C. M., Navarro, J. M., Nilsson, G. E., . . . Portner, H. O. (2018). Experimental strategies to assess the biological ramifications of multiple drivers of global ocean change—A review. *Global Change Biology*, 24(6), 2239-2261. <https://doi.org/10.1111/gcb.14102>.
- Boyd, P. W., & Hutchins, D. A. (2012). Understanding the responses of ocean biota to a complex matrix of cumulative anthropogenic change. *Marine Ecology Progress Series*, 470, 125-135. <https://doi.org/10.3354/meps10121>.
- Bradford, M. M. (1976). A rapid and sensitive method for the quantitation of microgram quantities of protein utilizing the principle of protein-dye binding. *Analytical Biochemistry*, 72(1-2), 248-254. [https://doi.org/10.1016/0003-2697\(76\)90527-3](https://doi.org/10.1016/0003-2697(76)90527-3).
- Brahmi, C., Chapron, L., Le Moullac, G., Soyez, C., Beliaeff, B., Lazareth, C. E., Gaertner-Mazouni, N., & Vidal-Dupiol, J. (2021). Effects of elevated temperature and $p\text{CO}_2$ on the respiration, biomineralization and photophysiology of the giant clam *Tridacna maxima*. *Conservation Physiology*, 9(1), coab041. <https://doi.org/10.1093/conphys/coab041>.
- Bray, L., Pancucci-Papadopoulou, M. A., & Hall-Spencer, J. M. (2014). Sea urchin response to rising $p\text{CO}_2$ shows ocean acidification may fundamentally alter the chemistry of marine skeletons. *Mediterranean Marine Science*, 15(3). <https://doi.org/10.12681/mms.579>.
- Breitburg, D., Salisbury, J., Bernhard, J., Cai, W.-J., Dupont, S., Doney, S., Kroeker, K., Levin, L., Long, W. C., Milke, L., Miller, S., Phelan, B., Passow, U., Seibel, B., Todgham, A., & Tarrant, A.

- (2015). And on top of all that... Coping with ocean acidification in the midst of many stressors. *Oceanography*, 25(2), 48-61. <https://doi.org/10.5670/oceanog.2015.31>.
- Brennand, H. S., Soars, N., Dworjanyn, S. A., Davis, A. R., & Byrne, M. (2010). Impact of ocean warming and ocean acidification on larval development and calcification in the sea urchin *Tripneustes gratilla*. *PLoS One*, 5(6), e11372. <https://doi.org/10.1371/journal.pone.0011372>.
- Brett, M. T., Müller-Navarra, D. C., & Persson, J. (2009). Crustacean zooplankton fatty acid composition. In M. Kainz, M. Brett, & M. Arts (Eds.), *Lipids in aquatic ecosystems* (pp. 115-146). Springer. https://doi.org/10.1007/978-0-387-89366-2_6.
- Brierley, A. S., & Kingsford, M. J. (2009). Impacts of climate change on marine organisms and ecosystems. *Current Biology*, 19(14), R602-614. <https://doi.org/10.1016/j.cub.2009.05.046>.
- Briffa, M., de la Haye, K., & Munday, P. L. (2012). High CO₂ and marine animal behaviour: Potential mechanisms and ecological consequences. *Marine Pollution Bulletin*, 64(8), 1519-1528. <https://doi.org/10.1016/j.marpolbul.2012.05.032>.
- Burton, E. A., & Walter, L. M. (1987). Relative precipitation rates of aragonite and Mg calcite from seawater: Temperature or carbonate ion control?. *Geology*, 15(2), 111-114. [https://doi.org/10.1130/0091-7613\(1987\)15<111:Rproaa>2.0.Co;2](https://doi.org/10.1130/0091-7613(1987)15<111:Rproaa>2.0.Co;2).
- Busacker, G. P., & Chavin, W. (1981). Characterization of Na⁺ + K⁺ -ATPase and Mg²⁺-ATPases from the gill and the kidney of the goldfish (*Carassius auratus* L.). *Comparative Biochemistry and Physiology Part B: Comparative Biochemistry*, 69(2), 249-256. [https://doi.org/10.1016/0305-0491\(81\)90237-6](https://doi.org/10.1016/0305-0491(81)90237-6).
- Butow, B., Wynne, D., Sukenik, A., Hadas, O., & Tel-Or, E. (1998). The synergistic effect of carbon concentration and high temperature on lipid peroxidation in *Peridinium gatunense*. *Journal of Plankton Research*, 20(2), 355-369. <https://doi.org/10.1093/plankt/20.2.355>.
- Byrne, M. (2006). Life history diversity and evolution in the Asterinidae. *Integrative and Comparative Biology*, 46(3), 243-254. <https://doi.org/10.1093/icb/icj033>.
- Byrne, M. (2011). Impact of ocean warming and ocean acidification on marine invertebrate life history stages: Vulnerabilities and potential for persistence in a changing ocean. In R. N. Gibson, R. J. A. Atkinson, J. D. M. Gordon, I. P. Smith, & D. J. Hughes (Eds.), *Oceanography and marine biology: An annual review* (Vol. 49, pp. 1-42). CRC Press.
- Byrne, M., & Fitzer, S. (2019). The impact of environmental acidification on the microstructure and mechanical integrity of marine invertebrate skeletons. *Conservation Physiology*, 7(1), coz062. <https://doi.org/10.1093/conphys/coz062>.

- Byrne, M., Gonzalez-Bernat, M., Doo, S., Foo, S., Soars, N., & Lamare, M. (2013). Effects of ocean warming and acidification on embryos and non-calcifying larvae of the invasive sea star *Patiriella regularis*. *Marine Ecology Progress Series*, 473, 235-246. <https://doi.org/10.3354/meps10058>.
- Byrne, M., & Hernández, J. C. (2020). Sea urchins in a high CO₂ world: Impacts of climate warming and ocean acidification across life history stages. In J. M. Lawrence (Ed.), *Sea urchins: Biology and ecology* (Vol. 43, pp. 281-297). Elsevier. <https://doi.org/10.1016/B978-0-12-819570-3.00016-0>.
- Byrne, M., & Przeslawski, R. (2013). Multistressor impacts of warming and acidification of the ocean on marine invertebrates' life histories. *Integrative and Comparative Biology*, 53(4), 582-596. <https://doi.org/10.1093/icb/ict049>.
- Byrne, M., Smith, A. M., West, S., Collard, M., Dubois, P., Grabalandy, A., & Dworjanyn, S. A. (2014). Warming influences Mg²⁺ content, while warming and acidification influence calcification and test strength of a sea urchin. *Environmental Science & Technology*, 48(21), 12620-12627. <https://doi.org/10.1021/es5017526>.
- Cabral, H., Fonseca, V., Sousa, T., & Costa Leal, M. (2019). Synergistic effects of climate change and marine pollution: An overlooked interaction in coastal and estuarine areas. *Int J Environ Res Public Health*, 16(15). <https://doi.org/10.3390/ijerph16152737>.
- Caetano, L. S., Pereira, T. M., Evangelista, J. D., Cabral, D. S., Carvalho Coppo, G., de Souza, L. A., Anderson, A. B., Heringer, O. A., & Chippari-Gomes, A. R. (2021). Impact on fertility rate and embryo-larval development due to the association acidification, ocean warming and lead contamination of a sea urchin *Echinometra lucunter* (Echinodermata: Echinoidea). *Bulletin of Environmental Contamination and Toxicology*, 106(6), 923-928. <https://doi.org/10.1007/s00128-021-03225-4>.
- Caldeira, K., & Wickett, M. E. (2003). Anthropogenic carbon and ocean pH. *Nature*, 425(6956), 365. <https://doi.org/10.1038/425365a>.
- Calder, P. C. (2010). Omega-3 fatty acids and inflammatory processes. *Nutrients*, 2(3), 355-374. <https://doi.org/10.3390/nu2030355>.
- Calder, P. C., & Grimble, R. F. (2002). Polyunsaturated fatty acids, inflammation and immunity. *European Journal of Clinical Nutrition*, 56 Suppl 3, S14-19. <https://doi.org/10.1038/sj.ejcn.1601478>.
- Cameron, L. P., Reymond, C. E., Müller-Lundin, F., Westfield, I., Grabowski, J. H., Westphal, H., & Ries, J. B. (2019). Effects of temperature and ocean acidification on the extrapallial fluid pH, calcification rate, and condition factor of the king scallop *Pecten maximus*. *Journal of Shellfish Research*, 38(3), 763-777. <https://doi.org/10.2983/035.038.0327>.

- Carey, N., Harianto, J., & Byrne, M. (2016). Sea urchins in a high-CO₂ world: Partitioned effects of body size, ocean warming and acidification on metabolic rate. *Journal of Experimental Biology*, 219(Pt 8), 1178-1186. <https://doi.org/10.1242/jeb.136101>.
- Carrier-Belleau, C., Drolet, D., McKindsey, C. W., & Archambault, P. (2021). Environmental stressors, complex interactions and marine benthic communities' responses. *Scientific Reports*, 11(1), 4194. <https://doi.org/10.1038/s41598-021-83533-1>.
- Carta, G., Murru, E., Banni, S., & Manca, C. (2017). Palmitic acid: Physiological role, metabolism and nutritional implications. *Frontiers in Physiology*, 8, 902. <https://doi.org/10.3389/fphys.2017.00902>.
- Chai, G., Li, J., & Li, Z. (2024). The interactive effects of ocean acidification and warming on bioeroding sponge *Sphaciospongia vesparium* microbiome indicated by metatranscriptomics. *Microbiological Research*, 278, 127542. <https://doi.org/10.1016/j.micres.2023.127542>.
- Challener, R. C., & McClintock, J. B. (2013). Exposure to extreme hypercapnia under laboratory conditions does not impact righting and covering behavior of juveniles of the common sea urchin *Lytechinus variegatus*. *Marine and Freshwater Behaviour and Physiology*, 46(3), 191-199. <https://doi.org/10.1080/10236244.2013.800759>.
- Challener, R. C., McClintock, J. B., & Makowsky, R. (2013). Effects of reduced carbonate saturation state on early development in the common edible sea urchin *Lytechinus variegatus*: Implications for land-based aquaculture. *Journal of Applied Aquaculture*, 25(2), 154-175. <https://doi.org/10.1080/10454438.2013.791911>.
- Chan, K.-M., Delfert, D., & Junger, K. D. (1986). A direct colorimetric assay for Ca²⁺-stimulated ATPase activity. *Analytical Biochemistry*, 157(2), 375-380. [https://doi.org/10.1016/0003-2697\(86\)90640-8](https://doi.org/10.1016/0003-2697(86)90640-8).
- Chan, K. Y. K., Grünbaum, D., & O'Donnell, M. J. (2011). Effects of ocean-acidification-induced morphological changes on larval swimming and feeding. *Journal of Experimental Biology*, 214(22), 3857-3867. <https://doi.org/10.1242/jeb.054809>.
- Chave, K. E. (1954). Aspects of the biogeochemistry of magnesium 1. Calcareous marine organisms. *Journal of Geology*, 62(3), 266-283. <https://doi.org/10.1086/626162>.
- Chave, K. E. (1962). Factors influencing the mineralogy of carbonate sediments. *Limnology and Oceanography*, 7(2), 218-223. <https://doi.org/10.4319/lo.1962.7.2.0218>.
- Chave, K. E. (1984). Physics and chemistry of biomineralization. *Annual Review of Earth and Planetary Sciences*, 12(1), 293-305. <https://doi.org/10.1146/annurev.ea.12.050184.001453>.

- Cheng, L., Abraham, J., Trenberth, K. E., Boyer, T., Mann, M. E., Zhu, J., Wang, F., Yu, F., Locarnini, R., Fasullo, J., Zheng, F., Li, Y., Zhang, B., Wan, L., Chen, X., Wang, D., Feng, L., Song, X., Liu, Y., . . . Lu, Y. (2024). New record ocean temperatures and related climate indicators in 2023. *Advances in Atmospheric Sciences*. <https://doi.org/10.1007/s00376-024-3378-5>.
- Cheng, L., Abraham, J., Trenberth, K. E., Fasullo, J., Boyer, T., Locarnini, R., Zhang, B., Yu, F., Wan, L., Chen, X., Song, X., Liu, Y., Mann, M. E., Reseghetti, F., Simoncelli, S., Gouretski, V., Chen, G., Mishonov, A., Reagan, J., & Zhu, J. (2021). Upper ocean temperatures hit record high in 2020. *Advances in Atmospheric Sciences*, 38(4), 523-530. <https://doi.org/10.1007/s00376-021-0447-x>.
- Cheng, L., von Schuckmann, K., Abraham, J. P., Trenberth, K. E., Mann, M. E., Zanna, L., England, M. H., Zika, J. D., Fasullo, J. T., Yu, Y., Pan, Y., Zhu, J., Newsom, E. R., Bronselaer, B., & Lin, X. (2022). Past and future ocean warming. *Nature Reviews Earth & Environment*, 3(11), 776-794. <https://doi.org/10.1038/s43017-022-00345-1>.
- Chevin, L. M., & Hoffmann, A. A. (2017). Evolution of phenotypic plasticity in extreme environments. *Philosophical Transactions of the Royal Society of London B Biological Sciences*, 372(1723). <https://doi.org/10.1098/rstb.2016.0138>.
- Chown, S. L., Hoffmann, A. A., Kristensen, T. N., Angilletta, M. J., Stenseth, N. C., & Pertoldi, C. (2010). Adapting to climate change: a perspective from evolutionary physiology. *Climate Research*, 43(1), 3-15. <https://doi.org/10.3354/cr00879>.
- Christensen, A. B., Nguyen, H. D., & Byrne, M. (2011). Thermotolerance and the effects of hypercapnia on the metabolic rate of the ophiuroid *Ophionereis schayeri*: Inferences for survivorship in a changing ocean. *Journal of Experimental Marine Biology and Ecology*, 403(1-2), 31-38. <https://doi.org/10.1016/j.jembe.2011.04.002>.
- Christensen, A. B., Radivojevic, K. O., & Pyne, M. I. (2017). Effects of CO₂, pH and temperature on respiration and regeneration in the burrowing brittle stars *Hemipholis cordifera* and *Microphiopholis gracillima*. *Journal of Experimental Marine Biology and Ecology*, 495, 13-23. <https://doi.org/10.1016/j.jembe.2017.05.012>.
- Christie, W. W. (1998). Gas chromatography-mass spectrometry methods for structural analysis of fatty acids. *Lipids*, 33(4), 343-353. <https://doi.org/10.1007/s11745-998-0214-x>.
- Clark, A. M., & Downey, M. E. (1992). *Starfishes of the Atlantic*. Chapman & Hall.
- Clark, M. S. (2020). Molecular mechanisms of biomineralization in marine invertebrates. *Journal of Experimental Biology*, 223(Pt 11). <https://doi.org/10.1242/jeb.206961>.
- Clark, T. D., Sandblom, E., & Jutfelt, F. (2013). Aerobic scope measurements of fishes in an era of climate change: Respirometry, relevance and recommendations. *Journal of Experimental Biology*, 216(Pt 15), 2771-2782. <https://doi.org/10.1242/jeb.084251>.

- Clements, J. C., & Hunt, H. L. (2015). Marine animal behaviour in a high CO₂ ocean. *Marine Ecology Progress Series*, 536, 259-279. <https://doi.org/10.3354/meps11426>.
- Cohen-Rengifo, M., Aguera, A., Bouma, T., M'Zoudi, S., Flammang, P., & Dubois, P. (2019). Ocean warming and acidification alter the behavioral response to flow of the sea urchin *Paracentrotus lividus*. *Ecology and Evolution*, 9(21), 12128-12143. <https://doi.org/10.1002/ece3.5678>.
- Cohen, A. L., & Holcomb, M. (2009). Why corals care about ocean acidification: uncovering the mechanism. *Oceanography*, 22(4), 118-127. <https://doi.org/https://www.jstor.org/stable/24861029>.
- Cole, V. J., Parker, L. M., O'Connor, S. J., O'Connor, W. A., Scanes, E., Byrne, M., & Ross, P. M. (2016). Effects of multiple climate change stressors: ocean acidification interacts with warming, hyposalinity, and low food supply on the larvae of the brooding flat oyster *Ostrea angasi*. *Marine Biology*, 163(5). <https://doi.org/10.1007/s00227-016-2880-4>.
- Collard, M., Catarino, A. I., Bonnet, S., Flammang, P., & Dubois, P. (2013). Effects of CO₂-induced ocean acidification on physiological and mechanical properties of the starfish *Asterias rubens*. *Journal of Experimental Marine Biology and Ecology*, 446, 355-362. <https://doi.org/10.1016/j.jembe.2013.06.003>.
- Cornwall, C. E., Revill, A. T., Hall-Spencer, J. M., Milazzo, M., Raven, J. A., & Hurd, C. L. (2017). Inorganic carbon physiology underpins macroalgal responses to elevated CO₂. *Scientific Reports*, 7, 46297. <https://doi.org/10.1038/srep46297>.
- Côté, I. M., & Darling, E. S. (2010). Rethinking ecosystem resilience in the face of climate change. *PLoS Biology*, 8(7). <https://doi.org/10.1371/journal.pbio.1000438>.
- Courtney, T., Westfield, I., & Ries, J. B. (2013). CO₂-induced ocean acidification impairs calcification in the tropical urchin *Echinometra viridis*. *Journal of Experimental Marine Biology and Ecology*, 440, 169-175. <https://doi.org/10.1016/j.jembe.2012.11.013>.
- Cyronak, T., Schulz, K. G., & Jokieli, P. L. (2016). The Omega myth: what really drives lower calcification rates in an acidifying ocean. *ICES Journal of Marine Science*, 73(3), 558-562. <https://doi.org/10.1093/icesjms/fsv075>.
- da Costa Filho, B. M., Duarte, A. C., & Rocha-Santos, T. A. P. (2022). Environmental monitoring approaches for the detection of organic contaminants in marine environments: A critical review. *Trends in Environmental Analytical Chemistry*, 33. <https://doi.org/10.1016/j.teac.2022.e00154>.
- Dahlke, F. T., Wohlrab, S., Butzin, M., & Portner, H. O. (2020). Thermal bottlenecks in the life cycle define climate vulnerability of fish. *Science*, 369(6499), 65-70. <https://doi.org/10.1126/science.aaz3658>.

- Dalgaard, J., St. John, M., Kattner, G., Müller-Navarra, D., & Hagen, W. (2003). Fatty acid trophic markers in the pelagic marine environment. In A. J. Southward, P. A. Tyler, C. M. Young, & L. A. Fuiman (Eds.), *Advances in Marine Biology* (Vol. 46, pp. 225-340). Academic Press. [https://doi.org/10.1016/S0065-2881\(03\)46005-7](https://doi.org/10.1016/S0065-2881(03)46005-7).
- Davies, M. S., & Hatcher, A. M. (1998). The energy budget: A useful tool? *Annales Zoologici Fennici*, 35(4), 231-240.
- Davis, K. J., Dove, P. M., & De Yoreo, J. J. (2000). The role of Mg^{2+} as an impurity in calcite growth. *Science*, 290(5494), 1134-1137. <https://doi.org/10.1126/science.290.5494.1134>.
- Dawson, T. P., Jackson, S. T., House, J. I., Prentice, I. C., & Mace, G. M. (2011). Beyond predictions: biodiversity conservation in a changing climate. *Science*, 332(6025), 53-58. <https://doi.org/10.1126/science.1200303>.
- de Goeyse, S., Webb, A. E., Reichart, G.-J., & de Nooijer, L. J. (2021). Carbonic anhydrase is involved in calcification by the benthic foraminifer *Amphistegina lessonii*. *Biogeosciences*, 18(2), 393-401. <https://doi.org/10.5194/bg-18-393-2021>.
- de Mendiburu, F. (2021). *Agricolae*: statistical procedures for agricultural research. <https://cran.r-project.org/web/packages/agricolae/index.html>.
- de Souza, C. O., Vannice, G. K., Rosa Neto, J. C., & Calder, P. C. (2018). Is palmitoleic acid a plausible nonpharmacological strategy to prevent or control chronic metabolic and inflammatory disorders? *Molecular Nutrition & Food Research*, 62(1), 1700504. <https://doi.org/10.1002/mnfr.201700504>.
- Dermawan, D., Wang, Y. F., You, S. J., Jiang, J. J., & Hsieh, Y. K. (2022). Impact of climatic and non-climatic stressors on ocean life and human health: A review. *Science of the Total Environment*, 821, 153387. <https://doi.org/10.1016/j.scitotenv.2022.153387>.
- Deutsch, C., Penn, J. L., & Lucey, N. (2023). Climate, oxygen, and the future of marine biodiversity. *Annual Review of Marine Science*. <https://doi.org/10.1146/annurev-marine-040323-095231>.
- Di Lorenzo, F., Rodríguez-Galán, R. M., & Prieto, M. (2018). Kinetics of the solvent-mediated transformation of hydromagnesite into magnesite at different temperatures. *Mineralogical Magazine*, 78(6), 1363-1372. <https://doi.org/10.1180/minmag.2014.078.6.02>.
- Dickson, A. G. (1990). Standard potential of the reaction: $AgCl(s) + 12H_2(g) = Ag(s) + HCl(aq)$, and the standard acidity constant of the ion HSO_4^- in synthetic sea water from 273.15 to 318.15 K. *The Journal of Chemical Thermodynamics*, 22(2), 113-127. [https://doi.org/10.1016/0021-9614\(90\)90074-z](https://doi.org/10.1016/0021-9614(90)90074-z).

- Dickson, A. G., & Millero, F. J. (1987). A comparison of the equilibrium constants for the dissociation of carbonic acid in seawater media. *Deep Sea Research Part A. Oceanographic Research Papers*, 34(10), 1733-1743. [https://doi.org/10.1016/0198-0149\(87\)90021-5](https://doi.org/10.1016/0198-0149(87)90021-5).
- Dickson, A. G., & Riley, J. P. (1979). The estimation of acid dissociation constants in seawater media from potentiometric titrations with strong base. I. The ionic product of water - K_w . *Marine Chemistry*, 7(2), 89-99. [https://doi.org/10.1016/0304-4203\(79\)90001-x](https://doi.org/10.1016/0304-4203(79)90001-x).
- Dickson, A. G., Sabine, C. L., & Christian, J. R. (Eds.). (2007). *Guide to best practices for ocean CO₂ measurements. PICES special publication 3* (Vol. 3). North Pacific Marine Science Organization.
- Dickson, J. A. (2002). Fossil echinoderms as monitor of the Mg/Ca ratio of Phanerozoic oceans. *Science*, 298(5596), 1222-1224. <https://doi.org/10.1126/science.1075882>.
- Dissanayake, A., & Ishimatsu, A. (2011). Synergistic effects of elevated CO₂ and temperature on the metabolic scope and activity in a shallow-water coastal decapod (*Metapenaeus joyneri*; Crustacea: Penaeidae). *ICES Journal of Marine Science*, 68(6), 1147-1154. <https://doi.org/10.1093/icesjms/fsq188>.
- Dissard, D., Nehrke, G., Reichart, G. J., & Bijma, J. (2010). The impact of salinity on the Mg/Ca and Sr/Ca ratio in the benthic foraminifera *Ammonia tepida*: Results from culture experiments. *Geochimica et Cosmochimica Acta*, 74(3), 928-940. <https://doi.org/10.1016/j.gca.2009.10.040>.
- Dodd, J. R. (1967). Magnesium and strontium in calcareous skeletons: A review. *Journal of Paleontology*, 41(6), 1313-1329. <http://www.jstor.org/stable/1302184>.
- Donachy, J. E., Watabet, N., & Showman, R. M. (1989). Na⁺, K⁺-ATPase, Mg²⁺-ATPase and Ca²⁺-ATPase activity during arm regeneration in the starfish *Asterias forbesi*. *Comp. Biochem. Physiol. Part A Mol. Integr. Physiol.*, 94(1), 57-60. [https://doi.org/10.1016/0300-9629\(89\)90784-6](https://doi.org/10.1016/0300-9629(89)90784-6).
- Donelson, J. M., Salinas, S., Munday, P. L., & Shama, L. N. S. (2018). Transgenerational plasticity and climate change experiments: Where do we go from here? *Global Change Biology*, 24(1), 13-34. <https://doi.org/10.1111/gcb.13903>.
- Donelson, J. M., Sunday, J. M., Figueira, W. F., Gaitan-Espitia, J. D., Hobday, A. J., Johnson, C. R., Leis, J. M., Ling, S. D., Marshall, D., Pandolfi, J. M., Pecl, G., Rodgers, G. G., Booth, D. J., & Munday, P. L. (2019). Understanding interactions between plasticity, adaptation and range shifts in response to marine environmental change. *Philosophical Transactions of the Royal Society of London B Biological Sciences*, 374(1768), 20180186. <https://doi.org/10.1098/rstb.2018.0186>.

- Doney, S., Bopp, L., & Long, M. (2014). Historical and future trends in ocean climate and biogeochemistry. *Oceanography*, 27(1), 108-119. <https://doi.org/10.5670/oceanog.2014.14>.
- Doney, S. C., Fabry, V. J., Feely, R. A., & Kleypas, J. A. (2009). Ocean acidification: The other CO₂ problem. *Annual Review of Marine Science*, 1, 169-192. <https://doi.org/10.1146/annurev.marine.010908.163834>.
- Doney, S. C., Ruckelshaus, M., Duffy, J. E., Barry, J. P., Chan, F., English, C. A., Galindo, H. M., Grebmeier, J. M., Hollowed, A. B., Knowlton, N., Polovina, J., Rabalais, N. N., Sydeman, W. J., & Talley, L. D. (2012). Climate change impacts on marine ecosystems. *Annual Review of Marine Science*, 4, 11-37. <https://doi.org/10.1146/annurev-marine-041911-111611>.
- Dong, Y. W., Yu, S. S., Wang, Q. L., & Dong, S. L. (2011). Physiological responses in a variable environment: relationships between metabolism, hsp and thermotolerance in an intertidal-subtidal species. *PLoS One*, 6(10), e26446. <https://doi.org/10.1371/journal.pone.0026446>.
- Doo, S. S., Kealoha, A., Andersson, A., Cohen, A. L., Hicks, T. L., Johnson, Z. I., Long, M. H., McElhany, P., Mollica, N., Shamberger, K. E. F., Silbiger, N. J., Takeshita, Y., Busch, D. S., & Browman, H. (2020). The challenges of detecting and attributing ocean acidification impacts on marine ecosystems. *ICES Journal of Marine Science*, 77(7-8), 2411-2422. <https://doi.org/10.1093/icesjms/fsaa094>.
- du Pontavice, H., Gascuel, D., Reygondeau, G., Maureaud, A., & Cheung, W. W. L. (2020). Climate change undermines the global functioning of marine food webs. *Global Change Biology*, 26(3), 1306-1318. <https://doi.org/10.1111/gcb.14944>.
- Dubois, P. (2014). The skeleton of postmetamorphic echinoderms in a changing world. *The Biological Bulletin*, 226(3), 223-236. <https://doi.org/10.1086/BBLv226n3p223>.
- Dubois, P., & Chen, C. P. (1989). Calcification in echinoderms. In M. Jangoux & J. M. Lawrence (Eds.), *Echinoderm Studies* (Vol. 3, pp. 109-178). A. A. Balkema.
- Dupont, S., Ortega-Martinez, O., & Thorndyke, M. (2010). Impact of near-future ocean acidification on echinoderms. *Ecotoxicology*, 19(3), 449-462. <https://doi.org/10.1007/s10646-010-0463-6>.
- Dupont, S., & Pörtner, H.-O. (2013). A snapshot of ocean acidification research. *Marine Biology*, 160(8), 1765-1771. <https://doi.org/10.1007/s00227-013-2282-9>.
- Dupont, S., & Thorndyke, M. (2012). Relationship between CO₂-driven changes in extracellular acid–base balance and cellular immune response in two polar echinoderm species. *Journal of Experimental Marine Biology and Ecology*, 424-425, 32-37. <https://doi.org/10.1016/j.jembe.2012.05.007>.

- Duquette, A., McClintock, J. B., Amsler, C. D., Perez-Huerta, A., Milazzo, M., & Hall-Spencer, J. M. (2017). Effects of ocean acidification on the shells of four Mediterranean gastropod species near a CO₂ seep. *Marine Pollution Bulletin*, 124(2), 917-928. <https://doi.org/10.1016/j.marpolbul.2017.08.007>.
- Duquette, A., Vohra, Y. K., McClintock, J. B., & Angus, R. A. (2018). Near-future temperature reduces Mg/Ca ratios in the major skeletal components of the common subtropical sea urchin *Lytechinus variegatus*. *Journal of Experimental Marine Biology and Ecology*, 509, 1-7. <https://doi.org/10.1016/j.jembe.2018.08.007>.
- Durack, P., Gleckler, P., Purkey, S., Johnson, G., Lyman, J., & Boywe, T. (2018). Ocean warming: From the surface to the deep in observations and models. *Oceanography*, 31(2), 41-51. <https://doi.org/10.5670/oceanog.2018.227>.
- Dworjanyn, S. A., & Byrne, M. (2018). Impacts of ocean acidification on sea urchin growth across the juvenile to mature adult life-stage transition is mitigated by warming. *Proceedings of the Royal Society B: Biological Sciences*, 285(1876). <https://doi.org/10.1098/rspb.2017.2684>.
- Earhart, M. L., Blanchard, T. S., Harman, A. A., & Schulte, P. M. (2022). Hypoxia and high temperature as interacting stressors: Will plasticity promote resilience of fishes in a changing world?. *The Biological Bulletin*, 243(2), 149-170. <https://doi.org/10.1086/722115>.
- Ebert, T. A. (2021). Life-history analysis of asterinid starfishes. *The Biological Bulletin*, 241(3), 231-242. <https://doi.org/10.1086/716913>.
- Ehrlich, H., Elkin, Y. N., Artoukov, A. A., Stonik, V. A., Safronov, P. P., Bazhenov, V. V., Kurek, D. V., Varlamov, V. P., Born, R., Meissner, H., & Richter, G. (2011). Simple method for preparation of nanostructurally organized spines of sand dollar *Scaphechinus mirabilis* (Agassiz, 1863). *Marine Biotechnology*, 13(3), 402-410. <https://doi.org/10.1007/s10126-010-9310-2>.
- Erez, J., Reynaud, S., Silverman, J., Schneider, K., & Allemand, D. (2011). Coral Calcification Under Ocean Acidification and Global Change. In Z. Dubinsky & N. Stambler (Eds.), *Coral Reefs: An Ecosystem in Transition* (pp. 151-176). Springer. https://doi.org/10.1007/978-94-007-0114-4_10.
- Ericson, J. A., Hellesey, N., Kawaguchi, S., Nicol, S., Nichols, P. D., Hoem, N., & Virtue, P. (2018). Adult Antarctic krill proves resilient in a simulated high CO₂ ocean. *Communications Biology*, 1, 190. <https://doi.org/10.1038/s42003-018-0195-3>.

- Ernst, R., Ejsing, C. S., & Antonny, B. (2016). Homeoviscous adaptation and the regulation of membrane lipids. *Journal of Molecular Biology*, 428(24 Pt A), 4776-4791. <https://doi.org/10.1016/j.jmb.2016.08.013>.
- Etminan, M., Myhre, G., Highwood, E. J., & Shine, K. P. (2016). Radiative forcing of carbon dioxide, methane, and nitrous oxide: A significant revision of the methane radiative forcing. *Geophysical Research Letters*, 43(24). <https://doi.org/10.1002/2016gl071930>.
- Evans, T. G., & Hofmann, G. E. (2012). Defining the limits of physiological plasticity: how gene expression can assess and predict the consequences of ocean change. *Philosophical Transactions of the Royal Society of London B Biological Sciences*, 367(1596), 1733-1745. <https://doi.org/10.1098/rstb.2012.0019>.
- Fabricius, K. E., Langdon, C., Uthicke, S., Humphrey, C., Noonan, S., De'ath, G., Okazaki, R., Muehllehner, N., Glas, M. S., & Lough, J. M. (2011). Losers and winners in coral reefs acclimatized to elevated carbon dioxide concentrations. *Nature Climate Change*, 1(3), 165-169. <https://doi.org/10.1038/nclimate1122>.
- Fabry, V. J., Seibel, B. A., Feely, R. A., & Orr, J. C. (2008). Impacts of ocean acidification on marine fauna and ecosystem processes. *ICES Journal of Marine Science*, 65(3), 414-432. <https://doi.org/10.1093/icesjms/fsn048>.
- Faleiro, F., Baptista, M., Santos, C., Aurelio, M. L., Pimentel, M., Pegado, M. R., Paula, J. R., Calado, R., Repolho, T., & Rosa, R. (2015). Seahorses under a changing ocean: the impact of warming and acidification on the behaviour and physiology of a poor-swimming bony-armoured fish. *Conservation Physiology*, 3(1), cov009. <https://doi.org/10.1093/conphys/cov009>.
- Fawzy, S., Osman, A. I., Doran, J., & Rooney, D. W. (2020). Strategies for mitigation of climate change: A review. *Environmental Chemistry Letters*, 18(6), 2069-2094. <https://doi.org/10.1007/s10311-020-01059-w>.
- Feely, R., Doney, S., & Cooley, S. (2009). Ocean acidification: Present conditions and future changes in a high-CO₂ world. *Oceanography*, 22(4), 36-47. <http://www.jstor.org/stable/24861022>.
- Feely, R. A., Sabine, C. L., Lee, K., Berelson, W., Kleypas, J., Fabry, V. J., & Millero, F. J. (2004). Impact of anthropogenic CO₂ on the CaCO₃ system in the oceans. *Science*, 305(5682), 362-366. <https://doi.org/10.1126/science.1097329>.
- Feng, Q. (2011). Principles of calcium-based biomineralization. In W. E. G. Müller (Ed.), *Molecular biomineralization: Aquatic organisms forming extraordinary materials* (pp. 141-197). Springer. https://doi.org/10.1007/978-3-642-21230-7_6.
- Figuerola, B., Hancock, A. M., Bax, N., Cummings, V. J., Downey, R., Griffiths, H. J., Smith, J., & Stark, J. S. (2021). A review and meta-analysis of potential impacts of ocean acidification on

- marine calcifiers from the Southern Ocean. *Frontiers in Marine Science*, 8. <https://doi.org/10.3389/fmars.2021.584445>.
- Filimonova, V., Gonçalves, F., Marques, J. C., De Troch, M., & Gonçalves, A. M. M. (2016). Fatty acid profiling as bioindicator of chemical stress in marine organisms: A review. *Ecological Indicators*, 67, 657-672. <https://doi.org/10.1016/j.ecolind.2016.03.044>.
- Findlay, H. S., Wood, H. L., Kendall, M. A., Spicer, J. I., Twitchett, R. J., & Widdicombe, S. (2009). Calcification, a physiological process to be considered in the context of the whole organism. *Biogeosciences Discussions*, 6(1), 2267-2284. <https://doi.org/10.5194/bgd-6-2267-2009>.
- Fiske, C. H., & Subbarow, Y. (1925). The Colorimetric Determination of Phosphorus. *Journal of Biological Chemistry*, 66(2), 375-400. [https://doi.org/10.1016/s0021-9258\(18\)84756-1](https://doi.org/10.1016/s0021-9258(18)84756-1).
- Fitzer, S. C., Vittert, L., Bowman, A., Kamenos, N. A., Phoenix, V. R., & Cusack, M. (2015). Ocean acidification and temperature increase impact mussel shell shape and thickness: problematic for protection?. *Ecology and Evolution*, 5(21), 4875-4884. <https://doi.org/10.1002/ece3.1756>.
- Folt, C. L., Chen, C. Y., Moore, M. V., & Burnaford, J. (1999). Synergism and antagonism among multiple stressors. *Limnology and Oceanography*, 44(3part2), 864-877. https://doi.org/10.4319/lo.1999.44.3_part_2.0864.
- Fonseca, J. G., Laranjeiro, F., Freitas, D. B., Oliveira, I. B., Rocha, R. J. M., Machado, J., Hinzmann, M., Barroso, C. M., & Galante-Oliveira, S. (2020). Impairment of swimming performance in *Tritia reticulata* (L.) veligers under projected ocean acidification and warming scenarios. *Science of the Total Environment*, 731, 139187. <https://doi.org/10.1016/j.scitotenv.2020.139187>.
- Foo, S. A., & Byrne, M. (2016). Acclimatization and adaptive capacity of marine species in a changing ocean. *Advances in Marine Biology*, 74, 69-116. <https://doi.org/10.1016/bs.amb.2016.06.001>.
- Fox, J., & Weisberg, S. (2019). *An R companion to applied regression* (3rd ed.). Sage.
- Frederich, M., & Portner, H. O. (2000). Oxygen limitation of thermal tolerance defined by cardiac and ventilatory performance in spider crab, *Maja squinado*. *American Journal of Physiology Regulatory Integrative and Comparative Physiology*, 279(5), R1531-1538. <https://doi.org/10.1152/ajpregu.2000.279.5.R1531>.
- Friedlingstein, P., O'Sullivan, M., Jones, M. W., Andrew, R. M., Bakker, D. C. E., Hauck, J., Landschützer, P., Le Quéré, C., Lujikx, I. T., Peters, G. P., Peters, W., Pongratz, J., Schwingshackl, C., Sitch, S., Canadell, J. G., Ciais, P., Jackson, R. B., Alin, S. R., Anthoni, P.,

- . . . Zheng, B. (2023). Global carbon budget 2023. *Earth System Science Data*, 15(12), 5301-5369. <https://doi.org/10.5194/essd-15-5301-2023>.
- Frolicher, T. L., Fischer, E. M., & Gruber, N. (2018). Marine heatwaves under global warming. *Nature*, 560(7718), 360-364. <https://doi.org/10.1038/s41586-018-0383-9>.
- Fuller, A., Dawson, T., Helmuth, B., Hetem, R. S., Mitchell, D., & Maloney, S. K. (2010). Physiological mechanisms in coping with climate change. *Physiological and Biochemical Zoology*, 83(5), 713-720. <https://doi.org/10.1086/652242>.
- Galloway, A. W., Brett, M. T., Holtgrieve, G. W., Ward, E. J., Ballantyne, A. P., Burns, C. W., Kainz, M. J., Muller-Navarra, D. C., Persson, J., Ravet, J. L., Strandberg, U., Taipale, S. J., & Alhgren, G. (2015). A fatty acid based bayesian approach for inferring diet in aquatic consumers. *PLoS One*, 10(6), e0129723. <https://doi.org/10.1371/journal.pone.0129723>.
- Galloway, T. S., Brown, R. J., Browne, M. A., Dissanayake, A., Lowe, D., Jones, M. B., & Depledge, M. H. (2004). A multibiomarker approach to environmental assessment. *Environmental Science & Technology*, 38(6), 1723-1731. <https://doi.org/10.1021/es030570+>.
- Gao, K., Gao, G., Wang, Y., & Dupont, S. (2020). Impacts of ocean acidification under multiple stressors on typical organisms and ecological processes. *Marine Life Science & Technology*, 2(3), 279-291. <https://doi.org/10.1007/s42995-020-00048-w>.
- Gao, Y., Zheng, S. C., Zheng, C. Q., Shi, Y. C., Xie, X. L., Wang, K. J., & Liu, H. P. (2018). The immune-related fatty acids are responsive to CO₂ driven seawater acidification in a crustacean brine shrimp *Artemia sinica*. *Developmental & Comparative Immunology*, 81, 342-347. <https://doi.org/10.1016/j.dci.2017.12.022>.
- Garcês, A., & Pires, I. (2023). The guardians of the sea: Echinoderms as sentinels of marine pollution. *Toxicology International*, 541-552. <https://doi.org/10.18311/ti/2022/v29i4/30487>.
- Garcia, E., Clemente, S., & Hernandez, J. C. (2015). Ocean warming ameliorates the negative effects of ocean acidification on *Paracentrotus lividus* larval development and settlement. *Marine Environmental Research*, 110, 61-68. <https://doi.org/10.1016/j.marenvres.2015.07.010>.
- Gardner, J. L., Peters, A., Kearney, M. R., Joseph, L., & Heinsohn, R. (2011). Declining body size: a third universal response to warming? *Trends in Ecology & Evolution*, 26(6), 285-291. <https://doi.org/10.1016/j.tree.2011.03.005>.
- Garrabou, J., Gomez-Gras, D., Medrano, A., Cerrano, C., Ponti, M., Schlegel, R., Bensoussan, N., Turicchia, E., Sini, M., Gerovasileiou, V., Teixido, N., Mirasole, A., Tamburello, L., Cebrian, E., Rilov, G., Ledoux, J. B., Souissi, J. B., Khamassi, F., Ghanem, R., . . . Harmelin, J. G. (2022). Marine heatwaves drive recurrent mass mortalities in the Mediterranean Sea. *Global Change Biology*, 28(19), 5708-5725. <https://doi.org/10.1111/gcb.16301>.

- Garzke, J., Hansen, T., Ismar, S. M., & Sommer, U. (2016). Combined effects of ocean warming and acidification on copepod abundance, body size and fatty acid content. *PLoS One*, *11*(5), e0155952. <https://doi.org/10.1371/journal.pone.0155952>.
- Garzke, J., Sommer, U., & Ismar-Rebitz, S. M. H. (2020). Zooplankton growth and survival differentially respond to interactive warming and acidification effects. *Journal of Plankton Research*, *42*(2), 189-202. <https://doi.org/10.1093/plankt/fbaa005>.
- Gattuso, J. P., Magnan, A., Bille, R., Cheung, W. W., Howes, E. L., Joos, F., Allemand, D., Bopp, L., Cooley, S. R., Eakin, C. M., Hoegh-Guldberg, O., Kelly, R. P., Portner, H. O., Rogers, A. D., Baxter, J. M., Laffoley, D., Osborn, D., Rankovic, A., Rochette, J., . . . Turley, C. (2015). Contrasting futures for ocean and society from different anthropogenic CO₂ emissions scenarios. *Science*, *349*(6243), aac4722. <https://doi.org/10.1126/science.aac4722>.
- Gaymer, C. F., & Himmelman, J. H. (2008). A keystone predatory sea star in the intertidal zone is controlled by a higher-order predatory sea star in the subtidal zone. *Marine Ecology Progress Series*, *370*, 143-153. <https://doi.org/10.3354/meps07663>.
- Gazeau, F., Parker, L. M., Comeau, S., Gattuso, J.-P., O'Connor, W. A., Martin, S., Pörtner, H.-O., & Ross, P. M. (2013). Impacts of ocean acidification on marine shelled molluscs. *Marine Biology*, *160*(8), 2207-2245. <https://doi.org/10.1007/s00227-013-2219-3>.
- Gazeau, F., Quiblier, C., Jansen, J. M., Gattuso, J.-P., Middelburg, J. J., & Heip, C. H. R. (2007). Impact of elevated CO₂ on shellfish calcification. *Geophysical Research Letters*, *34*(7). <https://doi.org/10.1029/2006gl028554>.
- Gazeau, F., Urbini, L., Cox, T. E., Alliouane, S., & Gattuso, J. P. (2015). Comparison of the alkalinity and calcium anomaly techniques to estimate rates of net calcification. *Marine Ecology Progress Series*, *527*, 1-12. <https://doi.org/10.3354/meps11287>.
- Gerhardt, A. (2009). Bioindicator species and their use in biomonitoring. In H. I. Inyang & J. L. Daniels (Eds.), *Environmental monitoring* (Vol. 1, pp. 77-123). EOLSS Publishers.
- Gestoso, I., Arenas, F., & Olabarria, C. (2016). Ecological interactions modulate responses of two intertidal mussel species to changes in temperature and pH. *Journal of Experimental Marine Biology and Ecology*, *474*, 116-125. <https://doi.org/10.1016/j.jembe.2015.10.006>.
- Ghalambor, C. K., McKay, J. K., Carroll, S. P., & Reznick, D. N. (2007). Adaptive versus non-adaptive phenotypic plasticity and the potential for contemporary adaptation in new environments. *Functional Ecology*, *21*(3), 394-407. <https://doi.org/10.1111/j.1365-2435.2007.01283.x>.
- Gibbin, E. M., Massamba N'Siala, G., Chakravarti, L. J., Jarrold, M. D., & Calosi, P. (2017). The evolution of phenotypic plasticity under global change. *Scientific Reports*, *7*(1), 17253. <https://doi.org/10.1038/s41598-017-17554-0>.

- Gilbert, P. U. P. A., & Wilt, F. H. (2011). Molecular aspects of biomineralization of the echinoderm endoskeleton. In W. E. G. Müller (Ed.), *Molecular biomineralization: Aquatic organisms forming extraordinary materials* (pp. 199-223). Springer. https://doi.org/10.1007/978-3-642-21230-7_7.
- Gissi, E., Manea, E., Mazaris, A. D., Frascchetti, S., Almpandou, V., Bevilacqua, S., Coll, M., Guarnieri, G., Lloret-Lloret, E., Pascual, M., Petza, D., Rilov, G., Schonwald, M., Stelzenmuller, V., & Katsanevakis, S. (2021). A review of the combined effects of climate change and other local human stressors on the marine environment. *Science of the Total Environment*, 755(Pt 1), 142564. <https://doi.org/10.1016/j.scitotenv.2020.142564>.
- Gooding, R. A., Harley, C. D., & Tang, E. (2009). Elevated water temperature and carbon dioxide concentration increase the growth of a keystone echinoderm. *Proceedings of the National Academy of Sciences of the United States of America*, 106(23), 9316-9321. <https://doi.org/10.1073/pnas.0811143106>.
- Gorzalak, P. (2021). Functional micromorphology of the echinoderm skeleton. In C. D. Sumrall (Ed.), *Elements of paleontology* (pp. 44). Cambridge University Press. <https://doi.org/10.1017/9781108893886>.
- Gruber, N. (2011). Warming up, turning sour, losing breath: ocean biogeochemistry under global change. *Philosophical Transactions of the Royal Society of London Series A Mathematical Physical and Engineering Sciences*, 369(1943), 1980-1996. <https://doi.org/10.1098/rsta.2011.0003>.
- Gruber, N., Bakker, D. C. E., DeVries, T., Gregor, L., Hauck, J., Landschützer, P., McKinley, G. A., & Müller, J. D. (2023). Trends and variability in the ocean carbon sink. *Nature Reviews Earth & Environment*, 4(2), 119-134. <https://doi.org/10.1038/s43017-022-00381-x>.
- Guillermic, M., Cameron, L. P., De Corte, I., Misra, S., Bijma, J., de Beer, D., Reymond, C. E., Westphal, H., Ries, J. B., & Eagle, R. A. (2021). Thermal stress reduces pocilloporid coral resilience to ocean acidification by impairing control over calcifying fluid chemistry. *Science Advances*, 7(2). <https://doi.org/10.1126/sciadv.aba9958>.
- Guinotte, J. M., & Fabry, V. J. (2008). Ocean acidification and its potential effects on marine ecosystems. *Annals of the New York Academy of Sciences*, 1134, 320-342. <https://doi.org/10.1196/annals.1439.013>.
- Gunderson, A. R., Armstrong, E. J., & Stillman, J. H. (2016). Multiple stressors in a changing world: The need for an improved perspective on physiological responses to the dynamic marine environment. *Annual Review of Marine Science*, 8, 357-378. <https://doi.org/10.1146/annurev-marine-122414-033953>.

- Guppy, M., & Withers, P. (2007). Metabolic depression in animals: physiological perspectives and biochemical generalizations. *Biological Reviews*, 74(1), 1-40. <https://doi.org/10.1111/j.1469-185X.1999.tb00180.x>.
- Gurr, M. I., Harwood, J. L., & Frayn, K. N. (2002). *Lipid biochemistry* (5th ed.). Blackwell Science. <https://doi.org/10.1002/9780470774366>.
- Gutowky, L. F. G., Brownscombe, J. W., Wilson, A. D. M., Szekeres, P., & Cooke, S. J. (2016). Improved performance, within-individual consistency and between-individual differences in the righting behaviour of the Caribbean sea star, *Oreaster reticulatus*. *Behaviour*, 153(13-14), 1763-1776. <https://doi.org/10.1163/1568539x-00003401>.
- Haldar, S. K. (2020). *Introduction to mineralogy and petrology*. Elsevier. <https://doi.org/https://doi.org/10.1016/C2019-0-00625-5>.
- Hale, R., Calosi, P., McNeill, L., Mieszkowska, N., & Widdicombe, S. (2011). Predicted levels of future ocean acidification and temperature rise could alter community structure and biodiversity in marine benthic communities. *Oikos*, 120(5), 661-674. <https://doi.org/10.1111/j.1600-0706.2010.19469.x>.
- Hall-Spencer, J. M., & Harvey, B. P. (2019). Ocean acidification impacts on coastal ecosystem services due to habitat degradation. *Emerging Topics in Life Sciences*, 3(2), 197-206. <https://doi.org/10.1042/ETLS20180117>.
- Halpern, B. S., Frazier, M., Potapenko, J., Casey, K. S., Koenig, K., Longo, C., Lowndes, J. S., Rockwood, R. C., Selig, E. R., Selkoe, K. A., & Walbridge, S. (2015). Spatial and temporal changes in cumulative human impacts on the world's ocean. *Nature Communications*, 6, 7615. <https://doi.org/10.1038/ncomms8615>.
- Halpern, B. S., Walbridge, S., Selkoe, K. A., Kappel, C. V., Micheli, F., D'Agrosa, C., Bruno, J. F., Casey, K. S., Ebert, C., Fox, H. E., Fujita, R., Heinemann, D., Lenihan, H. S., Madin, E. M., Perry, M. T., Selig, E. R., Spalding, M., Steneck, R., & Watson, R. (2008). A global map of human impact on marine ecosystems. *Science*, 319(5865), 948-952. <https://doi.org/10.1126/science.1149345>.
- Hansson, I. (1973). A new set of acidity constants for carbonic acid and boric acid in sea water. *Deep Sea Research and Oceanographic Abstracts*, 20(5), 461-478. [https://doi.org/10.1016/0011-7471\(73\)90100-9](https://doi.org/10.1016/0011-7471(73)90100-9).
- Harley, C. D., Randall Hughes, A., Hultgren, K. M., Miner, B. G., Sorte, C. J., Thornber, C. S., Rodriguez, L. F., Tomanek, L., & Williams, S. L. (2006). The impacts of climate change in coastal marine systems. *Ecology Letters*, 9(2), 228-241. <https://doi.org/10.1111/j.1461-0248.2005.00871.x>.

- Harvey, B., Al-Janabi, B., Broszeit, S., Cioffi, R., Kumar, A., Aranguren-Gassis, M., Bailey, A., Green, L., Gsottbauer, C., Hall, E., Lechler, M., Mancuso, F., Pereira, C., Ricevuto, E., Schram, J., Stapp, L., Stenberg, S., & Rosa, L. (2014). Evolution of marine organisms under climate change at different levels of biological organisation. *Water*, 6(11), 3545-3574. <https://doi.org/10.3390/w6113545>.
- Harvey, B. P., Gwynn-Jones, D., & Moore, P. J. (2013). Meta-analysis reveals complex marine biological responses to the interactive effects of ocean acidification and warming. *Ecology and Evolution*, 3(4), 1016-1030. <https://doi.org/10.1002/ece3.516>.
- Hazan, Y., Wangensteen, O. S., & Fine, M. (2014). Tough as a rock-boring urchin: Adult *Echinometra* sp. EE from the Red Sea show high resistance to ocean acidification over long-term exposures. *Marine Biology*, 161(11), 2531-2545. <https://doi.org/10.1007/s00227-014-2525-4>.
- Hazel, J. R. (1995). Thermal adaptation in biological membranes: Is homeoviscous adaptation the explanation?. *Annual Review of Physiology*, 57, 19-42. <https://doi.org/10.1146/annurev.ph.57.030195.000315>.
- Hazel, J. R., & Williams, E. E. (1990). The role of alterations in membrane lipid composition in enabling physiological adaptation of organisms to their physical environment. *Progress in Lipid Research*, 29(3), 167-227. [https://doi.org/10.1016/0163-7827\(90\)90002-3](https://doi.org/10.1016/0163-7827(90)90002-3).
- Hegerl, G. C., Bronnimann, S., Schurer, A., & Cowan, T. (2018). The early 20th century warming: Anomalies, causes, and consequences. *WIREs Climate Change*, 9(4), e522. <https://doi.org/10.1002/wcc.522>.
- Hellberg, M. E., Balch, D. P., & Roy, K. (2001). Climate-driven range expansion and morphological evolution in a marine gastropod. *Science*, 292(5522), 1707-1710. <https://doi.org/10.1126/science.1060102>.
- Helmuth, B., Kingsolver, J. G., & Carrington, E. (2005). Biophysics, physiological ecology, and climate change: does mechanism matter? *Annual Review of Physiology*, 67, 177-201. <https://doi.org/10.1146/annurev.physiol.67.040403.105027>.
- Helmuth, B. S., & Hofmann, G. E. (2001). Microhabitats, thermal heterogeneity, and patterns of physiological stress in the rocky intertidal zone. *The Biological Bulletin*, 201(3), 374-384. <https://doi.org/10.2307/1543615>.
- Hendriks, I. E., Duarte, C. M., & Álvarez, M. (2010). Vulnerability of marine biodiversity to ocean acidification: A meta-analysis. *Estuarine, Coastal and Shelf Science*, 86(2), 157-164. <https://doi.org/10.1016/j.ecss.2009.11.022>.
- Hermans, J., André, L., Navez, J., Pernet, P., & Dubois, P. (2011). Relative influences of solution composition and presence of intracrystalline proteins on magnesium incorporation in

- calcium carbonate minerals: Insight into vital effects. *Journal of Geophysical Research*, 116(G1). <https://doi.org/10.1029/2010jg001487>.
- Hermans, J., Borremans, C., Willenz, P., André, L., & Dubois, P. (2010). Temperature, salinity and growth rate dependences of Mg/Ca and Sr/Ca ratios of the skeleton of the sea urchin *Paracentrotus lividus* (Lamarck): an experimental approach. *Marine Biology*, 157(6), 1293-1300. <https://doi.org/10.1007/s00227-010-1409-5>.
- Heuer, R. M., Hamilton, T. J., & Nilsson, G. E. (2019). The physiology of behavioral impacts of high CO₂. In M. Grosell, P. L. Munday, A. P. Farrell, & C. J. Brauner (Eds.), *Fish Physiology* (Vol. 37, pp. 161-194). Academic Press. <https://doi.org/10.1016/bs.fp.2019.08.002>.
- Heugens, E. H., Hendriks, A. J., Dekker, T., van Straalen, N. M., & Admiraal, W. (2001). A review of the effects of multiple stressors on aquatic organisms and analysis of uncertainty factors for use in risk assessment. *Critical Reviews in Toxicology*, 31(3), 247-284. <https://doi.org/10.1080/20014091111695>.
- Heymans, J. J., Coll, M., Libralato, S., Morissette, L., & Christensen, V. (2014). Global patterns in ecological indicators of marine food webs: a modelling approach. *PLoS One*, 9(4), e95845. <https://doi.org/10.1371/journal.pone.0095845>.
- Hill, R. W., Wyse, G. A., & Anderson, M. (2012). *Animal physiology* (3rd ed.). Sinauer Associates.
- Hillebrand, H., Brey, T., Gutt, J., Hagen, W., Metfies, K., Meyer, B., & Lewandowska, A. (2018). Climate change: Warming impacts on marine biodiversity. In M. Salomon & T. Markus (Eds.), *Handbook on marine environment protection* (1 ed., pp. 353-373). Springer. https://doi.org/10.1007/978-3-319-60156-4_18.
- Hochachka, P. W., & Somero, G. N. (2002). *Biochemical adaptation: Mechanism and process in physiological evolution*. Oxford University Press. <https://doi.org/10.1093/oso/9780195117028.001.0001>.
- Hoegh-Guldberg, O., & Bruno, J. F. (2010). The impact of climate change on the world's marine ecosystems. *Science*, 328(5985), 1523-1528. <https://doi.org/10.1126/science.1189930>.
- Hoffmann, A. A., & Sgro, C. M. (2011). Climate change and evolutionary adaptation. *Nature*, 470(7335), 479-485. <https://doi.org/10.1038/nature09670>.
- Hofmann, L. C., & Bischof, K. (2014). Ocean acidification effects on calcifying macroalgae. *Aquatic Biology*, 22, 261-279. <https://doi.org/10.3354/ab00581>.
- Holt, E., & Miller, S. (2010). Bioindicators: using organisms to measure environmental impacts. *Nature Education Knowledge*, 3(10), 8.
- Horwitz, R., Norin, T., Watson, S. A., Pistevos, J. C. A., Beldade, R., Hacquart, S., Gattuso, J. P., Rodolfo-Metalpa, R., Vidal-Dupiol, J., Killen, S. S., & Mills, S. C. (2020). Near-future ocean warming and acidification alter foraging behaviour, locomotion, and metabolic rate in a

- keystone marine mollusc. *Scientific Reports*, 10(1), 5461. <https://doi.org/10.1038/s41598-020-62304-4>.
- Hoshijima, U., Wong, J. M., & Hofmann, G. E. (2017). Additive effects of $p\text{CO}_2$ and temperature on respiration rates of the Antarctic pteropod *Limacina helicina antarctica*. *Conservation Physiology*, 5(1), cox064. <https://doi.org/10.1093/conphys/cox064>.
- Howell, K. L., Pond, D. W., Billett, D. S. M., & Tyler, P. A. (2003). Feeding ecology of deep-sea seastars (Echinodermata: Asteroidea): a fatty-acid biomarker approach. *Marine Ecology Progress Series*, 255, 193-206. <https://doi.org/10.3354/meps255193>.
- Hu, N., Bourdeau, P. E., Harlos, C., Liu, Y., & Hollander, J. (2022). Meta-analysis reveals variance in tolerance to climate change across marine trophic levels. *Science of the Total Environment*, 827, 154244. <https://doi.org/10.1016/j.scitotenv.2022.154244>.
- Hu, N., Bourdeau, P. E., & Hollander, J. (2024). Responses of marine trophic levels to the combined effects of ocean acidification and warming. *Nature Communications*, 15(1), 3400. <https://doi.org/10.1038/s41467-024-47563-3>.
- Hue, T., Chateau, O., Lecellier, G., Marin, C., Coulombier, N., Le Dean, L., Gossuin, H., Adjeroud, M., & Dumas, P. (2022). Impact of near-future ocean warming and acidification on the larval development of coral-eating starfish *Acanthaster cf. solaris* after parental exposure. *Journal of Experimental Marine Biology and Ecology*, 548. <https://doi.org/10.1016/j.jembe.2021.151685>.
- Hughes, I. I. (2000). Biological consequences of global warming: is the signal already apparent? *Trends in Ecology & Evolution*, 15(2), 56-61. [https://doi.org/10.1016/s0169-5347\(99\)01764-4](https://doi.org/10.1016/s0169-5347(99)01764-4).
- Hughes, S. J., Ruhl, H. A., Hawkins, L. E., Hauton, C., Boorman, B., & Billett, D. S. (2011). Deep-sea echinoderm oxygen consumption rates and an interclass comparison of metabolic rates in Asteroidea, Crinoidea, Echinoidea, Holothuroidea and Ophiuroidea. *Journal of Experimental Biology*, 214(Pt 15), 2512-2521. <https://doi.org/10.1242/jeb.055954>.
- Iglesias-Rodriguez, M. D., Halloran, P. R., Rickaby, R. E., Hall, I. R., Colmenero-Hidalgo, E., Gittins, J. R., Green, D. R., Tyrrell, T., Gibbs, S. J., von Dassow, P., Rehm, E., Armbrust, E. V., & Boessenkool, K. P. (2008). Phytoplankton calcification in a high- CO_2 world. *Science*, 320(5874), 336-340. <https://doi.org/10.1126/science.1154122>.
- IPCC. (1996). Climate change 1995: The science of climate change: contribution of working group I to the second assessment report of the Intergovernmental Panel on Climate Change. In J. T. Houghton, L. G. Meira Filho, B. A. Callander, N. Harris, A. Kattenberg, & K. Maskell (Eds.), *the second assessment report of the Intergovernmental Panel on Climate Change* (pp. 588). Cambridge University Press.

- IPCC. (2013). Climate change 2013: The physical science basis. Contribution of working group I to the fifth assessment report of the Intergovernmental Panel on Climate Change. In T. F. Stocker, D. Qin, G. K. Plattner, M. Tignor, S. K. Allen, J. Boschung, A. Nauels, Y. Xia, V. Bex, & P. M. Midgley (Eds.), *The fifth assessment report of the Intergovernmental Panel on Climate Change* (pp. 1535). Cambridge University Press. <https://doi.org/10.1017/CBO9781107415324>.
- IPCC. (2014). Climate change 2014: Synthesis report. Contribution of working groups I, II and III to the fifth assessment report of the Intergovernmental Panel on Climate Change. In Core Writing Team, R. K. Pachauri, & L. A. Meyer (Eds.), *The fifth assessment report of the Intergovernmental Panel on Climate Change* (pp. 151). IPCC.
- IPCC. (2019). Climate change and land: An IPCC special report on climate change, desertification, land degradation, sustainable land management, food security, and greenhouse gas fluxes in terrestrial ecosystems. In P. R. Shukla, J. Skea, E. Calvo Buendia, V. Masson-Delmotte, H.-O. Pörtner, D. C. Roberts, P. Zhai, R. Slade, S. Connors, R. van Diemen, M. Ferrat, E. Haughey, S. Luz, S. Neogi, M. Pathak, J. Petzold, J. Portugal Pereira, P. Vyas, E. Huntley, K. Kissick, M. Belkacemi, & J. Malley (Eds.), *IPCC special report* (pp. 896). Cambridge University Press. <https://doi.org/10.1017/9781009157988>.
- IPCC. (2021). Climate change 2021: The physical science basis. Contribution of working group I to the sixth assessment report of the Intergovernmental Panel on Climate Change. In V. Masson-Delmotte, P. Zhai, A. Pirani, S. L. Connors, C. Péan, S. Berger, N. Caud, Y. Chen, L. Goldfarb, M. I. Gomis, M. Huang, K. Leitzell, E. Lonnoy, J. B. R. Matthews, T. K. Maycock, T. Waterfield, O. Yelekçi, R. Yu, & B. Zhou (Eds.), *The Sixth Assessment Report of the Intergovernmental Panel on Climate Change* (pp. 2391). Cambridge University Press. <https://doi.org/10.1017/9781009157896>.
- IPCC. (2022). Climate change 2022: Impacts, adaptation, and vulnerability. Contribution of working group II to the sixth assessment report of the Intergovernmental Panel on Climate Change. In H.-O. Pörtner, D. C. D.C. Roberts, M. Tignor, E. S. Poloczanska, K. Mintenbeck, A. Alegría, M. Craig, S. Langsdorf, S. Lösckke, V. Möller, A. Okem, & B. Rama (Eds.), *The sixth assessment report of the Intergovernmental Panel on Climate Change* (pp. 3056). Cambridge University Press. <https://doi.org/10.1017/9781009325844>.
- IPCC. (2023). Climate change 2023: Synthesis report. Contribution of working groups I, II and III to the sixth assessment report of the Intergovernmental Panel on Climate Change. In Core Writing Team, H. Lee, & J. Romero (Eds.), *the Sixth Assessment Report of the Intergovernmental Panel on Climate Change* (pp. 184). IPCC. <https://doi.org/10.59327/ipcc/ar6-9789291691647>.

- IUPAC-IUB. (1977). IUPAC-IUB Commission on Biochemical Nomenclature (CBN). The nomenclature of lipids. Recommendations, 1976. *European Journal of Biochemistry*, 79, 11-21. <https://doi.org/10.1111/j.1432-1033.1977.tb11778.x>.
- Ivanina, A. V., Jarrett, A., Bell, T., Rimkevicius, T., Beniash, E., & Sokolova, I. M. (2020). Effects of seawater salinity and pH on cellular metabolism and enzyme activities in biomineralizing tissues of marine bivalves. *Comparative Biochemistry and Physiology Part A: Molecular & Integrative Physiology*, 248, 110748. <https://doi.org/10.1016/j.cbpa.2020.110748>.
- Ji, Y., & Gao, K. (2021). Effects of climate change factors on marine macroalgae: A review. In C. Sheppard (Ed.), *Advances in Marine Biology* (Vol. 88, pp. 91-136). Academic Press. <https://doi.org/10.1016/bs.amb.2020.11.001>.
- Jiang, L., Guo, Y. J., Zhang, F., Zhang, Y. Y., McCook, L. J., Yuan, X. C., Lei, X. M., Zhou, G. W., Guo, M. L., Cai, L., Lian, J. S., Qian, P. Y., & Huang, H. (2019). Diurnally fluctuating $p\text{CO}_2$ modifies the physiological responses of coral recruits under ocean acidification. *Frontiers in Physiology*, 9, 1952. <https://doi.org/10.3389/fphys.2018.01952>.
- Jiang, L., Zhang, F., Guo, M.-L., Guo, Y.-J., Zhang, Y.-Y., Zhou, G.-W., Cai, L., Lian, J.-S., Qian, P.-Y., & Huang, H. (2017). Increased temperature mitigates the effects of ocean acidification on the calcification of juvenile *Pocillopora damicornis*, but at a cost. *Coral Reefs*, 37(1), 71-79. <https://doi.org/10.1007/s00338-017-1634-1>.
- Jiang, L. Q., Dunne, J., Carter, B. R., Tjiputra, J. F., Terhaar, J., Sharp, J. D., Olsen, A., Alin, S., Bakker, D. C. E., Feely, R. A., Gattuso, J. P., Hogan, P., Ilyina, T., Lange, N., Lauvset, S. K., Lewis, E. R., Lovato, T., Palmieri, J., Santana-Falcón, Y., . . . Ziehn, T. (2023). Global surface ocean acidification indicators from 1750 to 2100. *Journal of Advances in Modeling Earth Systems*, 15(3). <https://doi.org/10.1029/2022ms003563>.
- Johnson, R., Harianto, J., Thomson, M., & Byrne, M. (2020). The effects of long-term exposure to low pH on the skeletal microstructure of the sea urchin *Heliocidaris erythrogramma*. *Journal of Experimental Marine Biology and Ecology*, 523. <https://doi.org/10.1016/j.jembe.2019.151250>.
- Joyce, P. W. S., Tang, W. Y., & Falkenberg, L. J. (2022). Marine heatwaves of different magnitudes have contrasting effects on herbivore behaviour. *Scientific Reports*, 12(1), 17309. <https://doi.org/10.1038/s41598-022-21567-9>.
- Kainz, M. J., & Fisk, A. T. (2009). Integrating lipids and contaminants in aquatic ecology and ecotoxicology. In M. Kainz, M. Brett, & M. Arts (Eds.), *Lipids in aquatic ecosystems* (pp. 93-114). Springer. https://doi.org/10.1007/978-0-387-89366-2_5.
- Kamya, P. Z., Byrne, M., Graba-Landry, A., & Dworjanyn, S. A. (2016). Near-future ocean acidification enhances the feeding rate and development of the herbivorous juveniles of the crown-of-

- thorns starfish, *Acanthaster planci*. *Coral Reefs*, 35(4), 1241-1251. <https://doi.org/10.1007/s00338-016-1480-6>.
- Kamya, P. Z., Byrne, M., Mos, B., & Dworjanyn, S. A. (2018). Enhanced performance of juvenile crown of thorns starfish in a warm-high CO₂ ocean exacerbates poor growth and survival of their coral prey. *Coral Reefs*, 37(3), 751-762. <https://doi.org/10.1007/s00338-018-1699-5>.
- Kamya, P. Z., Dworjanyn, S. A., Hardy, N., Mos, B., Uthicke, S., & Byrne, M. (2014). Larvae of the coral eating crown-of-thorns starfish, *Acanthaster planci* in a warmer-high CO₂ ocean. *Global Change Biology*, 20(11), 3365-3376. <https://doi.org/10.1111/gcb.12530>.
- Kaniewska, P., Campbell, P. R., Kline, D. I., Rodriguez-Lanetty, M., Miller, D. J., Dove, S., & Hoegh-Guldberg, O. (2012). Major cellular and physiological impacts of ocean acidification on a reef building coral. *PLoS One*, 7(4), e34659. <https://doi.org/10.1371/journal.pone.0034659>.
- Kattner, G., Hagen, W., Lee, R. F., Campbell, R., Deibel, D., Falk-Petersen, S., Graeve, M., Hansen, B. W., Hirche, H. J., Jónasdóttir, S. H., Madsen, M. L., Mayzaud, P., Müller-Navarra, D., Nichols, P. D., Paffenhöfer, G. A., Pond, D., Saito, H., Stübing, D., & Virtue, P. (2007). Perspectives on marine zooplankton lipids. *Canadian Journal of Fisheries and Aquatic Sciences*, 64(11), 1628-1639. <https://doi.org/10.1139/f07-122>.
- Kaustuv, R., Jablonski, D., & Valentine, J. W. (2001). Climate change, species range limits and body size in marine bivalves. *Ecology Letters*, 4(4), 366-370. <https://doi.org/10.1046/j.1461-0248.2001.00236.x>.
- Kawahata, H., Fujita, K., Iguchi, A., Inoue, M., Iwasaki, S., Kuroyanagi, A., Maeda, A., Manaka, T., Moriya, K., Takagi, H., Toyofuku, T., Yoshimura, T., & Suzuki, A. (2019). Perspective on the response of marine calcifiers to global warming and ocean acidification—Behavior of corals and foraminifera in a high CO₂ world “hot house”. *Progress in Earth and Planetary Science*, 6(1). <https://doi.org/10.1186/s40645-018-0239-9>.
- Kazmi, S. S. U. H., Wang, Y. Y. L., Cai, Y.-E., & Wang, Z. (2022). Temperature effects in single or combined with chemicals to the aquatic organisms: An overview of thermo-chemical stress. *Ecological Indicators*, 143. <https://doi.org/10.1016/j.ecolind.2022.109354>.
- Kelley, J. L., Brown, A. P., Therkildsen, N. O., & Foote, A. D. (2016). The life aquatic: Advances in marine vertebrate genomics. *Nature Reviews Genetics*, 17(9), 523-534. <https://doi.org/10.1038/nrg.2016.66>.
- Kelley, L. A., & Lunden, J. J. (2017). Meta-analysis identifies metabolic sensitivities to ocean acidification. *AIMS Environmental Science*, 4(5), 709-729. <https://doi.org/10.3934/environsci.2017.5.709>.

- Kelly, M. (2019). Adaptation to climate change through genetic accommodation and assimilation of plastic phenotypes. *Philosophical Transactions of the Royal Society of London B Biological Sciences*, 374(1768), 20180176. <https://doi.org/10.1098/rstb.2018.0176>.
- Kelly, M. W., Hofmann, G. E., & Hoffmann, A. (2013). Adaptation and the physiology of ocean acidification. *Functional Ecology*, 27(4), 980-990. <https://doi.org/10.1111/j.1365-2435.2012.02061.x>.
- Keppel, E. A., Scrosati, R. A., & Courtenay, S. C. (2014). Interactive effects of ocean acidification and warming on subtidal mussels and sea stars from Atlantic Canada. *Marine Biology Research*, 11(4), 337-348. <https://doi.org/10.1080/17451000.2014.932914>.
- Khalil, M., Doo, S. S., Stuhr, M., & Westphal, H. (2022). Ocean warming amplifies the effects of ocean acidification on skeletal mineralogy and microstructure in the asterinid starfish *Aquilonastra yairi*. *Journal of Marine Science and Engineering*, 10(8), 1065. <https://doi.org/10.3390/jmse10081065>.
- Khalil, M., Doo, S. S., Stuhr, M., & Westphal, H. (2023). Long-term physiological responses to combined ocean acidification and warming show energetic trade-offs in an asterinid starfish. *Coral Reefs*, 42(4), 845-858. <https://doi.org/10.1007/s00338-023-02388-2>.
- Khalil, M., Stuhr, M., Kunzmann, A., & Westphal, H. (2024a). *Ca-ATPase and Mg-ATPase enzyme activities of the tropical-subtropical starfish Aquilonastra yairi under ocean acidification and warming in the laboratory* [dataset]. PANGAEA. <https://doi.org/10.1594/PANGAEA.965905>.
- Khalil, M., Stuhr, M., Kunzmann, A., & Westphal, H. (2024b). *Fatty acid composition of the tropical-subtropical starfish Aquilonastra yairi under ocean acidification and warming in the laboratory* [dataset]. PANGAEA. <https://doi.org/10.1594/PANGAEA.965902>.
- Khalil, M., Stuhr, M., Kunzmann, A., & Westphal, H. (2024c). Simultaneous ocean acidification and warming do not alter the lipid-associated biochemistry but induce enzyme activities in an asterinid starfish. *Science of the Total Environment*, 932, 173000. <https://doi.org/10.1016/j.scitotenv.2024.173000>.
- Khalil, M., Stuhr, M., Kunzmann, A., & Westphal, H. (2024d). *Total lipids of the tropical-subtropical starfish Aquilonastra yairi under ocean acidification and warming in the laboratory* [dataset]. PANGAEA. <https://doi.org/10.1594/PANGAEA.965904>.
- Khan, F. U., Chen, H., Gu, H., Wang, T., Dupont, S., Kong, H., Shang, Y., Wang, X., Lu, W., Hu, M., & Wang, Y. (2021). Antioxidant responses of the mussel *Mytilus coruscus* co-exposed to ocean acidification, hypoxia and warming. *Marine Pollution Bulletin*, 162, 111869. <https://doi.org/10.1016/j.marpolbul.2020.111869>.

- Khan, F. U., Hu, M., Kong, H., Shang, Y., Wang, T., Wang, X., Xu, R., Lu, W., & Wang, Y. (2020). Ocean acidification, hypoxia and warming impair digestive parameters of marine mussels. *Chemosphere*, 256, 127096. <https://doi.org/10.1016/j.chemosphere.2020.127096>.
- Kidawa, A., Potocka, M., & Janecki, T. (2010). The effects of temperature on the behaviour of the Antarctic sea star *Odontaster validus*. *Polish Polar Research*, 31(3), 273-284. <https://doi.org/10.2478/v10183-010-0003-3>.
- Killian, C. E., & Wilt, F. H. (1996). Characterization of the proteins comprising the integral matrix of *Strongylocentrotus purpuratus* embryonic spicules. *Journal of Biological Chemistry*, 271(15), 9150-9159. <https://doi.org/10.1074/jbc.271.15.9150>.
- Killian, C. E., & Wilt, F. H. (2008). Molecular aspects of biomineralization of the echinoderm endoskeleton. *Chemical Reviews*, 108(11), 4463-4474. <https://doi.org/10.1021/cr0782630>.
- Kisakürek, B., Eisenhauer, A., Böhm, F., Garbe-Schönberg, D., & Erez, J. (2008). Controls on shell Mg/Ca and Sr/Ca in cultured planktonic foraminiferan, *Globigerinoides ruber* (white). *Earth and Planetary Science Letters*, 273(3-4), 260-269. <https://doi.org/10.1016/j.epsl.2008.06.026>.
- Kleitman, N. (1941). The effect of temperature on the righting of Echinoderms. *The Biological Bulletin*, 80(3), 292-298. <https://doi.org/10.2307/1537716>.
- Klinger, T. S., McClintock, J. B., & Watts, S. A. (1997). Activities of digestive enzymes of polar and subtropical echinoderms. *Polar Biology*, 18(2), 154-157. <https://doi.org/10.1007/s003000050170>.
- Klymasz-Swartz, A. K., Allen, G. J. P., Treberg, J. R., Yoon, G. R., Tripp, A., Quijada-Rodriguez, A. R., & Weihrauch, D. (2019). Impact of climate change on the American lobster (*Homarus americanus*): Physiological responses to combined exposure of elevated temperature and pCO₂. *Comparative Biochemistry and Physiology Part A: Molecular & Integrative Physiology*, 235, 202-210. <https://doi.org/10.1016/j.cbpa.2019.06.005>.
- Knapp, B. D., & Huang, K. C. (2022). The effects of temperature on cellular physiology. *Annual Review of Biophysics*, 51, 499-526. <https://doi.org/10.1146/annurev-biophys-112221-074832>.
- Knights, A. M., Norton, M. J., Lemasson, A. J., & Stephen, N. (2020). Ocean acidification mitigates the negative effects of increased sea temperatures on the biomineralization and crystalline ultrastructure of *Mytilus*. *Frontiers in Marine Science*, 7. <https://doi.org/10.3389/fmars.2020.567228>.
- Knoll, A. H. (2003). Biomineralization and evolutionary history. *Reviews in Mineralogy & Geochemistry*, 54(1), 329-356. <https://doi.org/10.2113/0540329>.

- Ko, G. W., Dineshram, R., Campanati, C., Chan, V. B., Havenhand, J., & Thiyagarajan, V. (2014). Interactive effects of ocean acidification, elevated temperature, and reduced salinity on early-life stages of the pacific oyster. *Environmental Science & Technology*, *48*(17), 10079-10088. <https://doi.org/10.1021/es501611u>.
- Kokorin, A. I., Mirantsev, G. V., & Rozhnov, S. V. (2015). General features of echinoderm skeleton formation. *Paleontological Journal*, *48*(14), 1532-1539. <https://doi.org/10.1134/s0031030114140056>.
- Kolbuk, D., Di Giglio, S., M'Zoudi, S., Dubois, P., Stolarski, J., & Gorzelak, P. (2020). Effects of seawater Mg^{2+}/Ca^{2+} ratio and diet on the biomineralization and growth of sea urchins and the relevance of fossil echinoderms to paleoenvironmental reconstructions. *Geobiology*, *18*(6), 710-724. <https://doi.org/10.1111/gbi.12409>.
- Kristensen, E., Penha-Lopes, G., Delefosse, M., Valdemarsen, T., Quintana, C. O., & Banta, G. T. (2012). What is bioturbation? The need for a precise definition for fauna in aquatic sciences. *Marine Ecology Progress Series*, *446*, 285-302. <https://doi.org/10.3354/meps09506>.
- Kroeker, K. J., Kordas, R. L., Crim, R., Hendriks, I. E., Ramajo, L., Singh, G. S., Duarte, C. M., & Gattuso, J. P. (2013). Impacts of ocean acidification on marine organisms: quantifying sensitivities and interaction with warming. *Global Change Biology*, *19*(6), 1884-1896. <https://doi.org/10.1111/gcb.12179>.
- Kroeker, K. J., Kordas, R. L., Crim, R. N., & Singh, G. G. (2010). Meta-analysis reveals negative yet variable effects of ocean acidification on marine organisms. *Ecology Letters*, *13*(11), 1419-1434. <https://doi.org/10.1111/j.1461-0248.2010.01518.x>.
- Kroeker, K. J., Sanford, E., Jellison, B. M., & Gaylord, B. (2014). Predicting the effects of ocean acidification on predator-prey interactions: a conceptual framework based on coastal molluscs. *Biol Bull*, *226*(3), 211-222. <https://doi.org/10.1086/BBLv226n3p211>.
- Kronstadt, S. M., Darnell, M. Z., & Munguia, P. (2013). Background and temperature effects on *Uca panacea* color change. *Marine Biology*, *160*(6), 1373-1381. <https://doi.org/10.1007/s00227-013-2189-5>.
- Lan, X., Tans, P., & Thoning, K. W. (2023). *Trends in globally-averaged CO₂ determined from NOAA Global Monitoring Laboratory measurements. Version 2023-07*. <https://doi.org/10.15138/9N0H-ZH07>.
- Lang, B. J., Caballes, C. F., Uthicke, S., Doll, P. C., Donelson, J. M., & Pratchett, M. S. (2022). Impacts of ocean warming on the settlement success and post-settlement survival of Pacific crown-of-thorns starfish (*Acanthaster cf. solaris*). *Coral Reefs*, *42*(1), 143-155. <https://doi.org/10.1007/s00338-022-02314-y>.

- Lang, B. J., Donelson, J. M., Bairos-Novak, K. R., Wheeler, C. R., Caballes, C. F., Uthicke, S., & Pratchett, M. S. (2023). Impacts of ocean warming on echinoderms: A meta-analysis. *Ecology and Evolution*, *13*(8), e10307. <https://doi.org/10.1002/ece3.10307>.
- Langan, J. A., Puggioni, G., Oviatt, C. A., Henderson, M. E., & Collie, J. S. (2021). Climate alters the migration phenology of coastal marine species. *Marine Ecology Progress Series*, *660*, 1-18. <https://doi.org/10.3354/meps13612>.
- Lardies, M. A., Benitez, S., Osores, S., Vargas, C. A., Duarte, C., Lohrmann, K. B., & Lagos, N. A. (2017). Physiological and histopathological impacts of increased carbon dioxide and temperature on the scallops *Argopecten purpuratus* cultured under upwelling influences in northern Chile. *Aquaculture*, *479*, 455-466. <https://doi.org/10.1016/j.aquaculture.2017.06.008>.
- Laurent, J., Venn, A., Tambutte, E., Ganot, P., Allemand, D., & Tambutte, S. (2014). Regulation of intracellular pH in cnidarians: response to acidosis in *Anemonia viridis*. *FEBS Journal*, *281*(3), 683-695. <https://doi.org/10.1111/febs.12614>.
- LaVigne, M., Hill, T. M., Sanford, E., Gaylord, B., Russell, A. D., Lenz, E. A., Hosfelt, J. D., & Young, M. K. (2013). The elemental composition of purple sea urchin (*Strongylocentrotus purpuratus*) calcite and potential effects of $p\text{CO}_2$ during early life stages. *Biogeosciences*, *10*(6), 3465-3477. <https://doi.org/10.5194/bg-10-3465-2013>.
- Lawrence, J. M. (1985). The energetic echinoderm. In B. F. Keegan & B. D. S. O'Connor (Eds.), *Echinodermata* (pp. 47-67). A.A. Balkema.
- Lawrence, J. M., & Cowell, B. C. (1996). The righting response as an indication of stress in *Stichaster striatus* (Echinodermata, Asteroidea). *Marine and Freshwater Behaviour and Physiology*, *27*(4), 239-248. <https://doi.org/10.1080/10236249609378969>.
- Le Quéré, C., Raupach, M. R., Canadell, J. G., Marland, G., Bopp, L., Ciais, P., Conway, T. J., Doney, S. C., Feely, R. A., Foster, P., Friedlingstein, P., Gurney, K., Houghton, R. A., House, J. I., Huntingford, C., Levy, P. E., Lomas, M. R., Majkut, J., Metzl, N., . . . Woodward, F. I. (2009). Trends in the sources and sinks of carbon dioxide. *Nature Geoscience*, *2*(12), 831-836. <https://doi.org/10.1038/ngeo689>.
- Lea, D. W., Mashiotto, T. A., & Spero, H. J. (1999). Controls on magnesium and strontium uptake in planktonic foraminifera determined by live culturing. *Geochimica et Cosmochimica Acta*, *63*(16), 2369-2379. [https://doi.org/10.1016/s0016-7037\(99\)00197-0](https://doi.org/10.1016/s0016-7037(99)00197-0).
- Lebrato, M., Andersson, A. J., Ries, J. B., Aronson, R. B., Lamare, M. D., Koeve, W., Oschlies, A., Iglesias-Rodriguez, M. D., Thatje, S., Amsler, M., Vos, S. C., Jones, D. O. B., Ruhl, H. A., Gates, A. R., & McClintock, J. B. (2016). Benthic marine calcifiers coexist with CaCO_3 -undersaturated seawater worldwide. *Global Biogeochemical Cycles*, *30*(7), 1038-1053. <https://doi.org/10.1002/2015gb005260>.

- Lee, Y. H., Jeong, C. B., Wang, M., Hagiwara, A., & Lee, J. S. (2020). Transgenerational acclimation to changes in ocean acidification in marine invertebrates. *Marine Pollution Bulletin*, *153*, 111006. <https://doi.org/10.1016/j.marpolbul.2020.111006>.
- Lemasson, A. J., Hall-Spencer, J. M., Kuri, V., & Knights, A. M. (2019). Changes in the biochemical and nutrient composition of seafood due to ocean acidification and warming. *Marine Environmental Research*, *143*, 82-92. <https://doi.org/10.1016/j.marenvres.2018.11.006>.
- Lenz, B., Fogarty, N. D., & Figueiredo, J. (2019). Effects of ocean warming and acidification on fertilization success and early larval development in the green sea urchin *Lytechinus variegatus*. *Marine Pollution Bulletin*, *141*, 70-78. <https://doi.org/10.1016/j.marpolbul.2019.02.018>.
- Leung, J. Y. S., Russell, B. D., Coleman, M. A., Kelaher, B. P., & Connell, S. D. (2021). Long-term thermal acclimation drives adaptive physiological adjustments of a marine gastropod to reduce sensitivity to climate change. *Science of the Total Environment*, *771*, 145208. <https://doi.org/10.1016/j.scitotenv.2021.145208>.
- Leung, J. Y. S., Russell, B. D., & Connell, S. D. (2019). Adaptive responses of marine gastropods to heatwaves. *One Earth*, *1*(3), 374-381. <https://doi.org/10.1016/j.oneear.2019.10.025>.
- Leung, J. Y. S., Russell, B. D., & Connell, S. D. (2020). Linking energy budget to physiological adaptation: How a calcifying gastropod adjusts or succumbs to ocean acidification and warming. *Science of the Total Environment*, *715*, 136939. <https://doi.org/10.1016/j.scitotenv.2020.136939>.
- Leung, J. Y. S., Zhang, S., & Connell, S. D. (2022). Is ocean acidification really a threat to marine calcifiers? a systematic review and meta-analysis of 980+ studies spanning two decades. *Small*, *18*(35), e2107407. <https://doi.org/10.1002/smll.202107407>.
- Levene, H. (1960). Robust tests for equality of variances. In I. Olkin (Ed.), *Contributions to probability and statistics* (pp. 278-292). Stanford University Press.
- Levin, L. A., Hönisch, B., & Frieder, C. A. (2015). Geochemical proxies for estimating faunal exposure to ocean acidification. *Oceanography*, *28*(2), 62-73. <http://www.jstor.org/stable/24861871>.
- Li, S., Liu, C., Huang, J., Liu, Y., Zheng, G., Xie, L., & Zhang, R. (2015). Interactive effects of seawater acidification and elevated temperature on biomineralization and amino acid metabolism in the mussel *Mytilus edulis*. *Journal of Experimental Biology*, *218*(Pt 22), 3623-3631. <https://doi.org/10.1242/jeb.126748>.
- Li, Z., England, M. H., & Groeskamp, S. (2023). Recent acceleration in global ocean heat accumulation by mode and intermediate waters. *Nat Commun*, *14*(1), 6888. <https://doi.org/10.1038/s41467-023-42468-z>.

- Lieth, H. (1974). Purposes of a phenology book. In H. Lieth (Ed.), *Phenology and seasonality modeling* (Vol. 8, pp. 3-19). Springer. https://doi.org/10.1007/978-3-642-51863-8_1.
- Lindsey, R. (2023). *Climate change: Atmospheric carbon dioxide*. NOAA NCEI Paleoclimatology Program. Retrieved 1 May 2024 from <https://www.climate.gov/news-features/understanding-climate/climate-change-atmospheric-carbon-dioxide>.
- Lischka, S., Greenacre, M. J., Riebesell, U., & Graeve, M. (2022). Membrane lipid sensitivity to ocean warming and acidification poses a severe threat to Arctic pteropods. *Frontiers in Marine Science*, 9. <https://doi.org/10.3389/fmars.2022.920163>.
- Livingston, B. T., Killian, C. E., Wilt, F., Cameron, A., Landrum, M. J., Ermolaeva, O., Sapojnikov, V., Maglott, D. R., Buchanan, A. M., & Etensohn, C. A. (2006). A genome-wide analysis of biomineralization-related proteins in the sea urchin *Strongylocentrotus purpuratus*. *Developmental Biology*, 300(1), 335-348. <https://doi.org/10.1016/j.ydbio.2006.07.047>.
- Long, X., Ma, Y., & Qi, L. (2014). Biogenic and synthetic high magnesium calcite - a review. *Journal of Structural Biology*, 185(1), 1-14. <https://doi.org/10.1016/j.jsb.2013.11.004>.
- Lonhart, S. I., Jeppesen, R., Beas-Luna, R., Crooks, J. A., & Lorda, J. (2019). Shifts in the distribution and abundance of coastal marine species along the eastern Pacific Ocean during marine heatwaves from 2013 to 2018. *Marine Biodiversity Records*, 12(1). <https://doi.org/10.1186/s41200-019-0171-8>.
- Lorens, R. B. (1981). Sr, Cd, Mn and Co distribution coefficients in calcite as a function of calcite precipitation rate. *Geochimica et Cosmochimica Acta*, 45(4), 553-561. [https://doi.org/10.1016/0016-7037\(81\)90188-5](https://doi.org/10.1016/0016-7037(81)90188-5).
- Lowenstam, H. A., & Weiner, S. (1989). *On Biomineralization*. Oxford University Press
- Mackenzie, F. T., Bischoff, W. D., Bishop, F. C., Loijens, M., Schoonmaker, J., & Wollast, R. (1983). Magnesian calcites: Low temperature occurrence, solubility and solid solution behavior. In J. R. Richard (Ed.), *Carbonates: Mineralogy and chemistry, reviews in mineralogy* (Vol. 11, pp. 97-144). Mineralogical Society of America.
- Magdalena, W., Piotr, D., & Andrzej, O. (2012). Intrinsically disordered proteins in biomineralization. In S. Jong (Ed.), *Advanced topics in biomineralization* (pp. Ch. 1). IntechOpen. <https://doi.org/10.5772/31121>.
- Mah, C. L. (2024). *World Asteroidea database* <https://doi.org/10.14284/653>.
- Mah, C. L., & Blake, D. B. (2012). Global diversity and phylogeny of the Asteroidea (Echinodermata). *PLoS One*, 7(4), e35644. <https://doi.org/10.1371/journal.pone.0035644>.
- Maia, S., Marques, S. C., Dupont, S., Neves, M., Pinto, H. J., Reis, J., & Leandro, S. M. (2022). Effects of ocean acidification and warming on the development and biochemical responses of

- juvenile shrimp *Palaemon elegans* (Rathke, 1837). *Marine Environmental Research*, 176, 105580. <https://doi.org/10.1016/j.marenvres.2022.105580>.
- Mann, S. (1983). Mineralization in biological systems. In P. H. Connert, H. Foltmann, M. Lammers, S. Mann, J. D. Odom, & K. E. Wetterhahn (Eds.), *Inorganic elements in biochemistry* (pp. 125-174). Springer.
- Manriquez, P. H., Gonzalez, C. P., Brokordt, K., Pereira, L., Torres, R., Lattuca, M. E., Fernandez, D. A., Peck, M. A., Cucco, A., Antognarelli, F., Marras, S., & Domenici, P. (2019). Ocean warming and acidification pose synergistic limits to the thermal niche of an economically important echinoderm. *Science of the Total Environment*, 693, 133469. <https://doi.org/10.1016/j.scitotenv.2019.07.275>.
- Manríquez, P. H., Torres, R., Matson, P. G., Lee, M. R., Jara, M. E., Seguel, M. E., Sepúlveda, F., & Pereira, L. (2017). Effects of ocean warming and acidification on the early benthic ontogeny of an ecologically and economically important echinoderm. *Marine Ecology Progress Series*, 563, 169-184. <https://doi.org/10.3354/meps11973>.
- Marceta, T., Matozzo, V., Alban, S., Badocco, D., Pastore, P., & Marin, M. G. (2020). Do males and females respond differently to ocean acidification? an experimental study with the sea urchin *Paracentrotus lividus*. *Environmental Science and Pollution Research*, 27(31), 39516-39530. <https://doi.org/10.1007/s11356-020-10040-7>.
- Markert, B. A., Breure, A. M., & Zechmeister, H. G. (2003). Definitions, strategies and principles for bioindication/biomonitoring of the environment. In *Bioindicators & biomonitors - principles, concepts and applications* (Vol. 6, pp. 3-39). [https://doi.org/10.1016/s0927-5215\(03\)80131-5](https://doi.org/10.1016/s0927-5215(03)80131-5).
- Martin, S., Castets, M.-D., & Clavier, J. (2006). Primary production, respiration and calcification of the temperate free-living coralline alga *Lithothamnion corallioides*. *Aquatic Botany*, 85(2), 121-128. <https://doi.org/10.1016/j.aquabot.2006.02.005>.
- Matoo, O. B., Lannig, G., Bock, C., & Sokolova, I. M. (2021). Temperature but not ocean acidification affects energy metabolism and enzyme activities in the blue mussel, *Mytilus edulis*. *Ecology and Evolution*, 11(7), 3366-3379. <https://doi.org/10.1002/ece3.7289>.
- Matranga, V., Bonaventura, R., Costa, C., Karakostis, K., Pinsino, A., Russo, R., & Zito, F. (2011). Echinoderms as blueprints for biocalcification: Regulation of skeletogenic genes and matrices. In W. E. G. Müller (Ed.), *Molecular biomineralization: Aquatic organisms forming extraordinary materials* (pp. 225-248). Springer. https://doi.org/10.1007/978-3-642-21230-7_8.

- Matranga, V., Pinsino, A., Bonaventura, R., Costa, C., Karakostis, K., Martino, C., Russo, R., & Zito, F. (2013). Cellular and molecular bases of biomineralization in sea urchin embryos. *Cahiers de Biologie Marine*, 54, 467-478. <https://doi.org/10.21411/CBM.A.D5976C17>.
- Matson, P. G., Yu, P. C., Sewell, M. A., & Hofmann, G. E. (2012). Development under elevated $p\text{CO}_2$ conditions does not affect lipid utilization and protein content in early life-history stages of the purple sea urchin, *Strongylocentrotus purpuratus*. *The Biological Bulletin*, 223(3), 312-327. <https://doi.org/10.1086/BBLv223n3p312>.
- Maureaud, A., Gascuel, D., Colleter, M., Palomares, M. L. D., Du Pontavice, H., Pauly, D., & Cheung, W. W. L. (2017). Global change in the trophic functioning of marine food webs. *PLoS One*, 12(8), e0182826. <https://doi.org/10.1371/journal.pone.0182826>.
- McCarthy, I. D., Whiteley, N. M., Fernandez, W. S., Ragagnin, M. N., Cornwell, T. O., Suckling, C. C., & Turra, A. (2020). Elevated $p\text{CO}_2$ does not impair performance in autotomised individuals of the intertidal predatory starfish *Asterias rubens* (Linnaeus, 1758). *Marine Environmental Research*, 104841. <https://doi.org/10.1016/j.marenvres.2019.104841>.
- McCaw, B. A., Stevenson, T. J., & Lancaster, L. T. (2020). Epigenetic responses to temperature and climate. *Integrative and Comparative Biology*, 60(6), 1469-1480. <https://doi.org/10.1093/icb/icaa049>.
- McClintock, J. B., Amsler, M. O., Angus, R. A., Challener, R. C., Schram, J. B., Amsler, C. D., Mah, C. L., Cuce, J., & Baker, B. J. (2011). The Mg-calcite composition of antarctic echinoderms: Important implications for predicting the impacts of ocean acidification. *The Journal of Geology*, 119(5), 457-466. <https://doi.org/10.1086/660890>.
- McElroy, D. J., Nguyen, H. D., & Byrne, M. (2012). Respiratory response of the intertidal seastar *Parvulastra exigua* to contemporary and near-future pulses of warming and hypercapnia. *Journal of Experimental Marine Biology and Ecology*, 416-417, 1-7. <https://doi.org/10.1016/j.jembe.2012.02.003>.
- McLaren, E. J., & Byrne, M. (2022). The effect of ocean acidification on the escape behaviour of the sea star *Parvulastra exigua* to its sea star predator *Meridiastra calcar*. *Journal of Experimental Marine Biology and Ecology*, 555. <https://doi.org/10.1016/j.jembe.2022.151779>.
- McManus, L. C., Vasconcelos, V. V., Levin, S. A., Thompson, D. M., Kleypas, J. A., Castruccio, F. S., Curchitser, E. N., & Watson, J. R. (2020). Extreme temperature events will drive coral decline in the Coral Triangle. *Global Change Biology*, 26(4), 2120-2133. <https://doi.org/10.1111/gcb.14972>.

- Medeiros, I. P. M., & Souza, M. M. (2023). Acid times in physiology: A systematic review of the effects of ocean acidification on calcifying invertebrates. *Environmental Research*, 231(Pt 1), 116019. <https://doi.org/10.1016/j.envres.2023.116019>.
- Mehrbach, C., Culberson, C. H., Hawley, J. E., & Pytkowicz, R. M. (1973). Measurement of the apparent dissociation constants of carbonic acid in seawater at atmospheric pressure. *Limnology and Oceanography*, 18(6), 897-907. <https://doi.org/10.4319/lo.1973.18.6.0897>.
- Melzner, F., Gutowska, M. A., Langenbuch, M., Dupont, S., Lucassen, M., Thorndyke, M. C., Bleich, M., & Pörtner, H. O. (2009). Physiological basis for high CO₂ tolerance in marine ectothermic animals: pre-adaptation through lifestyle and ontogeny?. *Biogeosciences*, 6(10), 2313-2331. <https://doi.org/10.5194/bg-6-2313-2009>.
- Melzner, F., Mark, F. C., Seibel, B. A., & Tomanek, L. (2020). Ocean acidification and coastal marine invertebrates: Tracking CO₂ effects from seawater to the cell. *Annual Review of Marine Science*, 12, 499-523. <https://doi.org/10.1146/annurev-marine-010419-010658>.
- Menge, B. A., Iles, A. C., & Freidenburg, T. L. (2013). Keystone species. In *Encyclopedia of biodiversity* (pp. 442-457). <https://doi.org/10.1016/b978-0-12-384719-5.00081-2>.
- Menge, B. A., & Sanford, E. (2013). Ecological role of sea stars from populations to meta ecosystems. In J. M. Lawrence (Ed.), *Starfish: Biology and ecology of the Asteroidea* (pp. 67-80). The Johns Hopkins University Press.
- Meretta, P. E., & Ventura, C. R. R. (2021). Locomotion and righting behavior of sea stars: A study case on the bat star *Asterina stellifera* (Asterinidae). *Revista de Biologia Tropical*, 69(Suppl.1), S501-S513. <https://doi.org/10.15517/rbt.v69iSuppl.1.46392>.
- Mieszowska, N. (2021). Intertidal indicators of climate and global change. In T. M. Letcher (Ed.), *Climate change: Observed impacts on planet earth* (pp. 465-482). Elsevier. <https://doi.org/10.1016/b978-0-12-821575-3.00022-0>.
- Migliaccio, O., Pinsino, A., Maffioli, E., Smith, A. M., Agnisola, C., Matranga, V., Nonnis, S., Tedeschi, G., Byrne, M., Gambi, M. C., & Palumbo, A. (2019). Living in future ocean acidification, physiological adaptive responses of the immune system of sea urchins resident at a CO₂ vent system. *Science of the Total Environment*, 672, 938-950. <https://doi.org/10.1016/j.scitotenv.2019.04.005>.
- Miles, H., Widdicombe, S., Spicer, J. I., & Hall-Spencer, J. (2007). Effects of anthropogenic seawater acidification on acid-base balance in the sea urchin *Psammechinus miliaris*. *Marine Pollution Bulletin*, 54(1), 89-96. <https://doi.org/10.1016/j.marpolbul.2006.09.021>.
- Miller, N., & Stillman, J. (2012). Physiological optima and critical limits. *Nature Education Knowledge*, 3(10), 1.

- Montgomery, E. M. (2014). Predicting crawling speed relative to mass in sea stars. *Journal of Experimental Marine Biology and Ecology*, 458, 27-33. <https://doi.org/10.1016/j.jembe.2014.05.009>.
- Moreau, C., Jossart, Q., Danis, B., Eléaume, M., Christiansen, H., Guillaumot, C., Downey, R., & Saucède, T. (2021). The high diversity of Southern Ocean sea stars (Asteroidea) reveals original evolutionary pathways. *Progress in Oceanography*, 190. <https://doi.org/10.1016/j.pocean.2020.102472>.
- Morley, S. A., Peck, L. S., Sunday, J. M., Heiser, S., Bates, A. E., & Algar, A. (2019). Physiological acclimation and persistence of ectothermic species under extreme heat events. *Global Ecology and Biogeography*, 28(7), 1018-1037. <https://doi.org/10.1111/geb.12911>.
- Morley, S. A., Suckling, C. C., Clark, M. S., Cross, E. L., & Peck, L. S. (2016). Long-term effects of altered pH and temperature on the feeding energetics of the Antarctic sea urchin, *Sterechinus neumayeri*. *Biodiversity*, 17(1-2), 34-45. <https://doi.org/10.1080/14888386.2016.1174956>.
- Morse, J. W., Andersson, A. J., & Mackenzie, F. T. (2006). Initial responses of carbonate-rich shelf sediments to rising atmospheric $p\text{CO}_2$ and “ocean acidification”: Role of high Mg-calcites. *Geochimica et Cosmochimica Acta*, 70(23), 5814-5830. <https://doi.org/10.1016/j.gca.2006.08.017>.
- Morse, J. W., Wang, Q., & Tsio, M. Y. (1997). Influences of temperature and Mg:Ca ratio on CaCO_3 precipitates from seawater. *Geology*, 25(1). [https://doi.org/10.1130/0091-7613\(1997\)025<0085:lotamc>2.3.Co;2](https://doi.org/10.1130/0091-7613(1997)025<0085:lotamc>2.3.Co;2).
- Mos, B., Mesic, N., & Dworjanyn, S. A. (2023). Variable food alters responses of larval crown-of-thorns starfish to ocean warming but not acidification. *Commun Biol*, 6(1), 639. <https://doi.org/10.1038/s42003-023-05028-1>.
- Mouneyrac, C., & Amiard-Triquet, C. (2013). Biomarkers of ecological relevance in ecotoxicology. In J.-F. Féraud & C. Blaise (Eds.), *Encyclopedia of aquatic ecotoxicology* (pp. 221-236). Springer. https://doi.org/10.1007/978-94-007-5704-2_22.
- Mousseau, T. A., & Fox, C. W. (1998). The adaptive significance of maternal effects. *Trends in Ecology & Evolution*, 13(10), 403-407. [https://doi.org/10.1016/s0169-5347\(98\)01472-4](https://doi.org/10.1016/s0169-5347(98)01472-4).
- Mucci, A. (1983). The solubility of calcite and aragonite in seawater at various salinities, temperatures, and one atmosphere total pressure. *American Journal of Science*, 283(7), 780-799. <https://doi.org/10.2475/ajs.283.7.780>.
- Mucci, A. (1987). Influence of temperature on the composition of magnesian calcite overgrowths precipitated from seawater. *Geochimica et Cosmochimica Acta*, 51(7), 1977-1984. [https://doi.org/10.1016/0016-7037\(87\)90186-4](https://doi.org/10.1016/0016-7037(87)90186-4).

- Mucci, A., & Morse, J. W. (1983). The incorporation of Mg^{2+} and Sr^{2+} into calcite overgrowths: influences of growth rate and solution composition. *Geochimica et Cosmochimica Acta*, 47(2), 217-233. [https://doi.org/10.1016/0016-7037\(83\)90135-7](https://doi.org/10.1016/0016-7037(83)90135-7).
- Mueller, B., Bos, A. R., Graf, G., & Gumanao, G. S. (2011). Size-specific locomotion rate and movement pattern of four common Indo-Pacific sea stars (Echinodermata; Asteroidea). *Aquatic Biology*, 12(2), 157-164. <https://doi.org/10.3354/ab00326>.
- Munday, P. L., Warner, R. R., Monro, K., Pandolfi, J. M., Marshall, D. J., & Wootton, T. (2013). Predicting evolutionary responses to climate change in the sea. *Ecology Letters*, 16(12), 1488-1500. <https://doi.org/10.1111/ele.12185>.
- Murphy, D. J. (2001). The biogenesis and functions of lipid bodies in animals, plants and microorganisms. *Progress in Lipid Research*, 40(5), 325-438. [https://doi.org/10.1016/s0163-7827\(01\)00013-3](https://doi.org/10.1016/s0163-7827(01)00013-3).
- Nagelkerken, I., & Munday, P. L. (2016). Animal behaviour shapes the ecological effects of ocean acidification and warming: moving from individual to community-level responses. *Global Change Biology*, 22(3), 974-989. <https://doi.org/10.1111/gcb.13167>.
- Nakamura, M. T., & Nara, T. Y. (2004). Structure, function, and dietary regulation of $\Delta 6$, $\Delta 5$, and $\Delta 9$ desaturases. *Annual Review of Nutrition*, 24, 345-376. <https://doi.org/10.1146/annurev.nutr.24.121803.063211>.
- Nguyen, H. D., & Byrne, M. (2014). Early benthic juvenile *Parvulastra exigua* (Asteroidea) are tolerant to extreme acidification and warming in its intertidal habitat. *Journal of Experimental Marine Biology and Ecology*, 453, 36-42. <https://doi.org/10.1016/j.jembe.2013.12.007>.
- Nguyen, H. D., Doo, S. S., Soars, N. A., & Byrne, M. (2012). Noncalcifying larvae in a changing ocean: warming, not acidification/hypercapnia, is the dominant stressor on development of the sea star *Meridiastra calcar*. *Global Change Biology*, 18(8), 2466-2476. <https://doi.org/10.1111/j.1365-2486.2012.02714.x>.
- Nguyen, K. D., Morley, S. A., Lai, C. H., Clark, M. S., Tan, K. S., Bates, A. E., & Peck, L. S. (2011). Upper temperature limits of tropical marine ectotherms: Global warming implications. *PLoS One*, 6(12), e29340. <https://doi.org/10.1371/journal.pone.0029340>.
- NOAA. (2023). *Climate at a glance: Global time series*. NOAA National Centers for Environmental information. <https://www.ncei.noaa.gov/access/monitoring/climate-at-a-glance/global/time-series>.
- O'Loughlin, P. M., & Rowe, F. W. E. (2006). A systematic revision of the asterinid genus *Aquilonastra* O'Loughlin, 2004 (Echinodermata: Asteroidea). *Memoirs of Museum Victoria*, 63(2), 257-287. <https://doi.org/10.24199/j.mmv.2006.63.18>.

- O'Brien, A. L., Dafforn, K., Chariton, A., Airoidi, L., Schäfer, R. B., & Mayer-Pinto, M. (2023). Multiple stressors. In A. Reichelt-Brushett (Ed.), *Marine pollution – monitoring, management and mitigation* (pp. 305-315). Springer, Cham. https://doi.org/10.1007/978-3-031-10127-4_14.
- O'Loughlin, P. M., & Waters, J. M. (2004). A molecular and morphological revision of genera of Asterinidae (Echinodermata: Asteroidea). *Memoirs of Museum Victoria*, 61(1), 1-40. <https://doi.org/10.24199/j.mmv.2004.61.1>.
- Occhipinti-Ambrogi, A. (2007). Global change and marine communities: Alien species and climate change. *Marine Pollution Bulletin*, 55(7-9), 342-352. <https://doi.org/10.1016/j.marpolbul.2006.11.014>.
- Olson, I. C., Kozdon, R., Valley, J. W., & Gilbert, P. U. (2012). Mollusk shell nacre ultrastructure correlates with environmental temperature and pressure. *Journal of the American Chemical Society*, 134(17), 7351-7358. <https://doi.org/10.1021/ja210808s>.
- Ong, E. Z., Briffa, M., Moens, T., & Van Colen, C. (2017). Physiological responses to ocean acidification and warming synergistically reduce condition of the common cockle *Cerastoderma edule*. *Marine Environmental Research*, 130, 38-47. <https://doi.org/10.1016/j.marenvres.2017.07.001>.
- Oomori, T., Kaneshima, H., Maezato, Y., & Kitano, Y. (1987). Distribution coefficient of Mg²⁺ ions between calcite and solution at 10–50°C. *Marine Chemistry*, 20(4), 327-336. [https://doi.org/10.1016/0304-4203\(87\)90066-1](https://doi.org/10.1016/0304-4203(87)90066-1).
- Orr, J. C., Fabry, V. J., Aumont, O., Bopp, L., Doney, S. C., Feely, R. A., Gnanadesikan, A., Gruber, N., Ishida, A., Joos, F., Key, R. M., Lindsay, K., Maier-Reimer, E., Matear, R., Monfray, P., Mouchet, A., Najjar, R. G., Plattner, G. K., Rodgers, K. B., . . . Yool, A. (2005). Anthropogenic ocean acidification over the twenty-first century and its impact on calcifying organisms. *Nature*, 437(7059), 681-686. <https://doi.org/10.1038/nature04095>.
- Padilla, D. K., & Savedo, M. M. (2013). A systematic review of phenotypic plasticity in marine invertebrate and plant systems. In M. Lesser (Ed.), *Advances in Marine Biology* (Vol. 65, pp. 67-94). Academic Press. <https://doi.org/10.1016/B978-0-12-410498-3.00002-1>.
- Paganini, A. W., Miller, N. A., & Stillman, J. H. (2014). Temperature and acidification variability reduce physiological performance in the intertidal zone porcelain crab *Petrolisthes cinctipes*. *Journal of Experimental Biology*, 217(Pt 22), 3974-3980. <https://doi.org/10.1242/jeb.109801>.
- Paine, R. T. (1966). Food web complexity and species diversity. *The American Naturalist*, 100(910), 65-75.

- Pan, T. C., Applebaum, S. L., & Manahan, D. T. (2015). Experimental ocean acidification alters the allocation of metabolic energy. *Proceedings of the National Academy of Sciences of the United States of America*, *112*(15), 4696-4701. <https://doi.org/10.1073/pnas.1416967112>.
- Parker, E. D., Forbes, V. E., Nielsen, S. L., Ritter, C., Barata, C., Baird, D. J., Admiraal, W., Levin, L., Loeschke, V., Lyytikäinen-Saarenmaa, P., Høgh-Jensen, H., Calow, P., & Ripley, B. J. (1999). Stress in ecological systems. *Oikos*, *86*(1). <https://doi.org/10.2307/3546584>.
- Parker, L. M., O'Connor, W. A., Raftos, D. A., Portner, H. O., & Ross, P. M. (2015). Persistence of positive carryover effects in the oyster, *Saccostrea glomerata*, following transgenerational exposure to ocean acidification. *PLoS One*, *10*(7), e0132276. <https://doi.org/10.1371/journal.pone.0132276>.
- Parmar, T. K., Rawtani, D., & Agrawal, Y. K. (2016). Bioindicators: the natural indicator of environmental pollution. *Frontiers in Life Science*, *9*(2), 110-118. <https://doi.org/10.1080/21553769.2016.1162753>.
- Parrish, C. C. (2013). Lipids in marine ecosystems. *ISRN Oceanography*, *2013*, 604045. <https://doi.org/10.5402/2013/604045>.
- Pawson, D. L. (2007). Phylum Echinodermata. *Zootaxa*, *1668*(1), 749-764. <https://doi.org/10.11646/zootaxa.1668.1.31>.
- Pechenik, J. A. (2006). Larval experience and latent effects--metamorphosis is not a new beginning. *Integrative and Comparative Biology*, *46*(3), 323-333. <https://doi.org/10.1093/icb/icj028>.
- Peck, L. S., Clark, M. S., Morley, S. A., Massey, A., & Rossetti, H. (2009). Animal temperature limits and ecological relevance: effects of size, activity and rates of change. *Functional Ecology*, *23*(2), 248-256. <https://doi.org/10.1111/j.1365-2435.2008.01537.x>.
- Peck, L. S., Webb, K. E., Miller, A., Clark, M. S., & Hill, T. (2008). Temperature limits to activity, feeding and metabolism in the Antarctic starfish *Odontaster validus*. *Marine Ecology Progress Series*, *358*, 181-189. <https://doi.org/10.3354/meps07336>.
- Pelletier, G., Lewis, E., & Wallace, D. (2007a). CO₂SYS.xls: A calculator for the CO₂ system in seawater for Microsoft Excel/VBA.
- Pelletier, G., Lewis, E., & Wallace, D. (2007b). CO₂SYS.xls: A calculator for the CO₂ System in Seawater for Microsoft Excel/VBA. In Washington State Department for Ecology, Olympia, WA.
- Peng, C., Zhao, X., Liu, S., Shi, W., Han, Y., Guo, C., Peng, X., Chai, X., & Liu, G. (2017). Ocean acidification alters the burrowing behaviour, Ca²⁺/Mg²⁺-ATPase activity, metabolism, and gene expression of a bivalve species, *Sinonovacula constricta*. *Marine Ecology Progress Series*, *575*, 107-117. <https://doi.org/10.3354/meps12224>.

- Pereira, T. M., Gnocchi, K. G., Mercon, J., Mendes, B., Lopes, B. M., Passos, L. S., & Chippari Gomes, A. R. (2020). The success of the fertilization and early larval development of the tropical sea urchin *Echinometra lucunter* (Echinodermata: Echinoidea) is affected by the pH decrease and temperature increase. *Marine Environmental Research*, *161*, 105106. <https://doi.org/10.1016/j.marenvres.2020.105106>.
- Petersen, O. H., & Verkhatsky, A. (2016). Calcium and ATP control multiple vital functions. *Philosophical Transactions of the Royal Society of London B Biological Sciences*, *371*(1700). <https://doi.org/10.1098/rstb.2015.0418>.
- Peterson, R. A. (2021). Finding optimal normalizing transformations via bestNormalize. *The R Journal*, *13*(1), 310-329. <https://doi.org/10.32614/rj-2021-041>.
- Piersma, T., & Drent, J. (2003). Phenotypic flexibility and the evolution of organismal design. *Trends in Ecology & Evolution*, *18*(5), 228-233. [https://doi.org/10.1016/s0169-5347\(03\)00036-3](https://doi.org/10.1016/s0169-5347(03)00036-3).
- Piersma, T., & Lindström, Å. (1997). Rapid reversible changes in organ size as a component of adaptive behaviour. *Trends in Ecology & Evolution*, *12*(4), 134-138. [https://doi.org/10.1016/s0169-5347\(97\)01003-3](https://doi.org/10.1016/s0169-5347(97)01003-3).
- Piggott, J. J., Townsend, C. R., & Matthaei, C. D. (2015). Reconceptualizing synergism and antagonism among multiple stressors. *Ecology and Evolution*, *5*(7), 1538-1547. <https://doi.org/10.1002/ece3.1465>.
- Pigliucci, M., Murren, C. J., & Schlichting, C. D. (2006). Phenotypic plasticity and evolution by genetic assimilation. *Journal of Experimental Biology*, *209*(12), 2362-2367. <https://doi.org/10.1242/jeb.02070>.
- Pincebourde, S., Sanford, E., & Helmuth, B. (2009). An intertidal sea star adjusts thermal inertia to avoid extreme body temperatures. *American Naturalist*, *174*(6), 890-897. <https://doi.org/10.1086/648065>.
- Pinsky, M. L., Selden, R. L., & Kitchel, Z. J. (2020). Climate-driven shifts in marine species ranges: Scaling from organisms to communities. *Annual Review of Marine Science*, *12*, 153-179. <https://doi.org/10.1146/annurev-marine-010419-010916>.
- Politi, Y., Arad, T., Klein, E., Weiner, S., & Addadi, L. (2004). Sea urchin spine calcite forms via a transient amorphous calcium carbonate phase. *Science*, *306*(5699), 1161-1164. <https://doi.org/10.1126/science.1102289>.
- Poloczanska, E. S., Brown, C. J., Sydeman, W. J., Kiessling, W., Schoeman, D. S., Moore, P. J., Brander, K., Bruno, J. F., Buckley, L. B., Burrows, M. T., Duarte, C. M., Halpern, B. S., Holding, J., Kappel, C. V., O'Connor, M. I., Pandolfi, J. M., Parmesan, C., Schwing, F., Thompson, S. A., & Richardson, A. J. (2013). Global imprint of climate change on marine life. *Nature Climate Change*, *3*(10), 919-925. <https://doi.org/10.1038/nclimate1958>.

- Poloczanska, E. S., Burrows, M. T., Brown, C. J., García Molinos, J., Halpern, B. S., Hoegh-Guldberg, O., Kappel, C. V., Moore, P. J., Richardson, A. J., Schoeman, D. S., & Sydeman, W. J. (2016). Responses of marine organisms to climate change across oceans. *Frontiers in Marine Science*, 3. <https://doi.org/10.3389/fmars.2016.00062>.
- Pörtner, H. (2008). Ecosystem effects of ocean acidification in times of ocean warming: A physiologist's view. *Marine Ecology Progress Series*, 373, 203-217. <https://doi.org/10.3354/meps07768>.
- Pörtner, H. O. (2002). Climate variations and the physiological basis of temperature dependent biogeography: systemic to molecular hierarchy of thermal tolerance in animals. *Comparative Biochemistry and Physiology, Part A: Molecular & Integrative Physiology*, 132(4), 739-761. [https://doi.org/10.1016/s1095-6433\(02\)00045-4](https://doi.org/10.1016/s1095-6433(02)00045-4).
- Pörtner, H. O. (2012). Integrating climate-related stressor effects on marine organisms: unifying principles linking molecule to ecosystem-level changes. *Marine Ecology Progress Series*, 470, 273-290. <https://doi.org/10.3354/meps10123>.
- Pörtner, H. O., & Farrell, A. P. (2008). Physiology and climate change. *Science*, 322(5902), 690-692. <https://doi.org/10.1126/science.1163156>.
- Pörtner, H. O., Langenbuch, M., & Reipschläger, A. (2004). Biological impact of elevated ocean co2 concentrations: Lessons from animal physiology and earth history. *Journal of Oceanography*, 60(4), 705-718. <https://doi.org/10.1007/s10872-004-5763-0>.
- Prazeres, M., & Pandolfi, J. M. (2016). Effects of elevated temperature on the shell density of the large benthic foraminifera *Amphistegina lobifera*. *Journal of Eukaryotic Microbiology*, 63(6), 786-793. <https://doi.org/10.1111/jeu.12325>.
- Prazeres, M., Uthicke, S., & Pandolfi, J. M. (2015). Ocean acidification induces biochemical and morphological changes in the calcification process of large benthic foraminifera. *Proceedings of the Royal Society B: Biological Sciences*, 282(1803), 20142782. <https://doi.org/10.1098/rspb.2014.2782>.
- Przeslawski, R., Byrne, M., & Mellin, C. (2015). A review and meta-analysis of the effects of multiple abiotic stressors on marine embryos and larvae. *Global Change Biology*, 21(6), 2122-2140. <https://doi.org/10.1111/gcb.12833>.
- Purgstaller, B., Mavromatis, V., Goetschl, K. E., Steindl, F. R., & Dietzel, M. (2021). Effect of temperature on the transformation of amorphous calcium magnesium carbonate with near-dolomite stoichiometry into high Mg-calcite. *CrystEngComm*, 23(9), 1969-1981. <https://doi.org/10.1039/d0ce01679a>.
- R Core Team. (2022). R: A language and environment for statistical computing. R Foundation for Statistical Computing. <http://www.r-project.org/>.

- R Core Team. (2023). R: A language and environment for statistical computing. R Foundation for Statistical Computing. <http://www.r-project.org/>.
- Radha, A. V., Fernandez-Martinez, A., Hu, Y., Jun, Y.-S., Waychunas, G. A., & Navrotsky, A. (2012). Energetic and structural studies of amorphous $\text{Ca}_{1-x}\text{Mg}_x\text{CO}_3 \cdot n\text{H}_2\text{O}$ ($0 \leq x \leq 1$). *Geochimica et Cosmochimica Acta*, *90*, 83-95. <https://doi.org/10.1016/j.gca.2012.04.056>.
- Rahman, M. A., Molla, M. H. R., Megwalu, F. O., Asare, O. E., Tchoundi, A., Shaikh, M. M., & Jahan, B. (2018). The sea stars (Echinodermata: Asteroidea): Their biology, ecology, evolution and utilization. *SF Journal of Biotechnology and Biomedical Engineering*, *1*(2), 1007.
- Ramesh, K., Hu, M. Y., Thomsen, J., Bleich, M., & Melzner, F. (2017). Mussel larvae modify calcifying fluid carbonate chemistry to promote calcification. *Nature Communications*, *8*(1), 1709. <https://doi.org/10.1038/s41467-017-01806-8>.
- Ramonet, M., Chatterjee, A., Ciais, P., Levin, I., Sha, M. K., Steinbacher, M., & Sweeney, C. (2023). CO_2 in the atmosphere: Growth and trends since 1850. In *Oxford Research Encyclopedia of Climate Science*. <https://doi.org/10.1093/acrefore/9780190228620.013.863>.
- Randall, D. J., Burggren, W., & French, K. (1997). *Eckert animal physiology: Mechanisms and adaptations* (4th ed.). W. H. Freeman and Company.
- Ratcliffe, P. J., Jones, N. V., & Walters, N. J. (1981). The survival of *Macoma balthica* (L.) in mobile sediments. In N. V. Jones & W. J. Wolff (Eds.), *Feeding and survival strategies of estuarine organisms* (pp. 91-108). https://doi.org/10.1007/978-1-4613-3318-0_8.
- Rathburn, A. E., & De Deckker, P. (1997). Magnesium and strontium compositions of recent benthic foraminifera from the Coral Sea, Australia and Prydz Bay, Antarctica. *Marine Micropaleontology*, *32*(3-4), 231-248. [https://doi.org/10.1016/s0377-8398\(97\)00028-5](https://doi.org/10.1016/s0377-8398(97)00028-5).
- Raz, S., Weiner, S., & Addadi, L. (2000). Formation of high-magnesian calcites via an amorphous precursor phase: Possible biological implications. *Advanced Materials*, *12*(1), 38-42. [https://doi.org/10.1002/\(sici\)1521-4095\(200001\)12:1<38::Aid-adma38>3.0.Co;2-i](https://doi.org/10.1002/(sici)1521-4095(200001)12:1<38::Aid-adma38>3.0.Co;2-i).
- Reynaud, S., Ferrier-Pagès, C., Meibom, A., Mostefaoui, S., Mortlock, R., Fairbanks, R., & Allemand, D. (2007). Light and temperature effects on Sr/Ca and Mg/Ca ratios in the scleractinian coral *Acropora* sp. *Geochimica et Cosmochimica Acta*, *71*(2), 354-362. <https://doi.org/10.1016/j.gca.2006.09.009>.
- Ries, J. B. (2011). A physicochemical framework for interpreting the biological calcification response to CO_2 -induced ocean acidification. *Geochimica et Cosmochimica Acta*, *75*(14), 4053-4064. <https://doi.org/10.1016/j.gca.2011.04.025>.
- Ries, J. B., Cohen, A. L., & McCorkle, D. C. (2009). Marine calcifiers exhibit mixed responses to CO_2 -induced ocean acidification. *Geology*, *37*(12), 1131-1134. <https://doi.org/10.1130/g30210a.1>.

- Ries, J. B., Ghazaleh, M. N., Connolly, B., Westfield, I., & Castillo, K. D. (2016). Impacts of seawater saturation state ($\Omega_A=0.4-4.6$) and temperature (10, 25 °C) on the dissolution kinetics of whole-shell biogenic carbonates. *Geochimica et Cosmochimica Acta*, *192*, 318-337. <https://doi.org/10.1016/j.gca.2016.07.001>.
- Rodolfo-Metalpa, R., Lombardi, C., Cocito, S., Hall-Spencer, J. M., & Gambi, M. C. (2010). Effects of ocean acidification and high temperatures on the bryozoan *Myriapora truncata* at natural CO₂ vents. *Marine Ecology*, *31*, 447-456. <https://doi.org/10.1111/j.1439-0485.2009.00354.x>.
- Roleda, M. Y., Boyd, P. W., & Hurd, C. L. (2012). Before ocean acidification: Calcifier chemistry lessons. *Journal of Phycology*, *48*(4), 840-843 <https://doi.org/10.1111/j.1529-8817.2012.01195.x>.
- Root, T. L., Price, J. T., Hall, K. R., Schneider, S. H., Rosenzweig, C., & Pounds, J. A. (2003). Fingerprints of global warming on wild animals and plants. *Nature*, *421*(6918), 57-60. <https://doi.org/10.1038/nature01333>.
- Rosenthal, Y., Boyle, E. A., & Slowey, N. (1997). Temperature control on the incorporation of magnesium, strontium, fluorine, and cadmium into benthic foraminiferal shells from Little Bahama Bank: Prospects for thermocline paleoceanography. *Geochimica et Cosmochimica Acta*, *61*(17), 3633-3643. [https://doi.org/10.1016/s0016-7037\(97\)00181-6](https://doi.org/10.1016/s0016-7037(97)00181-6).
- Ross, P. M., Parker, L., O'Connor, W. A., & Bailey, E. A. (2011). The impact of ocean acidification on reproduction, early development and settlement of marine organisms. *Water*, *3*(4), 1005-1030. <https://doi.org/10.3390/w3041005>.
- Ross, P. M., Scanes, E., Byrne, M., Ainsworth, T. D., Donelson, J. M., Foo, S. A., Hutchings, P., Thiyagarajan, V., Parker, & Laura, M. (2023). Surviving the anthropocene: The resilience of marine animals to climate change. In S. J. Hawkins, B. D. Russell, & T. P. A. (Eds.), *Oceanography and Marine Biology* (Vol. 61, pp. 35-80). CRC Press. <https://doi.org/10.1201/9781003363873-3>.
- Rossoll, D., Bermudez, R., Hauss, H., Schulz, K. G., Riebesell, U., Sommer, U., & Winder, M. (2012). Ocean acidification-induced food quality deterioration constrains trophic transfer. *PLoS One*, *7*(4), e34737. <https://doi.org/10.1371/journal.pone.0034737>.
- Rothig, T., Trevathan-Tackett, S. M., Voolstra, C. R., Ross, C., Chaffron, S., Durack, P. J., Warmuth, L. M., & Sweet, M. (2023). Human-induced salinity changes impact marine organisms and ecosystems. *Global Change Biology*, *29*(17), 4731-4749. <https://doi.org/10.1111/gcb.16859>.

- Ruela, R., Sousa, M. C., deCastro, M., & Dias, J. M. (2020). Global and regional evolution of sea surface temperature under climate change. *Global and Planetary Change*, 190. <https://doi.org/10.1016/j.gloplacha.2020.103190>.
- Russell, A. D., Hönisch, B., Spero, H. J., & Lea, D. W. (2004). Effects of seawater carbonate ion concentration and temperature on shell U, Mg, and Sr in cultured planktonic foraminifera. *Geochimica et Cosmochimica Acta*, 68(21), 4347-4361. <https://doi.org/10.1016/j.gca.2004.03.013>.
- Sabine, C. L., Feely, R. A., Gruber, N., Key, R. M., Lee, K., Bullister, J. L., Wanninkhof, R., Wong, C. S., Wallace, D. W., Tilbrook, B., Millero, F. J., Peng, T. H., Kozyr, A., Ono, T., & Rios, A. F. (2004). The oceanic sink for anthropogenic CO₂. *Science*, 305(5682), 367-371. <https://doi.org/10.1126/science.1097403>.
- Safuan, C. D. M., Samshuri, M. A., Jaafar, S. N., Tan, C. H., & Bachok, Z. (2021). Physiological response of shallow-water hard coral *Acropora digitifera* to heat stress via fatty acid composition. *Frontiers in Marine Science*, 8. <https://doi.org/10.3389/fmars.2021.715167>.
- Saier, B. (2001). Direct and indirect effects of seastars *Asterias rubens* on mussel beds (*Mytilus edulis*) in the Wadden Sea. *Journal of Sea Research*, 46(1), 29-42. [https://doi.org/10.1016/s1385-1101\(01\)00067-3](https://doi.org/10.1016/s1385-1101(01)00067-3).
- Sampaio, E., Santos, C., Rosa, I. C., Ferreira, V., Portner, H. O., Duarte, C. M., Levin, L. A., & Rosa, R. (2021). Impacts of hypoxic events surpass those of future ocean warming and acidification. *Nature Ecology & Evolution*, 5(3), 311-321. <https://doi.org/10.1038/s41559-020-01370-3>.
- Schalkhauser, B., Bock, C., Stemmer, K., Brey, T., Pörtner, H.-O., & Lannig, G. (2012). Impact of ocean acidification on escape performance of the king scallop, *Pecten maximus*, from Norway. *Marine Biology*, 160(8), 1995-2006. <https://doi.org/10.1007/s00227-012-2057-8>.
- Schmitz, G., & Ecker, J. (2008). The opposing effects of n-3 and n-6 fatty acids. *Progress in Lipid Research*, 47(2), 147-155. <https://doi.org/10.1016/j.plipres.2007.12.004>.
- Schulte, P. M. (2011). Effects of temperature: An introduction. In A. P. Farrell (Ed.), *Encyclopedia of fish physiology* (pp. 1688-1694). Academic Press. <https://doi.org/10.1016/B978-0-12-374553-8.00159-3>.
- Schulte, P. M. (2015). The effects of temperature on aerobic metabolism: towards a mechanistic understanding of the responses of ectotherms to a changing environment. *Journal of Experimental Biology*, 218(Pt 12), 1856-1866. <https://doi.org/10.1242/jeb.118851>.

- Schulte, P. M., Healy, T. M., & Fague, N. A. (2011). Thermal performance curves, phenotypic plasticity, and the time scales of temperature exposure. *Integrative and Comparative Biology*, 51(5), 691-702. <https://doi.org/10.1093/icb/icr097>.
- Schwaner, C., Barbosa, M., Schwemmer, T. G., Pales Espinosa, E., & Allam, B. (2023). Increased food resources help eastern oyster mitigate the negative impacts of coastal acidification. *Animals*, 13(7). <https://doi.org/10.3390/ani13071161>.
- Seebacher, F., White, C. R., & Franklin, C. E. (2014). Physiological plasticity increases resilience of ectothermic animals to climate change. *Nature Climate Change*, 5(1), 61-66. <https://doi.org/10.1038/nclimate2457>.
- Seibel, B. A., & Drazen, J. C. (2007). The rate of metabolism in marine animals: environmental constraints, ecological demands and energetic opportunities. *Philosophical Transactions of the Royal Society of London B Biological Sciences*, 362(1487), 2061-2078. <https://doi.org/10.1098/rstb.2007.2101>.
- Seibel, B. A., & Walsh, P. J. (2001). Carbon cycle. Potential impacts of CO₂ injection on deep-sea biota. *Science*, 294(5541), 319-320. <https://doi.org/10.1126/science.1065301>.
- Seibel, B. A., & Walsh, P. J. (2003). Biological impacts of deep-sea carbon dioxide injection inferred from indices of physiological performance. *Journal of Experimental Biology*, 206(4), 641-650. <https://doi.org/10.1242/jeb.00141>.
- Shannon, R. D. (1976). Revised effective ionic radii and systematic studies of interatomic distances in halides and chalcogenides. *Acta Crystallographica Section A*, 32(5), 751-767. <https://doi.org/10.1107/s0567739476001551>.
- Shapiro, S. S., & Wilk, M. B. (1965). An analysis of variance test for normality (complete samples). *Biometrika*, 52(3/4), 591-611. <https://doi.org/10.2307/2333709>.
- Shirayama, Y. (2005). Effect of increased atmospheric CO₂ on shallow water marine benthos. *Journal of Geophysical Research*, 110(C9). <https://doi.org/10.1029/2004jc002618>.
- Simeoni, C., Furlan, E., Pham, H. V., Critto, A., de Juan, S., Tregarot, E., Cornet, C. C., Meesters, E., Fonseca, C., Botelho, A. Z., Krause, T., N'Guetta, A., Cordova, F. E., Failler, P., & Marcomini, A. (2023). Evaluating the combined effect of climate and anthropogenic stressors on marine coastal ecosystems: Insights from a systematic review of cumulative impact assessment approaches. *Science of the Total Environment*, 861, 160687. <https://doi.org/10.1016/j.scitotenv.2022.160687>.
- Simonetti, S., Zupo, V., Gambi, M. C., Luckenbach, T., & Corsi, I. (2022). Unraveling cellular and molecular mechanisms of acid stress tolerance and resistance in marine species: New frontiers in the study of adaptation to ocean acidification. *Marine Pollution Bulletin*, 185(Pt B), 114365. <https://doi.org/10.1016/j.marpolbul.2022.114365>.

- Sinclair, E. L. E., Thompson, M. B., & Seebacher, F. (2006). Phenotypic flexibility in the metabolic response of the limpet *Cellana tramoserica* to thermally different microhabitats. *Journal of Experimental Marine Biology and Ecology*, 335(1), 131-141. <https://doi.org/10.1016/j.jembe.2006.03.010>.
- Sinensky, M. (1974). Homeoviscous adaptation—A homeostatic process that regulates the viscosity of membrane lipids in *Escherichia coli*. *Proceedings of the National Academy of Sciences of the United States of America*, 71(2), 522-525. <https://doi.org/10.1073/pnas.71.2.522>.
- Skinner, H. C. W., & Ehrlich, H. (2014). Biomineralization. In H. D. Holland & K. K. Turekian (Eds.), *Treatise on Geochemistry* (Vol. 10, pp. 105-162). Elsevier. <https://doi.org/10.1016/b978-0-08-095975-7.00804-4>.
- Slein, M. A., Bernhardt, J. R., O'Connor, M. I., & Fey, S. B. (2023). Effects of thermal fluctuations on biological processes: a meta-analysis of experiments manipulating thermal variability. *Proc Biol Sci*, 290(1992), 20222225. <https://doi.org/10.1098/rspb.2022.2225>.
- Smale, D. A., Wernberg, T., Oliver, E. C. J., Thomsen, M., Harvey, B. P., Straub, S. C., Burrows, M. T., Alexander, L. V., Benthuyzen, J. A., Donat, M. G., Feng, M., Hobday, A. J., Holbrook, N. J., Perkins-Kirkpatrick, S. E., Scannell, H. A., Sen Gupta, A., Payne, B. L., & Moore, P. J. (2019). Marine heatwaves threaten global biodiversity and the provision of ecosystem services. *Nature Climate Change*, 9(4), 306-312. <https://doi.org/10.1038/s41558-019-0412-1>.
- Smith, A. M., Clark, D. E., Lamare, M. D., Winter, D. J., & Byrne, M. (2016). Risk and resilience: variations in magnesium in echinoid skeletal calcite. *Marine Ecology Progress Series*, 561, 1-16. <https://doi.org/10.3354/meps11908>.
- Smith, A. M., Key, M. M., & Gordon, D. P. (2006). Skeletal mineralogy of bryozoans: Taxonomic and temporal patterns. *Earth-Science Reviews*, 78(3-4), 287-306. <https://doi.org/10.1016/j.earscirev.2006.06.001>.
- Smith, K. E., Burrows, M. T., Hobday, A. J., King, N. G., Moore, P. J., Sen Gupta, A., Thomsen, M. S., Wernberg, T., & Smale, D. A. (2023). Biological impacts of marine heatwaves. *Annual Review of Marine Science*, 15, 119-145. <https://doi.org/10.1146/annurev-marine-032122-121437>.
- Sokal, R. R., & Rohlf, F. J. (2012). *Biometry: the principles and practice of statistics in biological research* (4 ed.). W.H. Freeman and Co. <https://doi.org/10.1002/iroh.19710560218>.
- Sokolova, I. M., Frederich, M., Bagwe, R., Lannig, G., & Sukhotin, A. A. (2012). Energy homeostasis as an integrative tool for assessing limits of environmental stress tolerance in aquatic invertebrates. *Marine Environmental Research*, 79, 1-15. <https://doi.org/10.1016/j.marenvres.2012.04.003>.

- Somero, G. N. (1978). Temperature adaptation of enzymes: Biological optimization through structure-function compromises. *Annual Review of Ecology and Systematics*, 9(1), 1-29. <https://doi.org/10.1146/annurev.es.09.110178.000245>.
- Somero, G. N. (2002). Thermal physiology and vertical zonation of intertidal animals: optima, limits, and costs of living. *Integrative and Comparative Biology*, 42(4), 780-789. <https://doi.org/10.1093/icb/42.4.780>.
- Somero, G. N. (2010). The physiology of climate change: how potentials for acclimatization and genetic adaptation will determine 'winners' and 'losers'. *Journal of Experimental Biology*, 213(6), 912-920. <https://doi.org/10.1242/jeb.037473>.
- Somero, G. N. (2012). The physiology of global change: Linking patterns to mechanisms. *Annual Review of Marine Science*, 4, 39-61. <https://doi.org/10.1146/annurev-marine-120710-100935>.
- Sonnenholzner, J. I., Montaña-Moctezuma, G., & Searcy-Bernal, R. (2010). Effect of three tagging methods on the growth and survival of the purple sea urchin *Strongylocentrotus purpuratus*. *Pan-American Journal of Aquatic Sciences*, 5(3), 414-420.
- Stanley-Samuelson, D. W. (1987). Physiological roles of prostaglandins and other eicosanoids in invertebrates. *The Biological Bulletin*, 173(1), 92-109. <https://doi.org/10.2307/1541865>.
- Stanley, S. M., Ries, J. B., & Hardie, L. A. (2002). Low-magnesium calcite produced by coralline algae in seawater of Late Cretaceous composition. *Proceedings of the National Academy of Sciences of the United States of America*, 99(24), 15323-15326. <https://doi.org/10.1073/pnas.232569499>.
- Staudinger, M. D., Carter, S. L., Cross, M. S., Dubois, N. S., Duffy, J. E., Enquist, C., Griffis, R., Hellmann, J. J., Lawler, J. J., O'Leary, J., Morrison, S. A., Sneddon, L., Stein, B. A., Thompson, L. M., & Turner, W. (2013). Biodiversity in a changing climate: A synthesis of current and projected trends in the US. *Frontiers in Ecology and the Environment*, 11(9), 465-473. <https://doi.org/10.1890/120272>.
- Stevens, A. M., & Gobler, C. J. (2018). Interactive effects of acidification, hypoxia, and thermal stress on growth, respiration, and survival of four North Atlantic bivalves. *Marine Ecology Progress Series*, 604, 143-161. <https://doi.org/10.3354/meps12725>.
- Stickle, W. B., & Diehl, W. J. (1987). Effects of salinity on echinoderms. In M. Jangoux & J. M. Lawrence (Eds.), *Echinoderm Studies* (Vol. 2, pp. 235-285). A. A. Balkema.
- Stock, C. A., Cheung, W. W. L., Sarmiento, J. L., & Sunderland, E. M. (2019). Changing ocean systems: A short synthesis. In A. M. Cisneros-Montemayor, W. W. L. Cheung, & Y. Ota (Eds.), *Predicting future oceans* (pp. 19-34). Elsevier. <https://doi.org/10.1016/b978-0-12-817945-1.00002-2>.

- Stoll, H. M., Rosenthal, Y., & Falkowski, P. (2002). Climate proxies from Sr/Ca of coccolith calcite: Calibrations from continuous culture of *Emiliania huxleyi*. *Geochimica et Cosmochimica Acta*, 66(6), 927-936. [https://doi.org/10.1016/s0016-7037\(01\)00836-5](https://doi.org/10.1016/s0016-7037(01)00836-5).
- Strahl, J., Francis, D. S., Doyle, J., Humphrey, C., & Fabricius, K. E. (2016). Biochemical responses to ocean acidification contrast between tropical corals with high and low abundances at volcanic carbon dioxide seeps. *ICES Journal of Marine Science*, 73(3), 897-909. <https://doi.org/10.1093/icesjms/fsv194>.
- Stuart-Smith, R. D., Edgar, G. J., & Bates, A. E. (2017). Thermal limits to the geographic distributions of shallow-water marine species. *Nat Ecol Evol*, 1(12), 1846-1852. <https://doi.org/10.1038/s41559-017-0353-x>.
- Stuckless, B., Hamel, J. F., Aguzzi, J., & Mercier, A. (2023). Intra- and interspecific foraging and feeding interactions in three sea stars and a gastropod from the deep sea. *Biology*, 12(6). <https://doi.org/10.3390/biology12060774>.
- Stuhr, M., Cameron, L. P., Blank-Landeshammer, B., Reymond, C. E., Doo, S. S., Westphal, H., Sickmann, A., & Ries, J. B. (2021). Divergent proteomic responses offer insights into resistant physiological responses of a reef-foraminifera to climate change scenarios. *Oceans*, 2(2), 281-314. <https://doi.org/10.3390/oceans2020017>.
- Stumpff, M., & Hu, M. Y. (2017). pH regulation and excretion in echinoderms. In D. Weihrauch & M. O'Donnell (Eds.), *Acid-base balance and nitrogen excretion in invertebrates* (pp. 261-273). Springer. https://doi.org/10.1007/978-3-319-39617-0_10.
- Stumpff, M., Hu, M. Y., Melzner, F., Gutowska, M. A., Dorey, N., Himmerkus, N., Holtmann, W. C., Dupont, S. T., Thorndyke, M. C., & Bleich, M. (2012). Acidified seawater impacts sea urchin larvae pH regulatory systems relevant for calcification. *Proceedings of the National Academy of Sciences of the United States of America*, 109(44), 18192-18197. <https://doi.org/10.1073/pnas.1209174109>.
- Suggett, D. J., & Smith, D. J. (2020). Coral bleaching patterns are the outcome of complex biological and environmental networking. *Global Change Biology*, 26(1), 68-79. <https://doi.org/10.1111/gcb.14871>.
- Sunday, J. M., Bates, A. E., & Dulvy, N. K. (2012). Thermal tolerance and the global redistribution of animals. *Nature Climate Change*, 2(9), 686-690. <https://doi.org/10.1038/nclimate1539>.
- Sydeman, W. J., & Bograd, S. J. (2009). Marine ecosystems, climate and phenology: introduction. *Marine Ecology Progress Series*, 393, 185-188. <https://doi.org/10.3354/meps08382>.
- Tang, Y., Du, X., Sun, S., Shi, W., Han, Y., Zhou, W., Zhang, J., Teng, S., Ren, P., & Liu, G. (2022). Circadian rhythm and neurotransmitters are potential pathways through which ocean

- acidification and warming affect the metabolism of thick-shell mussels. *Environmental Science & Technology*, 56(7), 4324-4335. <https://doi.org/10.1021/acs.est.1c06735>.
- Tattersall, G. J., Sinclair, B. J., Withers, P. C., Fields, P. A., Seebacher, F., Cooper, C. E., & Maloney, S. K. (2012). Coping with thermal challenges: Physiological adaptations to environmental temperatures. *Comprehensive Physiology*, 2(3), 2151-2202. <https://doi.org/10.1002/cphy.c110055>.
- Tesoriero, A. J., & Pankow, J. F. (1996). Solid solution partitioning of Sr²⁺, Ba²⁺, and Cd²⁺ to calcite. *Geochimica et Cosmochimica Acta*, 60(6), 1053-1063. [https://doi.org/10.1016/0016-7037\(95\)00449-1](https://doi.org/10.1016/0016-7037(95)00449-1).
- Tewksbury, J. J., Huey, R. B., & Deutsch, C. A. (2008). Ecology. Putting the heat on tropical animals. *Science*, 320(5881), 1296-1297. <https://doi.org/10.1126/science.1159328>.
- Thackeray, S. J., Henrys, P. A., Hemming, D., Bell, J. R., Botham, M. S., Burthe, S., Helaouet, P., Johns, D. G., Jones, I. D., Leech, D. I., Mackay, E. B., Massimino, D., Atkinson, S., Bacon, P. J., Brereton, T. M., Carvalho, L., Clutton-Brock, T. H., Duck, C., Edwards, M., . . . Wanless, S. (2016). Phenological sensitivity to climate across taxa and trophic levels. *Nature*, 535(7611), 241-245. <https://doi.org/10.1038/nature18608>.
- Thomas, J. T., Munday, P. L., & Watson, S.-A. (2020). Toward a mechanistic understanding of marine invertebrate behavior at elevated CO₂. *Frontiers in Marine Science*, 7. <https://doi.org/10.3389/fmars.2020.00345>.
- Thushari, G. G. N., & Senevirathna, J. D. M. (2020). Plastic pollution in the marine environment. *Heliyon*, 6(8), e04709. <https://doi.org/10.1016/j.heliyon.2020.e04709>.
- Tocher, D. R. (2010). Metabolism and functions of lipids and fatty acids in teleost fish. *Reviews in Fisheries Science*, 11(2), 107-184. <https://doi.org/10.1080/713610925>.
- Todd, P. A. (2008). Morphological plasticity in scleractinian corals. *Biological Reviews of the Cambridge Philosophical Society*, 83(3), 315-337. <https://doi.org/10.1111/j.1469-185x.2008.00045.x>.
- Todgham, A. E., & Stillman, J. H. (2013). Physiological responses to shifts in multiple environmental stressors: Relevance in a changing world. *Integrative and Comparative Biology*, 53(4), 539-544. <https://doi.org/10.1093/icb/ict086>.
- Tomanek, L. (2010). Variation in the heat shock response and its implication for predicting the effect of global climate change on species' biogeographical distribution ranges and metabolic costs. *Journal of Experimental Biology*, 213(6), 971-979. <https://doi.org/10.1242/jeb.038034>.

- Towle, E. K., Enochs, I. C., & Langdon, C. (2015). Threatened Caribbean coral is able to mitigate the adverse effects of ocean acidification on calcification by increasing feeding rate. *PLoS One*, *10*(4), e0123394. <https://doi.org/10.1371/journal.pone.0123394>.
- Toyofuku, T., Kitazato, H., Kawahata, H., Tsuchiya, M., & Nohara, M. (2000). Evaluation of Mg/Ca thermometry in foraminifera: Comparison of experimental results and measurements in nature. *Paleoceanography*, *15*(4), 456-464. <https://doi.org/10.1029/1999pa000460>.
- Toyofuku, T., Matsuo, M. Y., de Nooijer, L. J., Nagai, Y., Kawada, S., Fujita, K., Reichart, G. J., Nomaki, H., Tsuchiya, M., Sakaguchi, H., & Kitazato, H. (2017). Proton pumping accompanies calcification in foraminifera. *Nature Communications*, *8*, 14145. <https://doi.org/10.1038/ncomms14145>.
- Tracy, A. M., Pielmeier, M. L., Yoshioka, R. M., Heron, S. F., & Harvell, C. D. (2019). Increases and decreases in marine disease reports in an era of global change. *Proceedings of the Royal Society B: Biological Sciences*, *286*(1912), 20191718. <https://doi.org/10.1098/rspb.2019.1718>.
- Tresguerres, M. (2016). Novel and potential physiological roles of vacuolar-type H⁺-ATPase in marine organisms. *Journal of Experimental Biology*, *219*(Pt 14), 2088-2097. <https://doi.org/10.1242/jeb.128389>.
- Tucker, M. E., & Wright, V. P. (1990). Carbonate mineralogy and chemistry. In *Carbonate sedimentology* (pp. 284-313). <https://doi.org/https://doi.org/10.1002/9781444314175.ch6>.
- Ulbricht, R. J. (1973). Effect of temperature acclimation on the metabolic rate of sea urchins. *Marine Biology*, *19*(4), 273-277. <https://doi.org/10.1007/bf00348893>.
- Uppström, L. R. (1974). The boron/chlorinity ratio of deep-sea water from the Pacific Ocean. *Deep Sea Research and Oceanographic Abstracts*, *21*(2), 161-162. [https://doi.org/10.1016/0011-7471\(74\)90074-6](https://doi.org/10.1016/0011-7471(74)90074-6).
- Uthicke, S., Liddy, M., Nguyen, H. D., & Byrne, M. (2014). Interactive effects of near-future temperature increase and ocean acidification on physiology and gonad development in adult Pacific sea urchin, *Echinometra* sp. A. *Coral Reefs*, *33*(3), 831-845. <https://doi.org/10.1007/s00338-014-1165-y>.
- Valles-Regino, R., Tate, R., Kelaher, B., Savins, D., Dowell, A., & Benkendorff, K. (2015). Ocean warming and CO₂-induced acidification impact the lipid content of a marine predatory gastropod. *Marine Drugs*, *13*(10), 6019-6037. <https://doi.org/10.3390/md13106019>.
- Vargas, C. A., Lagos, N. A., Lardies, M. A., Duarte, C., Manriquez, P. H., Aguilera, V. M., Broitman, B., Widdicombe, S., & Dupont, S. (2017). Species-specific responses to ocean acidification

- should account for local adaptation and adaptive plasticity. *Nature Ecology & Evolution*, 1(4), 84. <https://doi.org/10.1038/s41559-017-0084>.
- Venables, W. N., & Ripley, B. D. (2002). *Modern applied statistics with S* (4th ed.). Springer <https://doi.org/10.1007/978-0-387-21706-2>.
- Venegas, R. M., Acevedo, J., & Treml, E. A. (2023). Three decades of ocean warming impacts on marine ecosystems: A review and perspective. *Deep Sea Research Part II: Topical Studies in Oceanography*, 212. <https://doi.org/10.1016/j.dsr2.2023.105318>.
- Vijayavel, K., Gopalakrishnan, S., & Balasubramanian, M. P. (2007). Sublethal effect of silver and chromium in the green mussel *Perna viridis* with reference to alterations in oxygen uptake, filtration rate and membrane bound ATPase system as biomarkers. *Chemosphere*, 69(6), 979-986. <https://doi.org/10.1016/j.chemosphere.2007.05.011>.
- Vinagre, C., Mendonca, V., Cereja, R., Abreu-Afonso, F., Dias, M., Mizrahi, D., & Flores, A. A. V. (2018). Ecological traps in shallow coastal waters—Potential effect of heat-waves in tropical and temperate organisms. *PLoS One*, 13(2), e0192700. <https://doi.org/10.1371/journal.pone.0192700>.
- von Schuckmann, K., Minière, A., Gues, F., Cuesta-Valero, F. J., Kirchengast, G., Adusumilli, S., Straneo, F., Ablain, M., Allan, R. P., Barker, P. M., Beltrami, H., Blazquez, A., Boyer, T., Cheng, L., Church, J., Desbruyeres, D., Dolman, H., Domingues, C. M., García-García, A., . . . Zemp, M. (2023). Heat stored in the Earth system 1960–2020: Where does the energy go? *Earth System Science Data*, 15(4), 1675-1709. <https://doi.org/10.5194/essd-15-1675-2023>.
- Wählström, I., Höglund, A., Almroth-Rosell, E., MacKenzie, B. R., Gröger, M., Eilola, K., Plikshs, M., & Andersson, H. C. (2020). Combined climate change and nutrient load impacts on future habitats and eutrophication indicators in a eutrophic coastal sea. *Limnology and Oceanography*, 65(9), 2170-2187. <https://doi.org/10.1002/lno.11446>.
- Wahlteinez, S. J., Kroll, K. J., Behringer, D. C., Arnold, J. E., Whitaker, B., Newton, A. L., Edmiston, K., Hewson, I., & Stacy, N. I. (2023). Common sea star (*Asterias rubens*) coelomic fluid changes in response to short-term exposure to environmental stressors. *Fishes*, 8(1). <https://doi.org/10.3390/fishes8010051>.
- Walter, L. M. (1984). Magnesian calcite stabilities: A reevaluation. *Geochimica et Cosmochimica Acta*, 48(5), 1059-1069. [https://doi.org/10.1016/0016-7037\(84\)90196-0](https://doi.org/10.1016/0016-7037(84)90196-0).
- Walther, K., Sartoris, F. J., Bock, C., & Pörtner, H. O. (2009). Impact of anthropogenic ocean acidification on thermal tolerance of the spider crab *Hyas araneus*. *Biogeosciences*, 6(10), 2207-2215. <https://doi.org/10.5194/bg-6-2207-2009>.

- Wang, Z. J., Liang, C. L., Li, G. M., Yu, C. Y., & Yin, M. (2007). Stearic acid protects primary cultured cortical neurons against oxidative stress. *Acta Pharmacologica Sinica*, 28(3), 315-326. <https://doi.org/10.1111/j.1745-7254.2007.00512.x>.
- Watson, A. J., Schuster, U., Shutler, J. D., Holding, T., Ashton, I. G. C., Landschutzer, P., Woolf, D. K., & Goddijn-Murphy, L. (2020). Revised estimates of ocean-atmosphere CO₂ flux are consistent with ocean carbon inventory. *Nature Communications*, 11(1), 4422. <https://doi.org/10.1038/s41467-020-18203-3>.
- Watson, S. A., Peck, L. S., Tyler, P. A., Southgate, P. C., Tan, K. S., Day, R. W., & Morley, S. A. (2012). Marine invertebrate skeleton size varies with latitude, temperature and carbonate saturation: Implications for global change and ocean acidification. *Global Change Biology*, 18(10), 3026-3038. <https://doi.org/10.1111/j.1365-2486.2012.02755.x>.
- Watts, S. A., & Lawrence, J. M. (1986). Seasonal effects of temperature and salinity on the organismal activity of the seastar *Luidia clathrata* (say) (Echinodermata: Asteroidea). *Marine Behaviour and Physiology*, 12(3), 161-169. <https://doi.org/10.1080/10236248609378643>.
- Watts, S. A., & Lawrence, J. M. (1990). The effect of temperature and salinity interactions on righting, feeding and growth in the sea star *Luidia clathrata* (say). *Marine Behaviour and Physiology*, 17(3), 159-165. <https://doi.org/10.1080/10236249009378765>.
- Weber, J. N. (1969). The incorporation of magnesium into the skeletal calcites of echinoderms. *American Journal of Science*, 267(5), 537-566. <https://doi.org/10.2475/ajs.267.5.537>.
- Weber, J. N. (1973). Temperature dependence of magnesium in echinoid and asteroid skeletal calcite: A reinterpretation of its significance. *Journal of Geology*, 81(5), 543-556. <https://doi.org/10.1086/627906>.
- Weiner, S. (1985). Organic matrixlike macromolecules associated with the mineral phase of sea urchin skeletal plates and teeth. *Journal of Experimental Zoology*, 234(1), 7-15. <https://doi.org/10.1002/jez.1402340103>.
- Weiner, S., & Dove, P. M. (2003). An overview of biomineralization processes and the problem of the vital effect. *Reviews in Mineralogy & Geochemistry*, 54(1), 1-29. <https://doi.org/10.2113/0540001>.
- Whiteley, N. M. (2011). Physiological and ecological responses of crustaceans to ocean acidification. *Marine Ecology Progress Series*, 430, 257-271. <https://doi.org/10.3354/meps09185>.
- Wickham, H. (2016). *ggplot2: Elegant graphics for data analysis*. Springer-Verlag. <https://doi.org/10.1007/978-3-319-24277-4>.

- Widdicombe, S., & Spicer, J. I. (2008). Predicting the impact of ocean acidification on benthic biodiversity: What can animal physiology tell us?. *Journal of Experimental Marine Biology and Ecology*, 366(1-2), 187-197. <https://doi.org/10.1016/j.jembe.2008.07.024>.
- Wikelski, M., & Cooke, S. J. (2006). Conservation physiology. *Trends in Ecology & Evolution*, 21(1), 38-46. <https://doi.org/10.1016/j.tree.2005.10.018>.
- Willmer, P., Stone, G., & Johnston, I. (2004). *Environmental physiology of animals* (2nd ed.). Blackwell Publishing.
- Wilson, D. F., & Matschinsky, F. M. (2021). Metabolic homeostasis in life as we know it: Its origin and thermodynamic basis. *Frontiers in Physiology*, 12, 658997. <https://doi.org/10.3389/fphys.2021.658997>.
- Wittmann, A. C., & Pörtner, H.-O. (2013). Sensitivities of extant animal taxa to ocean acidification. *Nature Climate Change*, 3(11), 995-1001. <https://doi.org/10.1038/nclimate1982>.
- Wolf-Gladrow, D. A., Zeebe, R. E., Klaas, C., Körtzinger, A., & Dickson, A. G. (2007). Total alkalinity: the explicit conservative expression and its application to biogeochemical processes. *Marine Chemistry*, 106(1-2), 287-300. <https://doi.org/10.1016/j.marchem.2007.01.006>.
- Wong, B. B. M., & Candolin, U. (2015). Behavioral responses to changing environments. *Behavioral Ecology*, 26(3), 665-673. <https://doi.org/10.1093/beheco/aru183>.
- Wood, H. L., Spicer, J. I., Kendall, M. A., Lowe, D. M., & Widdicombe, S. (2011). Ocean warming and acidification; implications for the Arctic brittlestar *Ophiocten sericeum*. *Polar Biology*, 34(7), 1033-1044. <https://doi.org/10.1007/s00300-011-0963-8>.
- Wood, H. L., Spicer, J. I., Lowe, D. M., & Widdicombe, S. (2010). Interaction of ocean acidification and temperature; the high cost of survival in the brittlestar *Ophiura ophiura*. *Marine Biology*, 157(9), 2001-2013. <https://doi.org/10.1007/s00227-010-1469-6>.
- Wood, H. L., Spicer, J. I., & Widdicombe, S. (2008). Ocean acidification may increase calcification rates, but at a cost. *Proceedings of the Royal Society B: Biological Sciences*, 275(1644), 1767-1773. <https://doi.org/10.1098/rspb.2008.0343>.
- WoRMS Editorial Board. (2024). *World Register of Marine Species (WoRMS)*. <https://doi.org/10.14284/170>.
- Yao, C.-L., & Somero, G. N. (2014). The impact of ocean warming on marine organisms. *Chinese Science Bulletin*, 59(5-6), 468-479. <https://doi.org/10.1007/s11434-014-0113-0>.
- Yoon, D. S., Byeon, E., Kim, D. H., Lee, M. C., Shin, K. H., Hagiwara, A., Park, H. G., & Lee, J. S. (2022). Effects of temperature and combinational exposures on lipid metabolism in aquatic invertebrates. *Comparative Biochemistry and Physiology Part C: Toxicology & Pharmacology*, 262, 109449. <https://doi.org/10.1016/j.cbpc.2022.109449>.

- Yoro, K. O., & Daramola, M. O. (2020). CO₂ emission sources, greenhouse gases, and the global warming effect. In M. R. Rahimpour, M. Farsi, & M. A. Makarem (Eds.), *Advances in carbon capture* (pp. 3-28). Woodhead Publishing. <https://doi.org/10.1016/B978-0-12-819657-1.00001-3>.
- Young, J. S., Peck, L. S., & Matheson, T. (2006a). The effects of temperature on peripheral neuronal function in eurythermal and stenothermal crustaceans. *Journal of Experimental Biology*, 209(Pt 10), 1976-1987. <https://doi.org/10.1242/jeb.02224>.
- Young, J. S., Peck, L. S., & Matheson, T. (2006b). The effects of temperature on walking and righting in temperate and Antarctic crustaceans. *Polar Biology*, 29(11), 978-987. <https://doi.org/10.1007/s00300-006-0140-7>.
- Yu, H., Zhang, C., Gao, Q., Dong, S., Ye, Z., & Tian, X. (2016). Impact of water temperature on the growth and fatty acid profiles of juvenile sea cucumber *Apostichopus japonicus* (Selenka). *Journal of Thermal Biology*, 60, 155-161. <https://doi.org/10.1016/j.jtherbio.2016.07.011>.
- Zeebe, R. E. (2012). History of seawater carbonate chemistry, atmospheric CO₂, and ocean acidification. *Annual Review of Earth and Planetary Sciences*, 40(1), 141-165. <https://doi.org/10.1146/annurev-earth-042711-105521>.
- Zeebe, R. E., & Wolf-Gladrow, D. (2001). CO₂ in seawater: Equilibrium, kinetics, isotopes. In D. Halpern (Ed.), *Elsevier Oceanography Series*. Elsevier.
- Zhan, Y., Li, J., Sun, J., Zhang, W., Li, Y., Cui, D., Hu, W., & Chang, Y. (2019). The impact of chronic heat stress on the growth, survival, feeding, and differential gene expression in the sea urchin *Strongylocentrotus intermedius*. *Frontiers in Genetics*, 10, 301. <https://doi.org/10.3389/fgene.2019.00301>.
- Zhang, Z.-Q. (2013). Animal biodiversity: An update of classification and diversity in 2013. *Zootaxa*, 3703(1), 5-11. <https://doi.org/10.11646/ZOOTAXA.3703.1.3>.
- Zhuang, X. Y., Zhang, Y. H., Xiao, A. F., Zhang, A. H., & Fang, B. S. (2022). Key enzymes in fatty acid synthesis pathway for bioactive lipids biosynthesis. *Frontiers in Nutrition*, 9, 851402. <https://doi.org/10.3389/fnut.2022.851402>.
- Zhukova, N. V. (2022). Fatty acids of echinoderms: Diversity, current applications and future opportunities. *Marine Drugs*, 21(1). <https://doi.org/10.3390/md21010021>.

Appendix

Munawar Khalil has also authored and co-authored journal articles which are not related to this doctoral study (2020-2024):

1. Dayrat, B., Goulding, T. C., Apte, D., Aslam, S., Bourke, A., Comendador, J., **Khalil, M.**, Ngo, X. Q., Tan, S. K., & Tan, S. H. (2020). Systematic revision of the genus *Peronia* Fleming, 1822 (Gastropoda, Euthyneura, Pulmonata, Onchidiidae). *Zookeys*, 972, 1-224. <https://doi.org/10.3897/zookeys.972.52853>.

Abstract. The genus *Peronia* Fleming, 1822 includes all the onchidiid slugs with dorsal gills. Its taxonomy is revised for the first time based on a large collection of fresh material from the entire Indo-West Pacific, from South Africa to Hawaii. Nine species are supported by mitochondrial (COI and 16S) and nuclear (ITS2 and 28S) sequences as well as comparative anatomy. All types available were examined and the nomenclatural status of each existing name in the genus is addressed. Of 31 *Peronia* species-group names available, 27 are regarded as invalid (twenty-one synonyms, sixteen of which are new, five *nomina dubia*, and one homonym), and four as valid: *Peronia peronii* (Cuvier, 1804), *Peronia verruculata* (Cuvier, 1830), *Peronia platei* (Hoffmann, 1928), and *Peronia madagascariensis* (Labbé, 1934a). Five new species names are created: *P. griffithsi* Dayrat & Goulding, sp. nov., *P. okinawensis* Dayrat & Goulding, sp. nov., *P. setoensis* Dayrat & Goulding, sp. nov., *P. sydneyensis* Dayrat & Goulding, sp. nov., and *P. willani* Dayrat & Goulding, sp. nov. *Peronia* species are cryptic externally but can be distinguished using internal characters, with the exception of *P. platei* and *P. setoensis*. The anatomy of most species is described in detail here for the first time. All the secondary literature is commented on and historical specimens from museum collections were also examined to better establish species distributions. The genus *Peronia* includes two species that are widespread across the Indo-West Pacific (*P. verruculata* and *P. peronii*) as well as endemic species: *P. okinawensis* and *P. setoensis* are endemic to Japan, and *P. willani* is endemic to Northern Territory, Australia. Many new geographical records are provided, as well as a key to the species using morphological traits.

Keywords: Biodiversity, Coral Triangle, Indo-West Pacific, integrative taxonomy, mangrove, South-East Asia

Systematic revision of the genus *Peronia* Fleming, 1822 (Gastropoda, Euthyneura, Pulmonata, Onchidiidae)

Benoît Dayrat¹, Tricia C. Goulding¹, Deepak Apte², Sadar Aslam³,
Adam Bourke⁴, Joseph Comendador⁵, Munawar Khalil⁶,
Xuân Quảng Ngô^{7,8}, Siong Kiat Tan⁹, Shau Hwai Tan^{10,11}

1 Department of Biology, Pennsylvania State University, University Park, PA 16802, USA **2** Bombay Natural History Society, Hornbill House, Opp. Lion Gate, Shaheed Bhagat Singh Road, Mumbai 400 001, Maharashtra, India **3** Centre of Excellence in Marine Biology, University of Karachi, Karachi 75270, Pakistan **4** College of Engineering, Information Technology and the Environment, Charles Darwin University, Ellengowan Dr, Casuarina, NT 0810, Australia **5** National Museum of the Philippines, Taft Ave, Ermita, Manila, 1000, Metro Manila, Philippines **6** Department of Marine Science, Universitas Malikussaleh, Reuleut Main Campus, Kecamatan Muara Batu, North Aceh, Aceh, 24355, Indonesia **7** Institute of Tropical Biology, Vietnam Academy of Science and Technology, 85 Tran Quoc Toan Street, District 3, Ho Chi Minh City, Vietnam **8** Graduate University of Science and Technology, Vietnam Academy of Science and Technology, 18 Hoang Quoc Viet, Cau Giay, Hanoi, Vietnam **9** Lee Kong Chian Natural History Museum, 2 Conservatory Dr, National University of Singapore, 117377, Singapore **10** Centre for Marine and Coastal Studies, Universiti Sains Malaysia, 11800, Minden Penang, Malaysia **11** Marine Science Laboratory, School of Biological Sciences, Universiti Sains Malaysia, 11800, Minden Penang, Malaysia

Corresponding author: Benoît Dayrat (bad25@psu.edu)

Academic editor: Nathalie Yonow | Received 2 April 2020 | Accepted 13 August 2020 | Published 1 October 2020

<http://zoobank.org/79167494-2E92-42C3-8D1F-D4DE7264D7B7>

Citation: Dayrat B, Goulding TC, Apte D, Aslam S, Bourke A, Comendador J, Khalil M, Ngô XQ, Tan SK, Tan SH (2020) Systematic revision of the genus *Peronia* Fleming, 1822 (Gastropoda, Euthyneura, Pulmonata, Onchidiidae). ZooKeys 972: 1–224. <https://doi.org/10.3897/zookeys.972.52853>

Abstract

The genus *Peronia* Fleming, 1822 includes all the onchidiid slugs with dorsal gills. Its taxonomy is revised for the first time based on a large collection of fresh material from the entire Indo-West Pacific, from South Africa to Hawaii. Nine species are supported by mitochondrial (COI and 16S) and nuclear (ITS2 and 28S) sequences as well as comparative anatomy. All types available were examined and the nomenclatural status of each existing name in the genus is addressed. Of 31 *Peronia* species-group names available, 27 are regarded as invalid (twenty-one synonyms, sixteen of which are new, five *nomina dubia*, and one homo-

2. Goulding, T. C., Bourke, A. J., Comendador, J., **Khalil, M.**, Quang, N. X., Tan, S. H., Tan, S. K., & Dayrat, B. (2021). Systematic revision of *Platevindex* Baker, 1938 (Gastropoda: Euthyneura: Onchidiidae). *European Journal of Taxonomy*, 737, 1-133. <https://doi.org/10.5852/ejt.2021.737.1259>.

Abstract. In the Indo-West Pacific, intertidal slugs of the genus *Platevindex* Baker, 1938 are common in mangrove forests, where they typically live on the roots and trunks of mangrove trees. These slugs are easily distinguished from most onchidiids by their hard notum and narrow foot, but despite their large size and abundance, species diversity and geographic distributions have remained a mystery. With the aid of new collections from across the entire Indo-West Pacific, the taxonomy of *Platevindex* is revised using an integrative approach (natural history field observations, re-examination of type specimens, mitochondrial and nuclear DNA sequences, and comparative anatomy). In this monograph, nine species of *Platevindex* are recognized, including one new to science: *P. amboinae* (Plate, 1893), *P. applanatus* (Simroth, 1920) comb. nov., *P. aptei* Goulding & Dayrat sp. nov., *P. burnupi* (Collinge, 1902) comb. nov., *P. coriaceus* (Semper, 1880), *P. latus* (Plate, 1893), *P. luteus* (Semper, 1880), *P. martensi* (Plate, 1893) and *P. tigrinus* (Stoliczka, 1869) comb. nov. Five species names are recognized as junior synonyms, four of which are new, and two *Platevindex* names are regarded as *nomina dubia*. One new subspecies is also recognized: *P. coriaceus darwinensis* Goulding & Dayrat subsp. nov. Most species were previously known only from the type material and many new geographic records are provided across the Indo-West Pacific, from South Africa to the West Pacific (Japan, New Ireland and New Caledonia).

Keywords: Biodiversity, Indo-West Pacific, integrative taxonomy, revisionary systematics, South-East Asia

Monograph

urn:lsid:zoobank.org:pub:FE4ED74A-3FE6-4CA6-A116-CB3AF46826F7

**Systematic revision of *Platevindex* Baker, 1938
(Gastropoda: Euthyneura: Onchidiidae)**

Tricia C. GOULDING¹, Adam J. BOURKE², Joseph COMENDADOR³,
Munawar KHALIL⁴, Ngo Xuan QUANG⁵, Shau Hwai TAN⁶,
Siong Kiat TAN⁷ & Benoît DAYRAT^{8,*}

^{1,8} Department of Biology, Pennsylvania State University, University Park, PA 16802, USA.

¹ Current address: Smithsonian Institution, National Museum of Natural History,
PO Box 37012, MRC 163, Washington, DC, 20013, USA.

² College of Engineering, Information Technology and the Environment,
Charles Darwin University, Ellengowan Dr., Casuarina, NT 0810, Australia.

³ National Museum of the Philippines, Taft Ave., Ermita, Manila, 1000 Metro Manila, Philippines.

⁴ Department of Marine Science, Faculty of Agriculture, Universitas Malikussaleh,
Reuleut Main Campus, Kecamatan Muara Batu, North Aceh, Aceh, 24355, Indonesia.

⁵ Institute of Tropical Biology, Vietnam Academy of Science and Technology,
85 Tran Quoc Toan Street, District 3, Ho Chi Minh City, Vietnam.

⁵ Graduate University of Science and Technology, Vietnam Academy of Science and Technology,
18 Hoang Quoc Viet, Cau Giay, Hanoi, Vietnam.

⁶ Centre for Marine and Coastal Studies, Universiti Sains Malaysia, 11800 Minden Penang, Malaysia.

⁶ Marine Science Laboratory, School of Biological Sciences,
Universiti Sains Malaysia, 11800 Minden Penang, Malaysia.

⁷ Lee Kong Chian Natural History Museum, 2 Conservatory Dr,
National University of Singapore, 117377, Singapore.

* Corresponding author: bad25@psu.edu

¹ Email: tc.goulding@gmail.com

² Email: adamjohn.bourke@gmail.com

³ Email: joseph.comendador@gmail.com

⁴ Email: khalil@unimal.ac.id

⁵ Email: ngoxuanq@gmail.com

⁶ Email: aileen@usm.my

⁷ Email: nhmtsk@nus.edu.sg

¹ urn:lsid:zoobank.org:author:6009A165-E73E-4124-96C6-C143FC51B18F

² urn:lsid:zoobank.org:author:AAF38199-57BF-4E7E-A888-468A9B01720C

³ urn:lsid:zoobank.org:author:0EAAEF74-7E54-47BA-9A3A-D3A4ED40AD85

⁴ urn:lsid:zoobank.org:author:6D38234D-0DE1-4CDE-9F7E-603070C9B27D

⁵ urn:lsid:zoobank.org:author:AD2EB983-517E-435A-BEDB-B51BC442D42C

⁶ urn:lsid:zoobank.org:author:6E9B8F28-EFCC-42F1-A7C4-3957C92995AA

⁷ urn:lsid:zoobank.org:author:1BFA4D8E-30CE-4DC4-A6C2-64E0281996DF

⁸ urn:lsid:zoobank.org:author:192B0AF4-A4B0-4129-8422-DEF8D0FB4A45

3. **Khalil, M.**, Ezraneti, R., Rusydi, R., Yasin, Z., and Tan, S. H. (2021). Biometric relationship of *Tegillarca granosa* (Bivalvia: Arcidae) from the Northern Region of the Strait of Malacca. *Ocean Science Journal*, 56(2), 156-166. <https://doi.org/10.1007/s12601-021-00019-x>.

Abstract. This study on the growth pattern of the blood cockle *Tegillarca granosa* focused on the aspects of biometric prints on the shell, which aimed to predict the growth of the *T. granosa* population in the northern region of Malacca Strait. The local sample populations of the cockle were collected in three different intertidal areas called Lhokseumawe and Banda Aceh in Indonesia and Pulau Pinang in Malaysia. The biometric analysis showed that the length–weight relationship model of *T. granosa* populations in this region indicated that the cockle population generally had a negative allometric growth pattern ($b < 3$) or that shell length is more dominant compared to shell weight. Therefore, the result showed that the growth performance of *T. granosa* was not ideal, and the highest b value (the coefficient of biometric relationship) was recorded in Lhokseumawe, followed by Banda Aceh and Pulau Pinang. The value of the coefficient b could be affected by various factors such as environmental conditions, adaptation, and dietary patterns. Cluster analysis revealed that the population of *T. granosa* from the northern region of the Strait of Malacca was divided into two clusters, which were *T. granosa* from the northern Strait of Malacca (Banda Aceh and Lhokseumawe in Indonesia) and *T. granosa* from the Western Strait of Malacca (Pulau Pinang in Malaysia). The factors that might cause the differences in the biometric component of both clusters were at the geographical level on the source of population and local environmental parameters.

Keywords: Blood cockle, Bivalvia, Morphometric, Growth model, Malacca Strait



Biometric Relationship of *Tegillarca granosa* (Bivalvia: Arcidae) from the Northern Region of the Strait of Malacca

Munawar Khalil^{1,2} · Riri Ezraneti¹ · Rachmawati Rusydi³ · Zulfigar Yasin^{4,5} · Shau Hwai Tan^{4,5}

Received: 20 July 2020 / Revised: 5 December 2020 / Accepted: 8 December 2020 / Published online: 7 May 2021
© Korea Institute of Ocean Science & Technology (KIOST) and the Korean Society of Oceanography (KSO) and Springer Nature B.V. 2021

Abstract

This study on the growth pattern of the blood cockle *Tegillarca granosa* focused on the aspects of biometric prints on the shell, which aimed to predict the growth of the *T. granosa* population in the northern region of Malacca Strait. The local sample populations of the cockle were collected in three different intertidal areas called Lhokseumawe and Banda Aceh in Indonesia and Pulau Pinang in Malaysia. The biometric analysis showed that the length–weight relationship model of *T. granosa* populations in this region indicated that the cockle population generally had a negative allometric growth pattern ($b < 3$) or that shell length is more dominant compared to shell weight. Therefore, the result showed that the growth performance of *T. granosa* was not ideal, and the highest b value (the coefficient of biometric relationship) was recorded in Lhokseumawe, followed by Banda Aceh and Pulau Pinang. The value of the coefficient b could be affected by various factors such as environmental conditions, adaptation, and dietary patterns. Cluster analysis revealed that the population of *T. granosa* from the northern region of the Strait of Malacca was divided into two clusters, which were *T. granosa* from the northern Strait of Malacca (Banda Aceh and Lhokseumawe in Indonesia) and *T. granosa* from the Western Strait of Malacca (Pulau Pinang in Malaysia). The factors that might cause the differences in the biometric component of both clusters were at the geographical level on the source of population and local environmental parameters.

Keywords Blood cockle · Bivalvia · Morphometric · Growth model · Malacca Strait

1 Introduction

Tegillarca granosa is one of the important fishery commodities in several areas of Southeast Asia. This species has been cultivated in countries such as Malaysia and Thailand due to limited natural stocks. However, this species in Indonesia

is still harvested directly from nature (Broom 1983; Khalil et al. 2017). Nevertheless, annual harvested-cockle data reveal a reduction in natural stocks in the last decade. One of the main factors for the significant reduction in natural stocks is overharvesting due to the high demand as a protein source. This condition may also be a result of the lack in management in controlling the wild cockle population stock. Therefore, the management of this species is required for the sustainability of this important species. Comprehensive information on biometrics (morphometric relationship pattern of the species) is necessary to predict the annual recruitment, as well as to interpret growth, mortality, reproductive biology, and survival data in the marine culture of species (Kim et al. 2006; Peharda et al. 2007; Pinn et al. 2005; Zelditch et al. 2004).

Length–weight is an essential variable for comparing growth, physiological processes, and environmental factors that affect aquatic organisms (Hemachandra and Thippeswamy 2008). Growth of bivalves can be defined as the increase of the length size of the shell and body weight (body mass) and these indicators have also been used extensively

✉ Munawar Khalil
khalil@unimal.ac.id

¹ Department of Marine Science, Faculty of Agriculture, Reuleut Main Campus, Universitas Malikussaleh, North Aceh 24351, Indonesia
² Leibniz Centre for Tropical Marine Research (ZMT), Bremen 28359, Germany
³ Department of Aquaculture, Faculty of Agriculture, Reuleut Main Campus, Universitas Malikussaleh, North Aceh 24351, Indonesia
⁴ School of Biological Sciences, Universiti Sains Malaysia, Penang 11800, Malaysia
⁵ Centre for Marine and Coastal Studies, Universiti Sains Malaysia, Penang 11800, Malaysia

4. Goulding, T. C., **Khalil, M.**, Tan, S. H., Cumming, R. A., & Dayrat, B. (2022). Global diversification and evolutionary history of onchidiid slugs (Gastropoda, Pulmonata). *Molecular Phylogenetics and Evolution*, 168, 107360. <https://doi.org/10.1016/j.ympev.2021.107360>.

Abstract. Many marine species are specialized to specific parts of a habitat. In a mangrove forest, for instance, species may be restricted to the mud surface, the roots and trunks of mangrove trees, or rotting logs, which can be regarded as distinct microhabitats. Shifts to new microhabitats may be an important driver of sympatric speciation. However, the evolutionary history of these shifts is still poorly understood in most groups of marine organisms, because it requires a well-supported phylogeny with relatively complete taxon sampling. Onchidiid slugs are an ideal case study for the evolutionary history of habitat and microhabitat shifts because onchidiid species are specialized to different tidal zones and microhabitats in mangrove forests and rocky shores, and the taxonomy of the family in the Indo-West Pacific has been recently revised in a series of monographs. Here, DNA sequences for onchidiid species from the North and East Pacific, the Caribbean, and the Atlantic are used to reconstruct phylogenetic relationships among *Onchidella* species, and are combined with new data for Indo-West Pacific species to reconstruct a global phylogeny of the family. The phylogenetic relationships of onchidiid slugs are reconstructed based on three mitochondrial markers (COI, 12S, 16S) and three nuclear markers (28S, ITS2, H3) and nearly complete taxon sampling (all 13 genera and 62 of the 67 species). The highly-supported phylogeny presented here suggests that ancestral onchidiids most likely lived in the rocky intertidal, and that a lineage restricted to the tropical Indo-West Pacific colonized new habitats, including mudflats, mangrove forests, and high-elevation rainforests. Many onchidiid species in the Indo-West Pacific diverged during the Miocene, around the same time that a high diversity of mangrove plants appears in the fossil record, while divergence among *Onchidella* species occurred earlier, likely beginning in the Eocene. It is demonstrated that ecological specialization to microhabitats underlies the divergence between onchidiid genera, as well as the diversification through sympatric speciation in the genera *Wallaconchis* and *Platevindex*. The geographic distributions of onchidiid species also indicate that allopatric speciation played a key role in the diversification of several genera, especially *Onchidella* and *Peronia*. The evolutionary history of several morphological traits (penial

gland, rectal gland, dorsal eyes, intestinal loops) is examined in relation to habitat and microhabitat evolutionary transitions and that the rectal gland of onchidiids is an adaptation to high intertidal and terrestrial habitats.

Keywords: Biogeography, Divergence time, Ecological speciation, Habitat transition, Mangroves, Rocky intertidal



Contents lists available at ScienceDirect

Molecular Phylogenetics and Evolution

journal homepage: www.elsevier.com/locate/ympev

Global diversification and evolutionary history of onchidiid slugs (Gastropoda, Pulmonata)

Tricia C. Goulding^{a,*}, Munawar Khalil^{b,1}, Shau Hwai Tan^{c,d}, Rebecca A. Cumming^a, Benoît Dayrat^a

^a Department of Biology, Pennsylvania State University, University Park, PA 16802, USA

^b Department of Marine Science, Universitas Malikussaleh, Reuleut Main Campus, Kecamatan Muara Batu, North Aceh, Aceh 24355, Indonesia

^c Centre for Marine and Coastal Studies, Universiti Sains Malaysia, 11800 Minden Penang, Malaysia

^d Marine Science Laboratory, School of Biological Sciences, Universiti Sains Malaysia, 11800 Minden Penang, Malaysia

ARTICLE INFO

Keywords:

Biogeography
Divergence time
Ecological speciation
Habitat transition
Mangroves
Rocky intertidal

ABSTRACT

Many marine species are specialized to specific parts of a habitat. In a mangrove forest, for instance, species may be restricted to the mud surface, the roots and trunks of mangrove trees, or rotting logs, which can be regarded as distinct microhabitats. Shifts to new microhabitats may be an important driver of sympatric speciation. However, the evolutionary history of these shifts is still poorly understood in most groups of marine organisms, because it requires a well-supported phylogeny with relatively complete taxon sampling. Onchidiid slugs are an ideal case study for the evolutionary history of habitat and microhabitat shifts because onchidiid species are specialized to different tidal zones and microhabitats in mangrove forests and rocky shores, and the taxonomy of the family in the Indo-West Pacific has been recently revised in a series of monographs. Here, DNA sequences for onchidiid species from the North and East Pacific, the Caribbean, and the Atlantic are used to reconstruct phylogenetic relationships among *Onchidella* species, and are combined with new data for Indo-West Pacific species to reconstruct a global phylogeny of the family. The phylogenetic relationships of onchidiid slugs are reconstructed based on three mitochondrial markers (COI, 12S, 16S) and three nuclear markers (28S, ITS2, H3) and nearly complete taxon sampling (all 13 genera and 62 of the 67 species). The highly-supported phylogeny presented here suggests that ancestral onchidiids most likely lived in the rocky intertidal, and that a lineage restricted to the tropical Indo-West Pacific colonized new habitats, including mudflats, mangrove forests, and high-elevation rainforests. Many onchidiid species in the Indo-West Pacific diverged during the Miocene, around the same time that a high diversity of mangrove plants appears in the fossil record, while divergence among *Onchidella* species occurred earlier, likely beginning in the Eocene. It is demonstrated that ecological specialization to microhabitats underlies the divergence between onchidiid genera, as well as the diversification through sympatric speciation in the genera *Wallaconchis* and *Platevindex*. The geographic distributions of onchidiid species also indicate that allopatric speciation played a key role in the diversification of several genera, especially *Onchidella* and *Peronia*. The evolutionary history of several morphological traits (penial gland, rectal gland, dorsal eyes, intestinal loops) is examined in relation to habitat and microhabitat evolutionary transitions and that the rectal gland of onchidiids is an adaptation to high intertidal and terrestrial habitats.

1. Introduction

Allopatric speciation has long been recognized as a driver of marine speciation through vicariance, especially following the formation of land barriers with changes in sea level (McManus, 1985; Macieira et al., 2015; Bowen et al., 2016). Dispersal of propagules to new regions can

also lead to diversification via founder speciation (Paulay and Meyer, 2002). Sympatric speciation, in which a species diverges into two lineages while remaining in close contact, is thought to occur due to disruptive selection, although there are many competing models for how this may transpire (Bolnick and Fitzpatrick, 2007). Evolutionary transitions to new habitats are a type of ecological specialization that can

* Corresponding author at: Smithsonian Institution, National Museum of Natural History, Washington, D.C. 20013, USA.

E-mail address: gouldingt@si.edu (T.C. Goulding).

¹ Present address: Leibniz Centre for Tropical Marine Research (ZMT), Fahrenheitstraße 6, 28359 Bremen, Germany.

<https://doi.org/10.1016/j.ympev.2021.107360>

Received 5 June 2021; Received in revised form 29 September 2021; Accepted 9 November 2021

Available online 15 November 2021

1055-7903/© 2021 Elsevier Inc. All rights reserved.

Index

A

acclimation, 23, 27, 32, 36, 46, 65, 78, 79, 89, 91, 94, 97, 139
acclimatization, 12, 22, 23, 76, 79, 159, 162, 168, 220
acidosis, 9, 60, 93, 166
adaptation, xiv, 12, 22, 24, 78, 89, 139, 170, 233, 236
adaptive, 22, 23, 24, 159, 166, 169, 170, 171, 172
 adaptive capacity, 7, 23, 24
 adaptive plasticity, 164, 172, 224
 adaptive potential, 7, 22, 24, 171
 adaptive response, 22, 23
additive, 11, 12, 44
algae, 11, 43, 46, 77
amorphous, 45, 60
anatomical characteristics, 29
antagonistic, iii, xiv, 11, 12, 18, 44, 76, 93, 95, 138, 163
anthropogenic, 1, 2, 23, 25, 158
aragonite, xxx, 4, 10, 18, 33, 42, 48, 63, 65, 98, 101, 141, 142, 167
asterinid starfish, i, vi, viii, xii, xiii, xiv, 27, 28, 29, 30, 35, 36, 39, 46, 63, 73, 79, 90, 108, 111, 113, 144, 150, 151, 158, 166, 167, 169, 170
Asteroidea, i, iii, 26, 27, 28, 29, 42, 46, 78
Atlantic, 29, 235
atmosphere, 1, 2
ATP, 14, 121, 137, 138, 160, 213

B

behavior, 7, 8, 9, 20, 28, 34, 36, 75, 79, 81, 82, 92, 93, 95, 96, 168
benthic, 25, 29, 64, 167

bicarbonate, xxviii, 4, 33, 43, 48, 60, 65, 98, 101, 141, 142
biochemical, xiv, 7, 8, 12, 23, 36, 94, 113, 114, 116, 117, 118, 136, 137, 139, 140, 159, 170, 174, 193, 204, 206, 214
biochemistry, vii, xiii, xiv, 28, 36, 111, 114, 168
bioecology, 79
biogeochemical, 11, 99
biogeographical movement, 22
bioindicators, vi, 25, 27, 30, 165
biological
 biological complexity, 8, 165, 168
 biological control, 45
 biological functions, vi, 8
 biological processes, viii, 8, 25
biomineralization, vi, vii, 10, 28, 35, 36, 37, 42, 43, 44, 45, 46, 60, 62, 114, 165, 169
biosynthesis, xiv, 139, 166, 170
bioturbation, 29

C

Ca-ATPase, vii, xiv, 13, 34, 114, 120, 121, 130, 131, 139, 144, 148, 151, 157, 168, 169
CaCO₃, xxviii, 4, 9, 10, 43, 45, 62, 82, 85, 93, 95, 99, 163, 174, 188, 204, 209
calcification, vii, xiii, xiv, 10, 13, 16, 18, 27, 28, 34, 36, 43, 61, 62, 63, 75, 76, 79, 82, 85, 87, 88, 93, 94, 95, 96, 99, 103, 114, 136, 139, 166, 169
calcifying organisms, 9, 10, 35, 42, 43, 95
calcite, vii, xxx, 4, 10, 18, 26, 33, 42, 43, 45, 48, 60, 61, 62, 63, 65, 98, 101, 141, 142, 167
carbonate, xxviii, xxix, 4, 27, 33, 43, 45, 47, 48, 50, 51, 52, 60, 62, 65, 80, 94, 98, 101, 141, 142
catalytic activity, 8
cell, 32, 45, 65, 98, 100, 141, 169

cellular, vi, 8, 23, 24, 63, 90, 93, 165, 166, 170
cement production, 1
chemical, vii, 1, 4, 27, 29, 33, 35, 45, 169
chronic conditions, vii, 167, 168
climate change, viii, xiii, 4, 22, 23, 24, 25, 76, 77,
79, 96, 158, 172
cnidaria, 7
CO₂, vi, vii, xxviii, 1, 2, 3, 4, 5, 6, 9, 10, 26, 27, 32,
37, 43, 47, 48, 65, 77, 79, 94, 95, 97, 98, 99, 101,
140, 141, 142, 165
CO₂SYs software, 33, 98, 141, 142
combined effects, vi, xiii, 36, 46, 76, 95, 114, 168
communities, 7, 30, 165
competitive capability, 7
conservation, viii, 25
coral bleaching, 8
corals, 9, 43, 44, 46, 77
crustaceans, 7, 25

D

deforestation, 1
deoxygenation, 158, 170
deuterostome division, 26
digestion, 8
dissertation, iv, xii, xxvi, xxvii, 28, 35, 37
dissolution, xiii, 4, 10, 26, 51, 57, 60, 62, 76, 93, 94,
95, 167
dorsal, xvi, xix, 29, 31, 34, 81, 99, 106, 229, 236

E

echinoderm, 9, 26, 27, 35, 42, 44, 45, 61, 165, 171
ecological, vi, viii, 8, 11, 25, 26, 29, 35, 46, 77, 96,
140, 159, 161, 169, 171, 235
ecosystem, vi, viii, xiii, 3, 7, 8, 9, 22, 23, 29, 77, 96,
114, 158, 165, 169, 171
ecosystems, viii, xiii, 3, 7, 8, 25, 29, 43, 114, 158,
159, 170
ectotherm, 26, 44, 77

ectothermic, 24, 30, 115, 117, 137, 159, 160, 172,
208, 209, 218
embryonic, 8
emission, vii, xxviii, 1, 2, 3, 4, 33, 50, 80
energetic regulation, 24
environmental disruptions, 30
environmental stressors, xiii, 7, 23, 29, 96, 158,
170, 171, 172
enzyme, iii, vii, xii, xiii, xiv, xvi, xx, xxi, xxiv, xxviii,
18, 19, 27, 28, 34, 36, 37, 90, 111, 114, 118,
121, 130, 131, 137, 138, 139, 140, 144, 157,
159, 161, 168, 170, 198, 200, 207
epigenetic, 22, 172
epithelial, 62
equilibrium, 4, 33, 66, 98, 141
evolution, 23, 25, 29
exoskeletons, 24
experimental design, 13, 69, 108
extracellular, 10, 90

F

factorial, vii, xvii, xxii, 13, 32, 69, 79, 119
FAMEs, 34, 120
fatty acids, xiv, 27, 28, 34, 36, 114, 119, 124, 128,
129, 139, 144, 156
fission, 30, 31
fitness, 7, 12, 23, 24, 90, 91, 92, 165, 166, 167
food web, 115, 158, 163
foraging, 7, 17, 19
foraminifera, 9, 11, 15, 44, 77
fossil fuel, 1
future research, 37, 165, 172

G

genetic, 12, 23, 170
geochemical, 4
global ocean change, i, vi, vii, 1, 22, 24, 27, 35, 36,
114, 158, 165, 166, 169, 170, 172, 178

growth, 7, 9, 14, 16, 17, 18, 20, 27, 43, 44, 77, 78, 233
Gulf of Suez, vii, 30, 79, 80

H

H⁺, xxviii, 4, 10, 94
homeostasis, 90, 139, 170
homeoviscous, xiv, 132, 139, 169
hypercapnia, 93, 166, 169, 171
hypoxia, 8, 116, 158, 160, 171, 178, 201, 221

I

immune, 77, 170
Indo-Pacific regions, 29
infectious disease outbreaks, 8
interactive effects, xiii, xiv, 12, 27, 37, 67, 76, 103, 151
interspecies, 163
intracellular, 45, 62, 90, 168
invasive species, 9
invertebrates, viii, 10, 13, 25, 29, 90, 158
ion, xxviii, xxix, 4, 33, 43, 48, 60, 65, 90, 98, 101, 141, 142
IPCC, vii, xxviii, 4, 79

J

juvenile, 14, 15, 16, 17, 20, 29, 79, 171

K

keystone, vi, 26, 29, 165

L

laboratory, 7, 25, 27, 30, 41, 64, 75, 79, 96, 113
life
 life history, 29, 30, 77, 78, 165, 171
 life performances, 8, 165, 171
 life stages, 9, 44, 45, 78, 91, 95, 171
lipid, vii, xiii, xiv, 19, 27, 28, 34, 36, 37, 111, 114, 119, 120, 122, 123, 128, 139, 140, 144, 151, 153, 168, 170

lipidomics, vi

locomotion, 19, 28, 63, 92, 93, 162, 163, 167, 195, 210

M

MAREE, xxvi, 31, 46, 79, 96, 97, 118, 140
marine organisms, vi, vii, xiii, 4, 7, 8, 9, 11, 22, 23, 24, 26, 35, 36, 42, 43, 44, 63, 76, 77, 78, 96, 158, 169, 171, 235
marine plants, 7
Mediterranean Sea, vi, 30, 46, 79
metabolic, vi, vii, xiii, xiv, xviii, xix, xxiii, 13, 15, 19, 26, 27, 28, 76, 77, 78, 82, 83, 84, 88, 89, 90, 92, 94, 96, 102, 103, 109, 113, 114, 116, 132, 137, 138, 159, 160, 161, 163, 166, 170, 181, 182, 184, 185, 196, 200, 212, 219, 223
metabolism, 7, 8, 9, 10, 24, 26, 27, 36, 76, 78, 89, 90, 93
Mg calcite, 10
Mg²⁺, vii, xxix, 45, 60, 61, 167, 169
Mg-ATPase, vii, xiv, 13, 34, 114, 120, 121, 130, 131, 139, 144, 149, 152, 168, 169
MgCO₃, 10, 43, 45, 167
microevolution, 22
microstructure, i, ii, xii, xvi, xvii, xxiii, 9, 28, 31, 33, 35, 37, 39, 42, 44, 45, 46, 50, 51, 56, 57, 59, 63, 95, 180, 198, 200
microstructures, 28, 42
migration, 3, 8, 22
mineralogy, vi, xii, 7, 27, 28, 33, 35, 39, 41, 42, 44, 45, 170
mitigate, vi, vii, 3, 4, 23, 24, 78, 94, 96, 158, 169, 170
molecular, vi, vii, 7, 8, 24, 114, 165, 168, 170
mollusks, 7, 9, 25, 43, 44, 77
morphogenesis, 43
morphological, 22, 24, 229, 236

mortality, xiii, 17, 18, 21, 36, 51, 75, 76, 79, 81, 84,
91, 96, 116, 138, 160, 162, 166, 167

MPMO, 161

MUFAs, xiv, xxi, xxiv, 34, 114, 117, 122, 124, 125,
128, 134, 136, 150, 156, 161, 168

multi-stressors, 7, 171

musculoskeletal fatigue, 93

mussel, 18, 45

N

neuromuscular, 93, 166

niche, 12, 23

nocturnal, 30, 79

O

objectives, 27, 31, 37

ocean

ocean acidification, vi, xii, xxix, 4, 6, 7, 13, 25,
35, 36, 39, 41, 42, 43, 65, 69, 73, 75, 76, 77,
79, 91, 94, 108, 111, 113, 114, 158, 159, 168

ocean warming, vi, xiii, xxix, 7, 13, 25, 35, 37,
41, 42, 43, 69, 75, 77, 113, 139, 161

ontogeny, vi

oxygen, xviii, xxix, 14, 18, 19, 34, 77, 81, 84, 89, 98,
99, 135, 162, 170, 174, 184, 196, 224

P

pathways, vi, 4, 23, 36, 61, 138, 160, 162, 166,
170, 172, 209, 222

pejus temperature, 160

pH, vii, xiii, xxix, 4, 6, 9, 10, 13, 15, 19, 26, 27, 43,
48, 60, 62, 63, 65, 76, 77, 78, 79, 89, 90, 92, 93,
94, 95, 96, 97, 114, 120, 121, 139, 141, 167, 169

phenological shift, 22

phenotypic, 12, 22, 23, 24, 62, 78, 172

phenotypic plasticity, 22, 23, 24, 62, 78

photosynthesis, 43

physicochemical, 165

physiochemical, iv, vii, xvi, xxv, 28, 31, 33, 36, 37,
158, 159, 160, 161, 162, 165, 167, 170, 171, 172

physiochemistry, vi, 75, 165

physiological, vi, vii, xii, xiii, 8, 9, 11, 12, 22, 23, 24,
26, 27, 28, 32, 36, 37, 45, 46, 47, 60, 61, 62, 63,
73, 76, 77, 78, 80, 83, 89, 91, 92, 93, 94, 96, 139,
158, 165, 166, 169, 170

physiology, vii, xiii, 26, 27, 30, 76, 77, 89, 91, 96,
114, 161

plastic pollution, 158

polymorphs, 10, 43

population, 1, 3, 7, 8, 22, 23, 166, 233

population dynamics, 25, 77

pteropods, 9

PUFAs, xiv, xxi, xxiv, 18, 34, 114, 117, 122, 124,
125, 128, 129, 134, 136, 150, 156, 161, 168

R

radiative forcing, 2

Red Sea, vi, 30, 39, 46, 73, 79

Representative Concentration Pathways, vii

reproduction, xvi, 7, 9, 22, 24, 27, 31, 115, 117,
134, 162, 216

reproductive biology, 9, 77

resilience, viii, 22, 62, 91, 132, 158, 159, 166, 169,
171, 172

S

saturation, xxix, xxx, 4, 10, 33, 43, 48, 62, 65, 94,
98, 101, 141, 142

sea surface temperature, 80

sea urchins, 26, 27, 90

seawater carbonate system, 9, 33, 65, 98, 141

settlement, 9

SFAs, xiv, xxi, xxiv, 34, 114, 117, 122, 124, 125,
128, 133, 136, 150, 156, 159, 168, 169

Shared Socioeconomic Pathways, 3

skeletal, vii, xii, xiii, 7, 8, 9, 14, 26, 27, 28, 33, 35,
37, 39, 41, 42, 44, 45, 50, 51, 52, 53, 54, 55,

56, 57, 59, 60, 61, 62, 63, 67, 76, 114, 167, 169,
170
skeletal mineralogy, 44
skeleton, vii, 8, 10, 14, 26, 31, 33, 35, 42, 43, 45,
46, 50, 51, 53, 57, 60, 62, 63, 77, 94, 95, 167
solubility, 11, 33, 66, 95, 98, 141
species-specific, xiii, 7, 24, 26, 44, 60, 61, 76, 90,
96
specimens, xiii, 32, 33, 35, 46, 50, 65, 79, 83, 89,
97, 120, 229, 231
stereom, 31, 42, 45, 51, 56, 57, 60, 62, 63
subtropical, vi, xiv, 4, 27, 28, 30, 35, 36, 114, 139,
165
survivability, 8, 28, 96, 166, 170
synergistic, vii, xiii, 11, 12, 27, 44, 76, 91

T

taxa, vi, 7, 9, 10, 45, 46, 159, 165, 172, 222, 226
taxonomic group, 10
thermal, 8, 12, 24, 26, 77, 78, 89, 92, 94, 116, 134,
159, 160, 161, 169, 171, 177, 189, 194, 204,
206, 213, 214, 219, 221, 222, 225
thermal biology, 24

thermal optimum, 95
thermal performance curve, 90
thermal pulse, 92
thermal sensitivity, 8, 89
thermal tolerance, 8, 26, 77, 78, 94
thermal windows, 12
thermostat, 32, 47, 80, 97, 119, 141
thesis, vi, xii, 27, 35, 158, 165, 166
thresholds, vi, 8, 159, 177
tolerance range, 26, 92
total lipid, 139, 153, 168
trade-offs, vi, xii, 23, 36, 63, 96
transgenerational, 22, 172
trophic, 9, 12, 25, 29, 45
tropical, vi, xiii, 4, 27, 28, 29, 30, 35, 36, 77, 79,
108, 114, 139, 165, 235

V

vaterite, 10
ventral, xvi, xix, 31, 34, 81, 99, 106

Z

ZMT, iv, v, xiii, xxvi, 32, 39, 46, 50, 64, 73, 79, 96,
97, 111, 118, 140